

# EUDIALYTE GEOCHRONOLOGY: INVESTIGATING THE TIMING OF REE MINERALIZATION IN THE GRENVILLE PROVINCE

Alexander Leich

A thesis

submitted to the Faculty of

the Department of Earth and Environmental Science

in partial fulfillment

of the requirements for the degree of

Master Science

Boston College

Morrissey College of Arts and Sciences  
Graduate School

December, 2020



## **EUDIALYTE GEOCHRONOLOGY: INVESTIGATING THE TIMING OF REE MINERALIZATION IN THE GRENVILLE PROVINCE**

Alexander H Leich

Advisor: Ethan F. Baxter PhD.

The Proterozoic Kipawa Syenite Complex and Red Wine Intrusive Suite have both been explored as potential REE ore bodies and are a heretofore unexploited REE resource. This study improves upon the internal-isochron eudialyte geochronology method developed by Sjöqvist et al. (2020) through the addition of Electron Microprobe mapping prior to precise MicroMill sampling to build Sm/Nd internal mineral isochrons to directly date this potential rare earth element ore mineral. We show that Nb and Ta concentrations correlate well with Sm/Nd ratios in zoned eudialyte crystals, providing a qualitative map to guide microsampling. At the Kipawa Syenite Complex two internal eudialyte isochrons yield ages of  $1066 \pm 56$  Ma (MSWD=1.7) and  $1109 \pm 53$  Ma (MSWD=1.2) while a multi-sample eudialyte bulk isochron produces an age of  $1092 \pm 53$  Ma (MWSD= 1.5). The weighted average of the three isochrons is  $1090 \pm 31$  Ma, and gives the age of eudialyte formation across the Kipawa Syenite Complex. Nd model ages confirm derivation from older continental crust with  $T_{DM}=2.28$ . At the Red Wine Intrusive Suite single internal eudialyte isochron yields an age of  $765 \pm 240$  Ma (MSWD=3.7) while the high-Nb sector of this crystal yields an age of  $704 \pm 120$  Ma (MSWD=1.6). A multi-sample eudialyte and mosandrite bulk isochron produces an age of  $989 \pm 150$  Ma (MSWD=15). The latter age reflects original Grenvillian crystallization of REE ore-minerals, while the age of the high-Nb zone reflects a younger, heretofore unrecognized recrystallization event. Nd model ages suggest derivation from the Proterozoic crust with  $T_{DM}=1.80$ . Examination of Nd model ages and geochemical data from five agpaitic deposits (Red Wine, Kipawa, Ilímaussaq, Norra Kärr, Lovozero) reveals three distinct deposit types identified as the Lovozero type, the Grenville type, and the Kipawa type.

## TABLE OF CONTENTS

<b>TABLE OF CONTENTS .....</b>	<b>i</b>
<b>LIST OF TABLES .....</b>	<b>iii</b>
<b>LIST OF FIGURES .....</b>	<b>iv</b>
<b>ACKNOWLEDGMENTS .....</b>	<b>vii</b>
<b>INTRODUCTION.....</b>	<b>viii</b>
<b>1.0 CHAPTER 1 BACKGROUND AND OBJECTIVES.....</b>	<b>1</b>
1.1 KEY QUESTIONS AND HYPOTHESES .....	1
1.2 RESEARCH METHODS .....	2
1.3 GEOLOGY OF THE GRENVILLE PROVINCE .....	3
<b>2.0 CHAPTER 2: EUDIALYTE GEOCHRONOLOGY OF THE KIPAWA SYENITE COMPLEX.....</b>	<b>8</b>
2.1 ABSTRACT .....	8
2.2 INTRODUCTION .....	9
2.2.1 Goals and Hypotheses .....	12
2.3 GEOLOGY AND GEOCHRONOLOGY .....	14
2.3.1 Kipawa Syenite Complex .....	15
2.3.2 Review of Existing Geochronology .....	18
2.4 SAMPLES .....	20
2.4.1 KP1 .....	21
2.4.2 KP2 .....	22
2.4.3 KP 9 .....	23
2.4.4 Eud122804.....	24
2.5 METHODS.....	25
2.5.1 Scanning Electron Microscopy (SEM).....	26
2.5.2 Laser Ablation Inductively Coupled Plasma Mass Spectrometry (LA-ICPMS)...	26
2.5.3 Electron Microprobe Mapping (EMP) .....	27
2.5.4 Micromill Sampling.....	28
2.5.5 Isotope Dilution Thermal Ionization Mass Spectrometry (ID-TIMS).....	29
2.6 RESULTS.....	30
2.6.1 SEM.....	30
2.6.2 LA-ICP-MS .....	31
2.6.3 Electron Microprobe.....	33
2.6.4 ID-TIMS .....	35

2.7	DISCUSSION.....	37
2.8	CONCLUSION.....	47
<b>3.0</b>	<b>CHAPTER 3: GEOCHRONOLOGY OF THE RED WINE INTRUSIVE SUITE.....</b>	<b>49</b>
3.1	ABSTRACT .....	49
3.2	REGIONAL GEOLOGY.....	50
3.2.1	Red Wine Intrusive Suite.....	50
3.3	SAMPLES .....	54
3.3.1	CBD 11-10-1 .....	55
3.3.2	CBD 11-10-2 .....	56
3.3.3	CB 02-12 .....	56
3.4	METHODS.....	57
3.5	RESULTS.....	59
3.5.1	SEM.....	59
3.5.2	LA-ICP-MS .....	60
3.5.3	Electron Microprobe.....	63
3.5.4	ID-TIMS .....	64
3.6	DISCUSSION.....	66
3.7	CONCLUSION.....	75
<b>4.0</b>	<b>REFERENCES.....</b>	<b>77</b>
<b>5.0</b>	<b>APPENDIX 1: DETAILED LABORATORY METHODS FOR EUDIALYTE GEOCHRONOLOGY .....</b>	<b>86</b>
<b>6.0</b>	<b>APPENDIX 2: SPIKE SUBTRACTION SHEETS.....</b>	<b>101</b>
<b>7.0</b>	<b>APPENDIX 3: DATA TABLES .....</b>	<b>163</b>
<b>8.0</b>	<b>APPENDIX 4: SAMPLE INVENTORY .....</b>	<b>253</b>
<b>9.0</b>	<b>APPENDIX 5: SUPPLEMENTAL IMAGES .....</b>	<b>254</b>

## LIST OF TABLES

Table 1. Formulae of HFSE minerals characteristic of agpaitic rocks.....	15
Table 2. Summary selected elements showing a relationship with $^{147}\text{Sm}/^{144}\text{Nd}$ ratio.....	31
Table 3. Kipawa Syenite Complex ID-TIMS data.....	35
Table 4. Summary selected elements showing a relationship with $^{147}\text{Sm}/^{144}\text{Nd}$ ratio.....	60
Table 5. Red Wine Intrusive Suite ID-TIMS data.....	65
Table 6. Oxide masses, with elemental mass and potential isobaric interferences.....	96
Table 7. LA-ICP-MS elemental concentration data.....	163
Table 8. Inventory of all samples acquired in the course of this study.....	253

## LIST OF FIGURES

### FIGURES FROM CHAPTER 1

Figure 1. Location and broad scale structure of the Grenville Province. ....	4
Figure 2. Location of Monocyclic and polycyclic metamorphic belts in the Grenville province.....	6

### FIGURES FROM CHAPTER 2

Figure 3. Location of Protoerzoic peralkaline complexes in relation to the Grenville Front Tectonic Zone (GFTZ).....	11
Figure 4. Broad scale structure of the Grenville Province.....	13
Figure 5. Geology and structure of the Kipawa Syenite complex and surrounding units.	16
Figure 6. Generalized structural column of the Kipawa region along transect A-B (Figure 5) and summary of previous geochronology. ....	18
Figure 7. Outcrop from which sample KP 1 was broken.....	20
Figure 8. Sample KP 1.....	21
Figure 9. Sample KP2.....	22
Figure 10. Sample KP 9.....	23
Figure 11. Sample EUD122804.....	24
Figure 12. Chondrite normalized rare earth element (REE) spider diagram from the Kipawa Syenite Complex (KSC). ....	32
Figure 13. LA-ICP-MS elemental concentrations (ppm) plotted against $^{147}\text{Sm}/^{144}\text{Nd}$ from three KSC eudialyte samples. ....	33
Figure 14. Electron Microprobe (EMP) maps of selected elements in the large eudialyte crystal from sample KP9.....	34
Figure 15. Isochrons plotted in the course of this study. ....	36
Figure 16. Chondrite normalized rare earth element (REE) spider diagram for all complexes measured in the course of this study .....	38
Figure 17. Electron Microprobe (EMP) map selected elements in several eudialyte crystals from sample KP1. ....	39
Figure 18. EMP map of Nb in a single large eudialyte crystal from sample KP9.....	41

Figure 19. Generalized structural column along transect A-B (Figure 5) and summary of relevant geochronology.....	43
Figure 20. Model for Nd isotopic evolution of KSC eudialyte.....	44
Figure 21. Model for Nd isotopic evolution of KSC and LV eudialyte. ....	46

## FIGURES FROM CHAPTER 3

Figure 22. Geologic provinces of Labrador.....	50
Figure 23. Geologic map of the Letitia Lake Area.....	51
Figure 24. Geology and relevant geochronology of the Red Wine Intrusive Suite.....	53
Figure 25. Map of Search Minerals diamond borehole drill sampling sites.....	54
Figure 26. True color scan of sample CBD 11-10-1.....	55
Figure 27. Sample CBD11-10-2. ....	56
Figure 28. Sample CB 02-12. ....	57
Figure 29. SEM BSE image of sample CBD11-10-2 with overlaid with EDS based mineral identifications. ....	58
Figure 30. SEM BSE image of sample CBD11-10-2 with overlaid with EDS based mineral identifications. ....	59
Figure 31. Chondrite normalized rare earth element (REE) spider diagram from the Red Wine Intrusive Suite (RWIS).....	61
Figure 32. LA-ICP-MS elemental concentrations (ppm) plotted against $^{147}\text{Sm}/^{144}\text{Nd}$ from two RWIS eudialyte samples.....	62
Figure 33. Electron Microprobe (EMP) maps of sample CBD 11-10-2.....	63
Figure 34. EMP map of La in sample CBD 11-10-2. ....	64
Figure 35. EMP map of NB in sample CBD 11-10-2.....	66
Figure 36. Chondrite normalized rare earth element (REE) spider diagram for all complexes measured in the course of this study.....	67
Figure 37. SEM BSE images and EDS maps of eudialyte from Ilímaussaq, Greenland..	68
Figure 38. Isochron diagrams from the RWIS.....	69
Figure 39. Geology and relevant geochronology of the Red Wine Intrusive Suite.....	71
Figure 40. Model for Nd isotopic evolution of RWIS eudialyte. ....	73
Figure 41. Model for Nd isotopic evolution of Grenvillian eudialyte. ....	74



## ACKNOWLEDGMENTS

I would like to thank a variety of individuals and organizations for their contributions to this work, without whom this project would not have been possible. These include Mike Tappa, Paul Starr, and Stephanie Walker for their help working in the lab, and answering many questions. Search Minerals, Quebec Precious Metals, The Harvard Mineralogical Museum, and Matthew Crocker for providing the sample material used in the study. Support from Search Minerals this also included access to the Kipawa Rare Metal Deposit in Temiscaming, Quebec. This work also relied on several excellent collaborators; Axel Sjöqvist and Thomas Zack at the University of Gothenburg, as well as Michael Williams at the University of Massachusetts, Amherst. Finally, I would like to thank my advisor Ethan Baxter who served as an excellent guide through the entire process of beginning a project and bringing it to a conclusion despite the disruptions of 2020.

## **INTRODUCTION**

This thesis consists of three chapters detailing this study focused on two Proterozoic Peralkaline Complexes from the Grenville Province. The first chapter introduces the guiding questions and motivations for this study as well as detailing some of the geologic underpinnings of the study. The geologic setting focuses on the Grenville Province where both field sites are located, and examines the complex history of this geologic province. Chapter two focuses on Sm-Nd eudialyte geochronology as a tool to investigate the timing of eudialyte formation at the Kipawa Syenite Complex in Southwestern Quebec. Chapter three similarly explores the geochronology of the Red Wine Intrusive Suite, Labrador, Canada. Taken together Chapter two and three constitute a draft manuscript for eventual publication in an undetermined scientific journal. An integrated manuscript exploring both locations may allow for the examination of new and more expansive hypotheses than presented herein. A detailed description of the laboratory procedures and methods for eudialyte geochronology can be found in the appendix.

## **1.0 CHAPTER 1 BACKGROUND AND OBJECTIVES**

### **1.1 KEY QUESTIONS AND HYPOTHESES**

This study seeks to further develop and utilize eudialyte internal mineral geochronology to inform our knowledge of Proterozoic agpaitic deposits in the Grenville province. Using this method, with the addition of high precision electron microprobe mapping, we can ask several questions. Was there some broadly distributed process acting during the Grenville orogeny that resulted in the formation of several large agpaitic deposits along the trace of the GFTZ? To explore this expansive question, we should begin by asking smaller and more focused questions. First, what is the age of eudialyte mineralization in the Red Wine Intrusive Suite and Kipawa Syenite Complex? Do these ages correspond with the age of initial igneous emplacement, or do they more closely align with regional metamorphic events? Second, what do Nd isotopic data and model ages reveal about the magmatic evolution of agpaitic source material and crustal residence time?

In order to address these research questions this study will test the following hypotheses:

- First, based on recent studies (Sjöqvist et al., 2020; Wu et al., 2016) we hypothesize that eudialyte Sm/Nd ages will correspond to Grenville age tectonometamorphism, thus suggesting syntectonic partial melting and enrichment of agpaitic ore, a process that has led to post magmatic REE enrichment at sites along the Grenville Front Tectonic Zone (GFTZ).

- Second, we hypothesize that Electron Microprobe (EMP) mapping of key elements such as Nb and Mn, will provide a better guide for micromill sampling for geochronology and will also illuminate evidence for potentially problematic open system behavior.

## 1.2 RESEARCH METHODS

The Boston College Center for Isotope Geochemistry encompasses an ultra-clean (1,000 ppcf) lab with 11 100-ppcf fume hoods, and an Isotopx Phoenix Thermal Ionization Mass Spectrometer (TIMS). The Isotope Geochemistry working group has worked extensively to explore Sm/Nd in garnets from a variety of environments (Baxter et al., 2017; Walker et al., 2019), including sampling individual growth zones within garnet crystals using a Micromill (Dragovic et al., 2012; Farrell, 2019).

The theoretical basis for internal mineral isochrons begins with Rakovan et al. (1997) who selectively sampled crystal faces in a single apatite crystal to constrain the timing of crystallization. More recently, Sjöqvist et al. (2020) successfully constructed an internal isochron in eudialyte using micromill extraction and Thermal Ionization Mass Spectrometry (TIMS) isotopic analysis. The work of Sjöqvist et al. (2020) serves as the theoretical framework for this study.

Sm/Nd geochronology is based on the radioactive decay of  $^{147}\text{Sm}$  to  $^{143}\text{Nd}$  by alpha particle emission with a half-life of 106 billion years (DePaolo and Wasserburg, 1976). Sm/Nd fractionation mostly occurs in the silicate portion of the planets, making Sm/Nd ratios a useful tool for exploring magma differentiation and similar processes (DePaolo,

1988). Sm/Nd geochronology relies on the isochron method where both the radioactive parent ( $^{147}\text{Sm}$ ) and daughter ( $^{143}\text{Nd}$ ) are presented as ratios relatively to non-radiogenic  $^{144}\text{Nd}$ . When  $^{147}\text{Sm}$  and  $^{143}\text{Nd}$  compositions are plotted relative to  $^{144}\text{Nd}$  the straight line between points can be described by the line:  $m = e^{\lambda t} - 1$ , solving for  $t$  will yield the age of the mineral (DePaolo, 1988). Whereas sector zoned garnet geochronology relies on external mineral points to provide a low point, internal mineral geochronology relies solely on the internal variation within a single crystal.

### 1.3 GEOLOGY OF THE GRENVILLE PROVINCE

The Grenville Province of Southeastern Canada is a complex amalgamation of predominantly Proterozoic amphibolite- and granulite-facies metamorphic rocks. K-Ar ages for metamorphic minerals are consistently reset to 1000-970 Ma across the province (Groulier et al., 2018). The Grenville Province extends along the southeastern Laurentian margin from Georgian Bay to the Labrador Sea in a northeasterly trending belt approximately 400 km across (Figure 1). Bounded to the northwest along much of its length by the Superior Province, the Grenville Province also borders the Makkovik, Southern Churchill, and Nain Provinces (Rivers, 1997) (Figure 1). The northern boundary of the Grenville Province is marked by the Grenville Front Tectonic Zone (GFTZ). This major southeasterly dipping crustal discontinuity is made up of multiple thrust faults and zones of mylonitization (Rivers et al., 1989) (Figure 1). The GFTZ marks where high-grade rocks of the Grenville Province were thrust onto the older and relatively low-grade rocks of the Canadian Shield, and is the northernmost boundary of K-Ar age resetting (Groulier

et al., 2018). Rivers et al. (1989) initially divided the Grenville Province into the Parautochthonous and Allochthonous Belts; two longitudinal belts (Figure 1) differentiated on the basis of age distribution and distinctive lithologies. The Parautochthonous Belt (PB) lies immediately to the south of the GFTZ and is characterized by lithologic continuity with the northern foreland (Rivers et al., 1997). Representing a section of northwesterly thrust Laurentian margin, the PB is composed of Archean and Paleoproterozoic age units (Dickin and Guo, 2001). The PB records the formation of Andean type arcs and backarcs

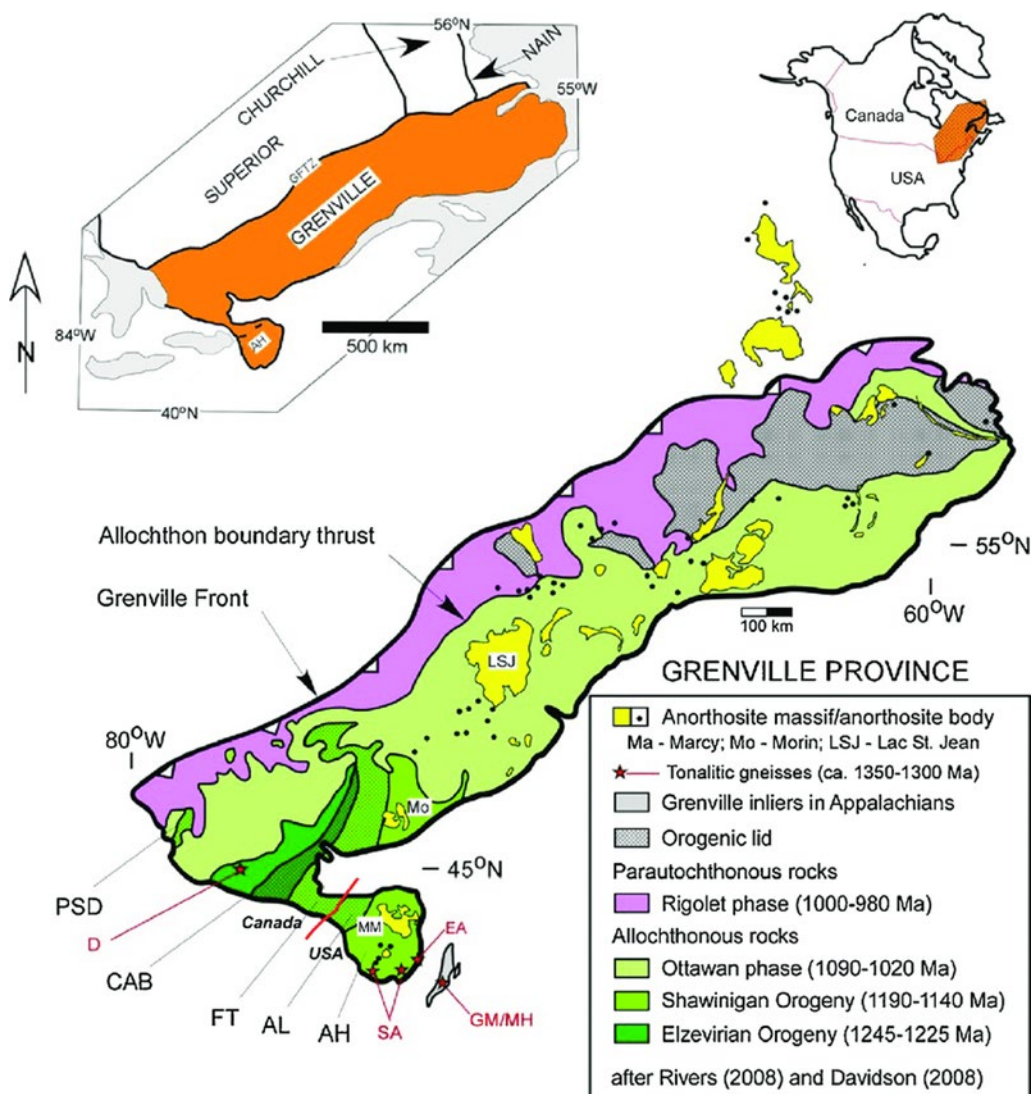


Figure 1. Location and broad scale structure of the Grenville Province. Image from Valentino et al. (2018).

and subsequent accretionary orogenesis from ~1.71 to 1.23 Ga (Gower and Krogh, 2002; Rivers et al., 1997). Much of the northwestern margin of the PB is characterized by shear zones and isoclinal folds with metamorphic grade generally increasing southeastward from the GFTZ (Rivers et al., 1989). The PB is bounded to the south by the Allochthon Boundary Thrust (ABT) marking where younger, distally-sourced rocks of the Allochthonous Belt (AB), lie structurally above the PB (Rivers et al., 1989) (Figure 1).

The Allochthon Boundary Thrust (ABT) (Figure 1, Figure 2) served as a large-scale ramp, leading to the exposure of deep crustal constituents through repeated thrusting and normal faulting (Herrell et al., 2006). The ABT was first identified along much of the Grenville province on the basis of aeromagnetic evidence (Rivers, et al., 1989), and has since been supported by structural, and geochronological studies (Dickin and Guo, 2001). The exact locations of some portions of the ABT remain in question, especially in southwestern areas where numerous shear zones and high-grade metamorphism have obscured the boundary (Herrell et al., 2006). Dikes related to the Sudbury dike swarm can be traced across the GFTZ into the PB (Berthune and Davidson, 1997), but do not cross the ABT (McLlland et al, 2010).

The AB is made up of younger and more lithologically variable terranes that do not correlate directly with the Laurentian foreland (Rivers et al, 1997). The AB is further divided into mono- and polycyclic belts, based on the apparent variation in deformational history (Figure 2) (Rivers et al., 1997). The Monocyclic Belt Boundary Zone separates the two allochthonous belts, and is variably expressed by ductile thrusting or mylonitization and subsequent brittle faulting (McLlland et al., 2010). In the Allochthonous Polycyclic Belt plutonic and supra-crustal rocks record deformation from multiple orogenies in

lithology characterized by high grade gneiss (Figure 2). The Allochthonous Monocyclic Belt is characterized by terrestrial rift and supracrustal rocks affected only by the younger Grenville Orogeny and has been interpreted as vestiges of an orogenic lid (Rivers et al., 1989) where rocks were thrust over the center of the orogenic belt and thus escaped high grade metamorphism (Figure 2).

Northeasterly thrusting accompanied the Shawinigan orogeny from 1190-1140 Ma. Intrusive suites from this interval are abundant in the Adirondack lowlands and the

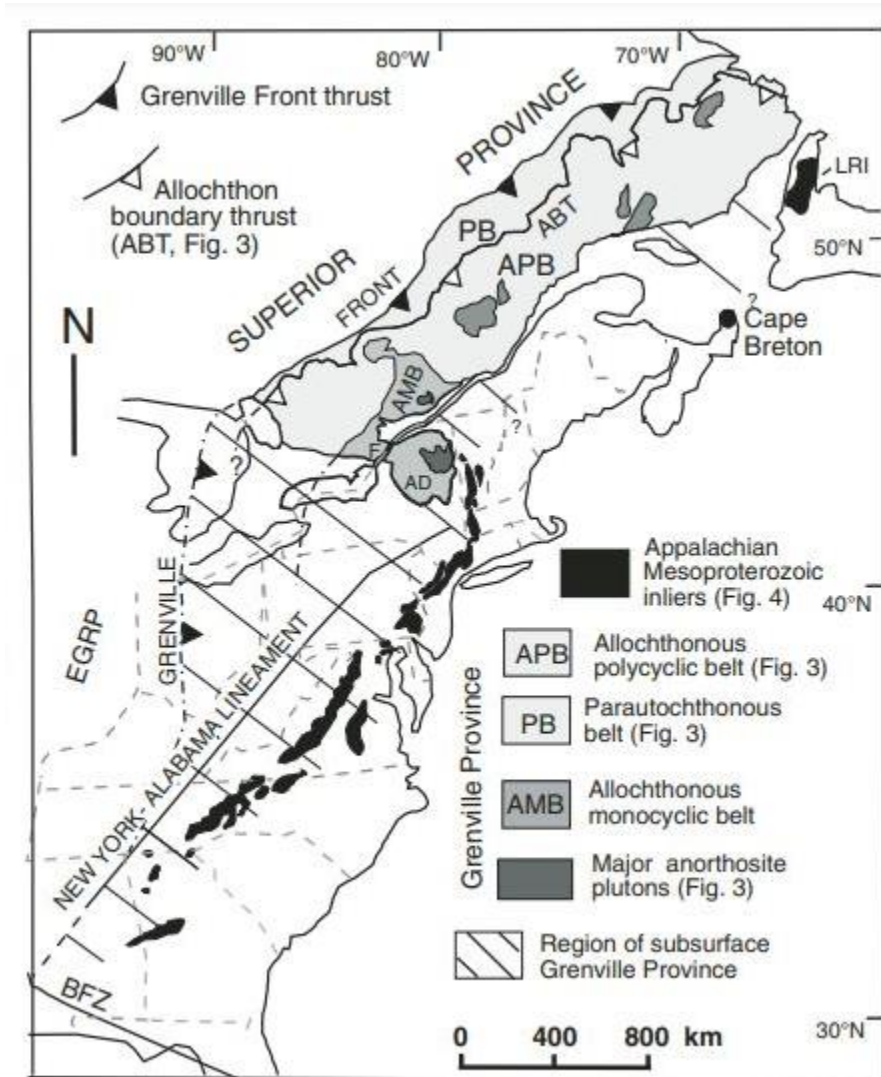


Figure 2. Location of Monocyclic and polycyclic metamorphic belts in the Grenville province. Image from McLelland et al. (2010).

southwest portion of the province. The eastern portion of the province was intruded by anorthosite-mangerite-charnockite-granite (AMCG) suites between 1155-1140 Ma in an environment characterized by mild extension, perhaps driven by crustal delamination (Figure 2) (McLlland et al., 1990). Following AMCG emplacement the Laurentian margin experienced a period of relative quiescence from 1140-1090 Ma, which came to an end with the onset of the Grenville orogeny from 1090 to 980 Ma. Two phases of the Greenville orogeny are recognized, the Ottawan phase from 1090-1020 Ma and the Rigolet phase from 1010-980 Ma. Both phases consist of northwestward thrusting followed by extensional collapse ultimately resulting in the exhumation of high grade terranes (Figure 1) (McLlland et al., 1990).

## **2.0 CHAPTER 2: EUDIALYTE GEOCHRONOLOGY OF THE KIPAWA SYENITE COMPLEX**

### **2.1 ABSTRACT**

The Proterozoic Kipawa Syenite complex has been explored as a potential REE ore body and is a heretofore unexploited REE resource. The petrogenesis of this and similar eudialyte ore bodies (i.e., Norra Kärr, Sweden) remains uncertain, including the role of metamorphic remobilization in ore formation. Accurate geochronology of eudialyte can help resolve whether the ore formed during Grenvillian metamorphism or earlier igneous emplacement. This study improves upon the internal-isochron eudialyte geochronology method developed by Sjöqvist et al. (2020) through the addition of Electron Microprobe mapping prior to precise MicroMill sampling to build Sm/Nd internal mineral isochrons to directly date this potential rare earth element ore mineral. We show that Nb and Ta concentrations correlate well with Sm/Nd ratios in zoned eudialyte crystals, providing a qualitative map to guide microsampling. Two internal eudialyte isochrons yield ages of  $1066 \pm 56$  Ma (MSWD=1.7) and  $1109 \pm 53$  Ma (MSWD=1.2) while a multi-sample eudialyte bulk isochron produces an age of  $1092 \pm 53$  Ma (MWSD= 1.5). The weighted average of the three isochrons is  $1090 \pm 31$  Ma, and gives the age of eudialyte formation across the Kipawa Syenite Complex. This age corresponds to the beginning of the Ottowan phase of the Grenville Orogeny. Nd model ages confirm derivation from older continental crust with  $T_{DM}=2.28$ . HREE enrichment in Kipawa eudialyte is likely related to this derivation

from continental source. Metamorphic reworking of enriched continental crust is crucial to the formation of this HREE-enriched eudialyte ore at Kipawa.

## 2.2 INTRODUCTION

The Rare Earth Elements (REE's) comprise the 15 elements of the lanthanide series (Lanthanum - Lutetium) as well as Yttrium. Based on a variety of unique physical properties related to lanthanide contraction REE's have become crucial elements for the manufacture of many modern technologies such as fluorescent lighting, batteries, and strong magnets (Chakhmouradian and Wall, 2012). Despite being less rare than other valuable elements such as gold and silver, deposits with concentrations of REEs are exceptionally rare thus economically viable resources are uncommon. REE's only occur in economic concentrations in a small number of geologic environments. Global REE demand is expected to increase due to their use in a variety of sectors such as communications, power generation, and power storage (Chakhmouradain and Wall, 2012). Currently most of global rare earth oxides are produced by China (Chakhmouradain and Wall, 2012). Increased demand has focused attention on examining nontraditional REE resources; peralkaline agpaitic deposits are one such type. Eudialyte hosted agpaitic REE deposits constitute a potential new resource, and are particularly interesting for those seeking to secure REE resources within the NAFTA free trade area.

Peralkaline rocks are defined by molar (Na+K)/Al ratios > 1 and commonly contain high concentrations of incompatible elements such as large ion lithophile elements (LILEs), high field strength elements (HFSEs), rare earth elements (REEs) and halogens

(Sørensen, 1992). Agpaitic rocks are distinguished from more common peralkaline compositions based on the presence of characteristic minerals like the REE-rich eudialyte instead of more common phases like zircon and titanite (Marks et al., 2011). The substitution of REE into the structure of eudialyte is poorly understood, by is thought to be most due to substitutions for Ca on the M1 site (Borst et al., 2020) Agpaitic rocks typically occur as minor silica-undersaturated constituents within larger units of silica-saturated peralkaline rocks, although not all agpaitic rocks are silica-undersaturated.

Eudialyte ( $\text{Na}_{15}\text{Ca}_6\text{Fe}_3\text{Zr}_3\text{Si}(\text{Si}_{25}\text{O}_{73})(\text{O},\text{OH},\text{H}_2\text{O})_3(\text{Cl},\text{OH})_2$ ) is named for a propensity to dissolve in acid making it an appealing target for both laboratory analysis and as an ore mineral (Chakraborty et al., 2011). Although processing at scale has proven difficult the prospect of a relatively easy and safe processing procedure remains on the horizon (Balinski et al., 2020). Unlike monazite and xenotime hosted deposits, eudialyte is mostly free of radioactive elements like uranium and thorium, although radioactive accessory minerals like thorite are found in some eudialyte-bearing deposits.

Understanding of agpaitic REE source materials, petrogenesis, and age relations are far from complete and warrant further inquiry. Here, we focus on the Proterozoic Kipawa Syenite Complex (KSC) located on the Southwestern portion of the Grenville Province of Southeastern Canada (Figure 3). Characteristic of agpaitic rocks, the KSC contains large amounts of eudialyte, which has been explored as a potential REE ore mineral and is a heretofore unexploited REE resource (Marks and Markl, 2017). The Kipawa deposit has been explored by Quebec Precious Metals through several proprietary drilling campaigns aimed at defining eudialyte mineralization; however, due to unstable prices and environmental concerns, the site has not seen production.

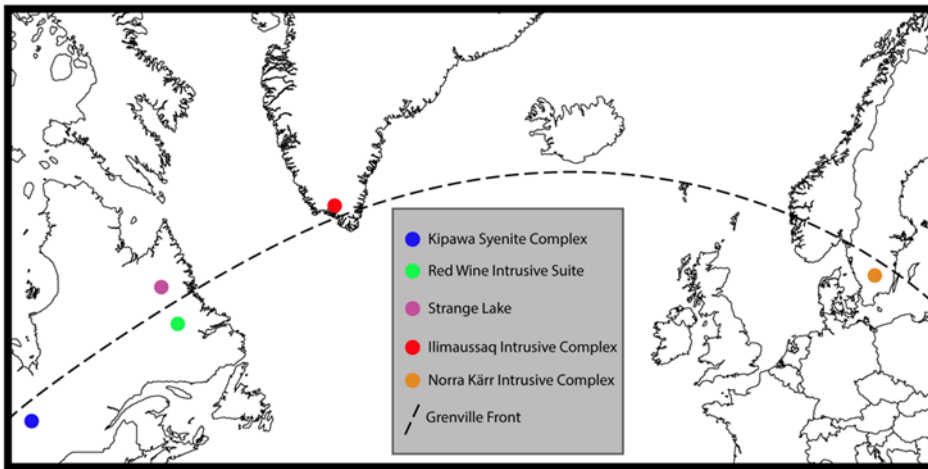


Figure 3. Location of Protoerzoic peralkaline complexes in relation to the Grenville Front Tectonic Zone (GFTZ) (dashed line) modified from Currie and van Breeman (1996).

Several authors (Currie and van Breeman 1996; Allan, 1992) have observed that five Proterozoic peralkaline complexes occur in close proximity to the Grenville Front Tectonic Zone (GFTZ) (Figure 3), Kipawa among them. The distribution of agpaitic rocks through time is not even, and the formation of agpaitic rocks appears to correlate negatively with the presence of supercontinents (Marks and Markl, 2017). The spatial and temporal association of these normally rare geologic formations along the GFTZ raises the prospect that some unique process was driving the formation of agpaitic rocks at this time. Ilímaussaq, Greenland, is located near the GFTZ but is far enough north to have avoided extensive Grenvillian deformation (Sørrensen, 1992) (Figure 3) and serves as a useful model for what other locations may have looked like prior to Grenvillian deformation.

A variety of techniques have been employed to constrain the age of the KSC and surrounding formations and have yielded a range of ages spanning 400 million years. The variety of methods and variable results reflect the difficulty associated with directly dating metamorphic agpaitic systems. This difficulty can be largely attributed to the lack of zircon in silica-undersaturated agpaitic rocks and the preponderance of evidence for open system behavior. A direct chronometer of the dominant REE ore mineral, eudialyte, will allow for

temporal constraints on possible open system behavior and ore mineralization. Sjöqvist et al., (2020) developed a new eudialyte geochronometer exploiting internal mineral Sm-Nd isochrons in sector zoned eudialyte crystals. LA-ICPMS characterization illuminate areas of higher and lower  $^{147}\text{Sm}/^{144}\text{Nd}$  that were targeted for micromill sampling. This new method was tested at the Nora Kärr agpaitic locale in Sweden, returning a eudialyte age of  $1144 \pm 53$  Ma. This age is significant because it is much younger than the well constrained primary igneous emplacement age of 1490 Ma, leading Sjöqvist et al., (2020) to conclude that ore mineralization was a metamorphic remobilization event.

### 2.2.1 Goals and Hypotheses

This study seeks to answer a fundamental question. What is the age of eudialyte mineralization in the Kipawa Syenite Complex? Do these ages correspond to older pre-Grenvillian initial igneous emplacement, or do they more closely align with regional Grenvillian metamorphic events? In an effort to better answer the above question we also seek to improve the novel microdrill internal-isochron methodology used to constrain the age of eudialyte mineralization, first attempted by Sjöqvist et al. (2020). Specifically, we explore whether Electron Microprobe (EMP) mapping of eudialyte crystals could provide a more efficient and effective pre-characterization tool prior to eudialyte geochronology.

In order to address these research questions this study will test the following hypotheses:

- First, based on recent studies (Sjöqvist et al., 2020; Wu et al., 2016) we hypothesize that eudialyte Sm/Nd ages will correspond to Grenville age tectonometamorphism, thus suggesting syntectonic partial melting and enrichment of agpaitic ore, a process that has led to post magmatic REE enrichment at sites along the GFTZ.

- Second, we hypothesize that Electron Microprobe (EMP) mapping of key elements such as Nb and Mn, will provide a better guide for micromill sampling for geochronology and will also illuminate evidence for potentially problematic open system behavior.

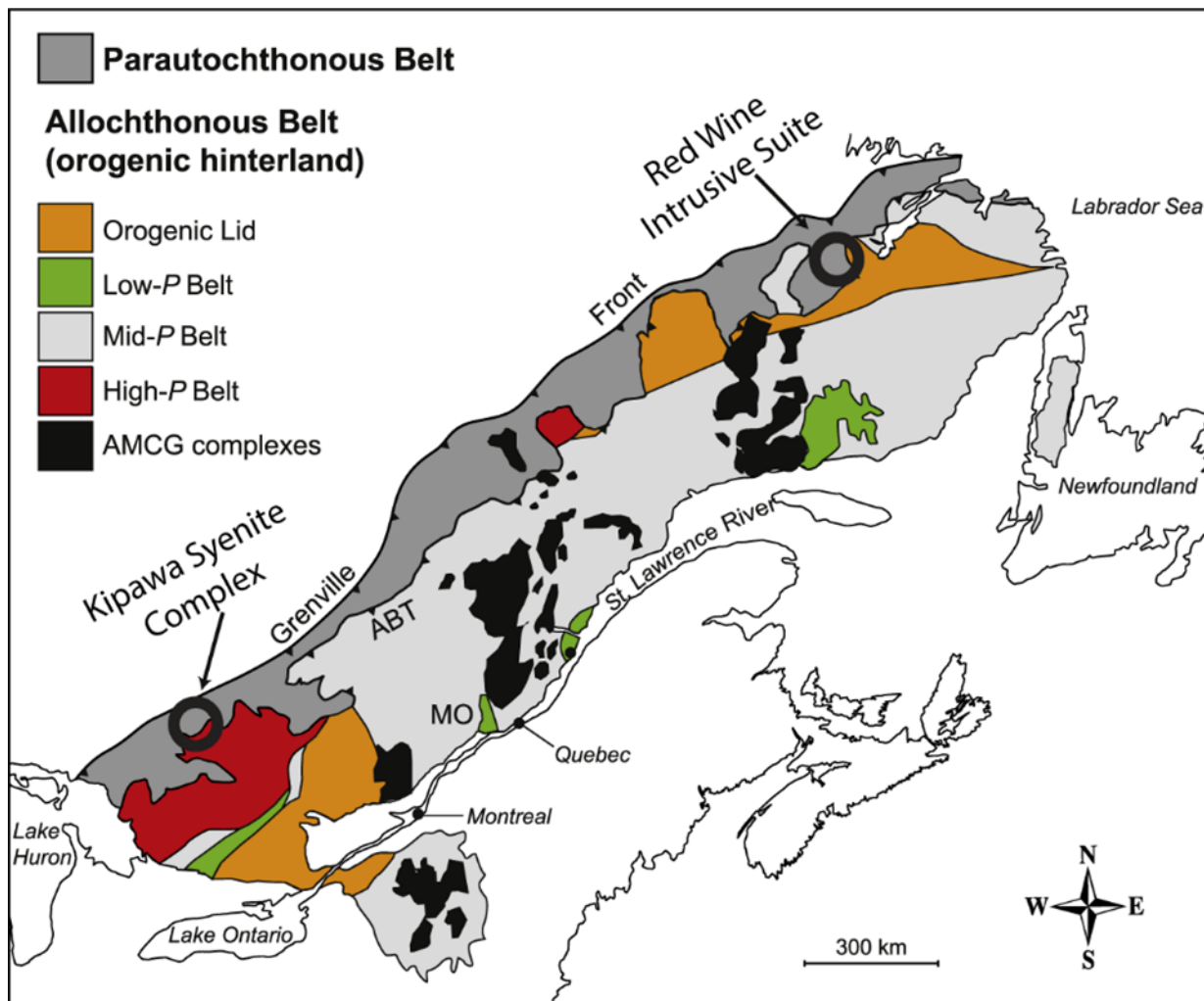


Figure 4. Broad scale structure of the Grenville Province. Location of Kipawa Syenite Complex (KSC) indicated by black circle. Modified from Groulier et al. (2018).

## 2.3 GEOLOGY AND GEOCHRONOLOGY

Peralkaline rocks are defined by molar (Na+K)/Al ratios > 1 and commonly contain high concentrations of incompatible elements such as large ion lithophile elements (LILEs), high field strength elements (HFSEs), rare earth elements (REEs) and halogens (Sørensen, 1992). Peralkaline rocks are further divided into two compositional categories, miaskitic and agpaitic. Agpaitic varieties are distinguished from more common miaskitic compositions based on the presence of characteristic minerals like eudialyte in the place of phases like zircon and titanite (Marks et al., 2011). Agpaitic rocks typically occur as minor silica-undersaturated constituents within larger units of silica-saturated peralkaline rocks. This common field relationship suggests agpaitic rocks represent the most highly evolved, residual liquids of peralkaline systems.

In Southeastern Canada, the GFTZ marks where high-grade rocks of the Grenville Province were thrust onto the older rocks of the Canadian Shield (Groulier et al., 2018). Ilímaussaq, Greenland, is located near the GFTZ, but is far enough north to have avoided extensive Grenvillian deformation (Sørensen, 1992) and serves as a useful model for what other locations may have looked like prior to Grenvillian deformation.

Eudialyte (Table 1) is named for a propensity to dissolve in acid making it an appealing target for both laboratory analysis and as an ore mineral. Although processing at scale has proven difficult the prospect of a relatively easy and safe processing procedure remains on the horizon. Unlike monazite and xenotime, eudialyte is mostly free of radioactive elements like Uranium and Thorium, although accessory minerals like thorite are common.

Agpaitic rocks are rare, even compared to peralkaline rocks and by definition contain a variety of rare minerals (Table 1). This rarity and unusual composition suggests specific processes must be required for their formation. The distribution of agpaitic rocks through time is not even, and the formation of agpaitic rocks appears to correlate negatively with the presence of supercontinents (Marks and Markl, 2017). The spatial and temporal association of these normally rare geologic formations along the GFTZ raises the prospect that some unique processes were acting on these rocks during the Grenville Orogeny.

### 2.3.1 Kipawa Syenite Complex

The Kipawa Syenite Complex is located 35 km east of Temiscaming, Quebec the Kipawa Syenite Complex (KSC) is on the northwestern margin of the Grenville Province, roughly 35 km from the GFTZ (Figure 4, Figure 5) (Allan, 1992) where Archean fault slices derived from the Superior Province are the primary bedrock constituent (Currie and van Breemen, 1996). Nd isotopic mapping reveals the presence of bimodal Archean crust

HFSE minerals typical of agpaitic rocks	
Aenigmatite	$\text{Na}_2\text{Fe}_5\text{TiSi}_6\text{O}_{20}$
Agrellite	$\text{NaCa}_2\text{Si}_4\text{O}_{10}\text{F}$
Catapleiite	$\text{Na}_2\text{Zr}(\text{Si}_3\text{O}_9) \cdot 2\text{H}_2\text{O}$
Eudialyte	$\text{Na}_{15}\text{Ca}_6\text{Fe}_3\text{Zr}_3\text{Si}(\text{Si}_{25}\text{O}_{73})(\text{O},\text{OH},\text{H}_2\text{O})_3(\text{Cl},\text{OH})_2$
Rinkite	$(\text{Ca},\text{REE})\text{Na}(\text{NaCa})\text{Ti}(\text{Si}_2\text{O}_7)_2(\text{OF})\text{F}_2$
Wöhlerite	$\text{Na}_2\text{Ca}_4\text{Zr}(\text{Nb},\text{Ti})(\text{Si}_2\text{O}_7)_2(\text{O},\text{F})_4$

Table 1. Formulae of HFSE minerals characteristic of agpaitic rocks.

in this region where isotopically undisturbed Archean crust yields model ages of  $\sim$ 2.6 Ga while reworked Archean crust yield model ages from 1.8-2.6 Ga (Dickin and Guo, 2001).

The KSC is a unit of nepheline syenite, amphibole syenite, quartz syenite, and alkali granite. At most 300 m thick, the KSC is traceable as a sheet-like body for about 100 km around the Kipawa syncline-anticline pair (Figure 5) (Currie and Van Breeman, 1996). The

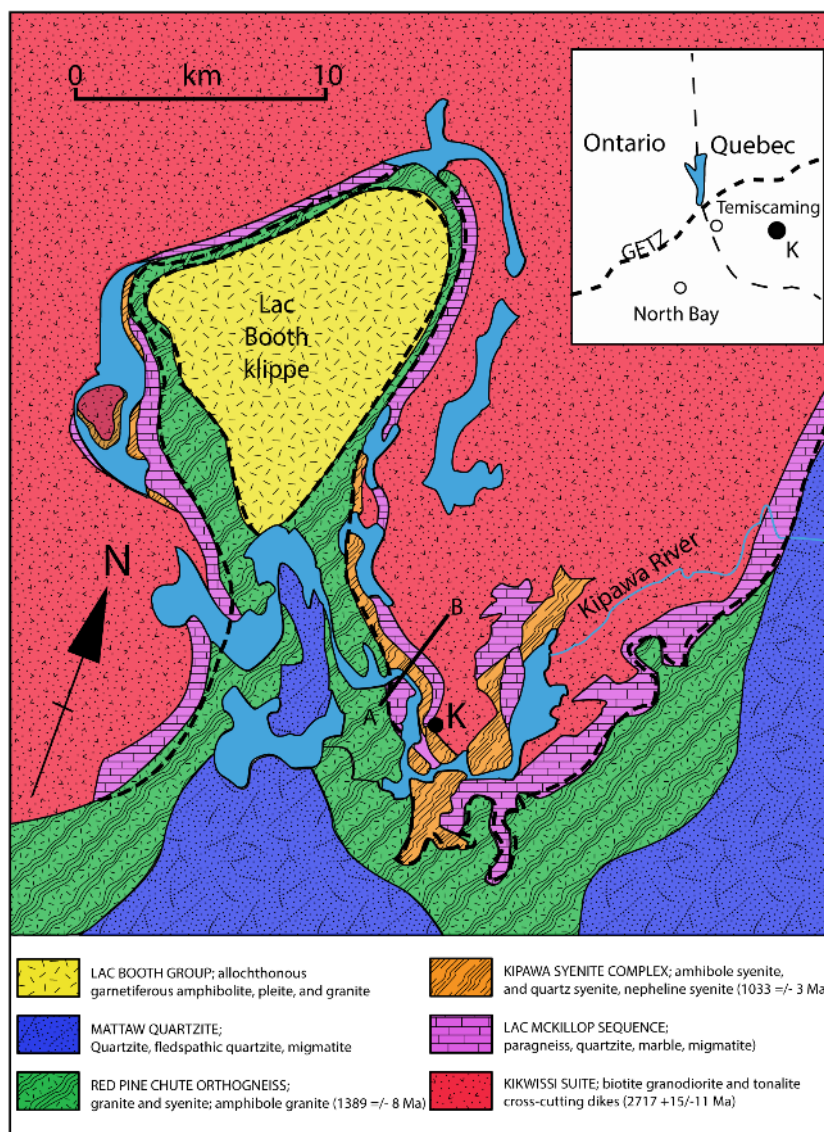


Figure 5. Geology and structure of the Kipawa Syenite complex and surrounding units. Modified from van Breeman and Currie (2004). K marks location of sampling site. Transect A-B indicates trace of generalized structural column.

composition of the KSC is roughly symmetrical with a core of amphibole-pyroxene syenite

and nepheline syenite, bounded by amphibole syenite, which is enclosed by quartz syenite and peralkaline granite (van Breeman and Currie, 2004). Contacts with other units show evidence of metasomatism, and no part of the syenite complex exhibits any recognizable primary igneous textures at the outcrop scale (van Breeman and Currie, 2004).

Silica-undersaturated rocks occur in lenses of varying size and extent, one particularly large lens (1300 m x 5 m) of amphibolite schist containing eudialyte, argellite ( $\text{NaCa}_2\text{Si}_4\text{O}_{10}\text{F}$ ) and other rare minerals constitutes the Kipawa rare metals deposit (Currie and van Breeman, 1996) from which the samples in the present study were collected.

### 2.3.2 Review of Existing Geochronology

Analyses of zircons from the Red Pine Chute orthogneiss yield a  $^{207}\text{Pb}/^{206}\text{Pb}$  age of  $1389 \pm 8$  Ma while small zircons from the Kipawa syenite complex margins yield an age of  $1033.4 \pm 3$  Ma (Figure 6) (van Breeman and Currie, 2004). The former age establishes a

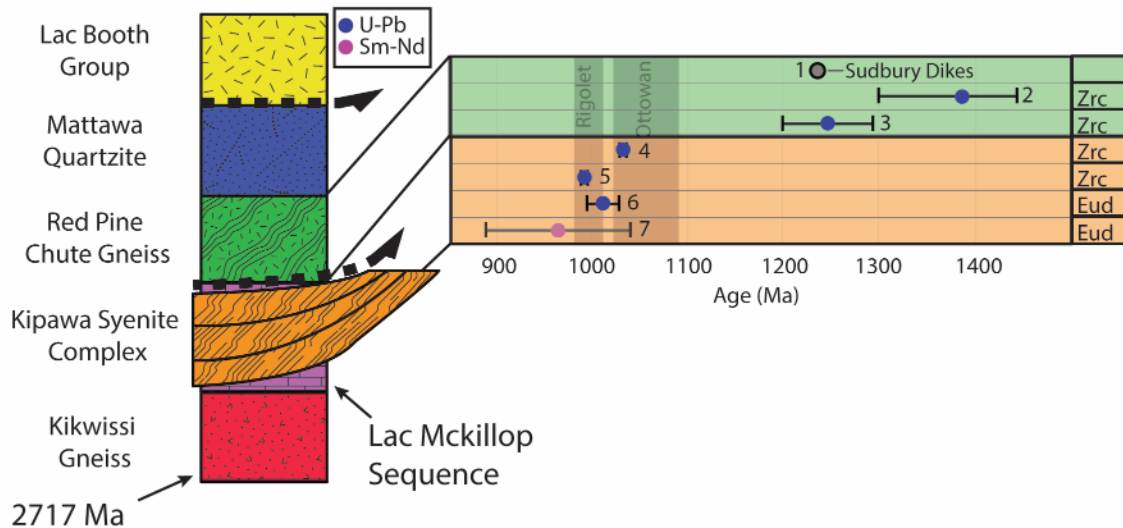


Figure 6. Generalized structural column of the Kipawa region along transect A-B (Figure 5) and summary of previous geochronology. Abbreviations: Zrc: zircon; Eud: eudialyte; Avg: weighted average. Data from: Currie and van Breeman, 1996 (points 1,5); van Breeman and Currie, 2004 (points 2,3,4); Wu et al., 2010 (points 6,7). Age of 2717Ma for the Kikwissi Gneiss is from van Breeman and Currie, 2004. Structural column modified from Matamec, 2011.

maximum emplacement age based on the age of the intruded unit (1389 Ma), while the latter age was interpreted as the emplacement age for the KSC (1033 Ma) coinciding with late Ottawan metamorphism (van Breeman and Currie, 2004). Zircons from marginal agpaitic pegmatites yield a U-Pb age of  $994 \pm 2$  Ma (Currie, and van Breeman, 1996). These youngest ages were interpreted to represent the lower limit for metasomatic zircon growth on the margins of the syenite complex at the end of the Rigolet phase (van Breeman and Currie, 2004).

In addition, Wu et al. (2010) used LA-ICP-MS to examine the U-Pb, Sr, Nd, and Hf isotopic compositions of eudialyte from nine agpaitic localities including the KSC. As part of their study, they constructed multi-point isochrons from in situ laser analysis of eudialyte. They reported a  $^{206}\text{Pb}/^{238}\text{U}$  age of  $1012 \pm 16$  Ma and a  $^{147}\text{Sm}/^{144}\text{Nd}$  age of  $965 \pm 75$  for Kipawa eudialytes (Figure 6). The U-Pb data are dominated by common lead making the isochron age calculation particularly susceptible to common lead uncertainties, as noted by the authors. The Sm-Nd age is based on 20 laser spot analyses, 18 of which cluster around  $^{147}\text{Sm}/^{144}\text{Nd} = 0.2438$  and  $^{143}\text{Nd}/^{144}\text{Nd} = 0.512403$ . Two other plotted data points appear to cluster around a single reported solution-ICP analysis from the same sample of  $^{147}\text{Sm}/^{144}\text{Nd}$  of 0.2079 and a  $^{143}\text{Nd}/^{144}\text{Nd}$  of 0.512205. No raw data for the 20 data points nor  $^{147}\text{Sm}/^{144}\text{Nd}$  uncertainties are reported, nor are any images of the zoned eudialytes to screen for open system disruption (e.g., as seen by Sjöqvist et al., 2020). While rigorous demonstration of the accuracy of  $^{143}\text{Nd}/^{144}\text{Nd}$  based on replicate analysis of a standard is reported, there is no such demonstration of the accuracy (nor precision) of their  $^{147}\text{Sm}/^{144}\text{Nd}$  data by LA-ICP. Furthermore, it is concerning that the solution ICP-MS analysis is completely different from the LA-ICP analyses.

## 2.4 SAMPLES

Kipawa hand samples were collected from a single quarry on the Kipawa Site at (46.80783, -78.50404) (Figure 5, ). Samples were selected based largely on crystal size and sample integrity. Thin sections for petrographic characterization were cut mostly from drill core samples, ultimately only one sample selected for isotopic analysis had an associated



Figure 7. Outcrop from which sample KP 1 was broken. Sampling location is indicated by K on Figure 5.

thin section. Below, the four samples selected for isotopic work in this project (KP1, KP2, KP9, Eud122804) are described. All other samples are listed in the appendix Table 8.

#### 2.4.1 KP1

Sample KP1 was broken directly off of outcrop where quarrying and mineral collecting has clearly been ongoing after initial exploration (Figure 7). This sample is

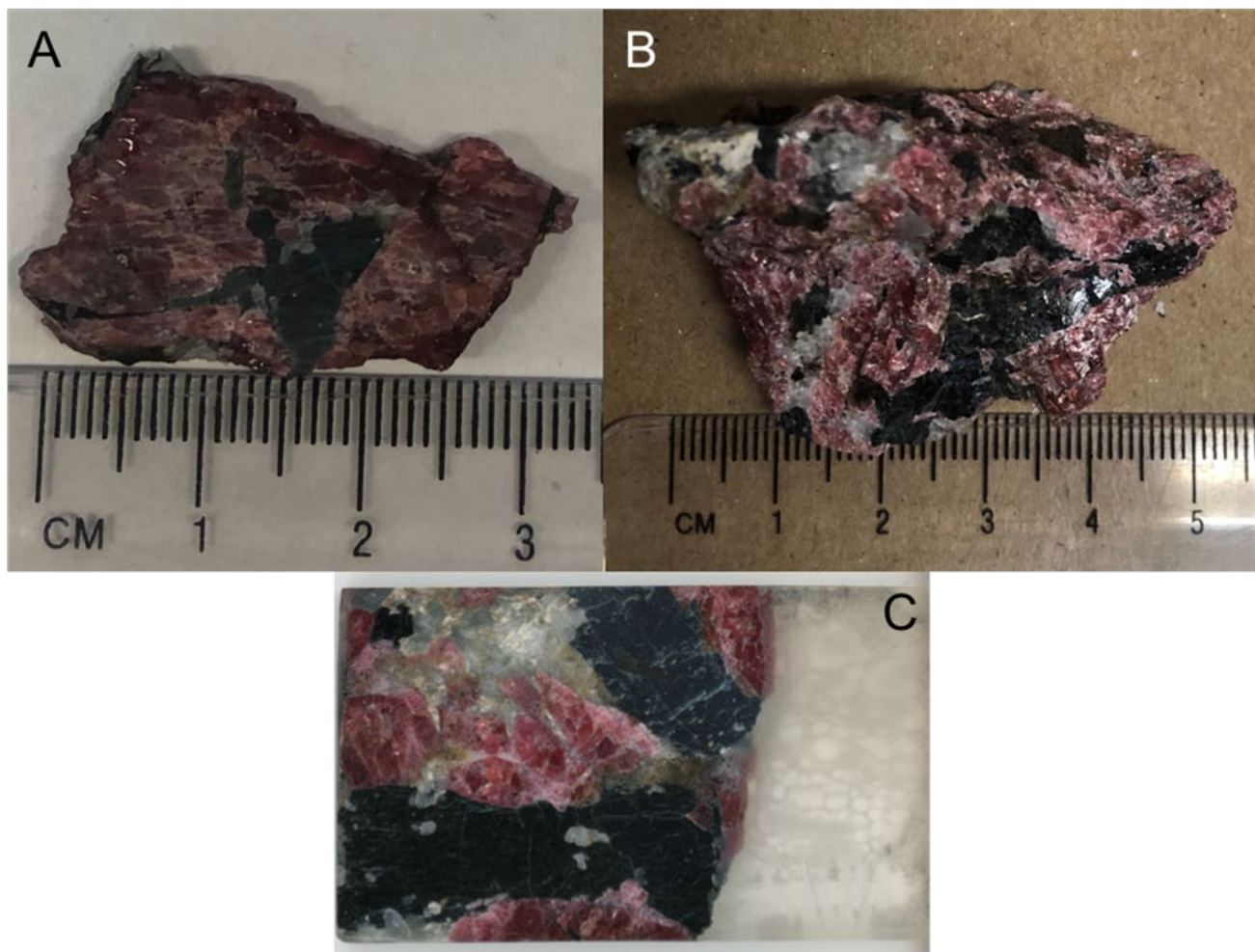


Figure 8. Sample KP 1. A) True color image of sample KP1 chip drilled for ID-TIMS. Pink mineral is eudialyte, black mineral is amphibole (kataphorite?). This sample was drilled 9 times by MicroMill, pits are not visible at this scale. B) KP1 representative hand sample as broken off outcrop. C) True color image of KP1 chip analyzed by LA-ICP-MS and EMP.

primarily comprised of coarse subhedral-anhedral eudialyte and amphibole (kataphorite) within a light-colored matrix of nepheline and minor mosandrite (Figure 8).

#### 2.4.2 KP2

Sample KP2 was acquired from quarry debris adjacent to outcrop. Similar to KP1 sample is primarily eudialyte and amphibole (kataphorite) with minor nepheline (Figure 9). Eudialyte is primarily equant with a granular appearance in hand sample. Subhedral amphibole is medium to fine grained, and deep black in color with nepheline as minor matrix. Microscopic examination reveals late-stage veins filled with britholite and fluorite.



Figure 9. Sample KP2. Hand sample from which eudialyte chips were broken off and analyzed.

### 2.4.3 KP 9

Sample KP9 was collected from quarry debris adjacent to the outcrop. The sample is light grey-white with several coarse (5 cm) eudialyte crystals (Figure 10). The Schistose matrix appears weathered, and primarily composed of argillite ( $\text{NaCa}_2\text{Si}_4\text{O}_{10}\text{F}$ ) and quartz

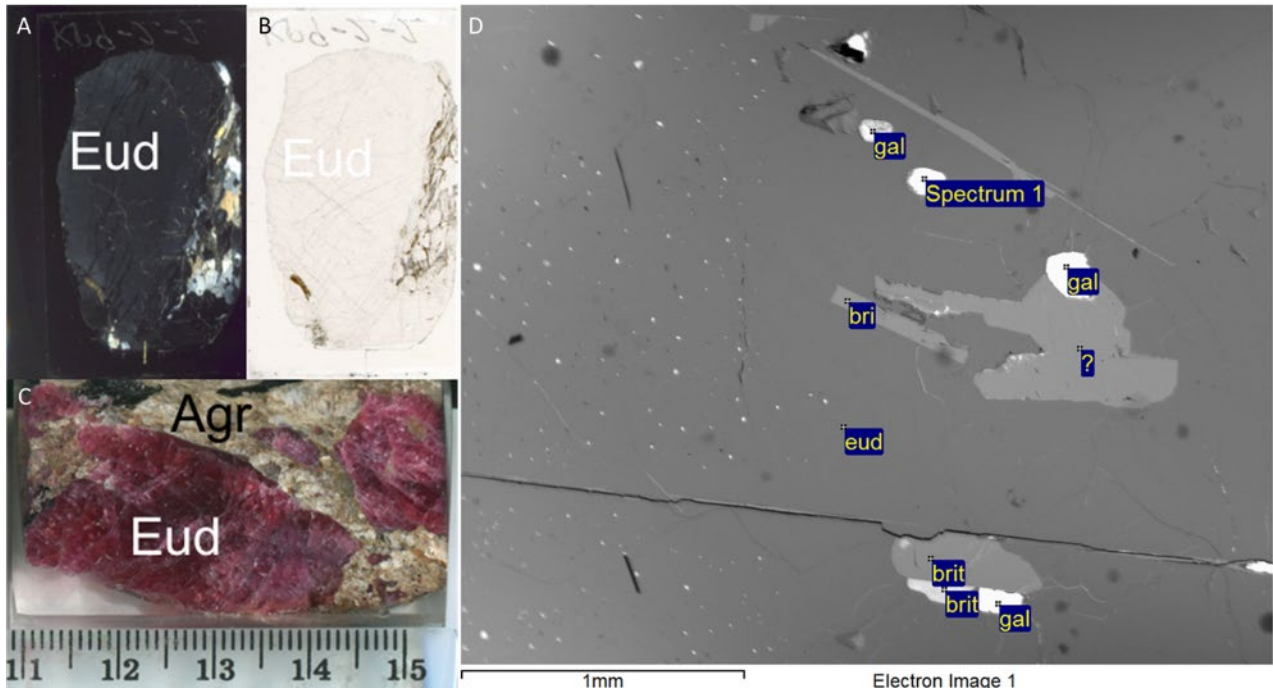


Figure 10. Sample KP 9. A) cross-polarized thin section image; B) cross-polarized thin section image, large grey mass is eudialyte; C) true color scan of sample chip analyzed of sample; D) BSE image of large eudialyte crystal with point locations for X-ray spectra. Abbreviations: Eud: eudialyte; Agr: Agrellite; Bri: Britholite; Gal: Galena.

(Figure 10). Thin section selection was mostly focused on a single large eudialyte grain and thus revealed little about surrounding matrix. The eudialyte crystal is visibly zoned under crossed polarized light and includes small inclusions of britholite, galena, quartz, and apatite (Figure 10).

#### 2.4.4 Eud122804

Sample Eud122804 consists of a small 20 oz. eudialyte crystal provided by the Harvard Mineralogical and Geological Museum, Cambridge, Massachusetts. The exact provenance of the sample is unknown with only “Kipawa River” listed for collection site. The portion of the sample provided by Harvard is red-pink with no obvious inclusions (Figure 11). The sample appears to be granular like some other samples as opposed to a single cohesive crystal. No thin section was made of this sample, and the only processing or analysis conducted was for bulk ID-TIMS as exact sample provenance is unknown.

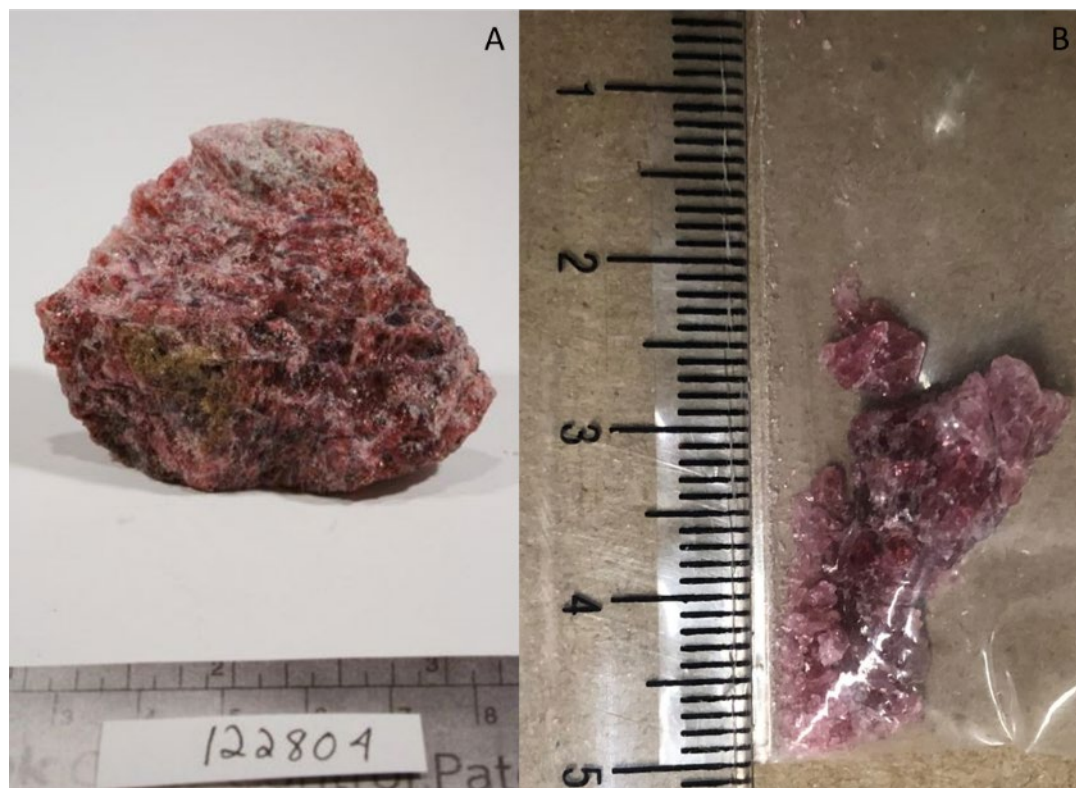


Figure 11. Sample EUD122804. A) Photo of full hand sample from Harvard Mineralogical Museum. B) Photo of loose material provided for this study.

## 2.5 METHODS

We use the method developed by Sjöqvist et al. (2020) to sample individual eudialyte crystals using a computer controlled microdrill for Sm/Nd isotopic analysis by Isotope Dilution Thermal Ionization Mass Spectrometry (ID-TIMS). Pairing the spatial control of microdrill sampling with the high precision of ID-TIMS provides the ability to construct robust internal mineral isochrons (e.g., Schoene & Baxter, 2017) to directly date eudialyte.

Sampling and analysis in this manner are time consuming and within any individual eudialyte crystal variation in  $^{147}\text{Sm}/^{144}\text{Nd}$  is relatively small. Thus, characterization by SEM and LA-ICP-MS prior to drilling and ID-TIMS proved critical in the examination of eudialyte crystals from Norra Kärr, Sweden by Sjöqvist et al. (2020). By identifying crystal zonations by SEM and then characterizing the Sm/Nd isotopic composition of each zone by LA-ICP-MS Sjöqvist et al. (2020) maximized the  $^{147}\text{Sm}/^{144}\text{Nd}$  spread among microdrilled pits in a large eudialyte crystal yielding an isochron age of  $1144 \pm 53$  Ma. Their SEM and LA-ICPMS pre-characterization also proved critical in rejecting a few points showing textural and chemical evidence for late stage open system remobilization. In our study, in an effort to explore other pre-characterization methods, Electron Microprobe mapping (e.g., Regan et al., 2019) of selected elements in eudialyte crystals was also conducted after SEM and LA-ICP-MS characterization.

### **2.5.1 Scanning Electron Microscopy (SEM)**

A Hitachi S-4300N Scanning electron microscope (SEM) with solid state Back Scatter Electron (BSE) detector was used to examine polished thick sections at the University of Gothenburg department of Earth Science. Samples were polished and set in epoxy to meet size constraints and to increase sample integrity. Contrast and brightness were manually tuned to reveal textures and crystal zonations within individual eudialyte crystals. Mineral identification was supported by qualitative X-ray spectrometry using oxford instruments X-MAX 20 mm<sup>2</sup> area silicon drift detector and INCA software.

### **2.5.2 Laser Ablation Inductively Coupled Plasma Mass Spectrometry (LA-ICPMS)**

After identifying zoned crystals with the SEM the isotopic composition of selected crystals were examined using Laser Ablation Inductively Coupled Plasma Mass Spectrometry (LA-ICP-MS) at the University of Gothenburg department of Earth Science. The instrument consisted of an ESL 213NWR laser ablation connected to Agilent 8800 ICP-QQQ in no-gas mode. Samples were ablated using pulsed laser beam with 20 µm diameter and 5Hz repetition rate at a fluence of 4.9 J/Cm<sup>2</sup>. Reference glasses analyzed alongside the samples were NIST SRM 610, NIST SRM 612, BHVO-2G, GSD\_1G, GSE\_1G, and BCR-2G. Matrix references run alongside samples were MAD, Th\_tnt, TH\_apa, Durango\_apt, and LREE. Eudialyte fragments of LVO1 (Wu et al, 2010) and NK (Sjöqvist et al., 2020) were ablated alongside samples to provide matrix samples. Elements

reported are: Na, Cl, Ca, Mn, Fe, Zr, Be, Mg, Si (fixed internal standard), Al, K, Ti, Ga, Rb, Sr, Y, Nb, Mo, Sn, Sb, Ba, La, Ce, Pr, 2Nd, Sm, Eu, Gd, Tb, Dy, Ho, Er, Tm, Yb, Lu, Hf, Ta, W, Pb, U, Th. Corresponding to the ionic species :  $^{23}\text{Na}^+$ ,  $^{35}\text{Cl}^+$ ,  $^{44}\text{Ca}^+$ ,  $^{55}\text{Mn}^+$ ,  $^{57}\text{Fe}^+$ ,  $^{90}\text{Zr}^+$ ,  $^9\text{Be}^+$ ,  $^{24}\text{Mg}^+$ ,  $^{29}\text{Si}^+$  (fixed internal standard),  $^{27}\text{Al}^+$ ,  $^{39}\text{K}^+$ ,  $^{49}\text{Ti}^+$ ,  $^{85}\text{Rb}^+$ ,  $^{88}\text{Sr}^+$ ,  $^{89}\text{Y}^+$ ,  $^{93}\text{Nb}^+$ ,  $^{95}\text{Mo}^+$ ,  $^{118}\text{Sn}^+$ ,  $^{121}\text{Sb}^+$ ,  $^{137}\text{Ba}^+$ ,  $^{139}\text{La}^+$ ,  $^{140}\text{Ce}^+$ ,  $^{141}\text{Pr}^+$ ,  $^{146}\text{Nd}^+$ ,  $^{147}\text{Sm}^+$ ,  $^{153}\text{Eu}^+$ ,  $^{157}\text{Gd}^+$ ,  $^{159}\text{Tb}^+$ ,  $^{163}\text{Dy}^+$ ,  $^{165}\text{Ho}^+$ ,  $^{166}\text{Er}^+$ ,  $^{169}\text{Tm}^+$ ,  $^{172}\text{Yb}^+$ ,  $^{175}\text{Lu}^+$ ,  $^{178}\text{Hf}^+$ ,  $^{181}\text{Ta}^+$ ,  $^{182}\text{W}^+$ ,  $^{208}\text{Pb}^+$ ,  $^{232}\text{U}^+$ ,  $^{238}\text{Th}^+$ . Ti was quantified from  $^{49}\text{Ti}^+$ , since  $^{47}\text{Ti}^+$  was subjected to isobaric overlap by abundant  $^{94}\text{Zr}^{++}$  during eudialyte analyses. Gallium was not reported due to  $^{71}\text{Ga}^+$  overlap with  $^{142}\text{Ce}^{++}$ , which is abundant in EGM, and  $^{69}\text{Ga}^+$  is overlapped by  $^{138}\text{Ba}^{++}$ .

Sm and Nd were estimated from measured concentrations, corrected for natural isotopic abundances of 14.99%  $^{147}\text{Sm}$  and 23.8%  $^{144}\text{Nd}$  (Rosman and Taylor, 1998). Measurements of Sm/Nd ratio of NIST SRM 610 glass during the two analytical sessions averaged  $1.034 \pm 0.52\%$  (1RSD, n=21) and  $1.034 \pm 0.60\%$  (1 RSD, n=25), respectively.

Elemental concentrations were plotted against  $^{147}\text{Sm}/^{144}\text{Nd}$  ratios for each sample in an effort to find strong correlations between elemental abundance and Sm/Nd ratio. An element with apparent zonation and a strong link to  $^{147}\text{Sm}/^{144}\text{Nd}$  could be a useful and more easily acquired proxy for mapping Sm/Nd ratio.

### 2.5.3 Electron Microprobe Mapping (EMP)

Full thick section compositional maps were made using Cameca SX-50 electron microprobe at the University of Massachusetts, Amherst, MA, USA. Scans were conducted with 15.0 KeV accelerating voltage and five spectrometers set to Mg, Mn, Nb, Ta, and Ti. These elements were chosen as they displayed the strongest correlations with Sm/Nd

according to LA-ICPMS analysis (see results below). Beam size was 30  $\mu\text{m}$  at 300 nA. Using a 25 ms dwell time the entire thin section was mapped.

High resolution grain maps were conducted on a Cameca SXFive-TACTIS electron microprobe at the University of Massachusetts, Amherst, MA, USA. Again, five spectrometers were set to Mg, Mn, Ti, Ta, and Nb, and background measurements were conducted at the first spot.

#### 2.5.4 Micromill Sampling

Based on LA-ICP-MS isotopic data coupled with EMP and SEM imagery eudialyte crystals from samples KP2 and KP9 were selectively drilled using the method developed by Charlier et al. (2006) and Sjöqvist et al. (2020). Using an ESL MicroMill computer controlled micro drill and a Brasseler 2500-0033 carbide bit a series of 150  $\mu\text{m}$  deep pits were drilled to yield spatially controlled samples. Drilling for each pit took place within a single drop of MQ H<sub>2</sub>O held in place by a parafilm with a single 4 mm hole. The MQ H<sub>2</sub>O serves to cool the drill bit as well as to capture the sample dust derived from the pit. After drilling the slurry was collected by pipette. Three more droplets of MQ H<sub>2</sub>O were placed over the pit, and again collected by pipette to collect any residual sample dust. The eudialyte samples would occasionally chip next to the drilled pits due to lateral pressure applied by the pipette tip while retrieving sample slurry.

Between drilling each pit, the parafilm dam was removed and the sample was rinsed thoroughly with MQ H<sub>2</sub>O and isopropanol. The drill bit was rinsed and ultrasonicated in MQ H<sub>2</sub>O, and rinsed with isopropanol between each sample pit.

Several samples (KP1, KP2, and EUD122804) were also sampled by dissolving small chips rather than by drill. These larger samples were used in preliminary analysis before drilling, and to provide accurate concentrations to guide subsequent analysis, as very small drilled samples proved difficult to weigh.

### **2.5.5 Isotope Dilution Thermal Ionization Mass Spectrometry (ID-TIMS)**

The dissolution procedure detailed below is adapted from procedures developed for garnet (Harvey and Baxter, 2009; Pollington and Baxter, 2010). While eudialyte can be dissolved in concentrated HNO<sub>3</sub> alone (Chakraborty et al., 2011), HCl and HF were used to eliminate potential residues, namely potentially problematic silica gels that may not have been visible in very small samples.

Sample dissolution began in 100 µL HF and 1000 µL 16N HNO<sub>3</sub> fluxed overnight followed by 1000 µL 16N HNO<sub>3</sub> and 1000 µL 6N HCl. Samples were then dried down and brought up in 1000 µl 16N HNO<sub>3</sub> and fluxed overnight to prevent the formation of secondary fluorides (Makishima, 2016). Finally, the sample was brought up in 4 mL 1.5N HCl and 0.5 mL 16N HNO<sub>3</sub> for spiking. Based on estimated Sm/Nd ratios samples were spiked with a well-calibrated <sup>147</sup>Sm-<sup>150</sup>Nd spike.

For TIMS analysis all other REE's must be removed to avoid deleterious isobaric interferences that would obscure measured ratios (Schoene and Baxter, 2017). Samples were refined through three stages of column chemistry following the procedure of Harvey and Baxter (2009). This procedure uses a short cation exchange column to remove Fe and most major elements, a Transuranic Specific (Tru-spec) column to isolate the REE, and a 2-methyllactic acid (MLA) column to separate cuts of Sm and Nd for analysis.

Isotope characterization was conducted using an Isotopx Phoenix Thermal Ionization Mass Spectrometer at the Boston College Center for Isotope Geochemistry. Nd was analyzed as an oxide ( $\text{NdO}^+$ ) on a Re filament. The samples were loaded in 2N  $\text{HNO}_3$  along with  $\text{Ta}_2\text{O}_5$  activator slurry (Harvey and Baxter, 2009). Sm was analyzed as a metal using Ta filaments prepared with HCL. Samples were loaded in 2N  $\text{HNO}_3$  and  $\text{H}_3\text{PO}_4$  was added after to aid ionization.

## 2.6 RESULTS

### 2.6.1 SEM

The examination of eudialyte samples (KP1, KP9) by BSE revealed little apparent zonation or textural zones even when brightness and contrast were optimized to focus on small changes within single crystals. Sample KP9 showed clear growth zones (Figure 10) under cross polarized light. Even so, no zonation was observed using BSE. Close inspection of the large crystal in this sample did reveal small lines of galena inclusions, which may define optical zonations. When brightness and contrast are adjusted to examine REE rich eudialyte other minerals are easily distinguished. Amphiboles, nepheline, and other non-REE phases are dark and unremarkable in contrast to eudialyte. Other REE phases like mosandrite, and britholite contrast well with eudialyte and are commonly observed as inclusions in eudialyte or as fill along cross cutting fractures (Figure 10). While not revealing vivid zonation, BSE images make it easy to distinguish clean, inclusion free eudialyte. Accidentally drilling and incorporating a small amount of galena in later stages would not

be problematic for eudialyte Sm/Nd analysis (whereas it could be quite detrimental to U-Pb efforts, i.e., Wu et al. 2010); however, even a small amount of britholite or mosandrite have the potential to significantly contaminate a drilled eudialyte sample due to its relatively high REE content.

### 2.6.2 LA-ICP-MS

Eudialyte from the KSC is known to have unusually high concentrations of HREE and constitutes a unique deposit in this sense (Wu et al., 2010). LA-ICP-MS analyses from three samples shows high concentrations of REE. Absent visible zonations, transects across crystals were analyzed in an effort to gain information across the crystal. Total rare earth elements (REE+Y) range from 3.42 to 5.16 wt.% along with 8.5 to 10.5 wt.% Zr, an essential component of eudialyte.

REE spider diagrams (Figure 12) highlight the high concentrations of REE in KSC eudialyte and particularly the enrichment of HREE relative to chondrite. Kipawa samples display a clear Eu anomaly consistent with other Grenvillian eudialyte samples.

<b>Element</b>	<b>Avg. R<sup>2</sup></b>
<b>Ta</b>	<b>0.668</b>
<b>La</b>	<b>0.631</b>
<b>Nb</b>	<b>0.603</b>
<b>Ti</b>	<b>0.496</b>
<b>Mn</b>	<b>0.480</b>
<b>Mg</b>	<b>0.331</b>
<b>Cl</b>	<b>0.294</b>
<b>Y</b>	<b>0.268</b>
<b>Zr</b>	<b>0.239</b>

Table 2. Summary selected elements showing a relationship with  $^{147}\text{Sm}/^{144}\text{Nd}$  ratio as measured by LA-ICP-MS, and the average  $R^2$  value for each element vs. the  $^{147}\text{Sm}/^{144}\text{Nd}$  ratio.

Several elements show variation in concentrations across transects corresponding to Sm/Nd ratio. These elements are Ta, La, Nb, Ti, Mn, Mg, Cl, Y, Zr listed in order of

average  $R^2$  value (Table 2). Ta shows strong negative relationship with  $^{147}\text{Sm}/^{144}\text{Nd}$  (Figure 13). Variation within single crystal is usually  $\sim 500$  ppm. Ti shows some relationship with Sm/Nd, this relationship is inconsistent across crystals and variation in crystal can vary from 250 ppm to 1500 ppm (Figure 13). Both Nb and Mn show a negative relationship with  $^{147}\text{Sm}/^{144}\text{Nd}$ , variation in concentration is generally large (Figure 13). La shows strong negative relationship with  $^{147}\text{Sm}/^{144}\text{Nd}$ . Large variation in concentration within single crystals,  $\sim 1500$  ppm variation (Figure 13). The other elements (Mg, Cl, Y, and Zr) are less consistent and effective proxies for  $^{147}\text{Sm}/^{144}\text{Nd}$  ratio and are not considered further.

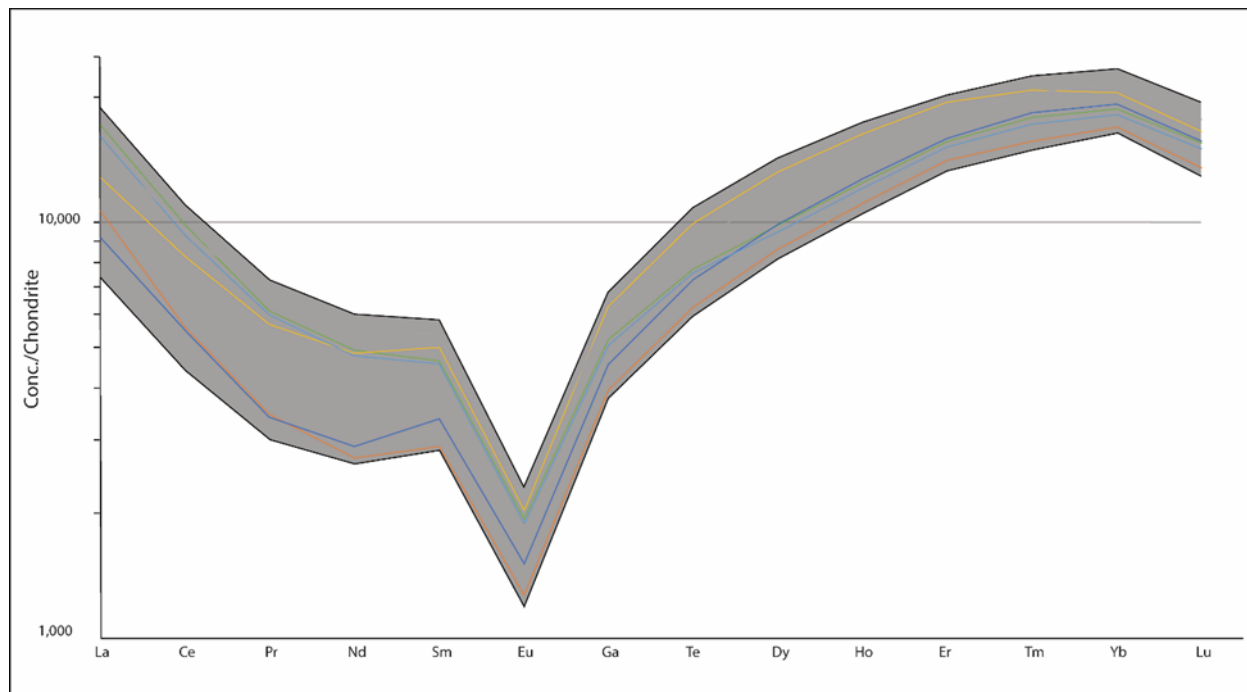


Figure 12. Chondrite normalized rare earth element (REE) spider diagram from the Kipawa Syenite Complex (KSC). The grey field indicates the range of measured values. Colored lines are average values for individual eudialyte crystals measured in this study. Chondrite values from (Sun and McDonough (1989)).

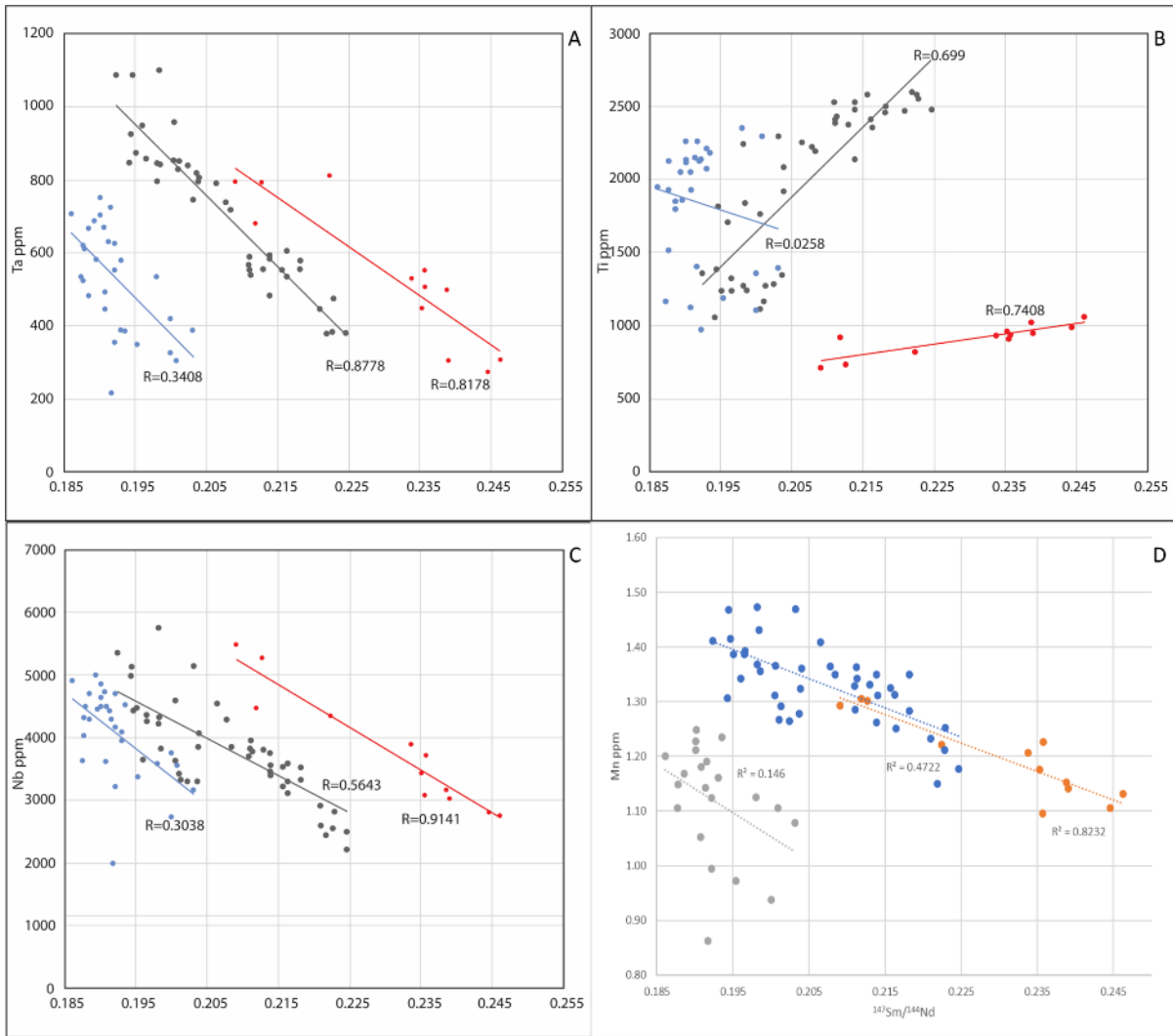


Figure 13. LA-ICP-MS elemental concentrations (ppm) plotted against  $^{147}\text{Sm}/^{144}\text{Nd}$  from three KSC eudialyte samples. A) All samples show a negative relationship between Sm/Nd ratio and Ta concentration. B) Two of three measured samples show a positive relationship between Sm/Nd ratio and Ti concentration. C) All samples show a negative relationship between Sm/Nd ratio and Nb concentration. D) All samples show a negative relationship between Sm/Nd ratio and Mn concentration.

### 2.6.3 Electron Microprobe

Two samples (KP1, KP9) were analyzed via EMP. Mapping reveals zonation in the distribution of certain elements mentioned above. Nb and Mn maps proved most useful for examining eudialyte due their relatively high concentrations and resulting easily distinguishable zoning contrast. Nb mapping of a single large eudialyte crystal from sample KP9 shows a complex pattern of zonation (Figure 14). This consists of clear growth zonations within a euhedral-subhedral crystal which is then surrounded by texturally overgrown eudialyte rim with a patchy and irregular Nb distribution. Mn mapping of the same crystal shows a similar pattern (Figure 14). Although growth zonation is more muted,

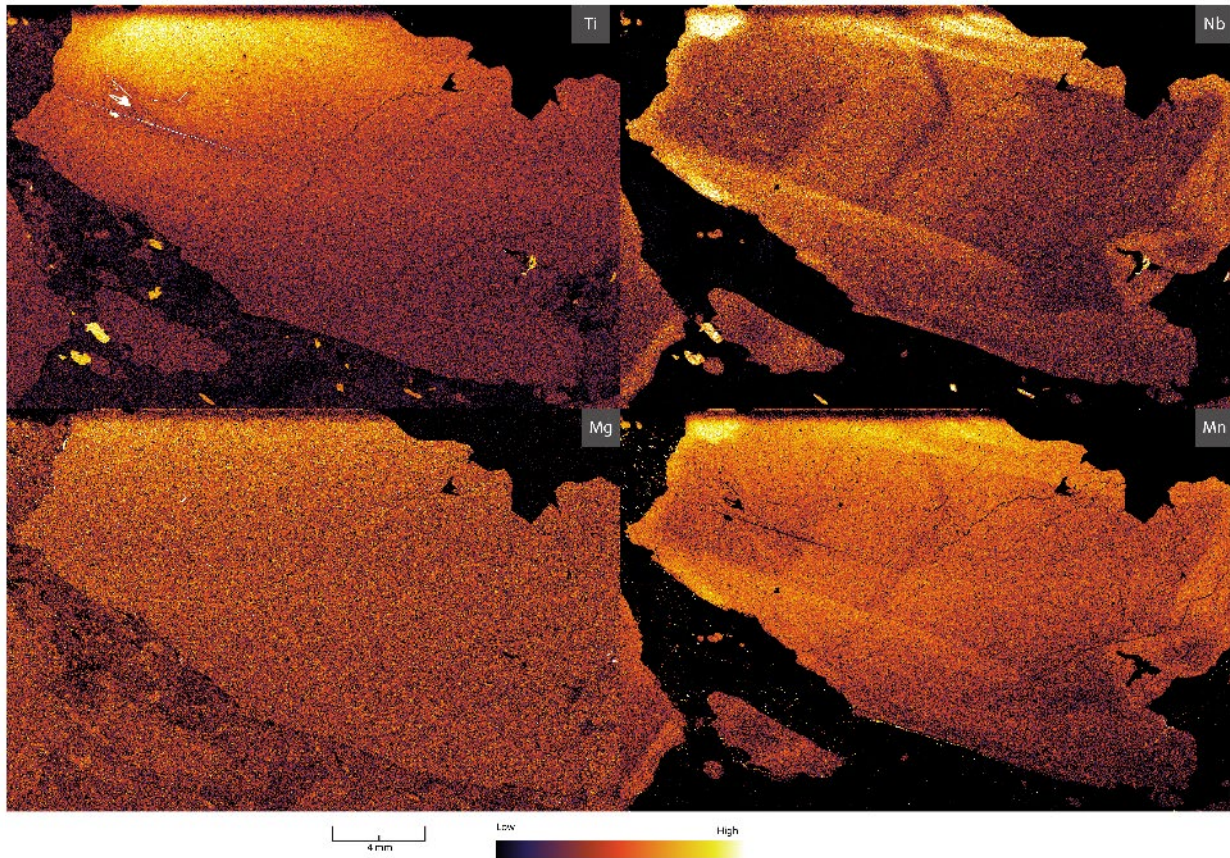


Figure 14. Electron Microprobe (EMP) maps of selected elements in the large eudialyte crystal from sample KP9. Mn and Nb mapping reveals two distinct crystal domains, a central core and a peripheral rim. The core displays faint oscillatory zoning. Bright orange to white indicates high concentrations.

the core and rim can be distinguished. Ta and Ti maps reveal little other than bright spots corresponding to small britholite inclusions.

#### 2.6.4 ID-TIMS

Two samples (KP1, KP9) were microdrilled for TIMS analysis, both samples yielded 8 drill pits. Full results of ID-TIMS isotopic analyses are presented in Table 3. The spread in  $^{147}\text{Sm}/^{144}\text{Nd}$  is relatively small, from 0.1752 to 0.2236 across all samples,  $^{143}\text{Nd}/^{144}\text{Nd}$  values ranged from 0.511955 to 0.512376 from 0.512074 to 0.512248. This range of  $^{147}\text{Sm}/^{144}\text{Nd}$  data are roughly consistent with the solution-ICP data of Wu et al.

Sample ID	$^{147}\text{Sm}/^{144}\text{Nd}$	$\pm 2 \text{ S.E.}$	$^{143}\text{Nd}/^{144}\text{Nd}$	$\pm 2 \text{ S.E.}$	$\epsilon\text{Nd}$	$^{150}\text{Nd}/^{144}\text{Nd}$	Notes
<b>eud12280</b>	0.223621	0.00007	0.512376	0.000014	-5.12	0.8861	bulk chip
<b>4</b>							
<b>KP1-2.1-1</b>	0.207030	0.00020	0.512248	0.000009	-7.60	1.9201	drilled
<b>KP1-2.1-2</b>	0.198791	0.00002	0.512203	0.000006	-8.48	3.3025	drilled
<b>KP1-2.1-3</b>	0.198987	0.00001	0.512191	0.000007	-8.72	3.6233	drilled
<b>KP1-2.1-4</b>	0.202541	0.00004	0.512230	0.000011	-7.96	3.3200	drilled
<b>KP1-2.1-6</b>	0.181609	0.00001	0.512074	0.000009	-11.00	3.1678	drilled
<b>KP1-2.1-7</b>	0.181656	0.00002	0.512084	0.000016	-10.80	6.9439	drilled
<b>KP1-2.1-8</b>	0.184082	0.00003	0.512086	0.000010	-10.76	2.3260	drilled
<b>KP1-2.1-9</b>	0.183603	0.00001	0.512093	0.000004	-10.63	2.5420	drilled
<b>KP1-2.1-10</b>	0.198806	0.00002	0.512198	0.000005	-8.59	1.2808	bulk chip
<b>KP2-1-2</b>	0.196243	0.00003	0.512169	0.000004	-9.14	1.1349	bulk chip
<b>KP2-1-3</b>	0.177599	0.00002	0.512045	0.000005	-11.56	1.0989	bulk chip
<b>KP9_1</b>	0.175205	0.00006	0.512020	0.000029	-12.06	15.6410	drilled
<b>KP9_2</b>	0.214392	0.00004	0.512309	0.000017	-6.43	8.3174	drilled
<b>KP9_3</b>	0.206532	0.00004	0.512270	0.000012	-7.18	12.3564	drilled
<b>KP9_4</b>	0.207536	0.00002	0.512281	0.000015	-6.97	8.8572	drilled
<b>KP9_5</b>	0.212032	0.00002	0.512301	0.000013	-6.58	4.1855	drilled
<b>KP9_6</b>	0.182213	0.00003	0.512086	0.000005	-10.76	1.1084	drilled
<b>KP9_7</b>	0.194570	0.00003	0.512170	0.000014	-9.13	2.9247	drilled
<b>KP9_8</b>	0.184699	0.00002	0.512107	0.000004	-10.36	1.0811	drilled

Table 3. Kipawa Syenite Complex ID-TIMS data.

(2010) ( $^{147}\text{Sm}/^{144}\text{Nd}=0.2079$ ), but much lower than their LA-ICP data ( $^{147}\text{Sm}/^{144}\text{Nd}=0.2438$ ).

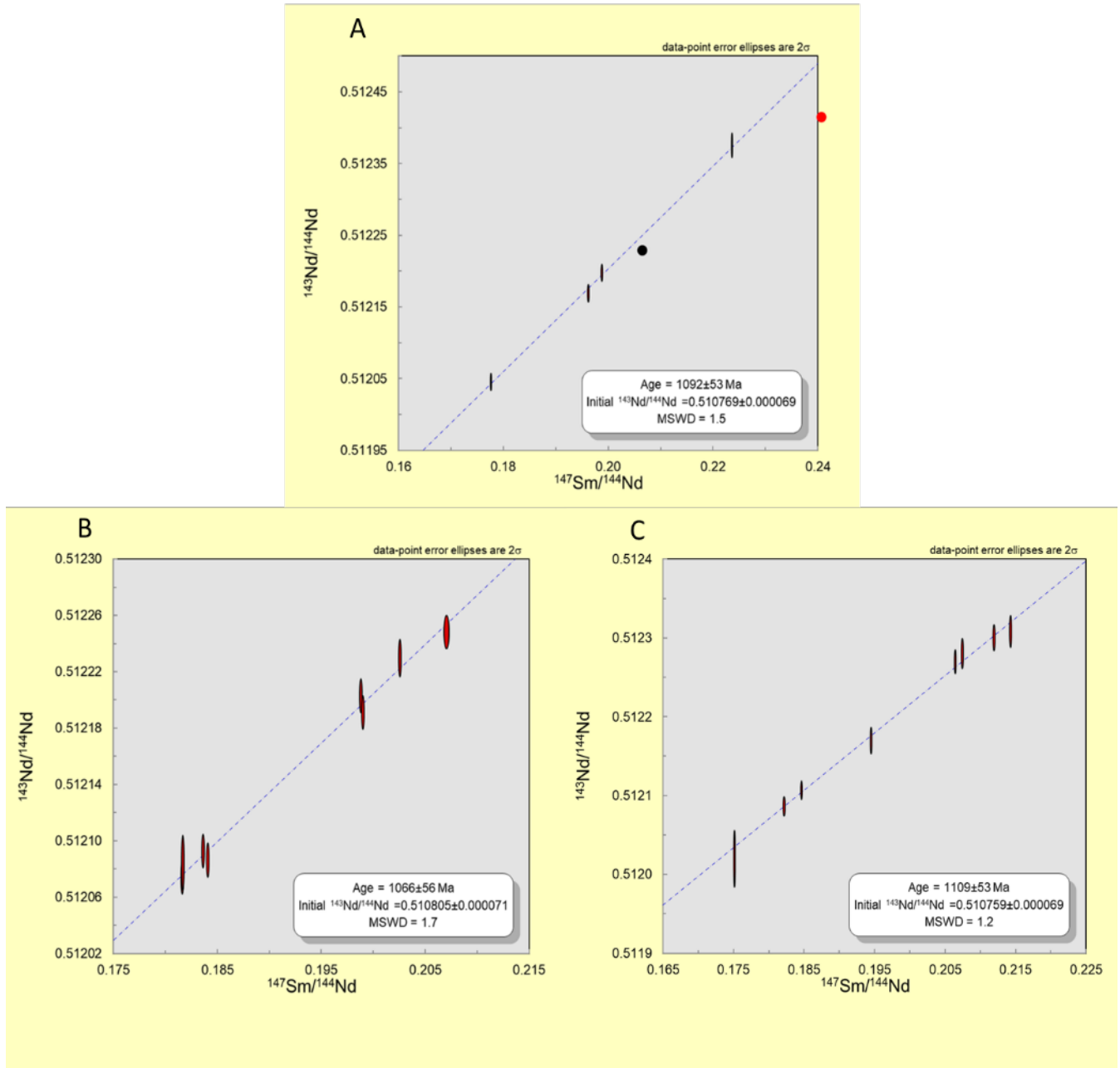


Figure 15. Isochrons plotted in the course of this study. A) Bulk isochron based on 4 ID-TIMS analyses of eudialyte ‘bulk chips’ from samples KP1, KP2, and EUD122804. Black dot shows Wu et al. (2010) solution-ICP results, red dot shows Wu et al. (2010) LA-ICP-MS results. B) Internal mineral isochron from sample KP1. C) Internal mineral isochron from sample KP9. All eight analyses were sampled using the micromill sampling procedure. All isochrons created using Isoplot.

Repeated analyses of 4ng AMES Nd standard solution run over the course of the study yield a  $^{143}\text{Nd}/^{144}\text{Nd}$  value of  $0.512152 \pm 0.000010$  (18.75 ppm,  $2\sigma$ ;  $n=36$ ). Analyses of 20 ppm Ames Sm standard solution yield a  $^{147}\text{Sm}/^{144}\text{Nd}$  reproducibility of 0.054%. External reproducibility was used for all age calculations except in instances where the internal reproducibility was worse. A procedural blank run alongside samples yielded a measured Nd value of 6.4 pg. Analyses of bulk chip samples where sample weights were accurately measured yield Sm and Nd concentrations consistent with LA-ICP-MS results.

Four isotope analyses by ID-TIMS of bulk chip aliquots from three KSC hand samples all plot on a line (MWSD= 1.5) corresponding to an age of  $1092 \pm 53$  Ma with an initial  $^{143}\text{Nd}/^{144}\text{Nd}$  of  $0.510769 \pm 0.000069$  for a ‘bulk isochron’ (Figure 15). Within a single crystal from sample KP1 an isochron based on 8 drilled aliquots yields an age of  $1066 \pm 56$  Ma (MSWD=1.7) and an initial  $^{143}\text{Nd}/^{144}\text{Nd}$  of  $0.510805 \pm 0.000071$  (Figure 15). Analysis of 8 drilled samples from sample KP 9 yield an age of  $1109 \pm 53$  Ma with an initial  $^{143}\text{Nd}/^{144}\text{Nd}$  of  $0.510759 \pm 0.000069$  (MSWD= 1.2) (Figure 15). The weighted average of these three isochron-based eudialyte ages is  $1090 \pm 31$  Ma.

## 2.7 DISCUSSION

Direct eudialyte geochronology has been attempted previously by Wu et al. (2010; Kipawa Syenite Complex and others), Crocker (2014; Red Wine Intrusive Suite), and Sjöqvist et al. (2020; Norra Kärr). Both Wu et al. (2010) and Crocker (2014) utilized the U-Pb system; the identification of galena (Figure 10) inclusions in eudialyte from the KSC

should raise concerns regarding common Pb here and elsewhere for those attempting to date eudialyte by U-Pb. Indeed Wu et al. (2010) conclude common Pb is problematic for eudialyte U-Pb without measuring other common accessory minerals like apatite and titanite to assess common Pb. The Wu et al. (2010) U-Pb age of  $1012 \pm 16$  Ma is cast in doubt given the identification of galena in Kipawa samples in this study. The Sm-Nd age of Wu et al. (2010) is essentially a three point isochron based largely on laser ablation data that does not correspond well to solution data from the same sample. In addition, the isotope data from Wu et al (2010) do not align with the data collected in our study (Figure 15). We conclude that analytical issues likely impacted the accuracy of the Wu et al. (2010) data, and without raw data or  $^{147}\text{Sm}/^{144}\text{Nd}$  uncertainties reported in their paper, it is difficult to assess their results.

Eudialyte samples from the KSC are enriched in all the REE relative to chondrite (Sun and McDonough, 1989 C1 chondrite) by a factor of ~1200 (Eu) to ~11,500 (Yb).

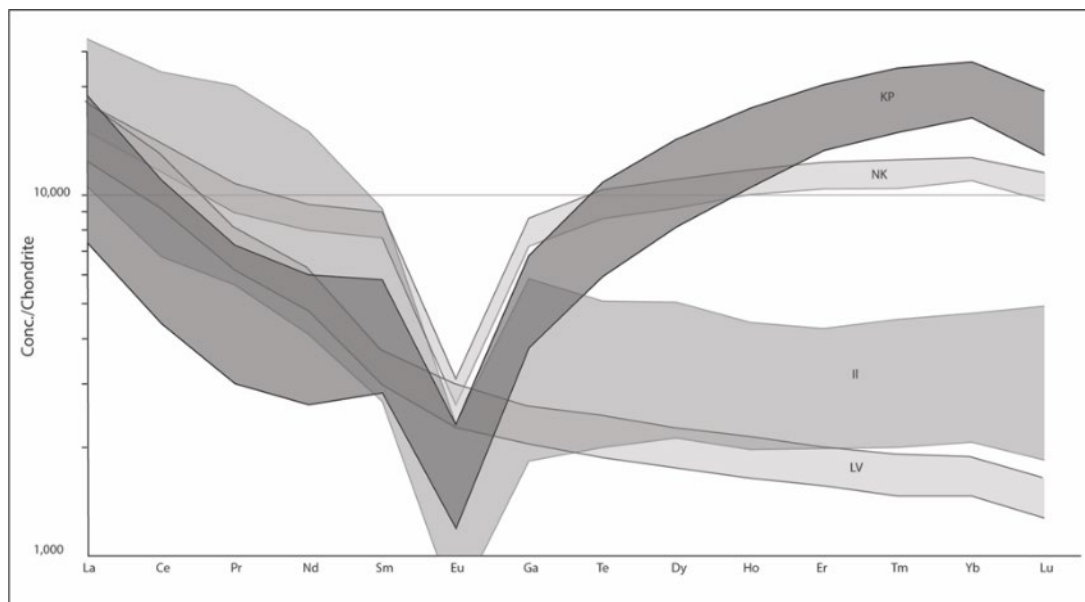


Figure 16. Chondrite normalized rare earth element (REE) spider diagram for all complexes measured in the course of this study and one additional (Ilímaussaq) for comparison. Abbreviations: KP: Kipawa Syenite Complex, NK: Norra Kärr, LV: Lovozero, IL: Ilímaussaq complex, data from Wu et al. (2010). Chondrite values from Sun and McDonough (1989).

HREE enrichment increases consistently from Gd to Yb (Figure 16). Chondrite normalized REE spider diagrams reveal unusual enrichment in HREE in the KSC compared to other eudialyte ore bodies near the Grenville Front (Nora Kärr, Ilímaussaq, Red Wine), taken from Sjöqvist et al. (2020), Wu et al. (2010) and Chapter 3, respectively. These analyses also show a pronounced negative Eu anomaly despite high enrichment over chondrite.

Strong Eu anomalies suggest derivation from a source where plagioclase had been previously fractionated, consistent with partial melting of older continental crust with plagioclase in the restite. Compared to other analyses of eudialyte from Grenvillian peralkaline complexes the REE profile of Kipawa samples shows exceptional HREE enrichment (Figure 16). The REE profile of Nora Kärr eudialyte is the most similar to KSC samples with both a strong europium anomaly and significant HREE enrichment. Red

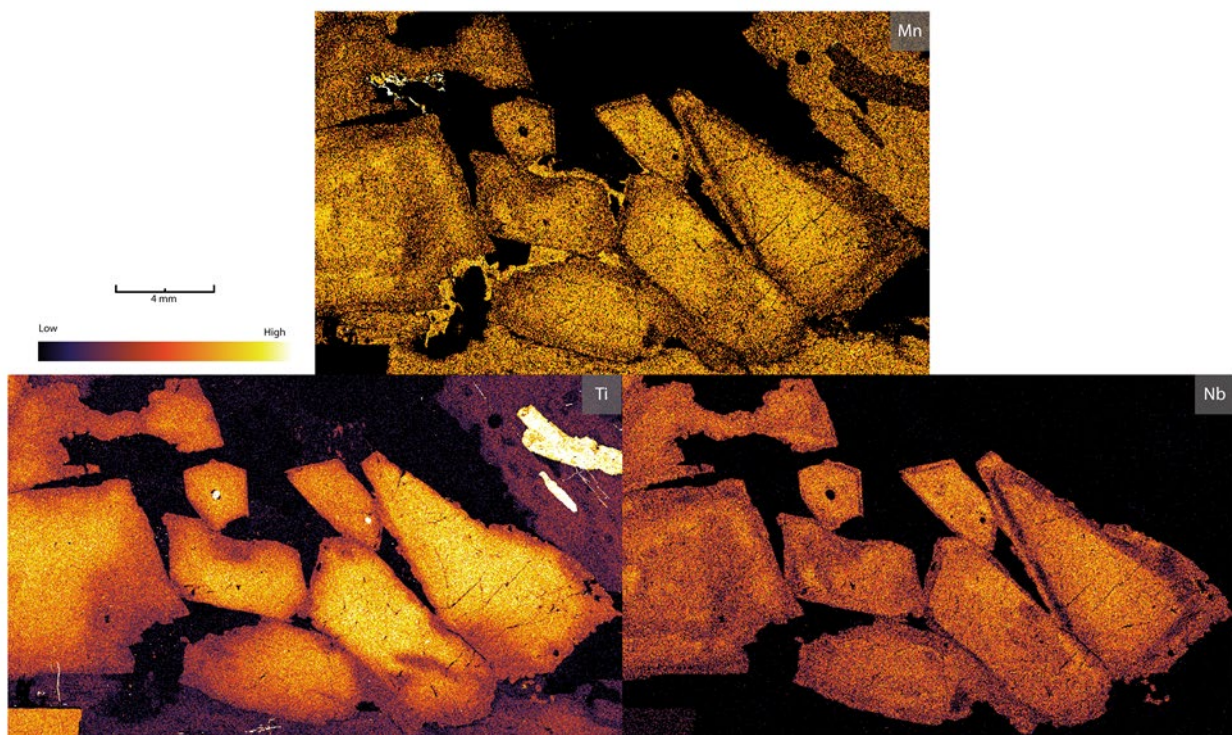


Figure 17. Electron Microprobe (EMP) map selected elements in several eudialyte crystals from sample KP1. Nb and Mn reveal faint concentric zonations similar to those revealed by Mn mapping.

Wine Intrusive Suite samples show a similar europium anomaly but less pronounced HREE enrichment, as do Ilímaussaq samples which share a geochemical affinity with Red Wine samples (Kerr, 2011). In contrast, samples from the much younger (370±7 Ma; Kramm and Kogarko, 1994) Lovozero Alkaline Massif lack both a europium anomaly and HREE enrichment. Overall the REE profile from Lovozero Massif is consistent with that of rock produced through the partial melting of a mantle source and only a short period of crustal residence. Van Breeman and Currie (2004) attributed the exceptional HREE content in the KSC to metasomatism by a Fluorine-rich fluid. However, the broad similarity of REE profiles across the samples associated in space and time suggest broader differences between Grenvillian samples and other eudialyte localities (such as Lovozero).

LA-ICP-MS data revealed correlations between some elements (Nb, Ta, Ti, Mn, Mg, and La) and Sm/Nd ratio (Figure 13). Subsequent high precision Electron Microprobe mapping of individual eudialyte crystals illuminated complex zonations for several of these elements. Based on the correlative relationships between certain elements (Nb, Ta, Ti, Mn, Mg, and La) and Sm/Nd ratio it was hypothesized that EMP maps can be used as proxies for Sm/Nd in eudialyte. Nb and Mn mapping proved most informative for mapping eudialyte with both relatively large concentrations and large variation in concentration across crystals. Mapping of sample KP1 revealed rhythmic concentric zonations within several euhedral-subhedral eudialyte crystals (Figure 17). A map of sample KP9 revealed similar rhythmic euhedral zonation within the core of a single large eudialyte crystal (Figure 18). The margins of the crystal core are regular and surrounded by a less clearly zoned rim. This mapping clearly reflects a more complex growth history, with at least two texturally distinct phases of growth.

Selective drilling and ID-TIMS analysis of crystal sectors in sample KP9 support the relationship between Nb, Mn and  $^{147}\text{Sm}/^{144}\text{Nd}$  (Figure 18). This confirms that EMP mapping of Nb or Mn can be used to map  $^{147}\text{Sm}/^{144}\text{Nd}$  by proxy. This new procedure will simplify the characterization of eudialyte, providing greater speed, and a higher likelihood of maximizing  $^{147}\text{Sm}/^{144}\text{Nd}$  differences and thus analytical precision; indeed, the EMP guided microdrilling of KP9 yielded a broader spread of  $^{147}\text{Sm}/^{144}\text{Nd}$  than sample KP1 which was done ‘blind’. The textures revealed by EMP mapping can also provide important context for the ages derived from drilling and ID-TIMS, such as open system remobilization of inclusion contamination.

Maps of a separate chip from sample KP1 produced after drilling reveal simple concentric zoning within eudialyte crystals consistent with a single growth generation (Figure 17). In contrast, the large crystal from KP9 appears shows a more complex,

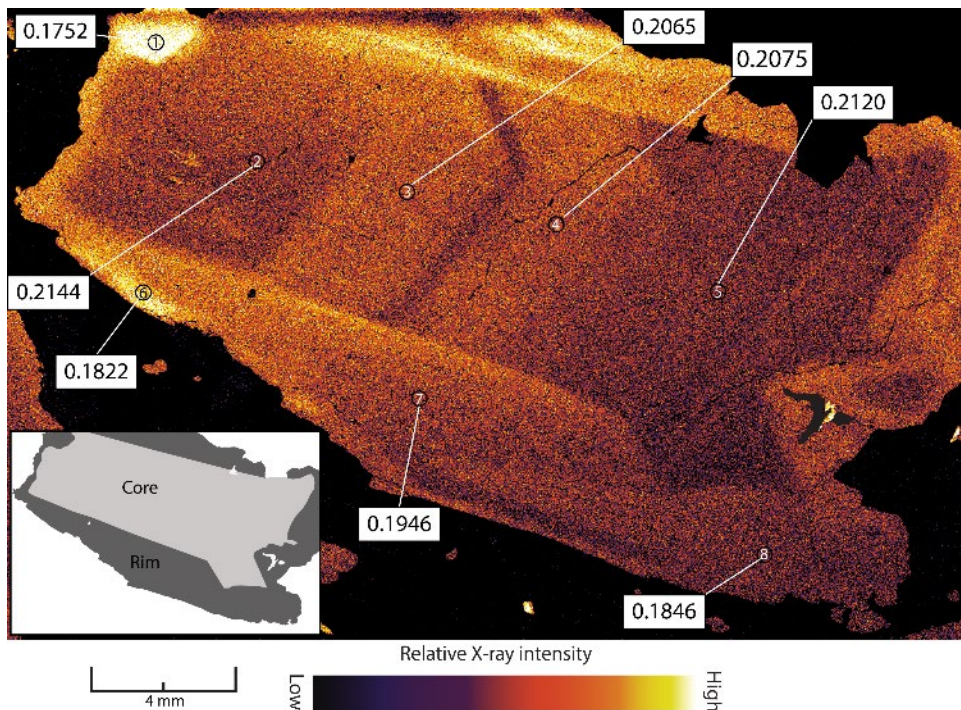


Figure 18. EMP map of Nb in a single large eudialyte crystal from sample KP9. The image is annotated with the location of drillholes and the measured  $^{147}\text{Sm}/^{144}\text{Nd}$  ratio. Results corroborate the negative relationship between Nb and  $^{147}\text{Sm}/^{144}\text{Nd}$  ratio.

multiphase history. Pit locations in KP 9 were selected in an attempt to examine the age relations between core and rim, should they be resolvably different (Figure 18). The low MSWD of all 8 points in sample KP9 (MSWD=1.2) is robust statistical confirmation of a true linear isochron relationship (i.e., Wendt & Carl 1991), thus evidence for a single age of growth, at least at the present level of precision. Furthermore, age concordance across all analyzed samples and isochrons (KP1, KP2, KP9, and EUD122804) from both bulk chip and drilled samples suggests a single uniform age across KSC eudialyte samples. The weighted average of these three robust isochron-based ages is  $1090 \pm 31$  Ma, interpreted here as the crystallization age for eudialyte throughout the Kipawa Syenite Complex.

The weighted mean of  $1090 \pm 31$  Ma is the oldest date yet determined for any portion of the KSC, predating the interpreted emplacement date of Currie and van Breeman (2004) by 58 Ma (Figure 19). Along with new constraints on eudialyte formation, we propose that the zircon U-Pb ages of  $1033 \pm 3$  Ma (van Breeman and Currie, 2004) and  $994 \pm 2$  (Currie and van Breeman, 1996) represent the range of metasomatic zircon growth as part of a late alteration assemblage (Karup-Møller et al., 2010) caused by the introduction of outside, possibly F-rich fluids during the waning stages of the Rigolet phase of the orogeny.

The  $1090 \pm 31$  Ma age of eudialyte formation falls at the onset of the Ottawan phase of the Grenville Orogeny suggesting a tectonic correlation with eudialyte ore mineralization. It is possible that this age corresponds to the initial igneous emplacement

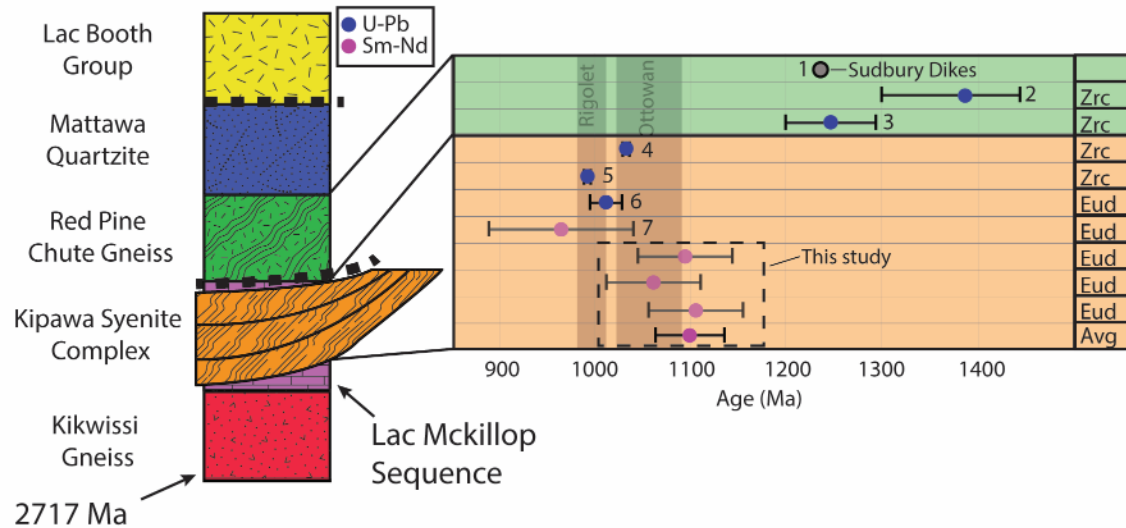


Figure 19. Generalized structural column along transect A-B (Figure 5) and summary of relevant geochronology. Abbreviations: Zrc: zircon; Eud: eudialyte; Avg: weighted average. Data from: Currie and van Breeman, 1996 (points 1,5); van Breeman and Currie, 2004 (points 2,3,4); Wu et al., 2010 (points 6,7). Age of 2717 Ma for the Kikwissi Gneiss is from van Breeman and Currie, 2004. Structural column modified from Matamec, 2011.

of the KPC within the surrounding rocks; however, there is no other igneous geochronology to support this. Perhaps a more likely scenario is that this age represents a metamorphic remobilization, enrichment, and ore mineralization event driven by Ottawan crustal heating of an older peralkaline rock. In this scenario, the age of primary igneous emplacement could be closer to the zircon ages recorded in the surrounding Red Pine Chute orthogneiss ( $1389 \pm 8$  Ma) (Figure 19). Such a genetic model would be consistent with the interpretation of Sjöqvist et al. (2020) for Nora Karr where eudialyte mineralization

corresponded to low-T metamorphic melting and re-mobilization nearly 300 Myr after primary igneous emplacement. At Kipawa, the conditions of Ottowan metamorphism were much hotter, perhaps high enough to obliterate or obscure any geochronologic record of an earlier primary igneous crystallization.

To help test this idea, the Nd-model ages were examined. Epsilon Nd ( $\epsilon_{\text{Nd}}$ ) values from these samples are strongly negative (-5.12 to -12.06) and plot well away from the modeled depleted mantle (cf. DePaolo et al. 1991) (Figure 20). Such low  $\epsilon_{\text{Nd}}$  data from these samples offer strong evidence for derivation from reworking of older preexisting continental crust. If eudialyte has been remobilized from older continental crust rather than directly from the mantle an appropriate crustal evolution trend must be used to calculate

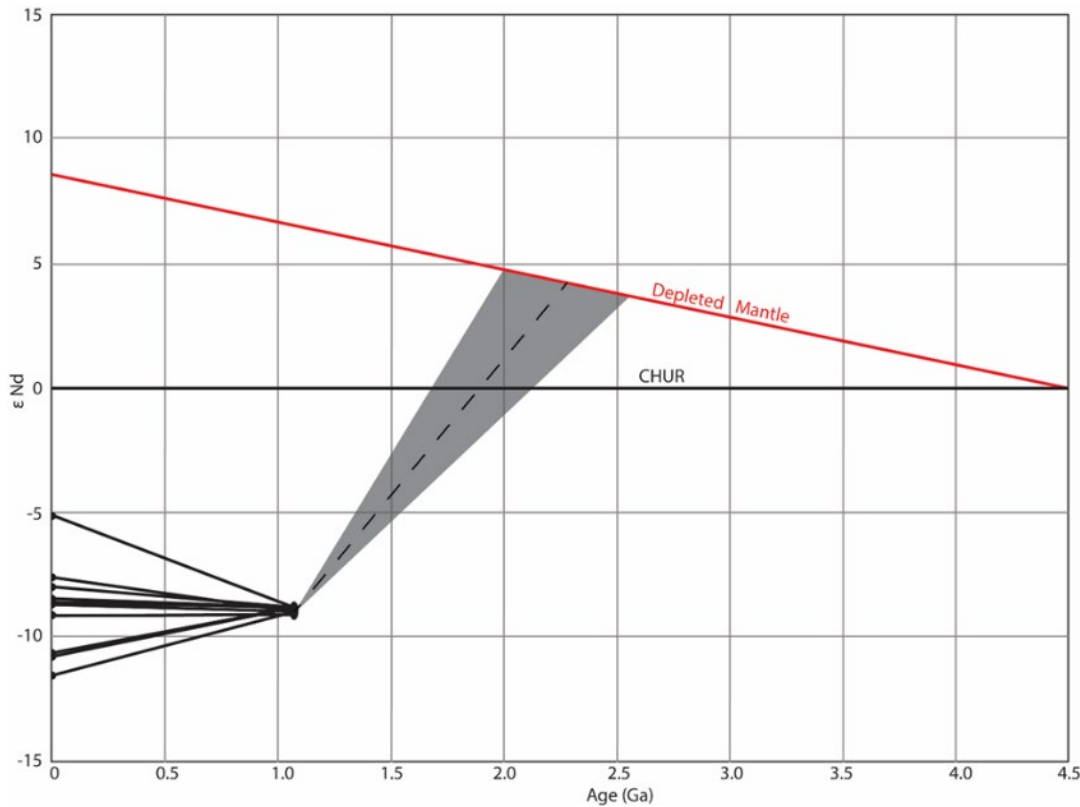


Figure 20. Model for Nd isotopic evolution of KSC eudialyte. Data points converge on an initial value of  $^{143}\text{Nd}/^{144}\text{Nd} = 0.510805$  ( $\epsilon_{\text{Nd}} = -8.9$ ). The grey field shows range of possible TDM ages based on regional whole rock  $^{147}\text{Sm}/^{144}\text{Nd}$  values (Dickin). Dotted line indicated evolution modeled using method of DePaolo et al. (1991).

an accurate model age. Using the range of  $^{147}\text{Sm}/^{144}\text{Nd}$  whole rock values (0.08-0.13) reported in this region from Nd model age mapping (Dickin and Guo, 2001) yields TDM ages ranging from 2.0 to 2.4 Ga (Figure 20). These represent the range of possible ages depending on whole rock composition. Based on the method of DePaolo et al. (1991) we calculate a model age for eudialyte samples of 2.28 Ga, which falls in the middle of the aforementioned range. Considering the agreement of the two methods, we consider the model age from the DePaolo et al. (1991) method of 2.28 Ga to be representative of the likely crustal evolution. Use of this method also provides consistency with other works (Kay et al., 2017; Borg and DePaolo, 1994). In this region of the Grenville Province Dickin and Guo (2001) interpret similar model ages (1.9-2.6 Ga) as characteristic of remelted Archean crust. This result suggests that eudialyte (and rare elements) were sourced from the reworking of Archean crust of the Canadian Shield onto which the Grenville Province was thrust. Clearly, the eudialytes of Kipawa are not primary mantle derivatives.

The Nd isotopic evolution of the KSC is distinctly different from that of the Lovozero Alkaline Massif. Isotopic data from Sjöqvist et al. (2020) and a crystallization age of  $370 \pm 7$  Ma (Kramm and Kogarko, 1994) indicate direct derivation from the mantle with a  $\epsilon\text{Nd}$  value of 4.7 (Figure 21). Taken together isotopic and geochemical illustrate two distinct deposit types (Figure 21). The KSC is derived from the reworking of older continental crust and shows unusual enrichment in HREE. The Lovozero Alkaline Massif, is mantle derived and lacks HREE enrichment or any trace of a europium anomaly (Figure 16).

It is also instructive to compare the Kipawa eudialytes to other Proterozoic eudialyte deposits at Ilímaussaq, and Nora Kärr which share a roughly similar geochemical pattern, age, and tectonic history. It is reasonable to infer that characteristic HREE enrichment noted at these sites is related to unique conditions or processes present at this time of orogenesis, likely the repeated cycles of compression and extension along the

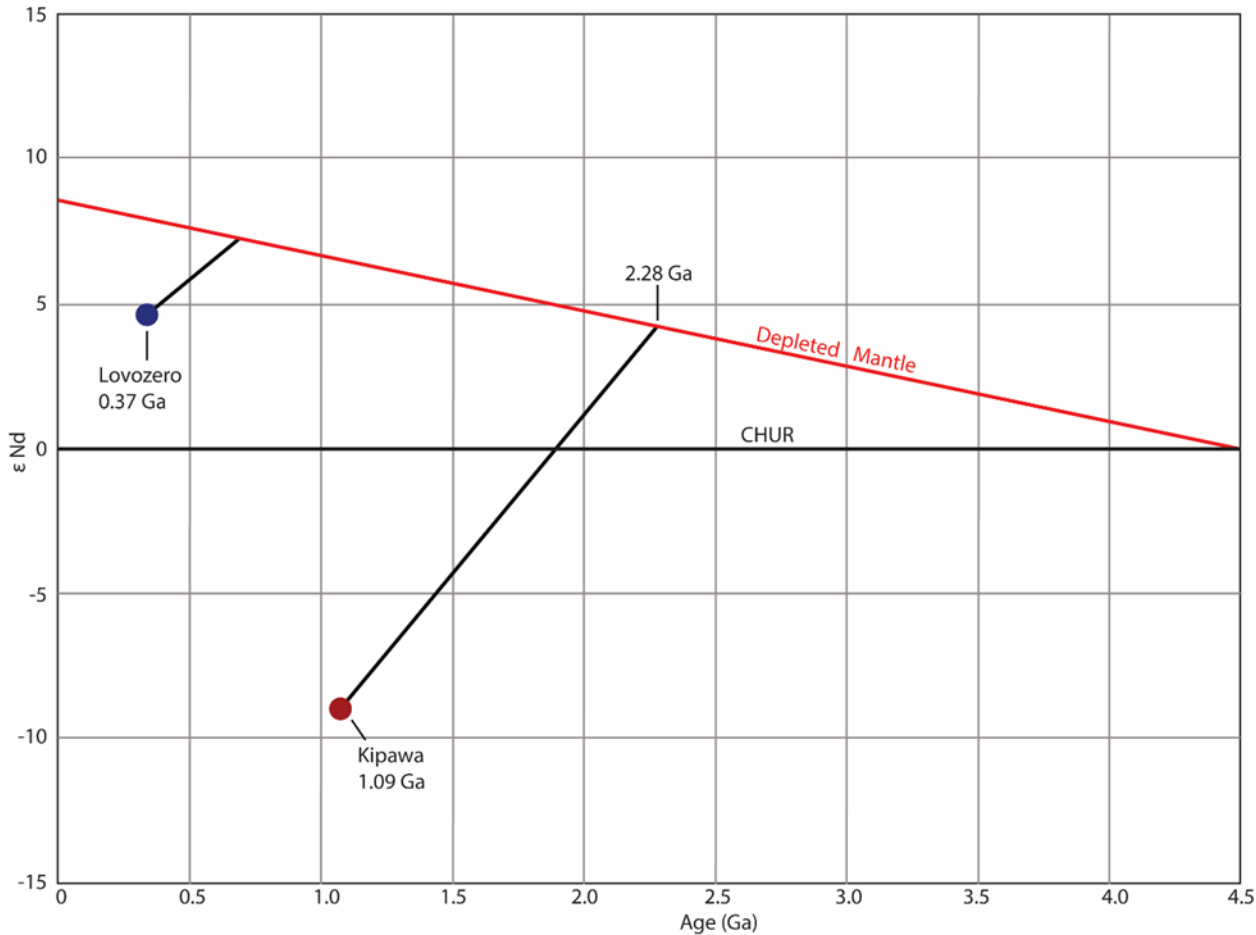


Figure 21. Model for Nd isotopic evolution of KSC and LV eudialyte. LV evolution is based on a crystallization age of 370 Ma. and isotopic ratios measured by Sjöqvist et al. (2020):  $^{143}\text{Nd}/^{144}\text{Nd}=0.512693$ ,  $^{147}\text{Sm}/^{144}\text{Nd}=0.119804$ .

Grenville Front resulting in the large-scale reworking of older continental crust. Furthermore, the magnitude of HREE enrichment seems be higher at Kipawa and Nora Karr (which experienced metamorphic reworking) as opposed to Ilímaussaq (which is a primary igneous body that escaped Grenville metamorphism). This would support the idea

that both Nora Karr and Kipawa acquired their higher HREE enrichment because of metamorphic remobilization. Ottowan metamorphism was deeper and hotter than at Nora Kärr perhaps leading to the even greater HREE enrichment in eudialytes observed.

## 2.8 CONCLUSION

The examination of KSC eudialyte by ID-TIMS yields two important results. First, eudialyte mineralization at the KSC is robustly constrained by both internal mineral isochrons and a bulk isochron. The weighted mean of these ages is the oldest age yet recorded from the KSC at  $1090 \pm 31$  Ma and represents the age of eudialyte ore mineralization. The lack of firm geochronological constraints on the primary emplacement age for the Kipawa syenite complex as a whole precludes a definitive conclusion regarding eudialyte remobilization through metamorphic partial melting such as those from Nora Kärr (Sjöqvist et al., 2020), although surrounding rocks do indicate older igneous ages of 1250-1450 Ma. However, Nd isotopic data suggest derivation from the reworking of older continental crust, and the extreme HREE enrichment of Kipawa eudialytes is consistent with the idea that Kipawa did experience a metamorphic remobilization from a preexisting peralkaline igneous rock. The age and Nd isotopic signature of KSC eudialyte are consistent with an origin in Archean continental crust most recently reworked in the early stages of the Ottowan phase of the Grenville Orogeny. We propose that this genetic model of metamorphic remobilization and ore mineralization following primary igneous emplacement is unique to agpaitic rocks along the Grenville Front that acquire the highest, and most economically favorable, HREE eudialytes.

Second, we demonstrate the utility of EMP elemental mapping of eudialyte for characterization of eudialyte prior to micromill sampling for ID-TIMS internal mineral geochronology. Strong negative correlations between elements such as Nb or Mn and  $^{147}\text{Sm}/^{144}\text{Nd}$  identified by LA-ICP-MS are vividly reflected in paired EMP mapping and MicroMill drilling. Crystal domains shown to have high concentrations of Nb have the lowest  $^{147}\text{Sm}/^{144}\text{Nd}$  values, and the areas with the lowest Nb concentrations have the highest  $^{147}\text{Sm}/^{144}\text{Nd}$  values. This method provides an effective and easily mapped proxy for Sm/Nd in eudialyte. EMP maps of Nb or Mn can be used to maximize  $^{147}\text{Sm}/^{144}\text{Nd}$  spread and age precision in future studies utilizing eudialyte internal mineral geochronology.

Future study could seek to establish a more concrete constraint on the timing of igneous emplacement for the KSC in order to test our genetic model hypothesis for the high HREE eudialytes at Kipawa. Furthermore, the examination of a larger suite of eudialyte samples, especially samples from late-stage agpaitic pegmatites described by van Breeman and Currie (2004), would add to our knowledge of age relationships and test our assertion of a single generation of eudialyte growth.

## **3.0 CHAPTER 3: GEOCHRONOLOGY OF THE RED WINE INTRUSIVE SUITE**

### **3.1 ABSTRACT**

The Proterozoic Red Wine Intrusive Suite has been explored as a potential REE ore body and is a heretofore unexploited REE resource. The petrogenesis of this and similar eudialyte ore bodies (i.e., Norra Kärr, Sweden) remains uncertain, including the role of metamorphic remobilization in ore formation. Accurate geochronology of eudialyte can help resolve whether the ore formed during Grenvillian metamorphism or earlier igneous emplacement. This study improves upon the internal-isochron eudialyte geochronology method developed by Sjöqvist et al. (2020) through the addition of Electron Microprobe mapping prior to precise MicroMill sampling to build Sm/Nd internal mineral isochrons to directly date this potential rare earth element ore mineral. We show that Nb and Mn concentrations correlate with Sm/Nd ratios in zoned eudialyte crystals, providing a qualitative map to guide microsampling. A single internal eudialyte isochron yields an ages of  $765 \pm 240$  Ma (MSWD=3.7) while the high-Nb sector of this crystal yields and age of  $704 \pm 120$  Ma (MSWD=1.6). A multi-sample eudialyte and mosandrite bulk isochron produces an age of  $989 \pm 150$  Ma (MSWD=15). The latter age reflects Grenvillian crystallization, while the age of the high-Nb zone reflects a younger recrystallization event. This young age emphasizes the sensitivity of eudialyte considering the relative quiescence of the region since the Grenville orogeny. Nd model ages suggest derivation from the mantle  $T_{DM}=1.80$ . Based on this model age and additional data three distinct deposit types are identified.

## 3.2 REGIONAL GEOLOGY

### 3.2.1 Red Wine Intrusive Suite

The Red Wine Intrusive Suite (RWIS) is located in Central Labrador ~100 km east of the three-way junction between the Grenville, Nain, and Southeastern Churchill provinces (Figure 22). In This portion of the Grenville Province most basement rocks are of Paleoproterozoic age and experienced extensive intrusion and deformation during the Mesoproterozoic (Gower and Krogh, 2002) (Figure 1). Located in close proximity to the GFTZ, many units in this area can be traced into adjacent provinces (Wardle et al., 1986).

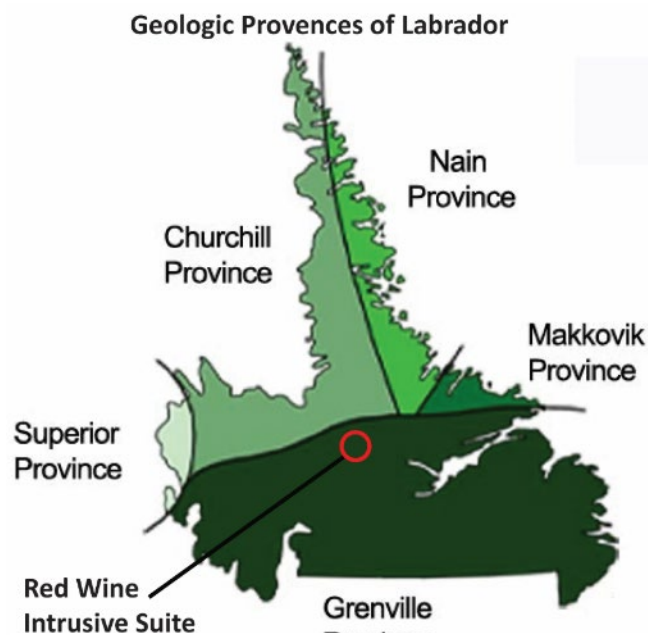


Figure 22. Geologic provinces of Labrador. Red Wine Intrusive Suite (RWIS) indicated by red circle, note proximity to province boundary. Illustration by Duleepa Wijayawardhana.

Several authors (Thomas, 1981; Miller, 1988; Kerr, 2011) have reported on the Letitia Lake Area (Figure 23) which hosts several zones of REE mineralization including the Red Wine Intrusive Suite all within the Parautochthonous Belt (Figure 4). Early mineral exploration in this area focused on radiometric anomalies to the north. Recent investigations have emphasized the intense nature of deformation in the area around Letitia

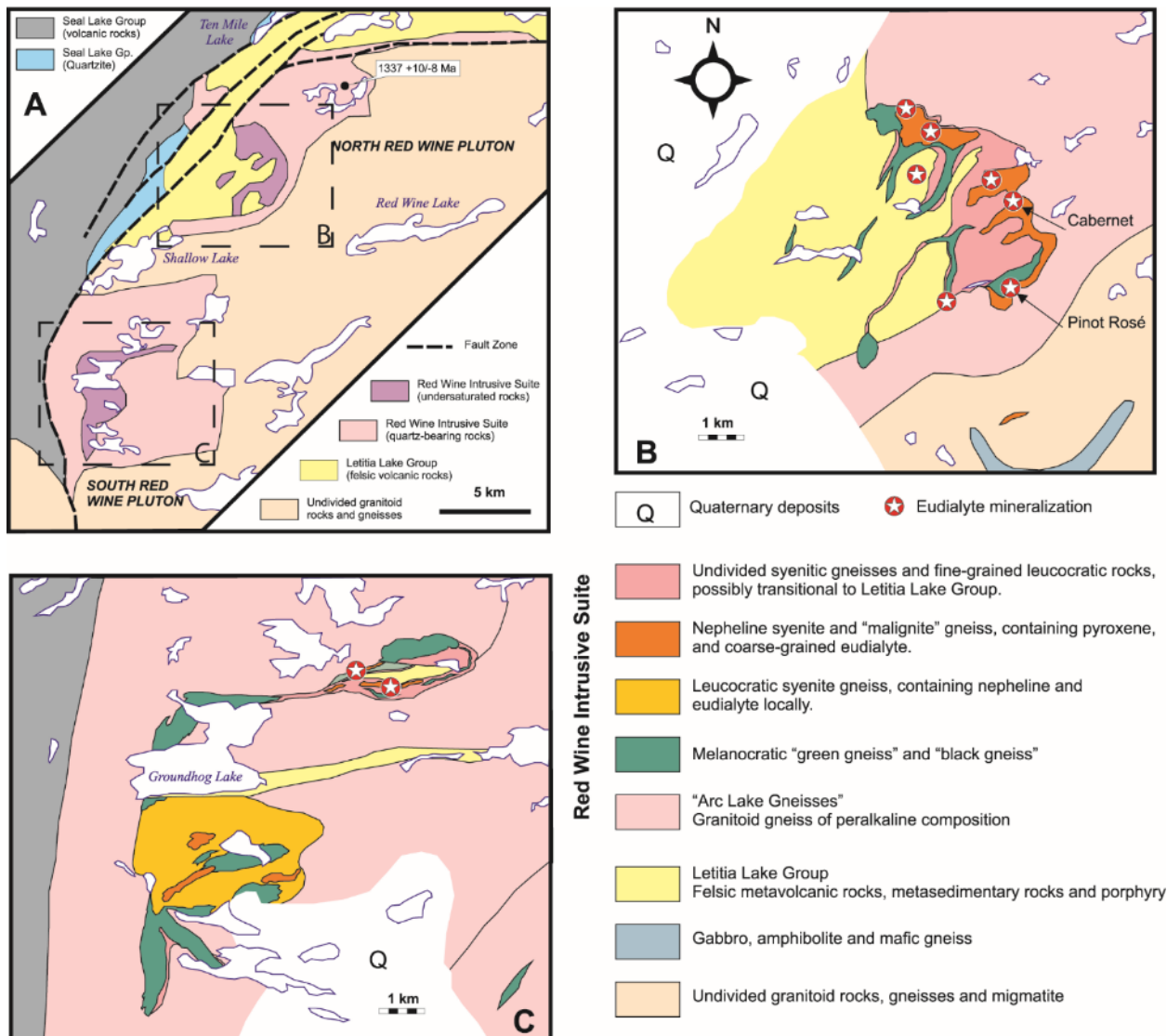


Figure 23. Geologic map of the Letitia Lake Area. A) regional map showing both the North and South Red Wine Plutons, breakout images are indicated by dashed lines. B) Geology of the North Red Wine Pluton. Samples examined in this study are from the Cabernet deposit. C) Geology of the South Red Wine Pluton. Modified from Kerr (2011).

Lake (Kerr, 2011), in contrast with earlier studies which fail to emphasize the intensity of deformation (Currie and Curtis, 1981; Thomas, 1981).

The Letitia Lake Group and Red Wine Intrusive Suite are the primary focus of local mineral exploration. The LLG contains areas of Zr, Nb, and Be mineralization within shear zones and the Red Wine Intrusive Suite hosts eudialyte and britholite ( $(Ce,Ca,Th,LA,Nd)_5(SiO_4, PO_4)_3(OH,F)$ ) mineralization in agpaitic units (Figure 23). Based on spatial proximity, geochemical similarities, and geochronological data, a cogenetic link between the LLG and the RWIS has been previously proposed (Gandhi et al., 1988). Such a model suggests that isolated syenitic bodies within the LLG are higher level constituents of the Red Wine Intrusive Suite (Kerr, 2011). The chondrite normalized REE profile of the Letitia Lake Group shows pronounced LREE enrichment, similar to what would be expected as a residual of partial melting (Kerr, 2011). By contrast the Red Wine Intrusive Suite shows a flat chondrite-normalized profile, reflecting relative HREE enrichment. These contrasting REE patterns have been cited, along with geochronological data, to suggest that the Red Wine Intrusive Suite was derived from the same source material as the Lake Letitia Group (Curtis and Currie, 1981). By invoking partial melting of a shared source LREE enrichment and HREE enrichment in the two units can be reconciled.

As many as eight zones of significant mineralization have been identified in the North Pluton, and similar occurrences have been discovered recently in the South Pluton (Kerr, 2011) (Figure 23). Two modes of mineralization are recognized. The first of which is as a disseminated constituent or discrete, concordant, layers of large crystals in syenite. Layers can be up to 50% eudialyte, and eudialyte crystals show signs of rotation within the

matrix (Kerr, 2011). Large crystals have been interpreted as phenocrysts or porphyroblasts present prior to deformation. Where multiple eudialyte-rich layers are present in a single locality disseminated eudialyte is usually present within the intervening syenite (Kerr, 2011).

The RWIS occurs as a large unit of peralkaline quartzofeldspathic gneiss containing isolated lenses of agpaitic gneiss (Figure 23) (Curtis and Currie, 1981). The primary occurrences of agpaitic gneiss form two plutonic centers uncreatively named North Red Wine Pluton and South Red Wine Pluton. Both plutonic centers become increasingly silica-undersaturated towards their centers where silica-undersaturated rocks are predominantly nepheline syenite (Currie and Curtis, 1981).

The surrounding peralkaline gneiss has been constrained by a U-Pb zircon date of  $1337 +10/-7$  Ma (Gandhi et al., 1988) while the nepheline syenites are dated only by a poorly constrained 11-point Rb-Sr isochron at  $1345 \pm 75$  Ma (Curtis and Currie, 1981) (Figure 24). Eudialyte occurs in syenite as a disseminated constituent or in discrete,

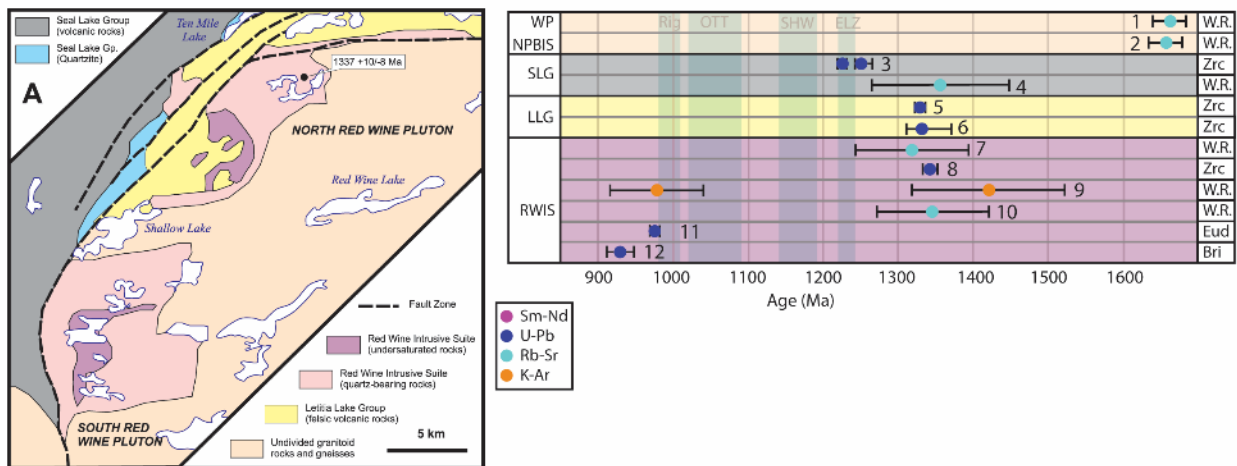


Figure 24. Geology and relevant geochronology of the Red Wine Intrusive Suite. Abbreviations: W.R.: Whole rock (multi-mineral isochron); Zrc: zircon; Bri: britholite; Eud: eudialyte. Data from: Thomas, 1981 (1,6); Hill and Thomas (2,5), 1983; Romer et al., 1995 (3); Curtis and Currie, 1981 (4,10); Blaxland and Curtis, 1977 (7); Gandhi et al., 1988 (8); Singh, 1972 (9); Crocker, 2014 (11,12). Map modified from Kerr (2011)

concordant layers of large crystals (Kerr, 2011). Significant mineralization also occurs in cross cutting leucocratic pegmatites, usually composed of albite, arfvedsonite, and eudialyte.

### 3.3 SAMPLES

Matthew Crocker formerly of Memorial University of Newfoundland provided several quarter cut drill core samples analyzed in his 2014 master's thesis, which was conducted in coordination with Search Minerals Inc. Materials from M. Crocker (including sample CB 02-12) were sourced from the Cabernet and Pinot Rose deposits (Figure 23 B). Search Minerals also provided half cut drill core samples from the Cabernet Deposit (Figure 23 B), the drill core CBD-11-10 was acquired as part of the 2011 drilling campaign.

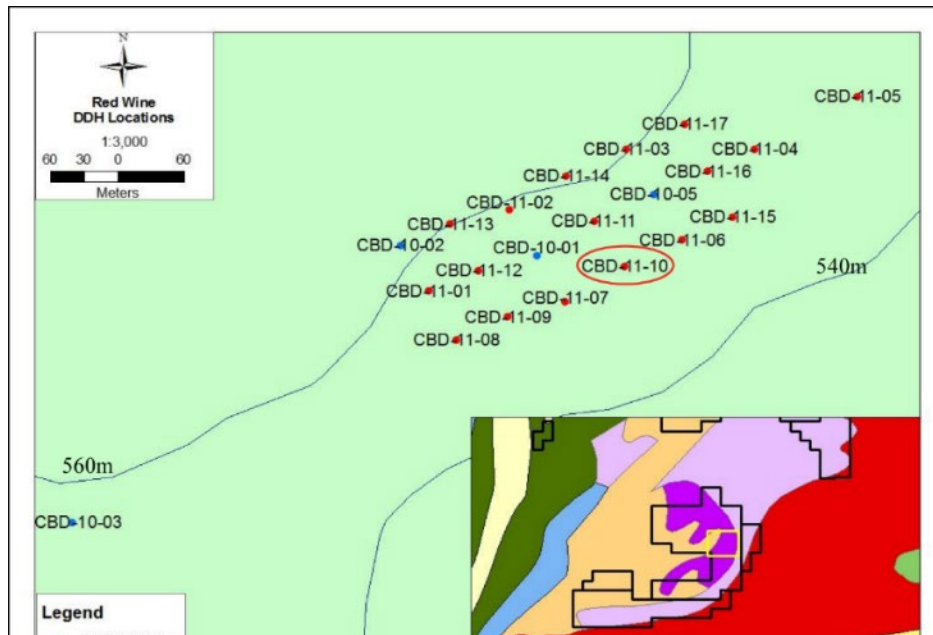


Figure 25. Map of Search Minerals diamond borehole drill sampling sites. Core CBD 11-10 circled in red. Inset shows generalized geology of the North Red Wine Pluton. Black polygon shows outline of Search Minerals prospect, yellow outline indicates location of area indicated. The outline of the inset is the same as Figure 23B. Modified from Crocker (2014).

RWIS samples for LA-ICP-MS and other analysis were selected from the larger half cut drill core samples based largely on sample size and quality, both from the Cabernet Deposit (CBD). Samples were cut to size at Boston College, samples CBD 11-10-1 and CBD 11-10-2 were polished for analysis at the University of Gothenburg. Sample CB 02-12 was thin sectioned by Wagner Petrographic.

### 3.3.1 CBD 11-10-1

Sample CB 11-10-1 was acquired directly from Search Minerals and is dark green-black with some lighter matrix components (Figure 26). Eudialyte grains are relatively small, equant, and disbursed. Minerals identified using SEM EDS include aenigmatite (Table 1), microcline, albite, arfvedsonite, aegerine, pyrite, nepheline, and eudialyte.



Figure 26. True color scan of sample CBD 11-10-1.  
Note dispersed pink eudialyte grains.

### 3.3.2 CBD 11-10-2

Sample CB 11-10-2 was acquired directly from Search Minerals. The sample is primarily dark green and pink (Figure 27). The pink color is due to a large eudialyte vein with white feldspars, and several large arfvedsonite crystals. The surrounding rock is comprised primarily of arfvedsonite, nepheline, and some minor constituents (Figure 27).

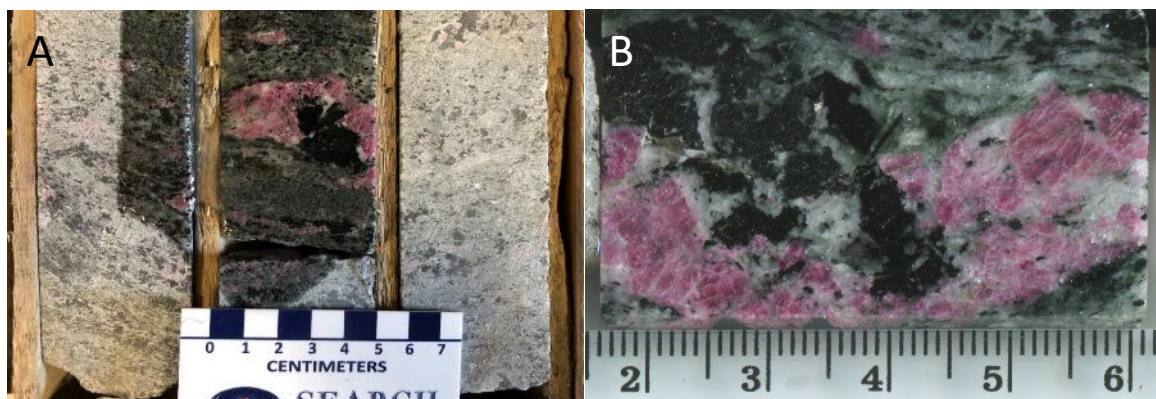


Figure 27. Sample CBD11-10-2. A) Photo of sample and surrounding drill core prior to cutting. Photo provided by Search Minerals. B) True color scan of sample billet. Note large eudialyte grains with associated amphibole.

### 3.3.3 CB 02-12

This sample was acquired from M. Crocker from materials he used for his Master's thesis. Sample is primarily green and white with clumps of pink eudialyte and black amphibole (Figure 28 B). White is nepheline and albite/microcline, green color is due to small grains of arfvedsonite. Sample is clearly deformed with a gneissic texture. Eudialyte grains are roughly equant and the clots of eudialyte and amphibole are reminiscent of garnets from more common gneisses. Thin section shows albite, microcline, arfvedsonite ( $\text{Na}_3(\text{Mg},\text{Fe})_4\text{AlSi}_8\text{O}_{22}(\text{OH},\text{F})_2$ ), eudialyte, nepheline, clinopyroxene, and aenigmatite ( $\text{Na}_2\text{Fe}_5\text{TiSi}_6\text{O}_{20}$ ) (Figure 28 A).

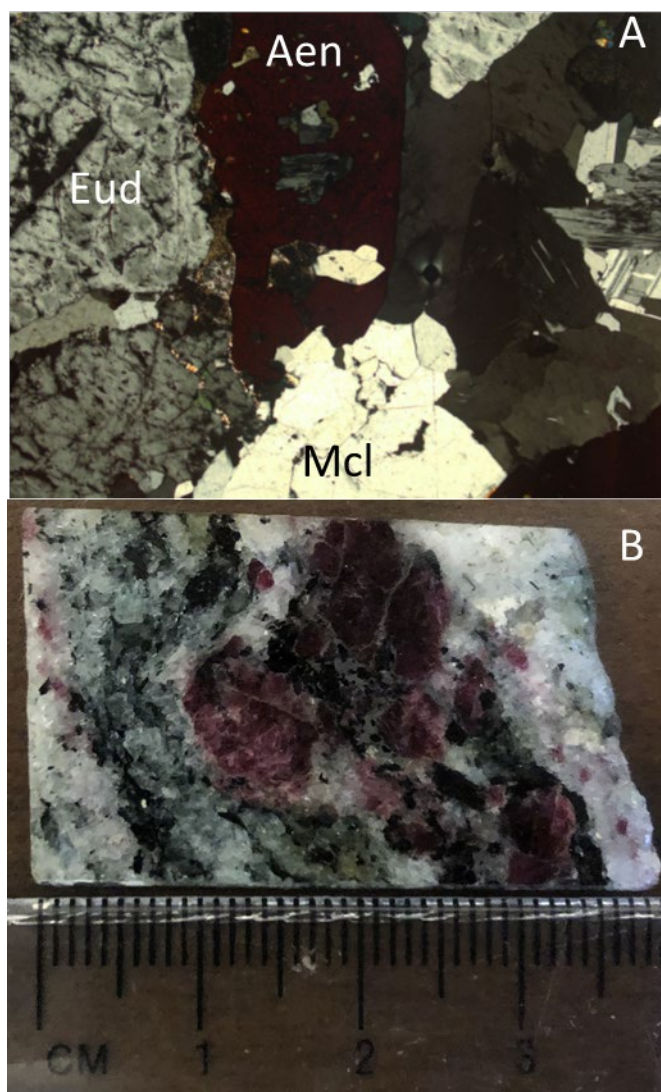


Figure 28. Sample CB 02-12.A) Thin section under cross polarized light. B) Photograph of sample chip, pink blots are eudialyte. Abbreviations: Aen: aenigmatite; Eud: eudialyte; Mcl: Microcline.

### 3.4 METHODS

See Chapter 2 for procedural details regarding laboratory methods. Sample were selected for examination primarily based on eudialyte crystal size. Sample CB 02-12 was received in the spring of 2019 and was cut and thin sectioned. After thin sectioning the chip was

sampled by hand for bulk TIMS analysis. Samples CBD 11-10-1 and CBD 11-10-2 were received in the fall of 2019 and slabbed for SEM, LA-ICP-MS, and EMP analysis based on large sample and crystal size. Following SEM and LA-ICP-MS analysis sample CBD 11-10-2 was selected for drilling and ID-TIMS. Six pits were drilled without the benefit of EMP mapping in February of 2020, based on zonation identified in LA-ICP-MS transects across individual eudialyte crystals. The remaining pits were drilled after EMP analysis in November 2020, drill sites were selected using combined LA-ICP-MS and EMP data.

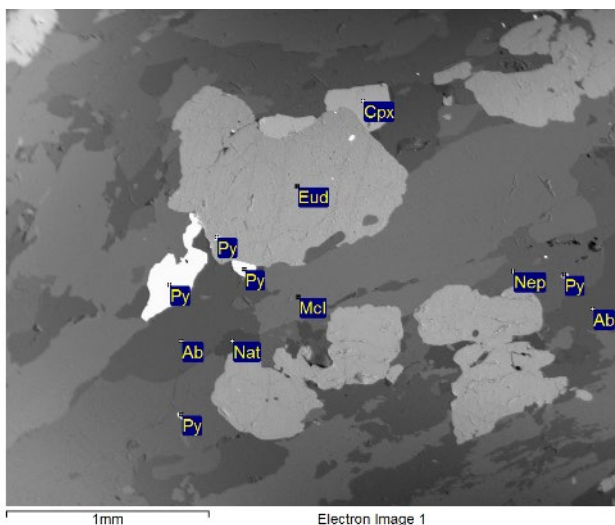


Figure 29. SEM BSE image of sample CBD11-10-2 with overlaid with EDS based mineral identifications. Abbreviations: Ab: albite; Nep: nepheline; Cpx: clinopyroxene (aegerine); McL: microcline; Py: pyrite; Eud: eudialyte.

### 3.5 RESULTS

#### 3.5.1 SEM

The examination of eudialyte samples (CBD 11-10-1, CBD 11-10-2) by BSE revealed little apparent zonation or textural zones even when brightness and contrast were optimized to focus on small changes within single crystals (Figure 29). While not revealing vivid zonation, BSE images make it easy to distinguish clean, inclusion free eudialyte. Accidentally drilling a small amount of aenigmatite or pyrite in later stages would not be

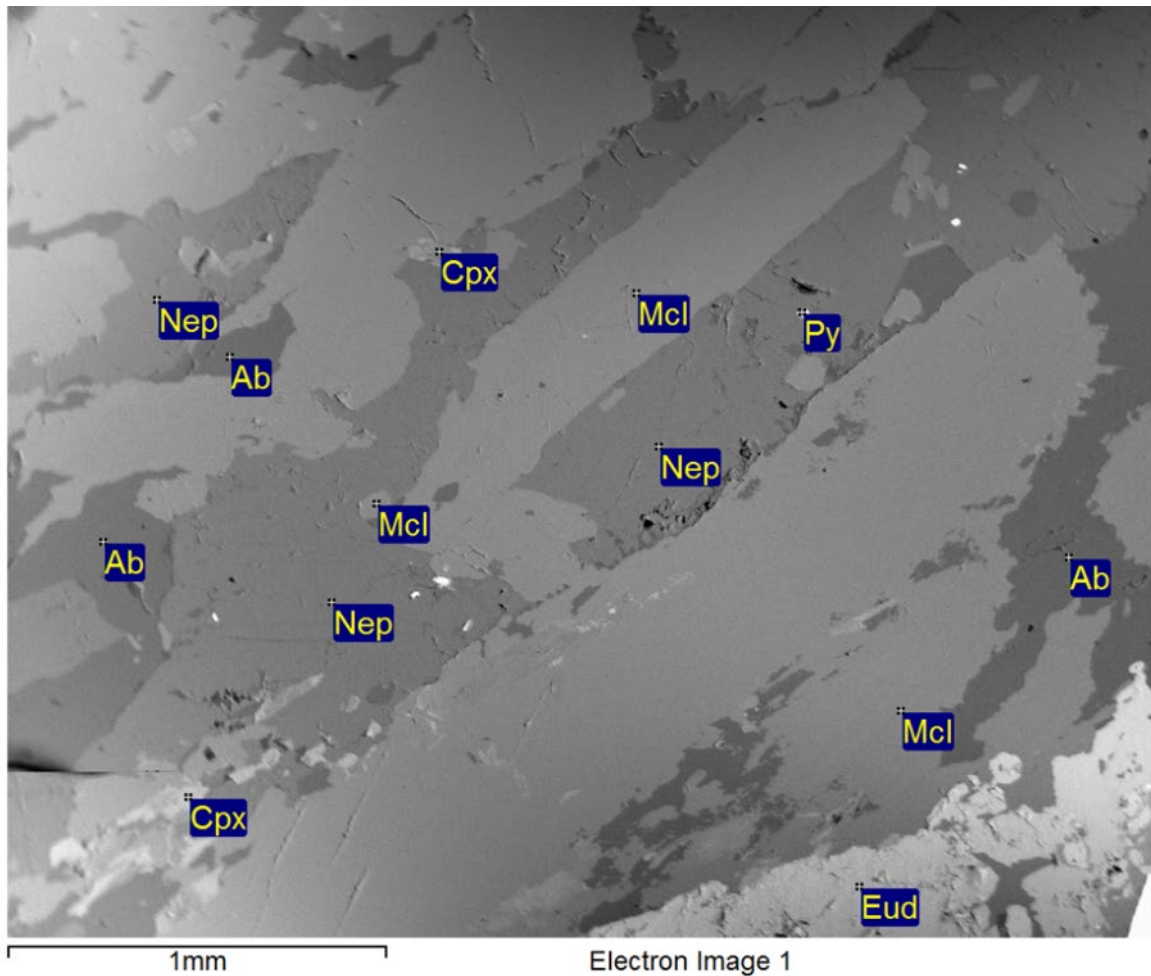


Figure 30. SEM BSE image of sample CBD11-10-2 with overlaid with EDS based mineral identifications. Abbreviations: Ab: albite; Nep: nepheline; Cpx: clinopyroxene (aegerine); Mcl: microcline; Py: pyrite; Eud: eudialyte.

problematic for eudialyte Sm/Nd analysis, however even a small amount of mosandrite have the potential to significantly contaminate a drilled eudialyte sample due to its relatively high REE content.

Through the use of EDS and INCA analytical software, several constituents were positively identified, consistent with findings from the CB 02-12 thin section (Figure 28). These minerals include microcline albite, nepheline, clinopyroxene, and pyrite. EDS analysis also informed the identification of natrolite ( $\text{Na}_2\text{Al}_2\text{Si}_3\text{O}_{10}\cdot 2\text{H}_2\text{O}$ ) and catapleiite ( $\text{Na}_2\text{ZrSi}_3\text{O}_9\cdot \text{H}_2\text{O}$ ) (Figure 29, Figure 30).

### 3.5.2 LA-ICP-MS

LA-ICP-MS analyses from samples CBD 11-10-1 and CBD-11-10-2 show high concentrations of REE in eudialyte. Absent visible zonations transects across eudialyte crystals were analyzed in an effort to gain information across the crystal. Total rare earth elements (REE+Y) range from 1.53 wt.% to 1.97 wt.% along with 8.59 to 10.42 wt.% Zr, an essential component of eudialyte. REE spider diagrams (Figure 31) highlight the high concentrations of REE in RW eudialyte and the moderate enrichment of HREE relative to chondrite.

The concentrations of most elements show a relatively poor correlation with  $^{147}\text{Sm}/^{144}\text{Nd}$ . Na, Nb, La, Mn, and Al all show a mix of weak positive and negative

Element	Avg. $R^2$
Y	0.208
Mg	0.145
La	0.118
Al	0.098
Nb	0.094
Mn	0.083
Ta	0.064
Na	0.027
Zr	0.023
Cl	0.011

Table 4. Summary selected elements showing a relationship with  $^{147}\text{Sm}/^{144}\text{Nd}$  ratio as measured by LA-ICP-MS, and the average  $R^2$  value for each element vs. the  $^{147}\text{Sm}/^{144}\text{Nd}$  ratio

relationships with  $^{147}\text{Sm}/^{144}\text{Nd}$  (Table 4, Figure 32). CB 11-10-1 shows a broader range of  $^{147}\text{Sm}/^{144}\text{Nd}$  values (0.1590 to 0.1996) but  $^{147}\text{Sm}/^{144}\text{Nd}$  does not correlate well with the concentration of most elements (Figure 32). By contrast, CBD 11-10-2 shows stronger correlations, but lower range of  $^{147}\text{Sm}/^{144}\text{Nd}$  ratios (0.1751 to 0.1923) (Figure 32). The five elements showing the best correlation with  $^{147}\text{Sm}/^{144}\text{Nd}$  (Na, Mn, Al, Nb, La (Table 4) were selected for EMP mapping.

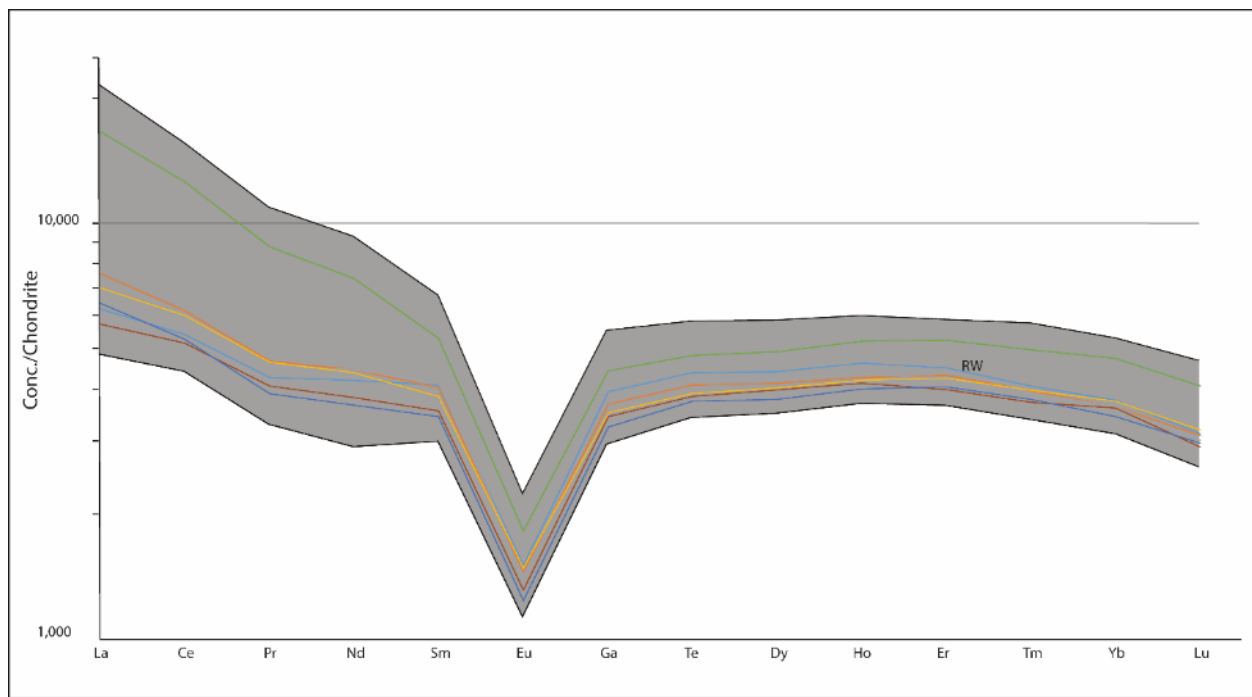


Figure 31. Chondrite normalized rare earth element (REE) spider diagram from the Red Wine Intrusive Suite (RWIS). The grey field indicates range of measured values. Colored lines are average values for individual eudialyte crystals in samples CBD 11-10-1 and CBD 11-10-2. Chondrite values from Sun and McDonough (1989).

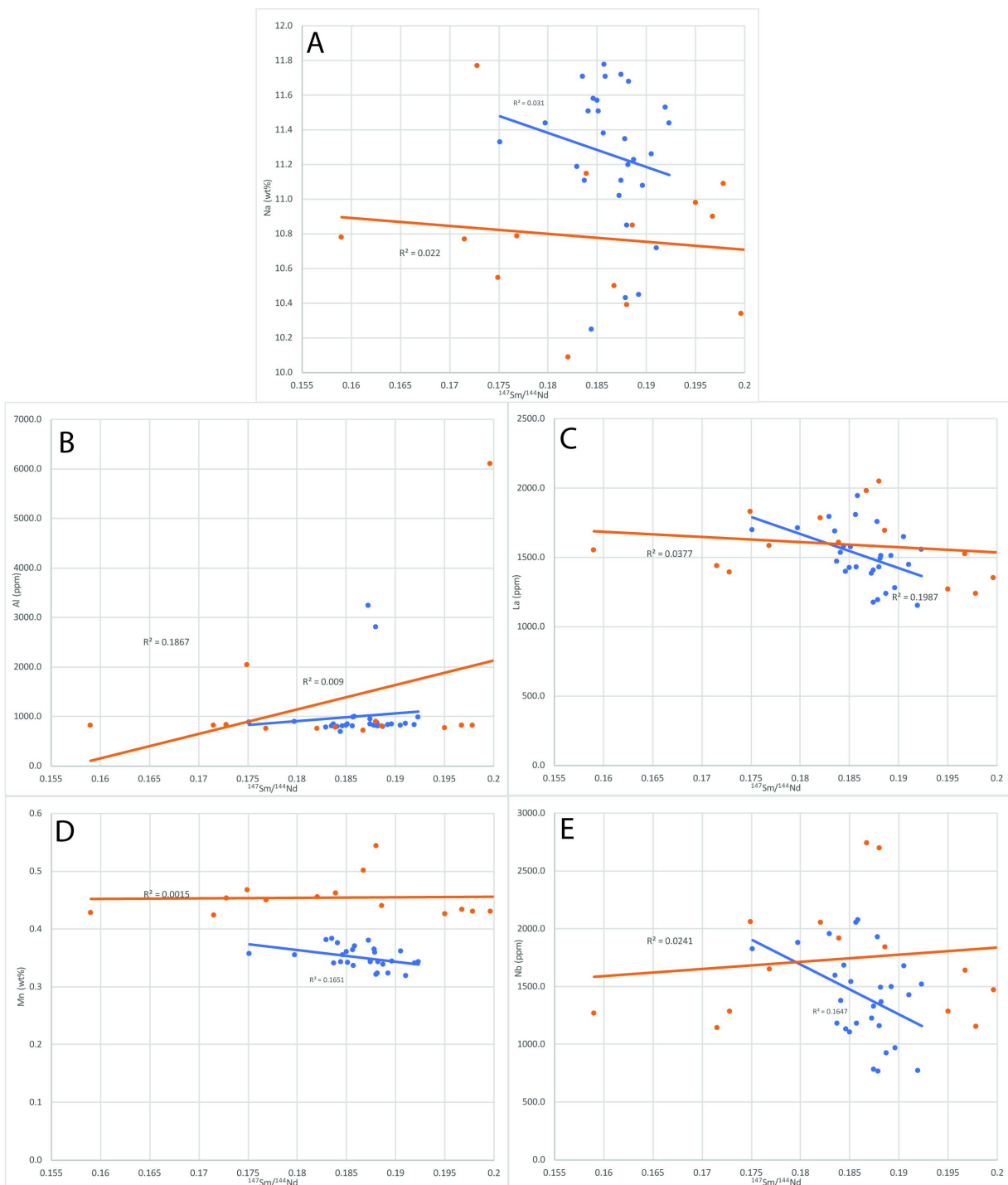


Figure 32. LA-ICP-MS elemental concentrations (ppm) plotted against  $^{147}\text{Sm}/^{144}\text{Nd}$  from two RWIS eudialyte samples. Sample CBD11-10-1 shown in orange, sample CBD11-10-2 shown in blue. Note stronger correlations in sample CBD11-10-2. A) Na. B) Al. C) La. D) Mn. E) Nb.

### 3.5.3 Electron Microprobe

Electron microprobe mapping of sample CBD 11-10-2 reveals zonation in the distribution of certain elements discussed above. Nb, Mn, and La maps proved most useful for examining eudialyte. Nb mapping of sample CBD11-10-2 revealed mild zonation in several eudialyte grains and clear zoning in one large crystal (Figure 33). Mn and La mapping reflect the same patterns but the zonation is less clearly defined. La mapping

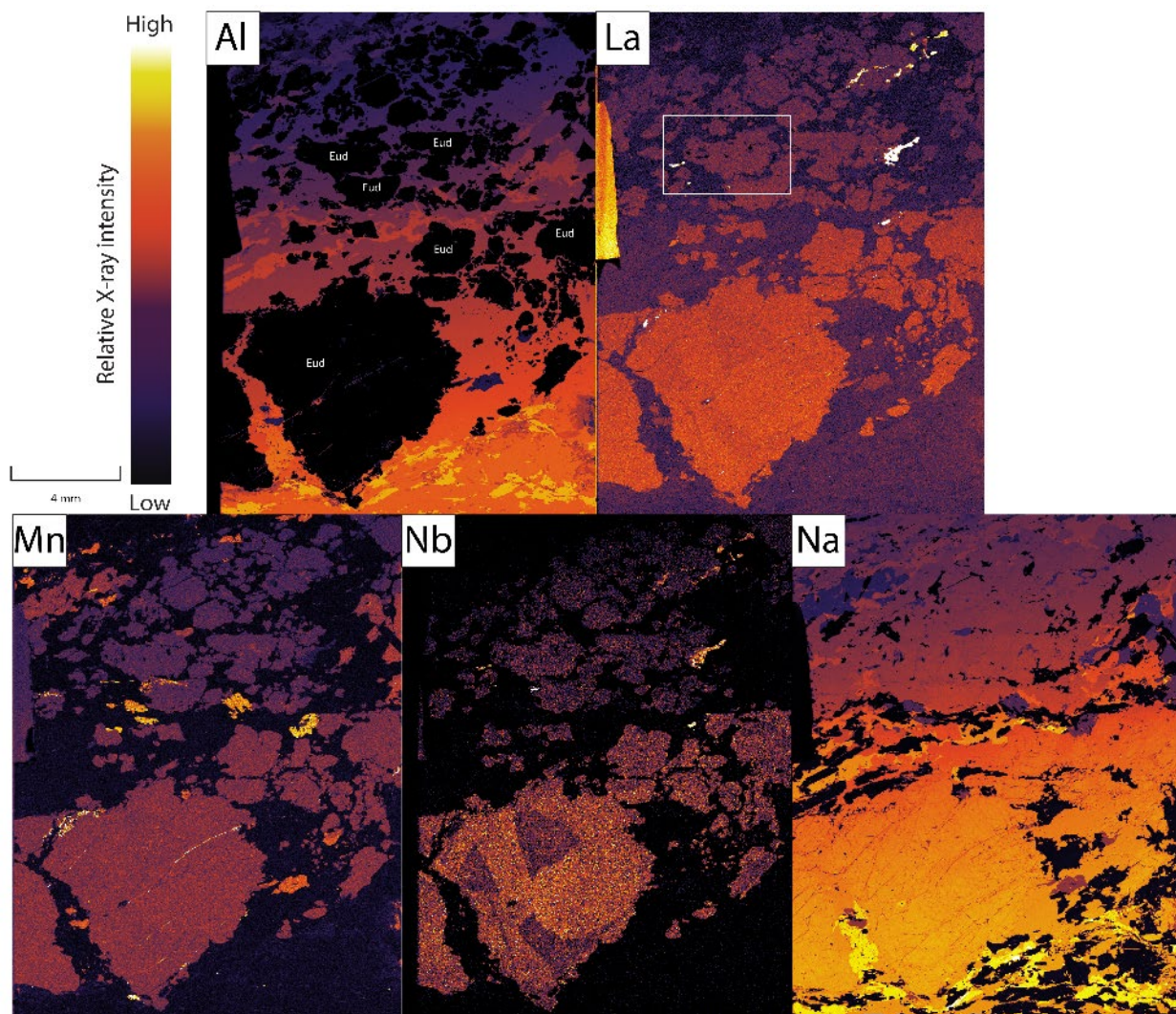


Figure 33. Electron Microprobe (EMP) maps of sample CBD 11-10-2. Element mapped indicated in upper left corner. White outline indicates outline of Figure 32. Note gradient in EMP color from top to bottom; this is likely an artifact of focusing on non-uniform thickness of the slab.

allows for the quick identification of mosandrite, a potentially problematic contaminant for Sm/Nd isotopic analyses (Figure 33).

### 3.5.4 ID-TIMS

Full results of ID-TIMS isotopic analyses are presented in Table 5. The spread in  $^{147}\text{Sm}/^{144}\text{Nd}$  is relatively small, from 0.1483 to 0.1812 across all samples (Figure 34, Figure 35),  $^{143}\text{Nd}/^{144}\text{Nd}$  values ranged from 0.510302 to 0.512574. A single mosandrite analysis provides a lower  $^{147}\text{Sm}/^{144}\text{Nd}$  of 0.115079 and  $^{143}\text{Nd}/^{144}\text{Nd}$  of 0.512012 (Figure 34).

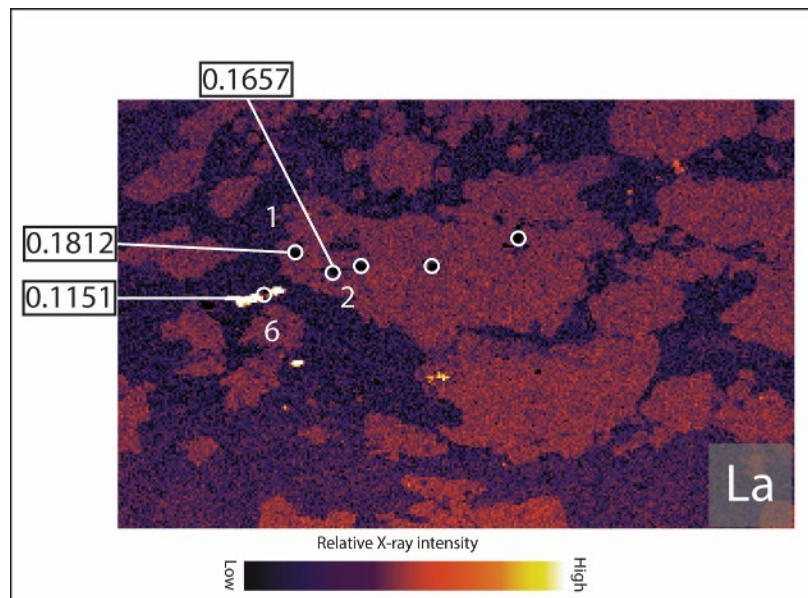


Figure 34. EMP map of La in sample CBD 11-10-2. Circles indicate drilled sample sites, and  $^{147}\text{Sm}/^{144}\text{Nd}$  ratios are displayed for successful analyses. Note poor zonation in sampled eudialyte crystal.

Repeated analyses of 4ng AMES Nd standard solution run over the course of the study yield a  $^{143}\text{Nd}/^{144}\text{Nd}$  value of  $0.512152 \pm 0.000010$  (18.75 ppm,  $2\sigma$ ;  $n=36$ ). Analyses of 20ppm Ames Sm standard solution yield a  $^{147}\text{Sm}/^{144}\text{Nd}$  reproducibility of 0.054%. External reproducibility was used for all age calculations except in instances where the

internal reproducibility was worse. A procedural blank run alongside samples yielded a measured Nd value of 6.4 pg. Analysis of a bulk chip sample from CB 02-12 where sample weights can be accurately measured yield Sm and Nd concentrations consistent with LA-ICP-MS results.

Sample ID	$^{147}\text{Sm}/^{144}\text{Nd}$	$\pm 2 \text{ S.E.}$	$^{143}\text{Nd}/^{144}\text{Nd}$	$\pm 2 \text{ S.E.}$	$\epsilon\text{Nd}$	$^{150}\text{Nd}/^{144}\text{Nd}$ raw	Nd ppm	Sm ppm	Mineral	Sample Type
CBD11-10-2-1	0.181217	0.00003	0.512409	0.000038	-4.46	7.82	N/A	N/A	Eudialyte	Drill
CBD11-10-2-2	0.165659	0.00016	0.512382	0.000008	-4.99	9.10	N/A	N/A	Eudialyte	Drill
CB-02-12	0.148292	0.00002	0.512201	0.000008	-8.53	0.89	2978	730	Eudialyte	Bulk Chip
CBD11-10-2-6	0.115079	0.00021	0.512012	0.000014	-12.21	10.48	N/A	N/A	Mosandrite	Drill
CBD11-10-2-eud-1	0.173085	0.00002	0.512351	0.000019	-5.60	2.83	N/A	N/A	Eudialyte	Drill
CBD11-10-2-eud-2	0.176071	0.00002	0.512409	0.000011	-4.48	2.02	N/A	N/A	Eudialyte	Drill
CBD11-10-2-eud-3	0.164252	0.00002	0.512334	0.000008	-5.92	1.84	N/A	N/A	Eudialyte	Drill
CBD11-10-2-eud-4	0.180841	0.00005	0.512408	0.000057	-4.48	2.76	N/A	N/A	Eudialyte	Drill
CBD11-10-2-eud-5	0.162094	0.00003	0.512322	0.000008	-6.16	1.52	N/A	N/A	Eudialyte	Drill
CBD11-10-2-eud-6	0.165508	0.00003	0.512354	0.000016	-5.53	1.97	N/A	N/A	Eudialyte	Drill
CBD11-10-2-eud-7	0.167126	0.00002	0.512341	0.000008	-5.78	1.83	N/A	N/A	Eudialyte	Drill
CBD11-10-2-eud-8	0.178451	0.00007	0.512399	0.000010	-4.65	2.17	N/A	N/A	Eudialyte	Drill

Table 5. Red Wine Intrusive Suite ID-TIMS data.

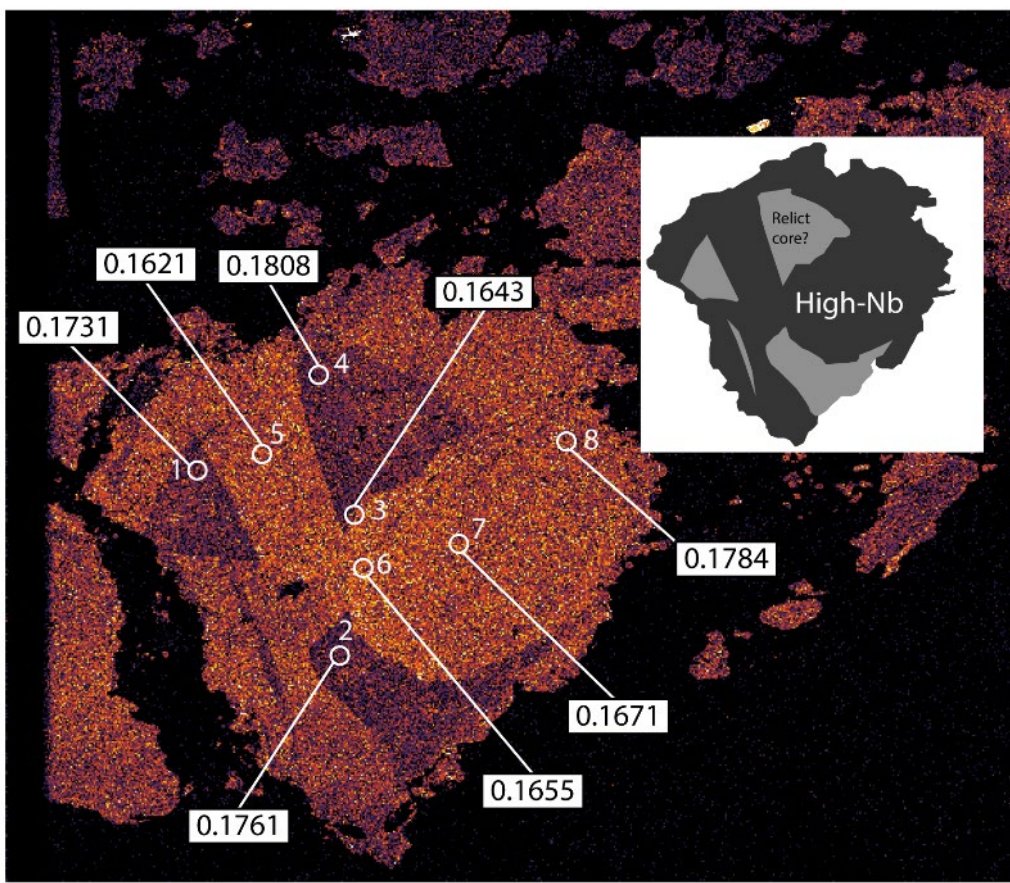


Figure 35. EMP map of Nb in sample CBD 11-10-2. Circles indicate drilled sample sites and corresponding  $^{147}\text{Sm}/^{144}\text{Nd}$  values. Point 3 straddles dark and light, but based on  $^{147}\text{Sm}/^{144}\text{Nd}$  ratio it is likely the light color, High-Nb zone was sampled. Inset shows schematic zonation.

### 3.6 DISCUSSION

SEM analysis shows little zonation in BSE imagery and reveals relatively little about the samples (Figure 30). This is a stark contrast to eudialyte from Norra Kärr described by Sjöqvist et al. (2020) where a large eudialyte crystal was clearly zoned in BSE. The general mineralogy first assessed in hand sample and thin section is confirmed

in addition to the identification of the accessory minerals natrolite and catapleiite (Figure 30).

LA-ICP-MS analyses of both samples analyzed reveal only weak relationships between  $^{147}\text{Sm}/^{144}\text{Nd}$  and elemental concentrations. Variation in  $^{147}\text{Sm}/^{144}\text{Nd}$  is small but present; however, it does not appear to clearly and consistently correlate with any of the elements measured (Figure 32). This is a stark contrast with Kipawa samples discussed in Chapter 2 that showed strong, clear, and consistent relationships between elemental (Ta, Ti, Nb, Mn) concentrations and  $^{147}\text{Sm}/^{144}\text{Nd}$  (Figure 13).

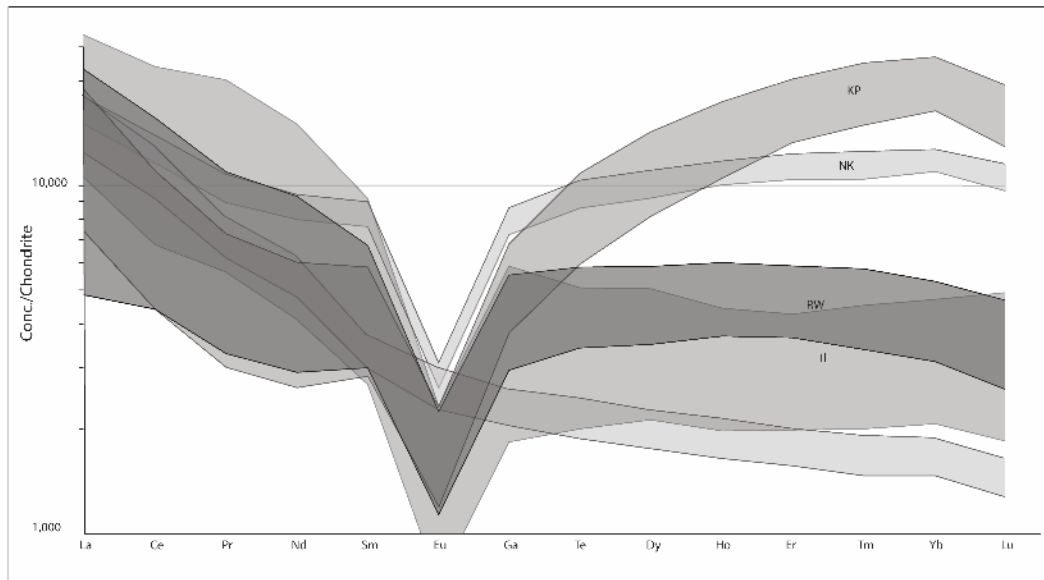


Figure 36. Chondrite normalized rare earth element (REE) spider diagram for all complexes measured in the course of this study. Abbreviations: KP: Kipawa Syenite Complex, NK: Norra Kärr, RW: Red Wine Intrusive Suite, LV: Lovozero Alkaline Massif. Chondrite values from Sun and McDonough (1989).

Eudialyte samples from the RWIS are enriched in all REE relative to chondrite (Sun and McDonough, 1989; C1 chondrite) by a factor of 1,050 (Eu) to 11,300 (La) (Figure 31). REE enrichment decreases from La to Lu. Chondrite normalized REE spider diagrams reveal enrichment in HREE in the RWIS compared to other localities (Lovozero, Ilímaussaq), but show markedly less HRRE enrichment than Norra Kärr or Kipawa (Figure 36). These analyses also show a pronounced Eu anomaly despite high enrichment over chondrite consistent with other Grenvillian samples. The broad similarity of REE profiles across the Grenvillian samples associated in both space and time emphasize the differences between Grenvillian samples and other eudialyte localities, such as Lovozero. Strong Eu anomalies suggest derivation from a source where plagioclase had been previously fractionated, consistent with plagioclase fractionation at some stage of magmatic evolution. In contrast, samples from the much younger ( $370 \pm 7$  Ma (Kramm and Kogarko, 1994)) Lovozero Alkaline Massif lack both a europium anomaly and HREE enrichment. Overall

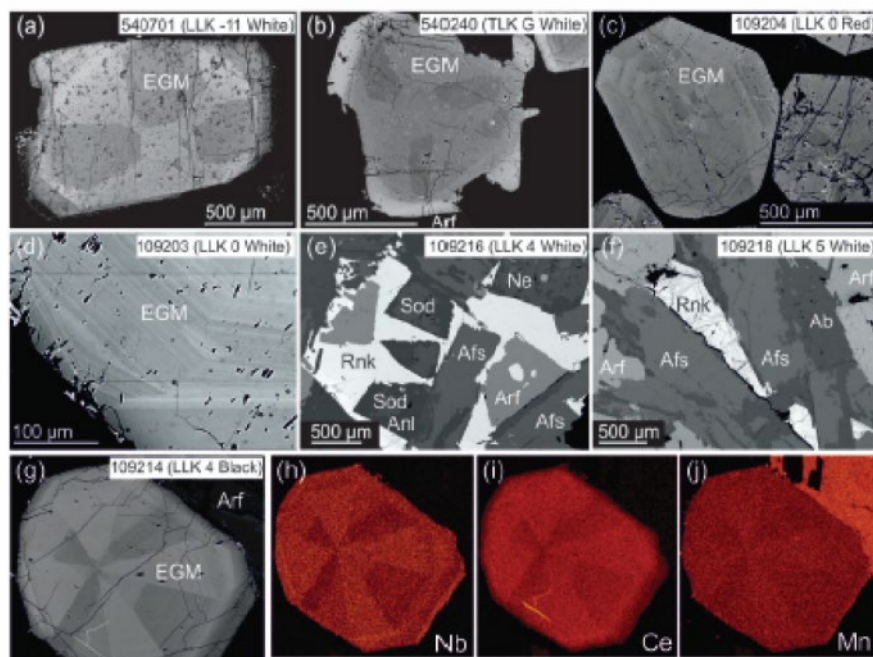


Figure 37. SEM BSE images and EDS maps of eudialyte from Ilímaussaq, Greenland. Note cleat sector zoning similar to sample CBD 11-10-2. Modified from Borst et al. (2018).

the REE profile from Lovozero Massif is consistent with that of rock produced through the partial melting of a mantle source (Figure 36).

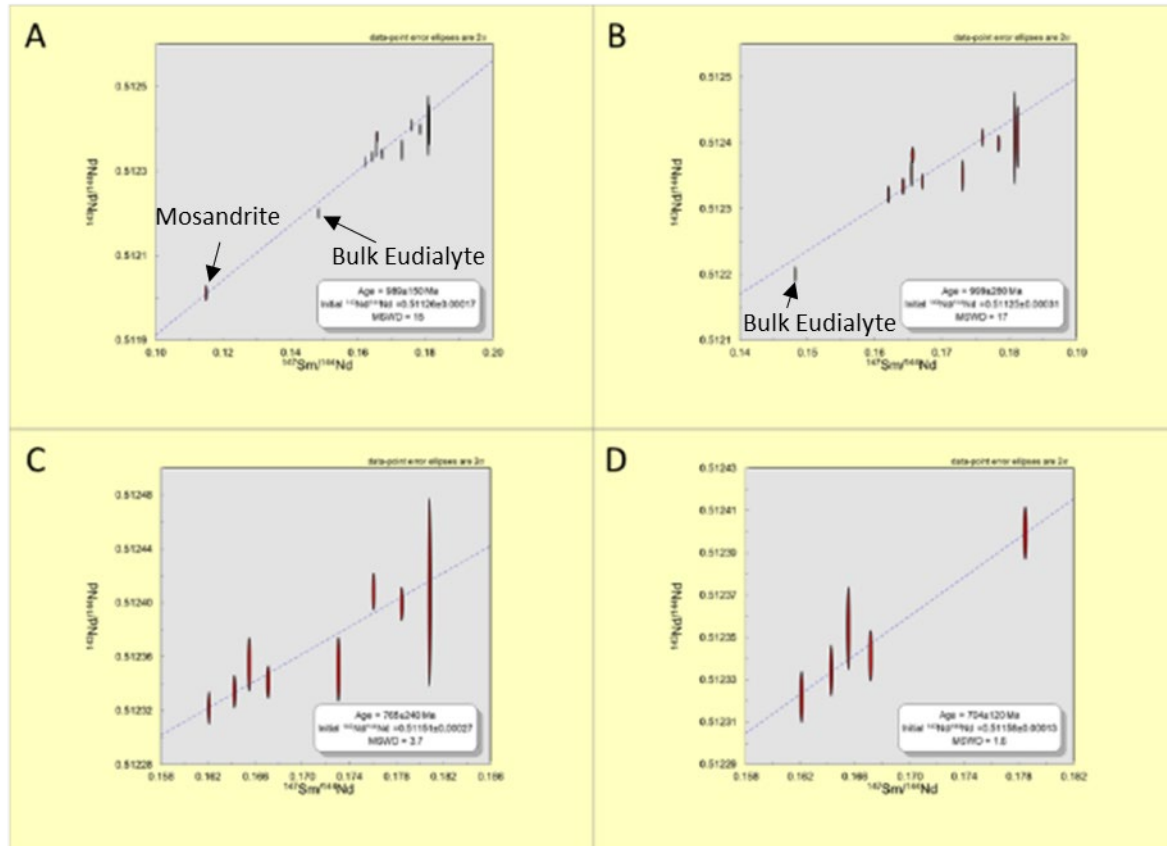


Figure 38. Isochron diagrams from the RWIS. A) Isochron based on all available analyses. B) Isochron based all eudialyte analyses, C) Internal mineral isochron from a single crystal in sample CBD 11-10-2. D) Isochron based solely on high-Nb crystal eudialyte (Figure 33). All plots made using Isoplot.

EMP mapping of sample CBD11-10-2 supports the general homogeneity within eudialyte crystals. However, there is some zoning, particularly in large (6mm), roughly equant crystals (Figure 33). The observed zoning bears a striking similarity to sector zoning in eudialyte from Ilímaussaq (Borst et al., 2018) (Figure 37). Even absent strong relationships between Mn, La, or Nb and  $^{147}\text{Sm}/^{144}\text{Nd}$  across all Red Wine samples, the sector zoning in eudialyte revealed by EMP mapping could prove fruitful in guiding microdrilling. Rakovan et al. (1997) and Sjöqvist et al. (2020) have previously demonstrated spread in  $^{147}\text{Sm}/^{144}\text{Nd}$  related to sector zonation in apatite and eudialyte. The

presence of sector zoning not revealed in the course of SEM examination underscores the utility of EMP characterization in eudialyte. Because  $^{147}\text{Sm}/^{144}\text{Nd}$  spread is a critical factor contributing to analytical precision in Sm/Nd geochronology, EMP mapping should be considered as a good first step for finding strongly zoned crystals where some zonation in  $^{147}\text{Sm}/^{144}\text{Nd}$  may be expected. Even if the zonation isn't true sector zoning, it may reveal different generations of crystal growth or re-precipitation that may each represent different ages and events; this may be the case at Red Wine.

ID-TIMS isotopic data provide new insight into the formation history of Red Wine eudialyte in several isochron plots. A 12-point isochron based on all available Red Wine analyses yield an isochron age of  $989\pm150$  Ma (MSWD=15) and an initial  $^{143}\text{Nd}/^{144}\text{Nd}$  of  $0.51126\pm0.00017$  (Figure 38) this age is probably most appropriate for establishing the time of primary REE ore mineral formation at Red Wine. Removing the mosandrite analysis from the isochron yields a similar age of  $999\pm280$  Ma (MSWD=17) and an initial  $^{143}\text{Nd}/^{144}\text{Nd}$  of  $0.51125\pm0.00031$  (Figure 38 A). Within a single crystal from sample CBD 11\_10\_2 an isochron based on 8 drilled aliquots yields an age of  $765\pm240$  Ma (MSWD=3.7) and an initial  $^{143}\text{Nd}/^{144}\text{Nd}$  of  $0.51151\pm0.00027$  (Figure 38 C). This age, while imprecise, is markedly younger. The high MSWD of these three isochrons (15, 17, and 3.7) suggests we may have sampled multiple age domains. To explore this idea, a five point isochron based solely on drill points from the high-Nb portions of the crystal yields a true isochron age of  $704\pm120$  Ma (MSWD=1.6) and an initial  $^{143}\text{Nd}/^{144}\text{Nd}$  of  $0.51158\pm0.00013$  (Figure 38 D).

ID-TIMS analyses have failed to produce a single precise age constraint for the age of eudialyte crystallization in the Red Wine Intrusive Suite (for example, in comparison to the results from Kipawa or Nora Kärr). However, some conclusions can still be drawn from the isotopic data. If all samples are considered together the isochron age is consistent with Grenvillian formation, but the precision of the age preclude any stronger conclusions regarding the particular phase of deformation involved (Figure 39). This isochron includes a mosandrite analysis which may violate the basic requirement of isotopic equilibrium. When mosandrite is removed the age is largely unchanged, but there is a deleterious effect on the age precision. With or without mosandrite the isotopic bare a distinctly Grenvillian

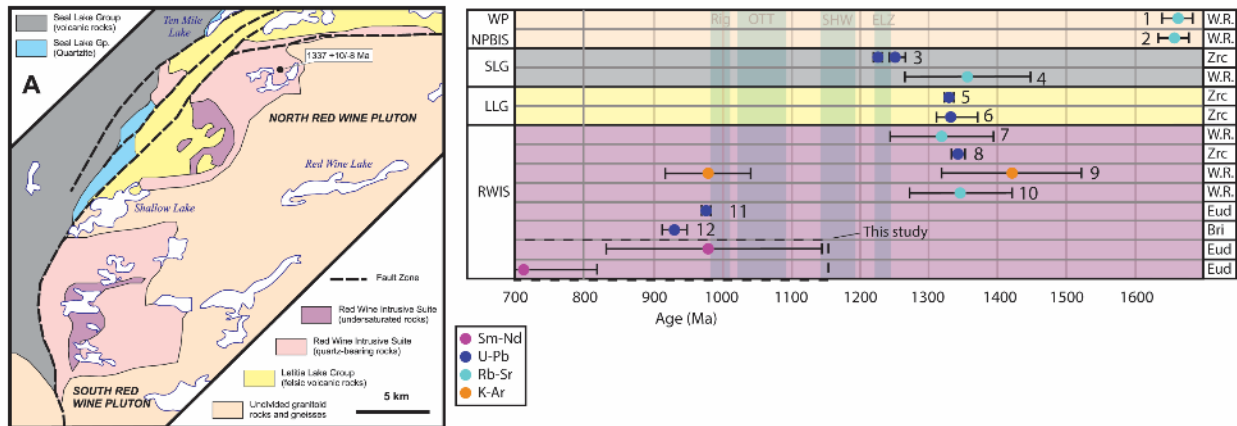


Figure 39. Geology and relevant geochronology of the Red Wine Intrusive Suite. Abbreviations: W.R.: Whole rock (multi-mineral isochron); Zrc: zircon; Bri: britholite; Eud: eudialyte. Data from: Thomas, 1981 (1,6); Hill and Thomas (2,5), 1983; Romer et al., 1995 (3); Curtis and Currie, 1981 (4,10); Blaxland and Curtis, 1977 (7); Gandhi et al., 1988 (8); Singh, 1972 (9); Crocker, 2014 (11,12).

age signal.

However when the large, zoned crystal, is examined alone a different signature becomes apparent. This age ( $765 \pm 240$  Ma) is younger and does not appear to correlate well with any recognized events in this region. The MSWD associated with this regression (3.7) still indicates significant geological scatter. The most robust age constraint produced here of  $704 \pm 120$  Ma (MSWD=1.6) is based on the high-Nb zone alone (samples 3,5,6,7,8)

(Figure 35). Prior to isotopic analysis the observed zonation was thought to reflect sector zoning reminiscent of that observed elsewhere (Figure 37), but the isotopic data instead suggest two distinct eudialyte age populations. These data suggest that instead of sector zoning, the observed zonations correspond to relict cores of Grenvillian age enveloped by a younger generation of recrystallized eudialyte characterized by high Nb concentrations.

The results show the very real disturbance of the  $^{147}\text{Sm}/^{144}\text{Nd}$  system by late-stage partial recrystallization, such that drilled samples do not meet the critical criteria of isotopic equilibrium. The isotopic scatter observed in the RWIS samples is striking in comparison to KSC samples where nearly all samples clearly fell on a line when  $^{143}\text{Nd}/^{144}\text{Nd}$  and  $^{147}\text{Sm}/^{144}\text{Nd}$  were plotted, indicating broad equilibrium in the  $^{147}\text{Sm}/^{144}\text{Nd}$  system and a single consistent mineralization age..

The uncertainties associated with the RWIS ages produced in this work are large. Such large uncertainties preclude any firm statements on the origin (primary igneous or tectonically remobilized) of the Grenvillian age eudialyte. However, the age derived from the high-Nb zone clearly records a post-Grenvillian event of some variety. Labrador is generally considered to have been tectonically stable since the end of Grenvillian deformation and the age described here does not correlate well with any previously described events. The properties of eudialyte may allow partial recrystallization due to the passage of low temperature acidic fluids around 700 Ma that may have escaped previous geochronologic observation.

Nd-model ages were examined to explore the source and crustal residence time recorded by Nd isotopes. Epsilon Nd ( $\epsilon_{\text{Nd}}$ ) values from these samples are negative (average= -6.07) and plot away from the modeled depleted mantle (cf. DePaolo et al., 1991)

(Figure 40). Absent a representative whole-rock sample the method of DePaolo et al. (1991) we calculate a model age for eudialyte samples of  $1.80 \pm 0.1$  Ga.

Comparison to other nearby Proterozoic peralkaline localities further informs the interpretation of Nd model ages. The Ilímaussaq Alkaline Complex was emplaced around  $1156 \pm 53$  Ma (Borst et al., 2019), and combined with weakly negative  $\epsilon_{\text{Nd}}$  values has a similar model age to that of RWIS calculated here (Figure 41). The Norra Kärr Alkaline Complex has a more complex evolutionary history, including significant metamorphic reworking (Sjöqvist et al., 2020), but has a similar model age at 1.69 Ma (Figure 41). These three Grenville localities all share a similar model age around 1.7 Ga. This suggests a similar crustal source, prior to remobilizing process that remelted the primary source and produced the rocks observed today. The RWIS, Norra Kärr, and Ilímaussaq show pronounced Eu anomalies (Figure 36) a notable difference from the less evolved Lovozero

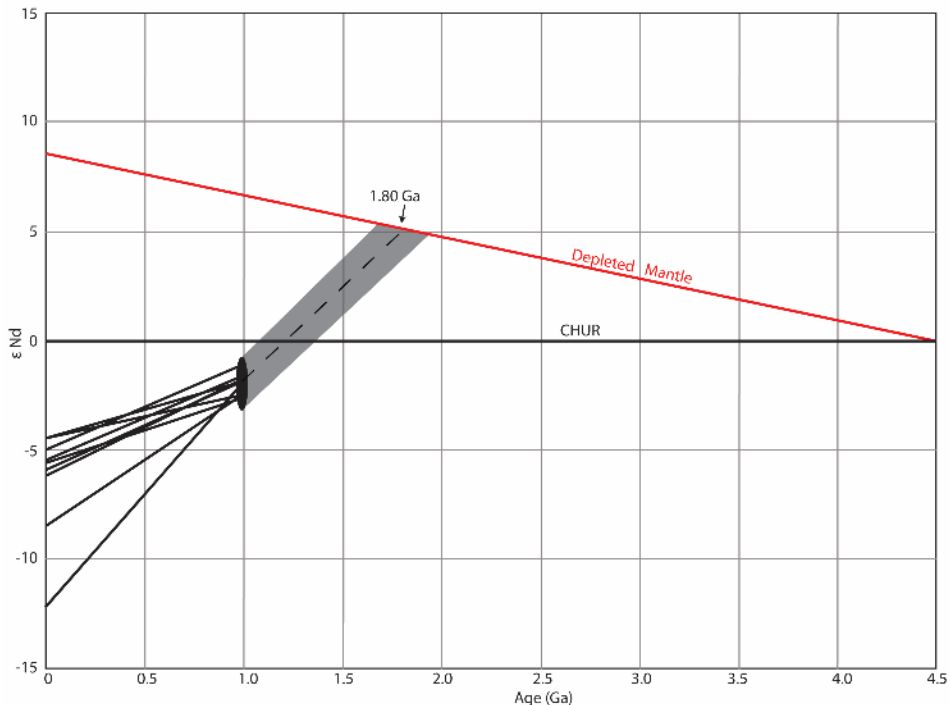


Figure 40. Model for Nd isotopic evolution of RWIS eudialyte. The grey field shows range of possible TDM ages based on range of measured values. Dotted line indicated evolution modeled using average measured composition and method of DePaolo et al. (1991).

Massif. The Kipawa Syenite Complex shows more strongly negative  $\epsilon$ Nd values and has a much older model age, ultimately resulting in a more HREE enrichment. It is worth noting that the Kipawa model age is very similar to the emplacement age of the much older (2.18 Ga) Néchalacho Layered Suite, Northwest Territories, Canada. When the isotopic composition of Néchalacho I plotted alongside data from Kipawa a similarity is clearly apparent, thus Néchalacho may serve as a useful model for the igneous precursor to the KSC in future studies.

Some drilling of eudialyte and mosandrite from sample CBD 11-10-2 took place prior to EMP mapping. Subsequent Mn and La maps show that the small eudialyte crystal sampled was mostly free of zonation (Figure 34). However, the second batch of drilled

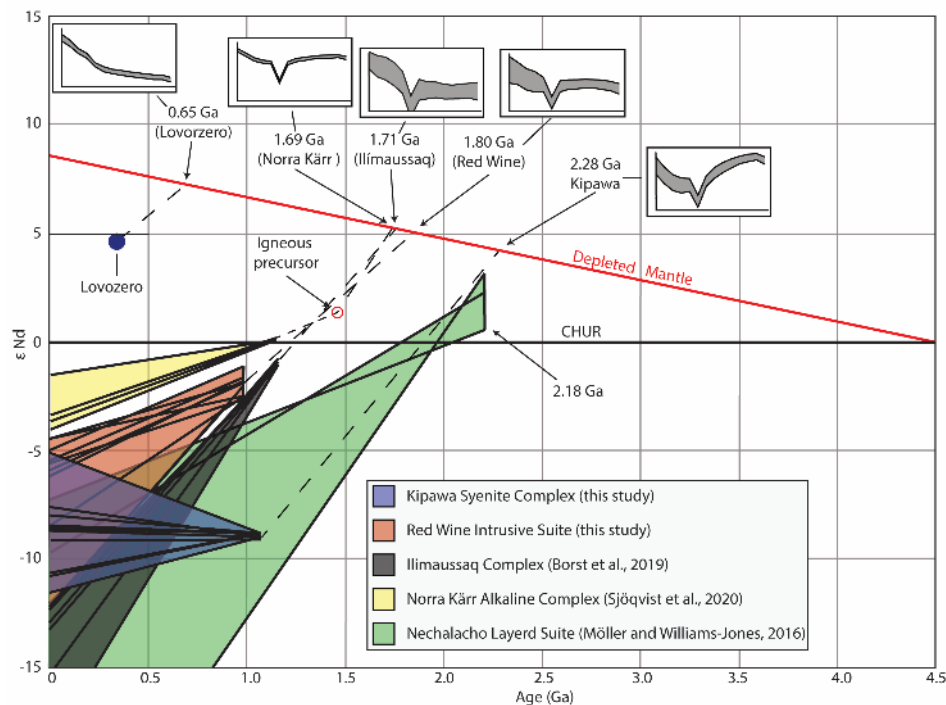


Figure 41. Model for Nd isotopic evolution of Grenvillian eudialyte. Colored fields indicate values from each location. Dotted lines indicate evolution modeled using average measured composition and method of DePaolo et al. (1991). Lovozero and Néchalacho added for context. Ilímaussaq data from Borst et al. (2018), Néchalacho data from Möller and Williams-Jones. (2016).

samples were selected with the benefit of EMP maps. ID-TIMS results do show that as expected  $^{147}\text{Sm}/^{144}\text{Nd}$  does correlate negatively with Nb (Figure 35) in this single zoned crystal. This qualitative assessment appears to confirm that Nb in single eudialyte crystals can serve as a useful proxy for  $^{147}\text{Sm}/^{144}\text{Nd}$  in eudialyte here similar to results from the Kipawa Syenite Complex (see chapter 2). The crystal sampled from sample CBD-11-10-2, is small compared to that examined from Kipawa and is anhedral. Future work should focus on finding and examining euhedral-subhedral eudialyte from the RWIS, especially for a better constraint on the age of Grenvillian crystallization.

### 3.7 CONCLUSION

This study aimed to examine the timing of eudialyte mineralization in the Red Wine Intrusive Suite of central Labrador using EMP guided internal mineral Sm-Nd geochronology. EMP has again shown to be an effective means of identifying strongly zoned eudialyte crystals even when zonation is not apparent in other imagery. Furthermore, based on correlative relationships between select elements and  $^{147}\text{Sm}/^{144}\text{Nd}$  EMP mapping of Nb and Mn can be used as a proxy map for  $^{147}\text{Sm}/^{144}\text{Nd}$  in eudialyte. A bulk isochron using all available data yields an age of  $989 \pm 150$  Ma (MSWD= 15) which is interpreted as a Grenvillian age signal. When drilled, a zoned crystal shows a small range of  $^{147}\text{Sm}/^{144}\text{Nd}$  and significant geologic scatter. Within this crystal two distinct age populations can be recognized with an older core surrounded by younger high-Nb eudialyte ( $704 \pm 120$  (MSWD= 1.6)). Overall, these results suggest a generally Grenvillian age for

the formation of most Red Wine eudialyte with a later remobilization event effecting some crystals.

Nd model ages also facilitate the identification of three distinct deposit types. The Lovozero type, with a young model age similar to crystallization age and lacking both Eu anomaly and HREE enrichment, is indicative of mantle derivation and a short period of evolution. The Grenville, type, with a model age of ~1.7 Ga and much younger ore growth. This type shows an Eu anomaly and moderate HREE enrichment. The Kipawa type, with an old (2.3 Ga) model age and long crustal residence. This type is characterized by an Eu anomaly and high HREE enrichment.

#### 4.0 REFERENCES

- Allan, J.F., 1992, Geology and Mineralization of the Kipawa Yttrium-Zirconium Prospect, Quebec: Exploration Mining Geology, v. 1, p. 283-295.
- Balinski, A., Wiche, O., Kelly, N., Reuter, M.A., and Scharf, C., 2020, Separation of rare earth elements from contaminants and valuable components by in-situ precipitation during the hydrometallurgical processing of eudialyte concentrate: Hydrometallurgy, v. 194, p. 105345.
- Baragar, W.R.A., 1981, Tectonic and regional relationships of the Seal Lake and Bruce River magmatic provinces: Geological Survey of Canada; Hull, Qué.: Available from Canadian Government.
- Baxter, E.F., Caddick, M.J., and Dragovic, B., 2017, Garnet: A Rock-Forming Mineral Petrochronometer: Reviews in Mineralogy and Geochemistry, v. 83, p. 469-533.
- Bethune, K.M., and Davidson, A., 1997, Grenvillian metamorphism of the Sudbury diabase dyke-swarm; from protolith to two-pyroxene--garnet coronite: The Canadian Mineralogist, v. 35, p. 1191-1220.
- Borg, S.G., and DePaolo, D.J., 1994, Laurentia, Australia, and Antarctica as a Late Proterozoic supercontinent: Constraints from isotopic mapping: Geology, v. 22, p. 307-310.
- Borst, A.M., Finch, A.A., Friis, H., Horsburgh, N.J., Gamaletsos, P.N., Goettlicher, J., Steininger, R., and Geraki, K., 2020, Structural state of rare earth elements in eudialyte-group minerals: Mineralogical Magazine, v. 84, p. 19-34.
- Borst, A.M., Friis, H., Nielsen, T.F.D., and Waight, T.E., 2018, Bulk and Mush Melt Evolution in Agpaitic Intrusions: Insights from Compositional Zoning in Eudialyte, Ilímaussaq Complex, South Greenland: Journal of Petrology, v. 59, p. 589-612.
- Borst, A.M., Waight, T.E., Finch, A.A., Storey, M., and Roux, P.J.L., 2019, Dating agpaitic rocks: A multi-system (U/Pb, Sm/Nd, Rb/Sr and 40Ar/39Ar) isotopic study of layered nepheline syenites from the Ilímaussaq complex, Greenland: Lithos, v. 324-325, p. 74-88.
- Bowring, J.F., McLean, N.M., and Bowring, S.A., 2011, Engineering cyber infrastructure for U-Pb geochronology: Tripoli and U-Pb\_Redux: Geochemistry, Geophysics, Geosystems, v. 12, .

Chakhmouradian, A., and Wall, F., 2012, Rare Earth Elements: Minerals, Mines, Magnets (and More): Elements, v. 8, p. 333-340.

Chakrabarty, A., Pruseth, K.L., and Sen, A.K., 2011, First report of eudialyte occurrence from the Sushina hill region, Purulia district, West Bengal: Journal of the Geological Society of India, v. 77, p. 12-16.

Chakhmouradian, A., and Wall, F., 2012, Rare Earth Elements: Minerals, Mines, Magnets (and More): Elements, v. 8, p. 333-340, doi: 10.2113/gselements.8.5.333.

Charlier, B.L.A., Ginibre, C., Morgan, D., Nowell, G.M., Pearson, D.G., Davidson, J.P., and Ottley, C.J., 2006, Methods for the microsampling and high-precision analysis of strontium and rubidium isotopes at single crystal scale for petrological and geochronological applications: Chemical Geology, v. 232, p. 114-133.

Crocker, M.G., 2014, A petrographic, geochemical, and geochronological study of rare earth element mineralization in the red wine intrusive suite, Labrador, Canada.[Ph.D. thesis]: Memorial University of Newfoundland, p. 766.

Currie, K.L., Curtis, L.W., and Gittins, J., 1975, Petrology of the Red Wine alkaline complexes, Central Labrador and a comparison with the Ilímaussaq Complex, South West Greenland: Geological Survey of Canada Paper, v. 75, p. 271-280.

Currie, K.L., and Gittins, J., 1993, Preliminary report on peralkaline silica-undersaturated rocks in the Kipawa syenite gneiss complex, western Quebec: Papers-Geological Survey of Canada, p. 197.

Currie, K., and Vanbreemen, O., 1996, The origin of rare minerals in the Kipawa Syenite Complex, western Quebec: Canadian Mineralogist, v. 34, p. 435-451.

Curtis, L.W., and Gittins, J., 1979, Aluminous and titaniferous clinopyroxenes from regionally metamorphosed agpaitic rocks in central Labrador: Journal of Petrology, v. 20, p. 165-186.

Curtis, L.W., and Currie, K.L., 1981, Geology and Petrology of The Red Wine Alkaline Complex, Central Labrador: Geological Survey of Canada, p. 61.

DePaolo, D.J., and Wasserburg, G.J., 1976, Nd isotopic variations and petrogenetic models: Geophysical Research Letters, v. 3, p. 249-252.

DePaolo, D.J., 1988, Neodymium isotope geochemistry: an introduction: Berlin; New York, Springer-Verlag.

Dickin, A.P., and Guo, A., 2001, The location of the Allochthon Boundary Thrust and the Archean-Proterozoic suture in the Mattawa area of the Grenville Province: Nd isotope evidence: Precambrian Research, v. 107, p. 31-43.

Dickin, A.P., 2004, Nd model ages and U-Pb zircon ages: dating crustal formation in the grenville province.

Dickin, A.P., 2005, Radiogenic isotope geology: Cambridge, UK; New York, Cambridge University Press.

Dragovic, B., Samanta, L.M., Baxter, E.F., and Silverstone, J., 2012, Using garnet to constrain the duration and rate of water-releasing metamorphic reactions during subduction: An example from Sifnos, Greece: Chemical Geology, v. 314, p. 9-22.

Easton, R.M., 1992, 1992 Friends of the Grenville Workshop: Geoscience Canada.

Farrell, T.P., 2019, Investigating the Tectonic Significance of Spiral Garnets from the Betic-Rif Arc of Southern Spain and Northern Morocco Using Sm-Nd Garnet Geochronology [Ph.D. thesis]: United States -- Massachusetts, Boston College.

Faure, G., Mensing, T.M., and Faure, G., 2005, Isotopes : principles and applications: Hoboken, N.J., Wiley.

Ferguson, J., 1970, On the schistose structure of some lujavrites: Bulletin of the Geological Society of Denmark, v. 20, p. 67-68.

Gandhi, S.S., 1971, Regional Geology of the Seal Lake area: Labrador', (Unpublished 1: 250,000 Scale Map, Prepared for Brinex Corp.

Gandhi, S.S., Krogh, T.E., and Corfu, F., 1988, U-Pb zircon and titanite dates on two granitic intrusions in the Makkovik Province and a perakaline granite of the Red Wine Intrusive Complex, central Labrador. GAC-MAC Meeting, Program with Abstracts, p. A42.

Gower, C.F., Ryan, A.B., and Rivers, T., 1990, Mid-Proterozoic Laurentia–Baltica: an overview of its geological evolution and a summary of the contributions made by this volume: Mid-Proterozoic Laurentia-Baltica, v. 38, p. 1-20.

Gower, C.F., and Krogh, T.E., 2002, AU-Pb geochronological review of the Proterozoic history of the eastern Grenville Province: Canadian Journal of Earth Sciences, v. 39, p. 795-829.

Groulier, P., Indares, A., Dunning, G., Moukhsil, A., and Jenner, G., 2018, Syn-orogenic magmatism over 100 m.y. in high crustal levels of the central Grenville Province: Characteristics, age and tectonic significance: Lithos, v. 312-313, p. 128-152.

Guo, A., and Dickin, A.P., 1994, Determination of the southern limit of Archean crust in the Grenville Province of western Quebec by Nd model age mapping: Geol. Assoc. Canada. Prog. with Abs, v. 19, p. A44.

Harvey, J., and Baxter, E.F., 2009, An improved method for TIMS high precision neodymium isotope analysis of very small aliquots (1–10 ng): Chemical Geology, v. 258, p. 251-257.

Hatch, G.P., 2012, Dynamics in the global market for rare earths: Elements, v. 8, p. 341-346.

Herrell, M.K., Dickin, A.P., and Morris, W.A., 2006, A test of detailed Nd isotope mapping in the Grenville Province: delineating a duplex thrust sheet in the Kipawa Mattawa region: Canadian Journal of Earth Sciences, v. 43, p. 421-432.

Hill, J.D., Miller, R.R., Gower, C.F., Rivers, T., and Ryan, A.B., 1990, A review of Middle Proterozoic epigenic felsic magmatism in Labrador: Mid-Proterozoic Laurentia-Baltica. Edited by CF Gower, T.Rivers, and AB Ryan. Geological Association of Canada, Special Paper, v. 38, p. 417-431.

Hill, J.D., and Thomas, A., 1983, Correlation of two Helikian peralkaline granite – volcanic centres in central Labrador: Canadian Journal of Earth Sciences, v. 20, p. 753-763.

Horwitz, E.P., Chiarizia, R., Dietz, M.L., Diamond, H., and Nelson, D.M., 1993, Separation and preconcentration of actinides from acidic media by extraction chromatography: Analytica Chimica Acta, v. 281, p. 361-372.

Karup-Møller, S., Rose-Hansen, J., and Sørensen, H., 2010, Eudialyte decomposition minerals with new hitherto undescribed phases from the Ilímaussaq complex, South Greenland: Bulletin of the Geological Society of Denmark, v. 58, p. 75-88.

Kay, A., Hepburn, J.C., Kuiper, Y.D., and Baxter, E.F., 2017, Geochemical evidence for a Ganderian arc/back-arc remnant in the Nashoba Terrane, SE New England, USA: American Journal of Science, v. 317, p. 413-448.

Kerr, A., 2011, Rare-Earth-Element (REE) Mineralization in Labrador: A review of Known Environments and the Geological Context of Current Exploration Activity : , 109-143 p.

Kish, L., and Tremblay-Clark, P., 1978, Le district radioactif de Kipawa (Comté de Témiscamingue): Ministère Des Richesses Naturelles, DP-579.

Kramm, U., and Kogarko, L.N., 1994, Nd and Sr isotope signatures of the Khibina and Lovozero agpaitic centres, Kola Alkaline Province, Russia: *Lithos*, v. 32, p. 225-242.

Krogh, T.E., Corfu, F., Davis, D.W., Dunning, G.R., Heaman, L.M., Kamo, S.L., Machado, N., Greenough, J.D., and Nakamura, E., 1987, Precise U–Pb isotopic ages of diabase dykes and mafic to ultramafic rocks using trace amounts of baddeleyite and zircon: Mafic Dyke Swarms.Edited by HC Halls and WF Fahrig.Geological Association of Canada, Special Paper, v. 34, p. 147-152.

Lorenz, M., Altenberger, U., Trumbull, R.B., Lira, R., López de Luchi, M., Günter, C., and Eidner, S., 2019, Chemical and textural relations of britholite-and apatite-group minerals from hydrothermal REE mineralization at the Rodeo de los Molles deposit, Central Argentina: *American Mineralogist: Journal of Earth and Planetary Materials*, v. 104, p. 1840-1850.

Ludwig, K., 2008, Manual for isoplot 3.7: Berkeley Geochronology Center Special Publication, v. 4, p. 77.

Lumbers, S.B., Heaman, L.M., Vertolli, V.M., Wu, T.W., Gower, C.F., Rivers, T., and Ryan, A.B., 1990, Nature and timing of Middle Proterozoic magmatism in the Central Metasedimentary Belt, Grenville Province, Ontario: Mid-Proterozoic Laurentia–Baltica.Edited by CF Gower, T.Rivers, and AB Ryan.Geological Association of Canada, Special Paper, v. 38, p. 243-276.

Macdonald, R., and Upton, B.G., 1993, The Proterozoic Gardar rift zone, South Greenland: comparisons with the East African rift system: Geological Society, London, Special Publications, v. 76, p. 427-442.

Makishima, A., 2016, Thermal ionization mass spectrometry (TIMS): silicate digestion, separation, and measurement: Wiley-VCH.

Marks, M.A.W., and Markl, G., 2017, A global review on agpaitic rocks: *Earth-Science Reviews*, v. 173, p. 229-258.

Marks, M.A., W., Hettmann, K., Schilling, J., Frost, B., Ronald, and Markl, G., 2011, The Mineralogical Diversity of Alkaline Igneous Rocks: Critical Factors for the Transition from Miaskitic to Agpaitic Phase Assemblages: *Journal of Petrology*, v. 52, p. 439-455.

McLlland, J.M., Selleck, B.W., Bickford, M.E., Tollo, R.P., Bartholomew, M.J., Hibbard, J.P., and Karabinos, P.M., 2010, Review of the Proterozoic evolution of the Grenville Province, its Adirondack outlier, and the Mesoproterozoic inliers of the Appalachians: From Rodinia to Pangea: The Lithotectonic Record of the Appalachian Region: Geological Society of America Memoir, v. 206, p. 21-49.

Miller, R.R., 1988, Yttrium (Y) and other rare metals (Be, Nb, REE, Ta, Zr) in Labrador: Current Research. Government of Newfoundland and Labrador, Department of Mines, Mineral Development Division, Report, v. 88, p. 229-245.

Möller, V., and Williams-Jones, A.E., 2016, Stable and radiogenic isotope constraints on the magmatic and hydrothermal evolution of the Nechalacho Layered Suite, northwest Canada: *Chemical Geology*, v. 440, p. 248-274,

Pin, C., and Joannon, S., 2002, Combined cation-exchange and extraction chromatography for the concomitant separation of Zr, Hf, Th, and the Lanthanides from geological materials: *Talanta*, v. 57, p. 393-403.

Pin, C., and Zalduogui, J.S., 1997, Sequential separation of light rare-earth elements, thorium and uranium by miniaturized extraction chromatography: application to isotopic analyses of silicate rocks: *Analytica Chimica Acta*, v. 339, p. 79-89.

Pollington, A.D., and Baxter, E.F., 2010, High resolution Sm–Nd garnet geochronology reveals the uneven pace of tectonometamorphic processes: *Earth and Planetary Science Letters*, v. 293, p. 63-71.

Pollington, A.D., and Baxter, E.F., 2011, High precision microsampling and preparation of zoned garnet porphyroblasts for Sm–Nd geochronology: *Chemical Geology*, v. 281, p. 270-282.

Potts, P.J., 2012, A handbook of silicate rock analysis: Springer Science & Business Media,

Rakovan, J., McDaniel, D.K., and Reeder, R.J., 1997, Use of surface-controlled REE sectoral zoning in apatite from Llallagua, Bolivia, to determine a single-crystal SmNd age: *Earth and Planetary Science Letters*, v. 146, p. 329-336.

Regan, S.P., Walsh, G.J., Williams, M.L., Chiarenzelli, J.R., Toft, M., and McAleer, R., 2019, Syn-collisional exhumation of hot middle crust in the Adirondack Mountains (New York, USA): Implications for extensional orogenesis in the southern Grenville province: *Geosphere*, v. 15, p. 1240-1261.

Rivers, T., Martignole, J., Gower, C.F., and Davidson, A., 1989, New tectonic divisions of the Grenville Province, Southeast Canadian Shield: *Tectonics*, v. 8, p. 63-84.

Rivers, T., 1997, Lithotectonic elements of the Grenville Province: review and tectonic implications: *Precambrian Research*, v. 86, p. 117-154.

Rosman, K., and Taylor, P., 1998, Isotopic compositions of the elements 1997 (Technical Report): Pure and Applied Chemistry, v. 70, p. 217-235.

Schoene, B., and Baxter, E.F., 2017, Petrochronology and TIMS: Reviews in Mineralogy and Geochemistry, v. 83, p. 231-260.

Sjöqvist, A.S., Zack, T., Honn, D.K., and Baxter, E.F., 2020, Modification of a rare-earth element deposit by low-temperature partial melting during metamorphic overprinting: Norra Kärr alkaline complex, southern Sweden: *Chemical Geology*, p. 119640.

Sørrensen, H., 1992, Agpaitic nepheline syenites: a potential source of rare elements: *Applied Geochemistry*, v. 7, p. 417-427.

Sun, S., and McDonough, W.F., 1989, Chemical and isotopic systematics of oceanic basalts: implications for mantle composition and processes: Geological Society, London, Special Publications, v. 42, p. 313-345.

Thomas, A., 1981, Geology along the southwestern margin of the Central Mineral Belt: St. John's: Mineral Development Division, Government of Newfoundland and Labrador.

Thomas, A., and Hibbs, D., 1980, Geology of the southwestern margin of the central mineral belt: Newfoundland Geologic Survey; Current Research, p. 166-176.

van Breemen, O., and Currie, K., 2004, Geology and U-Pb geochronology of the Kipawa Syenite Complex - a thrust related alkaline pluton - and adjacent rocks in the Grenville Province of western Quebec: *Canadian Journal of Earth Sciences*, v. 41, p. 431-455.

Valentino, D.W., Chiarenzelli, J.R., and Regan, S.P., 2019, Spatial and temporal links between shawinigan accretionary orogenesis and massif anorthosite intrusion, southern grenville province, New York, U.S.A. *Journal of Geodynamics*, v. 129, p. 80-97.

Van Gosen, B.S., Verplanck, P.L., Seal II, R.R., Long, K.R., and Gambogi, J., 2017, Rare-earth elements: , 44 p.

Walker, S., Baxter, E., BIRD, A., and Ague, J.J., 2019, Barrovian, Not So Fast: Insights Into the Timing and Rate of Metamorphism in NE Scotland Using Garnet Sm-Nd Geochronology: Agufm, v. 2019, p. V43F-0152.

Wardle, R.J., Rivers, T., Gower, C.F., Nunn, G., and Thomas, A., 1986, The northeastern Grenville Province: new insights: The Grenville Province.Edited by JM Moore, A.Davidson, and AJ Baer.Geological Association of Canada, Special Paper, v. 31, p. 13-29.

Wasserburg, G.J., Jacobsen, S.B., DePaolo, D.J., McCulloch, M.T., and Wen, T., 1981, Precise determination of Sm/Nd ratios, Sm and Nd isotopic abundances in standard solutions: Geochimica Et Cosmochimica Acta, v. 45, p. 2311-2323.

Wu, F., Yang, Y., Marks, M.A.W., Liu, Z., Zhou, Q., Ge, W., Yang, J., Zhao, Z., Mitchell, R.H., and Markl, G., 2010, In situ U–Pb, Sr, Nd and Hf isotopic analysis of eudialyte by LA-(MC)-ICP-MS: Chemical Geology, v. 273, p. 8-34.



## **5.0 APPENDIX 1: DETAILED LABORATORY METHODS FOR EUDIALYTE GEOCHRONOLOGY**

This section describes the laboratory and analytical methods used in this study in order to construct internal mineral isochrons with eudialyte samples. Much of the laboratory procedure is adapted from use in other minerals, most notably garnet (Harvey and Baxter, 2009; Pollington and Baxter, 2010). However, preparations for eudialyte are somewhat different than those used for garnet and other common minerals, the procedure and crucial differences from other minerals are detailed below.

Samples used in this study were acquired through several channels. The Harvard Museum furnished a small sample of eudialyte from the Kipawa Syenite Complex from their research collection. This sample allowed us to test lab and analytical techniques generally adapted from procedures established for garnet. Previous work by Wu et al. (2010) characterized the Sm/Nd content of eudialyte from the Kipawa Syenite Complex using LA-ICP-MS, and provided a good working estimate for initial work. Additional Kipawa samples were collect in June 2019 with the help of Quebec Precious Metals (QPM), and consist of drill cores and larger hand samples. Core samples from the Red Wine Intrusive Suite were furnished by Search Minerals and Matthew Crocker.

## 5.1 MICROMILL SAMPLING

One advantage of studies utilizing LA-ICP-MS is the ability to sample materials *in-situ*, commonly facilitating the analysis of individual zonations within a single crystal. However, due to isobaric interferences precision can be insufficient for measuring very small variations in isotopic ratios. TIMS analysis provides superior precision, especially with small samples, but *in-situ* analysis is impossible. Charlier et al. (2006) developed a method using a computer controlled milling machine to facilitate spatially controlled isotopic studies using TIMS instrumentation. This method involves drilling tiny (~150 nm) pits in a sample billet within a single droplet of MQ H<sub>2</sub>O (Fig. 3). The water serves to cool the bit and contain the sample dust derived from the pit. After drilling the slurry is collected by pipette and prepared for analysis.

Charlier et al. (2006) originally demonstrated the utility of this approach by examining Rb-Sr in feldspars. Micromill sampling has also been used to selectively sample zoned garnets (Pollington and Baxter, 2011; Dragovic et al., 2012). More recently Sjöqvist

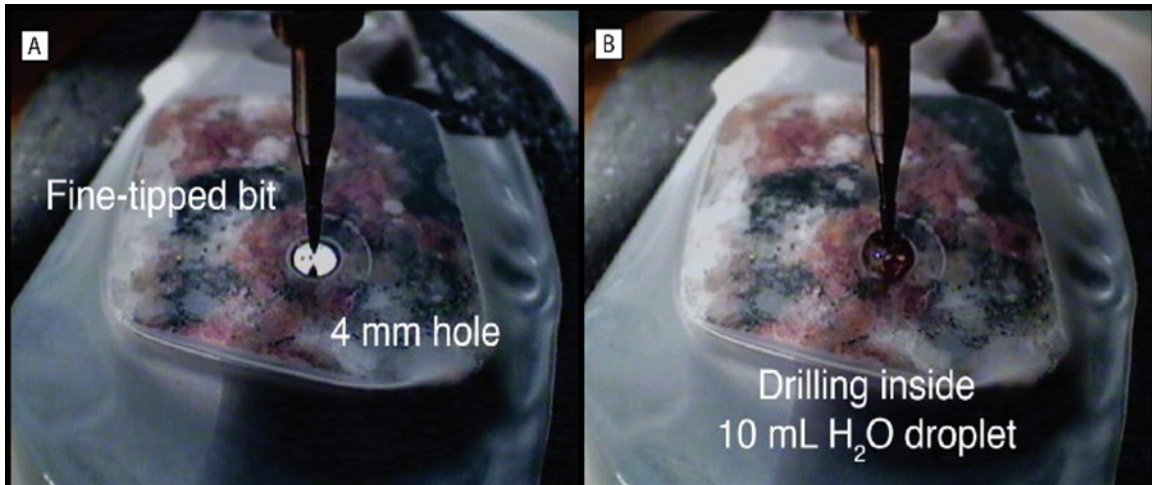


Figure 42. Photos showing the micromill drilling process. A- fine-tipped drill bit above the 4mm hole in Parafilm where drilling will occur. B- Drill in MQ H<sub>2</sub>O water droplet, water is held in place by 4mm hole in Parafilm shown in A. (Sjöqvist et al., 2020) I don't think this mentioned in text

et al. (2020) applied a similar technique to eudialyte. In the case of eudialyte, with exceptionally high Sm and Nd concentrations tiny pits ( $\sim 150 \mu\text{m}$ ) yield sufficient amounts of Sm and Nd ( $\sim 19 \text{ ng}$ ) for analysis (Sjöqvist et al., 2020).

The Micromill drilling unit is designed primarily as a miniature CNC machine in which a preprogramed track is cut by a high-speed drill bit. Using preprogramed tracks discrete growth zones in garnet and other minerals can be separated for subsequent analysis. The procedure for eudialyte drilling is far simpler and require less preparation but does require some adaptation. For accurate sampling the drill and microscope lens must be calibrated, this is most easily done by first pressing a pinprick hole in the parafilm around the drill site (Figure 42). The crosshairs of the microscope are then moved to intersect this small hole. Once calibrated the microscope can be used to select the drill site visually or based on supplemental images from SEM, LA-ICP-MS or EMP. Once the drill site is selected water should be added. The programmable motor steps in the z axis are too large for the desired bit size so the stage must be moved manually to ensure smooth drilling without cracking samples. The drill should be turned on before driving down into the water droplet to minimize the risk of water spray (Figure 42). Slowly driving bit down with a slow rotational speed has shown the best results in eudialyte.

With very high concentrations of Sm and Nd in eudialyte relative to garnet, 700 ppm Sm and 2400 ppm Nd vs. 3 ppm Sm and 4 ppm Nd (Farrell, 2020), contamination of other samples and clean spaces must be carefully considered. A typical drilled sample used in this study weighs between 0.03 mg and 0.06 mg after drying. This amount of material yields roughly 20 ng Sm and 70 ng Nd of material for sample analysis prior to aliquoting. Bulk samples derived from more traditional picking weight around 4.0 mg and yield 2.7

$\mu\text{g}$  Sm and  $8.2 \mu\text{g}$  Nd. Thus, micromill sampling conducted outside of the clean lab not only provides spatial control but also limits the amount of eudialyte that enters the lab to something similar in absolute terms to that of garnet limiting potential for contamination.

Similar to samples collected by more traditional methods of cutting, pulverizing, and picking, samples collected using the micromill must be accurately weighed prior to analysis in order to yield accurate determinations of Sm and Nd concentrations. The weight of the sample is important in the process of isotope dilution and spike subtraction after TIMS analysis to yield accurate concentration measurements (Faure and Mensing, 2005). The volume of sample furnished by the drilling procedure is very small, typically between 0.003 and 0.006 mg approaching the precision of the balance used in laboratory. This introduces some uncertainty into the sample mass, and thus into calculations of spike-subtracted concentrations. While not critical accurate determinations of Sm and Nd concentrations can be a useful check on proper dissolution and potential contamination from other minerals like britholite and mosandrite. Consistent and accurate weighing for small samples remains a possible area of improvement for this method.

## 5.2 DISSOLUTION

The dissolution procedure detailed below is partially adapted from procedures developed for garnet (Harvey and Baxter, 2009; Pollington and Baxter, 2010). It should be noted that eudialyte derives its name from a propensity to readily dissolve in acid (*eu*: well; *dialytos*: dissolved), and can be dissolved in concentrated  $\text{HNO}_3$  alone (Chakraborty et al., 2011).

Sample dissolution begins in 100 µL of concentrated HF and 1000 µL of 16N HNO<sub>3</sub> placed on a hotplate set at 120-140°c overnight. Clear-white sample residual is common in bulk samples where material is visible. The sample is then dried down and brought up in 16N HNO<sub>3</sub> and 6N HCL and fluxed overnight. Finally, to prevent the formation of secondary fluorides (Makishima, 2016).

For spiking and aliquoting the sample is once again dried and brought up in 1.5N HCL and 16N HNO<sub>3</sub>, which serves as the standard laboratory storage solution. As eudialyte has exceptionally high concentrations of Sm and Nd (900 ppm, 2400 ppm respectively) only a small aliquot (~0.03 µL or ~0.03 mg rock equivalent) in bulks samples, drilled samples are considerably smaller and all of the sample is typically used.

### 5.3 SPIKING

Absolute isotope concentrations are difficult to determine by mass spectrometry, however, isotopic ratios can be analyzed with very high precision (Potts, 2004). In what is known as isotope dilution, a spike artificially enriched in a particular isotope is added to the sample of natural composition to be analyzed. By measuring the isotopic composition of the spiked sample and subsequently ‘subtracting out’ the known composition and volume of the spike it possible to calculate elemental concentration as well as a very precise measurement of isotopic ratios (Dickin, 2004). Unlike in-situ techniques analyzing spike and sample concentrations together minimizes concerns of differential fractionation, and thus the precision accuracy of a derived date is tied to the known composition of the spike (Schoene and Baxter, 2017). Adding too much or too little spike can undermine the

precision of a measurement relying on isotope dilution by significantly increasing error magnification (Dickin, 2004). Accurately spiking a sample depends on an accurate estimate of Sm and Nd concentrations in a sample. Spike is added to sample aliquots in acid and must be accurately weighed to allow for precise spike subtraction following TIMS analysis. After spiking and weighing samples are dried down in preparation of cation exchange columns.

#### **5.4 CATION EXCHANGE COLUMNS**

After spiking the sample is ready to be refined for TIMS analysis. In the case of Sm/Nd, all other REE's must be removed to avoid deleterious isobaric interferences that would obscure measured ratios (Schoene and Baxter, 2017). The three stages of column chemistry required to reduce the sample to cuts of Sm and Nd are detailed below. Column chemistry procedures for eudialyte are identical to garnet and other minerals, after aliquoting a similar material to a garnet sample will need to be refined.

Iron and titanium are two metals commonly encountered in geologic materials.  $\text{Fe}^{3+}$  and Ti can interfere with TRU-Spec columns (discussed below) as these metals elute under the same conditions as the LREE's (Pin and Joannon, 2002). To facilitate better purification the first step of column chemistry is an iron clean up column. For iron columns our laboratory utilizes 13 cm columns made from disposable plastic pipettes filled with AG50w-X4 resin. After washing the resin with 6N HCL and conditioning with 1.5 N HCL the sample is rinsed in with 1.5N HCL to remove iron and titanium. After 1.5N HCL rinse the REE's are eluted in 6N HCL for the next stage of purification (Harvey and Baxter,

2009). When elution is completed the samples are dried and brought up in 2N HNO<sub>3</sub> in preparation for TRU-Spec columns.

While Fe<sup>3+</sup> has been shown to have the most detrimental effects on LREE yields, other cations must be removed after pretreatment for iron. TRU- Spec (**t**ransuranic-element **s**pecific) resin consists of octyl(phenyl)-N,N-diisobutyl-carbamoylmethyl phosphine oxide (CMPO) in tri-n-butyl phosphate (TBP) sorbed on a polymeric substrate known as Amberchrom (Horowitz et al., 1993). The substrate is fine grained (50-100 um), yielding narrower elution bands than previously available, coarser substrates (Pin and Santo Zalduegui, 1997). Lanthanides, Hf, Zr, and Th have the highest affinity for cation exchange resin with nitric acid. Other common cations (Ca, Na) are poorly retained (Pin and Joannon, 2002) and can be rinsed out of the sample. The cations retained by the TRU spec resin can then be selectively removed based on differential retention. Most importantly for Sm-Nd analysis LREE can be stripped by using very dilute HNO<sub>3</sub> (Horowitz et al., 1993; Pin and Santo Zalduegui, 1997).

Following the procedure of Harvey and Baxter (2009) the next stage of purification uses Eichrom TRU-spec in Teflon microcolumns with a 4ml reservoir over .2 ml of resin. After a thorough rinse with MQ H<sub>2</sub>O the resin is cleaned with 0.05N HNO<sub>3</sub> and conditioned with 2N HNO<sub>3</sub> before sample is loaded in 2N HNO<sub>3</sub>. The sample is then washed with an additional 3.8 mL 2N HNO<sub>3</sub> before the lanthanide portion is eluted from the column with 0.05N HNO<sub>3</sub>. Samples are dried down to a single small droplet, and brought up in 0.75N HCL. Complete dry down is avoided to ensure the samples stays in solution in the weak HCL used for subsequent columns. This process of drying down and diluting the sample

in 0.75N HCL is repeated once or more to remove any residual HNO<sub>3</sub>. Ultimately the sample is brought up in 0.75N HCL to be loaded into the next column.

Before TIMS analysis it is essential to remove all LREE's, and isolate Sm and Nd into separate cuts. This stage of purification uses a 294 mm column of AG50W-x4 in Teflon column with 10 mL reservoir (Harvey and Baxter, 2009). The resin used here is the same as the earlier iron cleanup columns, but follows a different, more complex, cleaning procedure prior to resin use. For these columns  $\alpha$ -hydroxyiso-butyric acid (HIBA; 2-methyl-lactic acid or MLA) is used to remove Sm and Nd from the other REE's, this process requires accurate calibration of MLA pH and temperature for consistent results (Schoene and Baxter, 2017). The MLA is purified by recrystallization in Teflon containers prior to dissolution in MQ H<sub>2</sub>O and buffered to the desired pH. The Boston College Isotope Geochemistry lab uses 0.2 M MLA buffered to pH of 4.6±0.02 with NH<sub>4</sub>OH.

The AG50W-x4 resin is conditioned with 0.2M MLA prior to sample loading in 0.75 M HCL. The sample is then washed into the column with an additional 100  $\mu$ L of 0.75N HCL and 200  $\mu$ L of 0.2N MLA before rinsing the sample with 0.2N MLA. Sm is eluted 0.2 MLA, and Nd is eluted in 0.2N H after a 2 mL rinse of 0.2N MLA. Yields are usually high, the calibration for the bottle of MLA used for this study produced a Sm yield of 87.50% and a Nd yield of 87.15%. The separate cuts of Sm and Nd are dried overnight before a 2-3 hour period of fluxing in 7N HNO<sub>3</sub> and 6N HCL. The samples are then dried and brought up in concentrated HNO<sub>3</sub> in an effort to remove any residual MLA, and again dried prior to loading for the TIMS.

## 5.5     LOADING

The Boston College TIMS facility analyzes Nd as the oxide NdO<sup>+</sup>, and Sm as a metal. At this stage in the preparation for TIMS analysis the procedures for the two elements diverge. Filaments are loaded under varying levels of stable current, allowing for the careful drying of samples onto the thin (0.7 mm x 0.04 mm) filaments. For both Sm and Nd analysis two small dams of Parafilm are melted onto the filament at 1.0 A. The Parafilm dams help to confine droplets of sample and activator to the middle third of the Re filament. Dry Nd cuts are dissolved in 1  $\mu$ L 2N HNO<sub>3</sub>, and loaded onto the filament at 0.6 A. The sample is allowed to dry until close to dry, before 2  $\mu$ L of activator (50 mg Ta<sub>2</sub>O<sub>5</sub> powder in 3 mL 5% H<sub>3</sub>PO<sub>4</sub>) is added at 0.6 A (Harvey and Baxter, 2009). The Ta<sub>2</sub>O<sub>5</sub> slurry provides a stable source of oxygen during analysis, and facilitates more precise measurements than the traditional gas bleed method. This procedural improvement is especially advantageous for small samples (Harvey and Baxter, 2009). After loading the activator, the current on the filament is increased to 1.0 A and the sample is dried for 10 minutes. Following the drying period the current is slowly increased until the middle portion of the filament glows red for ~5 seconds before current is shut off.

Sm is analyzed as a metal and analysis is conducted using a Ta filament. Similar to Nd loading, Parafilm dams are melted to the filament to help contain the sample and other solutions to the center of the thin Ta ribbon. 2N HCL is loaded and dried to a small droplet to which the sample, dissolved in 2N HNO<sub>3</sub>, is added at 0.6 A. Before final heating of filament H<sub>3</sub>PO<sub>4</sub> is added to the sample. Current on the filament is slowly ramped up until the filament briefly glows, usually around 2.5 A.

## **5.6     TIMS ANALYSIS**

Once the samples have been loaded onto filaments, they are securely fastened to the barrel of the TIMS. The Boston College Facility uses an Isotopx Phoenix instrument which is controlled using Isotopx Ion Vantage software. With the barrel installed into the source the instrument is allowed to pump to high vacuum, usually overnight. The line of sight is not opened until the vacuum is below  $5\text{e}^{-8}$ . Sm and Nd are run in two different manners, Sm is analyzed as a metal while Nd is analyzed as the oxide  $\text{NdO}^+$ . Sm analyses are run static, and the mass collected in each faraday cup is kept constant through the duration of the run.  $\text{NdO}^+$  is analyzed using a multi-dynamic method where the magnetic field fluctuates to switch the mass analyzed by each collector in effect scanning over a range of masses. The oxide mass collected in each faraday cup for the three sequences of the multi-dynamic analysis are shown in (Figure 43). By analyzing masses in different cups it is possible to monitor mass fractionation and correct for amplifier bias (Dickin, 2005).

## **5.7     DATA CORRECTION**

A variety of corrections are made by the Isotopx Ion Vantage software to account for oxygen isotopes, isobaric interferences, and mass fractionation within the instrument. While the data output from Ion Vantage includes raw ratios for review, these corrections are entirely automated. Such corrections are described briefly below.

Mass fractionation occurs in the TIMS instrument as ionization requires the breaking of bonds, which is a mass dependent process. Lighter isotopes are preferentially ionized, as result there is a trend towards heavier isotopes through the course of an analytical run. While this process follows a Rayleigh fractionation law fractionation can result in errors up to 1% measured ratios (Dickin, 2005). For elements with at least two non-radiogenic isotopes a mass fractionation correction can be applied (Potts, 2004). For example,  $^{143}\text{Nd}/^{144}\text{Nd}$  ratios are corrected for mass fractionation by using an exponential law to normalize to  $^{146}\text{Nd}/^{144}\text{Nd} = 0.7219$  (Wasserburg et al., 1981). Sm is similarly normalized to  $^{149}\text{Sm}/^{152}\text{Sm} = 0.51686$ . The corrections used assume that fractionation is independent of absolute mass and is controlled by relative mass difference alone. (Dickin,

Oxide mass	157	158	159	160	162	164	166	168	170
Element mass	141	142	143	144	146	148	150	152	154
Isotope required	$^{141}\text{Pr}^{16}\text{O}^+$	$^{142}\text{Nd}^{16}\text{O}^+$	$^{143}\text{Nd}^{16}\text{O}^+$	$^{144}\text{Nd}^{16}\text{O}^+$	$^{146}\text{Nd}^{16}\text{O}^+$	$^{148}\text{Nd}^{16}\text{O}^+$	$^{150}\text{Nd}^{16}\text{O}^+$	$^{152}\text{Sm}^{16}\text{O}^+$	$^{154}\text{Sm}^{16}\text{O}^+$
Possible isobaric interferences	$^{140}\text{Ce}^{17}\text{O}^+$	$^{141}\text{Pr}^{17}\text{O}^+$	$^{141}\text{Pr}^{18}\text{O}^+$	$^{144}\text{Sm}^{16}\text{O}^+$	$^{144}\text{Sm}^{18}\text{O}^+$	$^{146}\text{Nd}^{18}\text{O}^+$	$^{148}\text{Nd}^{18}\text{O}^+$	$^{150}\text{Nd}^{18}\text{O}^+$	$^{152}\text{Sm}^{18}\text{O}^+$
	$^{139}\text{La}^{18}\text{O}^+$	$^{140}\text{Ce}^{18}\text{O}^+$	$^{142}\text{Ce}^{17}\text{O}^+$	$^{142}\text{Ce}^{18}\text{O}^+$	$^{144}\text{Nd}^{18}\text{O}^+$	$^{147}\text{Sm}^{17}\text{O}^+$	$^{149}\text{Sm}^{18}\text{O}^+$	$^{150}\text{Sm}^{18}\text{O}^+$	
	$^{138}\text{Ba}^{19}\text{F}^+$	$^{142}\text{Ce}^{16}\text{O}^+$	$^{142}\text{Nd}^{17}\text{O}^+$	$^{143}\text{Nd}^{17}\text{O}^+$	$^{145}\text{Nd}^{17}\text{O}^+$	$^{148}\text{Sm}^{16}\text{O}^+$		$^{150}\text{Sm}^{16}\text{O}^+$	
				$^{142}\text{Nd}^{18}\text{O}^+$					

Table 6. Oxide masses, with elemental mass and potential isobaric interferences. Note recurring Nd masses with varying O mass. (Harvey and Baxter, 2009) 2005)

This facility analyzes Nd as the oxide  $\text{NdO}^+$  instead of as a metal which allows for analysis of significantly smaller sample volumes at lower temperatures. However, when analyzed as an oxide both the isotopic composition of Nd and O must be considered (Table 6). While  $^{16}\text{O}$  is the dominant isotope of oxygen (99.76%), the heavier isotopes  $^{17}\text{O}$  and  $^{18}\text{O}$  occur in sufficient quantities (0.04% and 0.20% respectively) to necessitate an oxygen correction to remove the influence of isobaric interferences caused by variable oxygen mass. For example, a collector set for  $^{146}\text{Nd}^{16}\text{O}^+$  would also collect  $^{144}\text{Nd}^{18}\text{O}^+$  and  $^{145}\text{Nd}^{17}\text{O}^+$ , more masses and potential interferences are presented in Table 1. Corrections rely on the measured ratios of  $^{17}\text{O}/^{16}\text{O}$  and  $^{18}\text{O}/^{16}\text{O}$  which can vary significantly between

laboratories (Harvey and Baxter, 2009). The particular value of  $^{17}\text{O}/^{16}\text{O}$  and  $^{18}\text{O}/^{16}\text{O}$  for the BC TIMS is embedded in the spreadsheet used for mass based corrections. These values were calculated by two primary methods after Harvey and Baxter (2009). First, a purified Pr solution was analyzed as oxide with collectors set for masses of 157, 158, and 159. Since Pr is monoisotopic these masses correspond to  $^{141}\text{Pr}^{16}\text{O}^+$ ,  $^{141}\text{Pr}^{17}\text{O}^+$ , and  $^{141}\text{Pr}^{16}\text{O}^+$ . Second,  $^{150}\text{NdO}^+$  was analyzed to similarly mass fractionation and simultaneously dispel concerns regarding about ionization efficiency in  $\text{PrO}^+$ .

It is also important to be able to correct for isobaric interferences caused by other elements such as  $^{140}\text{Ce}^{16}\text{O}^+$  and  $^{141}\text{Pr}^{16}\text{O}^+$  in  $\text{NdO}^+$  analysis, and  $^{152}\text{Gd}$  in Sm analysis. While cation exchange columns should remove the majority of this material, some fraction of other LREE often remains. Masses not associated with Sm or Nd isotopes are thus monitored to allow for isobaric interference corrections, in particular mass 156 ( $^{140}\text{Ce}^{16}\text{O}^+$ )

NdO Dynamic									
L5	L4	L3	L2	AX	H1	H2	H3	H4	
156	157	158	159	160	161	162	163	164	
157	158	159	160	161	162	163	164	165	
158	159	160	161	162	163	164	165	166	

Sm Static									
L5	L4	L3	L2	AX	H1	H2	H3	H4	
144	146	147	148	149	150	152	154	155	

Figure 43. Summary of mass analyzed during analysis, red highlights for emphasis of important masses.  $\text{NdO}^+$  multi-dynamic analysis (top) cycles through 3 configurations to ‘scan’ oxide masses 156-166. Sm static analysis utilizes a single configuration to measure masses 144-155.

and 157 ( $^{141}\text{Pr}^{16}\text{O}^+$ ) are used in Nd analysis to monitor for Ce and Pr oxides while  $^{155}\text{Gd}$  is used to correct for  $^{152}\text{Gd}$  interferences on  $^{152}\text{Sm}$  (Potts, 2012). In a manner, similar to the oxygen correction mentioned above, isobaric interferences can be corrected by combining the monitoring signals and natural isotopic abundances and subtracted from measured ratios.

## 5.8 DATA REDUCTION AND SPIKE SUBTRACTION

The data derived from the TIMS analysis in many cases needs to be further reduced to remove data shown to have run poorly or deviated significantly from ideal running conditions. The Isotopx Ion Vantage software used to control the TIMS run will remove individual measurements that fall outside 2 sigma standard deviation. For more intensive data reduction other software must be used. Tripoli was designed as a data visualization and data reduction interface by Charleston College and MIT. The software was first developed for use in U-Pb analyses but can be easily configured for Sm-Nd analyses. Tripoli includes interactive time series graphs of measured ratios, which allow the user to identify and exclude data points in real time (Bowring et al., 2011). In most cases data is removed when ratios begin to scatter near the end of analysis, which if included in the final data can unnecessarily decrease analytical precision. For example, data displaying anomalous fractionation trends can also be easily identified and removed in the Tripoli interface. As selections are made Tripoli recalculates isotopic ratios which are then used in the following steps to build an isochron.

While the corrections for isobaric interferences and fractionation trends described above are conducted automatically by modern instrumentation a correction for the spike solution or ‘spike subtraction’ must also be performed. This correction is performed in an excel spreadsheet, beginning with sample and spike weight and corrected ratios the known spike value are subtracted yielding concentrations (Dickin, 2005). However, because the spike solution added to the sample effects the ratios used for mass fractionation corrections ( $^{146}\text{Nd}/^{144}\text{Nd}=0.7219$ ;  $^{149}\text{Sm}/^{152}\text{Sm}=0.51686$ ) spike subtraction must be conducted iteratively. After the initial subtraction, the ratios must be renormalized, before again accounting for the spike solution.

## 5.9 ISO PLOT

The corrected and reduced data from are condensed into a single spreadsheet with the goal of finally creating an isochron. A two point isochron consists of a straight line between two points and is relatively easy to plot. The slope of the resulting line  $m$  is defined as  $m = e^{\lambda t} - 1$ , subsequently solving for  $t$  yields the age of the material analyzed (Faure and Mensing, 2005). However, most geochronological studies rely on more robust multi-point isochrons. In this case a more complex procedure for plotting a line of best fits required. Isoplot is an add-in for Microsoft Excel developed by the Berkley Geochronology Center designed to perform a wide variety of geochronology-specific functions. Importantly, Isoplot can quickly and accurately construct a multipoint isochron and calculate descriptive statistics important for critical data assessment like mean square weighted deviation (MSWD) and error associated with the calculated age (Ludwig, 2008).

For the calculation of age uncertainties, the poorer of internal and external reproducibility is used.

## 6.0 APPENDIX 2: SPIKE SUBTRACTION SHEETS

Full Sample Name: <b>KPI-2.1-1</b>	Date of TIMS analysis: <b>2/4/2020</b>	Position #: <b>7</b>														
estimated Nd load (ng): <b>25</b>																
<b>Rspike Values Nd [SmNd 0.15 A spike, 6-12-08 calib]</b>																
<table border="1" style="width: 100%; border-collapse: collapse;"> <tr> <td>142/144</td><td>143/144</td><td>145/144</td><td>146/144</td><td>148/144</td><td>150/144</td><td>[Nd150]</td></tr> <tr> <td>0.830433</td><td>0.494001</td><td>0.436936</td><td>0.885201</td><td>0.740574</td><td>198.371260</td><td>0.125778 nm/g</td></tr> </table>			142/144	143/144	145/144	146/144	148/144	150/144	[Nd150]	0.830433	0.494001	0.436936	0.885201	0.740574	198.371260	0.125778 nm/g
142/144	143/144	145/144	146/144	148/144	150/144	[Nd150]										
0.830433	0.494001	0.436936	0.885201	0.740574	198.371260	0.125778 nm/g										
Wt Sample (g)= <b>2.41074E-05</b> g																
Wt Spike (g)= <b>0.536385</b> g																
Mass Spectrometer Information:																
Number of cycles measured: <b>35</b>																
Number of cycles used: <b>30</b>																
Filament Current range: from <b>3.3</b>	start	average (from sheet) <b>3.31</b>	Amps													
Beam intensity range: from <b>0.5121638</b>		<b>0.5347674</b>	Volts 144Nd.16O													
Temperature range: from <b>1573</b>		<b>1609</b>	°C													
Final Ratio Data:																
Interference Values (oxide corrected; informational only... not used in this sheet)																
Ce140/Nd144 <b>0.012055378</b>																
Pr141/Nd144 <b>0.38976379</b>																
Sm149/Nd144 <b>5.56463E-05</b>																
for Ratios & %ISE: use grand mean oxygen corr, interference corr, exp normalized values																
142/144	143/144	145/144	146/144	148/144	150/144											
Ratios <b>1.1414329</b>	<b>0.512592</b>	<b>0.3488364</b>	<b>0.7219</b>	<b>0.24487933</b>	<b>1.9201098</b>											
%StdErr <b>0.001063062</b>	<b>0.000899</b>	<b>0.0011223</b>	<b>0</b>	<b>0.00245335</b>	<b>0.0025163</b>											
for comparison only																
142/144	143/144	145/144	146/144	148/144	150/144											
DePaolo 88, p.14, ln. B': 1.141854	na	0.348416	0.721882	0.241572	na											
<b>FINAL DATA TO REPORT: 146/144 set to 0.7219</b>																
142/144	143/144	145/144	146/144	148/144	150/144											
Ratios <b>1.141863</b>	<b>0.512248</b>	<b>0.348418</b>	<b>0.721900</b>	<b>0.241553</b>	<b>0.236478</b>											
± 2 S.E. <b>0.000024</b>	<b>0.000009</b>	<b>0.000008</b>	<b>0.000000</b>	<b>0.000012</b>	<b>0.000012</b>											
Epsilon143= -7.60 using (143/144)chur= 0.512638 ± 0.18 (Hamilton et al. 1983)																
linked from Sm sheet			[Nd144]= 1635.31977 nm/g ± 0.08609													
[Sm]= 338.559636 nm/g ± 0.327358			[Nd]= 991.78002 ppm ± 0.05221													
[Sm]= 339.442389 ppm ± 0.328212			TOT ng Sm= 8.18307345 TOT ng Nd= 23.9092376													
Sm147/Nd144= 0.207030 ± 2 S.E. 0.000200 ± 2RSE % 0%																

Full Sample Name: <b>KPI-2.1_2 Nd</b>	Date of TIMS analysis: <b>2/4/2020</b>	Position #: <b>8</b>																								
estimated Nd load (ng): <b>25</b>																										
<b>Rspike Values Nd {SmNd 0.15 A spike, 6-12-08 calib}</b>																										
<table border="1" style="width: 100%; border-collapse: collapse;"> <tr> <td>142/144</td><td>143/144</td><td>145/144</td><td>146/144</td><td>148/144</td><td>150/144</td><td>[Nd150]</td></tr> <tr> <td>0.830433</td><td>0.494001</td><td>0.436936</td><td>0.885201</td><td>0.740574</td><td>198.371260</td><td>0.125778</td></tr> <tr> <td></td><td></td><td></td><td></td><td></td><td></td><td>nm/g</td></tr> </table>			142/144	143/144	145/144	146/144	148/144	150/144	[Nd150]	0.830433	0.494001	0.436936	0.885201	0.740574	198.371260	0.125778							nm/g			
142/144	143/144	145/144	146/144	148/144	150/144	[Nd150]																				
0.830433	0.494001	0.436936	0.885201	0.740574	198.371260	0.125778																				
						nm/g																				
Wt Sample (g)= <b>2.41E-05</b> g Wt Spike (g)= <b>0.53577</b> g																										
Mass Spectrometer Information:																										
<table border="1" style="width: 100%; border-collapse: collapse;"> <tr> <td>Number of cycles measured: <b>180</b></td><td></td></tr> <tr> <td>Number of cycles used: <b>153</b></td><td></td></tr> <tr> <td style="text-align: center;">Filament Current range: from <b>3.61</b></td><td style="text-align: center;">average (from sheet) <b>3.64</b></td></tr> <tr> <td style="text-align: center;">Beam intensity range: from <b>1.1830612</b></td><td style="text-align: center;">Volts 144Nd.16O</td></tr> <tr> <td style="text-align: center;">Temperature range: from <b>1480</b></td><td style="text-align: center;">°C <b>1562</b></td></tr> </table>			Number of cycles measured: <b>180</b>		Number of cycles used: <b>153</b>		Filament Current range: from <b>3.61</b>	average (from sheet) <b>3.64</b>	Beam intensity range: from <b>1.1830612</b>	Volts 144Nd.16O	Temperature range: from <b>1480</b>	°C <b>1562</b>														
Number of cycles measured: <b>180</b>																										
Number of cycles used: <b>153</b>																										
Filament Current range: from <b>3.61</b>	average (from sheet) <b>3.64</b>																									
Beam intensity range: from <b>1.1830612</b>	Volts 144Nd.16O																									
Temperature range: from <b>1480</b>	°C <b>1562</b>																									
Final Ratio Data:																										
Interference Values (oxide corrected; informational only... not used in this sheet) Ce140/Nd144 <b>0.00019</b> Pr141/Nd144 <b>0.00252</b> Sm149/Nd144 <b>2E-05</b>																										
<i>for Ratios &amp; %ISE: use grand mean oxygen corr, interference corr, exp normalized values</i>																										
<table border="1" style="width: 100%; border-collapse: collapse;"> <tr> <td></td><td>142/144</td><td>143/144</td><td>145/144</td><td>146/144</td><td>148/144</td><td>150/144</td></tr> <tr> <td>Ratios</td><td><b>1.141019</b></td><td><b>0.512832</b></td><td><b>0.349177</b></td><td><b>0.7219</b></td><td><b>0.24764259</b></td><td><b>3.302541</b></td></tr> <tr> <td>%StdErr</td><td><b>0.000944</b></td><td><b>0.000619</b></td><td><b>0.0007918</b></td><td><b>0</b></td><td><b>0.00146111</b></td><td><b>0.0018778</b></td></tr> </table>				142/144	143/144	145/144	146/144	148/144	150/144	Ratios	<b>1.141019</b>	<b>0.512832</b>	<b>0.349177</b>	<b>0.7219</b>	<b>0.24764259</b>	<b>3.302541</b>	%StdErr	<b>0.000944</b>	<b>0.000619</b>	<b>0.0007918</b>	<b>0</b>	<b>0.00146111</b>	<b>0.0018778</b>			
	142/144	143/144	145/144	146/144	148/144	150/144																				
Ratios	<b>1.141019</b>	<b>0.512832</b>	<b>0.349177</b>	<b>0.7219</b>	<b>0.24764259</b>	<b>3.302541</b>																				
%StdErr	<b>0.000944</b>	<b>0.000619</b>	<b>0.0007918</b>	<b>0</b>	<b>0.00146111</b>	<b>0.0018778</b>																				
<i>for comparison only</i> DePaolo 88, p.14, ln. B': <b>1.141854</b> na <b>0.348416</b> <b>0.721882</b> <b>0.241572</b> na																										
<b>FINAL DATA TO REPORT:</b>																										
146/144 set to 0.7219																										
<table border="1" style="width: 100%; border-collapse: collapse;"> <tr> <td></td><td>142/144</td><td>143/144</td><td>145/144</td><td>146/144</td><td>148/144</td><td>150/144</td><td>150t/144s</td></tr> <tr> <td>Ratios</td><td><b>1.141814</b></td><td><b>0.512203</b></td><td><b>0.348412</b></td><td><b>0.721900</b></td><td><b>0.241578</b></td><td><b>0.236478</b></td><td><b>0.317073</b></td></tr> <tr> <td>± 2 S.E.</td><td><b>0.000022</b></td><td><b>0.000006</b></td><td><b>0.000000</b></td><td><b>0.000007</b></td><td><b>0.000009</b></td><td><b>0.000012</b></td><td></td></tr> </table>				142/144	143/144	145/144	146/144	148/144	150/144	150t/144s	Ratios	<b>1.141814</b>	<b>0.512203</b>	<b>0.348412</b>	<b>0.721900</b>	<b>0.241578</b>	<b>0.236478</b>	<b>0.317073</b>	± 2 S.E.	<b>0.000022</b>	<b>0.000006</b>	<b>0.000000</b>	<b>0.000007</b>	<b>0.000009</b>	<b>0.000012</b>	
	142/144	143/144	145/144	146/144	148/144	150/144	150t/144s																			
Ratios	<b>1.141814</b>	<b>0.512203</b>	<b>0.348412</b>	<b>0.721900</b>	<b>0.241578</b>	<b>0.236478</b>	<b>0.317073</b>																			
± 2 S.E.	<b>0.000022</b>	<b>0.000006</b>	<b>0.000000</b>	<b>0.000007</b>	<b>0.000009</b>	<b>0.000012</b>																				
<b>Epsilon143= -8.44 using (143/144)chur= 0.512638</b> ± 0.12 (Hamilton et al. 1983)																										
<i>linked from Sm sheet</i> [Sm147]= ##### nm/g ± 0.016131 [Sm]= ##### ppm ± 0.016173 TOT ng Sm= <b>4.258629</b>																										
[Nd144]= 886.77871 nm/g ± 0.03414 [Nd]= 537.80882 ppm ± 0.02071 TOT ng Nd= <b>12.9585036</b>																										
Sm147/Nd144= <b>0.198791</b> ± 2 S.E. <b>0.000020</b> ± 2RSE % <b>0%</b>																										

Full Sample Name: <b>KP1-2.1_3</b> Nd	Date of TIMS analysis: <b>1/29/2020</b>	Position #: <b>9</b>																								
estimated Nd load (ng): <b>25</b>																										
<b>Rspike Values Nd [SmNd 0.15 A spike, 6-12-08 calib]</b>																										
<table border="1" style="width: 100%; border-collapse: collapse;"> <tr> <td>142/144</td><td>143/144</td><td>145/144</td><td>146/144</td><td>148/144</td><td>150/144</td><td>[Nd150]</td></tr> <tr> <td>0.830433</td><td>0.494001</td><td>0.436936</td><td>0.885201</td><td>0.740574</td><td>198.371260</td><td>0.125778</td></tr> <tr> <td colspan="3" style="text-align: center;">nm/g</td><td></td><td></td><td></td><td></td></tr> </table>			142/144	143/144	145/144	146/144	148/144	150/144	[Nd150]	0.830433	0.494001	0.436936	0.885201	0.740574	198.371260	0.125778	nm/g									
142/144	143/144	145/144	146/144	148/144	150/144	[Nd150]																				
0.830433	0.494001	0.436936	0.885201	0.740574	198.371260	0.125778																				
nm/g																										
Wt Sample (g)= <b>2.4059E-05</b> g Wt Spike (g)= <b>0.535635</b> g																										
Mass Spectrometer Information:																										
Number of cycles measured: <b>47</b> Number of cycles used: <b>47</b> <table border="1" style="margin-left: auto; margin-right: auto; border-collapse: collapse;"> <tr> <td style="padding: 2px;">start</td><td style="padding: 2px;">average (from sheet)</td></tr> <tr> <td style="padding: 2px;">3.75</td><td style="padding: 2px;">3.77</td></tr> </table> Filament Current range: from <b>3.75</b> Amps Beam intensity range: from <b>1.2098757</b> Volts 144Nd.16O Temperature range: from <b>1540</b> °C			start	average (from sheet)	3.75	3.77																				
start	average (from sheet)																									
3.75	3.77																									
Final Ratio Data:																										
Interference Values (oxide corrected; informational only... not used in this sheet) Ce140/Nd144 <b>0.00499981</b> Pr141/Nd144 <b>0.93200147</b> Sm149/Nd144 <b>3.2847E-05</b>																										
<i>for Ratios &amp; %1SE: use grand mean oxygen corr, interference corr, exp normalized values</i>																										
<table border="1" style="width: 100%; border-collapse: collapse;"> <tr> <td></td><td>142/144</td><td>143/144</td><td>145/144</td><td>146/144</td><td>148/144</td><td>150/144</td></tr> <tr> <td>Ratios</td><td><b>1.1409431</b></td><td><b>0.512886</b></td><td><b>0.3492656</b></td><td><b>0.7219</b></td><td><b>0.24825795</b></td><td><b>3.6232708</b></td></tr> <tr> <td>%StdErr</td><td><b>0.00079596</b></td><td><b>0.000727</b></td><td><b>0.0004542</b></td><td><b>0</b></td><td><b>0.0016811</b></td><td><b>0.001641</b></td></tr> </table>				142/144	143/144	145/144	146/144	148/144	150/144	Ratios	<b>1.1409431</b>	<b>0.512886</b>	<b>0.3492656</b>	<b>0.7219</b>	<b>0.24825795</b>	<b>3.6232708</b>	%StdErr	<b>0.00079596</b>	<b>0.000727</b>	<b>0.0004542</b>	<b>0</b>	<b>0.0016811</b>	<b>0.001641</b>			
	142/144	143/144	145/144	146/144	148/144	150/144																				
Ratios	<b>1.1409431</b>	<b>0.512886</b>	<b>0.3492656</b>	<b>0.7219</b>	<b>0.24825795</b>	<b>3.6232708</b>																				
%StdErr	<b>0.00079596</b>	<b>0.000727</b>	<b>0.0004542</b>	<b>0</b>	<b>0.0016811</b>	<b>0.001641</b>																				
<i>for comparison only</i> DePaolo 88, p.14, ln. B': 1.141854 na 0.348416 0.721882 0.241572 na																										
<b>FINAL DATA TO REPORT:</b> <b>146/144 set to 0.7219</b> <table border="1" style="width: 100%; border-collapse: collapse;"> <tr> <td></td><td>142/144</td><td>143/144</td><td>145/144</td><td>146/144</td><td>148/144</td><td>150/144</td><td>150t/144s</td></tr> <tr> <td>Ratios</td><td><b>1.141824</b></td><td><b>0.512191</b></td><td><b>0.348420</b></td><td><b>0.721900</b></td><td><b>0.241556</b></td><td><b>0.236478</b></td><td><b>0.286246</b></td></tr> <tr> <td>± 2 S.E.</td><td><b>0.000018</b></td><td><b>0.000007</b></td><td><b>0.000003</b></td><td><b>0.000000</b></td><td><b>0.000008</b></td><td><b>0.000008</b></td><td><b>0.000009</b></td></tr> </table> <b>Epsilon143= -8.72 using (143/144)chur= 0.512638</b> <b>± 0.15 (Hamilton et al. 1983)</b>				142/144	143/144	145/144	146/144	148/144	150/144	150t/144s	Ratios	<b>1.141824</b>	<b>0.512191</b>	<b>0.348420</b>	<b>0.721900</b>	<b>0.241556</b>	<b>0.236478</b>	<b>0.286246</b>	± 2 S.E.	<b>0.000018</b>	<b>0.000007</b>	<b>0.000003</b>	<b>0.000000</b>	<b>0.000008</b>	<b>0.000008</b>	<b>0.000009</b>
	142/144	143/144	145/144	146/144	148/144	150/144	150t/144s																			
Ratios	<b>1.141824</b>	<b>0.512191</b>	<b>0.348420</b>	<b>0.721900</b>	<b>0.241556</b>	<b>0.236478</b>	<b>0.286246</b>																			
± 2 S.E.	<b>0.000018</b>	<b>0.000007</b>	<b>0.000003</b>	<b>0.000000</b>	<b>0.000008</b>	<b>0.000008</b>	<b>0.000009</b>																			
<i>linked from Sm sheet</i> [Sm147]= 159.499735 nm/g      [Nd144]= 801.55717 nm/g ± 0.007870      ± 0.02702 <table border="1" style="width: 100%; border-collapse: collapse;"> <tr> <td>[Sm]= 159.915611 ppm</td><td>[Nd]= 486.12412 ppm</td></tr> <tr> <td>± 0.007891</td><td>± 0.01639</td></tr> </table> TOT ng Sm= 3.84742568      TOT ng Nd= 11.6957088 <table border="1" style="width: 100%; border-collapse: collapse;"> <tr> <td style="text-align: center;">Sm147/Nd144= 0.198987 ± 2 S.E. 0.000012 ± 2RSE % 0%</td></tr> </table>			[Sm]= 159.915611 ppm	[Nd]= 486.12412 ppm	± 0.007891	± 0.01639	Sm147/Nd144= 0.198987 ± 2 S.E. 0.000012 ± 2RSE % 0%																			
[Sm]= 159.915611 ppm	[Nd]= 486.12412 ppm																									
± 0.007891	± 0.01639																									
Sm147/Nd144= 0.198987 ± 2 S.E. 0.000012 ± 2RSE % 0%																										

Full Sample Name:	KPI_2.1_4_Nd																							
Date of TIMS analysis:	2/5/2020	Position #:																						
estimated Nd load (ng):	25	10																						
<b>Rspike Values Nd [SmNd 0.15 A spike, 6-12-08 calib]</b>																								
<table border="1" style="width: 100%; border-collapse: collapse;"> <tr> <th>142/144</th><th>143/144</th><th>145/144</th><th>146/144</th><th>148/144</th><th>150/144</th><th>[Nd150]</th></tr> <tr> <td>0.830433</td><td>0.494001</td><td>0.436936</td><td>0.885201</td><td>0.740574</td><td>198.371260</td><td>0.125778</td></tr> <tr> <td colspan="3" style="text-align: center;">nm/g</td><td colspan="4"></td></tr> </table>			142/144	143/144	145/144	146/144	148/144	150/144	[Nd150]	0.830433	0.494001	0.436936	0.885201	0.740574	198.371260	0.125778	nm/g							
142/144	143/144	145/144	146/144	148/144	150/144	[Nd150]																		
0.830433	0.494001	0.436936	0.885201	0.740574	198.371260	0.125778																		
nm/g																								
Wt Sample (g)=	2.40301E-05	g	0.024030																					
Wt Spike (g)=	0.53473	g																						
Mass Spectrometer Information:																								
<table border="1" style="width: 100%; border-collapse: collapse;"> <tr> <td>Number of cycles measured:</td><td>45</td></tr> <tr> <td>Number of cycles used:</td><td>32</td></tr> <tr> <td>start</td><td>average (from sheet)</td></tr> <tr> <td>3.28</td><td>3.43</td></tr> <tr> <td>Beam intensity range: from</td><td>Amps</td></tr> <tr> <td>0.3614724</td><td>0.7244415</td></tr> <tr> <td>Temperature range: from</td><td>Volts 144Nd.16O</td></tr> <tr> <td>1507</td><td>1591</td></tr> <tr> <td></td><td>°C</td></tr> </table>			Number of cycles measured:	45	Number of cycles used:	32	start	average (from sheet)	3.28	3.43	Beam intensity range: from	Amps	0.3614724	0.7244415	Temperature range: from	Volts 144Nd.16O	1507	1591		°C				
Number of cycles measured:	45																							
Number of cycles used:	32																							
start	average (from sheet)																							
3.28	3.43																							
Beam intensity range: from	Amps																							
0.3614724	0.7244415																							
Temperature range: from	Volts 144Nd.16O																							
1507	1591																							
	°C																							
Final Ratio Data:																								
Interference Values (oxide corrected; informational only... not used in this sheet)																								
Ce140/Nd144	0.002742846																							
Pr141/Nd144	0.1247517																							
Sml49/Nd144	3.1462E-05																							
for Ratios & %ISE: use grand mean oxygen corr, interference corr, exp normalized values																								
	142/144	143/144	145/144	146/144	148/144	150/144																		
Ratios	1.141003	0.51286165	0.3491928	0.7219	0.24765777	3.319955																		
%StdErr	0.001663722	0.001051509	0.0010085	0	0.00146177	0.0027855																		
for comparison only	142/144	143/144	145/144	146/144	148/144	150/144																		
DePaolo 88, p.14, ln. B':	1.141854	na	0.348416	0.721882	0.241572	na																		
FINAL DATA TO REPORT:			146/144 set to 0.7219																					
	142/144	143/144	145/144	146/144	148/144	150/144																		
Ratios	1.141802	0.512230	0.348423	0.721900	0.241558	0.236478																		
± 2 S.E.	0.000038	0.000011	0.000007	0.000000	0.000007	0.000013																		
			Epsilon143= -7.96 using (143/144)chur= 0.512638																					
			± 0.21 (Hamilton et al. 1983)																					
linked from Sm sheet																								
[Sm147]= 178.702382 nm/g			[Nd144]= 882.30239 nm/g																					
± 0.037948			± 0.04971																					
[Sm]= 179.168327 ppm			[Nd]= 535.09405 ppm																					
± 0.038047			± 0.03015																					
TOT ng Sm= 4.305432816			TOT ng Nd= 12.8583636																					
Sm147/Nd144= 0.202541																								
± 2 S.E. 0.000044																								
± 2RSE % 0%																								

Full Sample Name: KP1-2.1_5	nd	Date of TIMS analysis: 7/14/2020	Position #: 3	estimated Nd load (ng): 25																					
<b>Rspike Values Nd [SmNd 0.15 A spike, 6-12-08 calib]</b> <table border="1" style="width: 100%; border-collapse: collapse;"> <tr> <th>142/144</th> <th>143/144</th> <th>145/144</th> <th>146/144</th> <th>148/144</th> <th>150/144</th> <th>[Nd150]</th> </tr> <tr> <td>0.830433</td> <td>0.494001</td> <td>0.436936</td> <td>0.885201</td> <td>0.740574</td> <td>198.371260</td> <td>0.125778</td> </tr> <tr> <td colspan="7" style="text-align: right;">nm/g</td> </tr> </table>					142/144	143/144	145/144	146/144	148/144	150/144	[Nd150]	0.830433	0.494001	0.436936	0.885201	0.740574	198.371260	0.125778	nm/g						
142/144	143/144	145/144	146/144	148/144	150/144	[Nd150]																			
0.830433	0.494001	0.436936	0.885201	0.740574	198.371260	0.125778																			
nm/g																									
Wt Sample (g)= 2.97421E-05	g	Wt Spike (g)= 0.75668	g																						
Mass Spectrometer Information:																									
Number of cycles measured: 83	Number of cycles used: 63																								
Filament Current range: from 3.36	3.49	Amps																							
Beam intensity range: from 0.0336008	0.1142898	Volts	144Nd.16O																						
Temperature range: from 1520	1595	°C																							
Final Ratio Data:																									
Interference Values (oxide corrected; informational only... not used in this sheet)																									
Ce140/Nd144 0.005080019																									
Pr141/Nd144 0.007303732																									
Sm149/Nd144 7.75586E-05																									
<i>for Ratios &amp; %ISE: use grand mean oxygen corr, interference corr, exp normalized values</i>																									
	142/144	143/144	145/144	146/144	148/144	150/144																			
Ratios	1.1406167	0.51313	0.3496566	0.7219	0.25123239	5.094146																			
%StdErr	0.002931565	0.002077	0.0031363	0	0.00858382	0.005651																			
for comparison only	142/144	143/144	145/144	146/144	148/144	150/144																			
DePaolo 88, p.14, ln. B':	1.141854	na	0.348416	0.721882	0.241572	na																			
<b>FINAL DATA TO REPORT:</b>																									
	142/144	143/144	145/144	146/144	148/144	150/144	146/144 set to 0.7219																		
Ratios	1.141902	0.512127	0.348438	0.721900	0.241608	0.236478	0.197014																		
± 2 S.E.	0.000067	0.000021	0.000022	0.000000	0.000041	0.000027	0.000022																		
Epsilon143=	-9.96	using (143/144)chur=	0.512638																						
	±	0.42	(Hamilton et al. 1983)																						
<i>linked from Sm sheet</i>																									
[Sm147]=	13.509010	nm/g	[Nd144]=	630.43866	nm/g																				
	± 0.010199			± 0.07133																					
[Sm]=	113.804971	ppm	[Nd]=	382.34508	ppm																				
	± 0.010225			± 0.04326																					
TOT ng Sm=	3.384798832		TOT ng Nd=	11.3717456																					
Sml47/Nd144=	0.180048																								
± 2 S.E.	0.000026																								
± 2RSE %	0%																								

Full Sample Name: KP_1_2.1_7_Nd	Date of TIMS analysis: 8/11/2020	Position #: 3				
estimated Nd load (ng): 25						
<b>Rspike Values Nd [SmNd 0.15 A spike, 6-12-08 calib]</b>						
142/144	143/144	145/144	146/144	148/144	150/144	[Nd150]
0.830433	0.494001	0.436936	0.885201	0.740574	198.371260	0.125778 nm/g
Wt Sample (g)= 2.41074E-05 g	Wt Spike (g)= 0.75857 g					
Mass Spectrometer Information:						
Number of cycles measured: 52	Number of cycles used: 31					
Filament Current range: from 3.56	start 3.56	average (from sheet) 3.56	Amps			
Beam intensity range: from 0.3488282	0.3488282	1.0291274	Volts 144Nd.16O			
Temperature range: from 1520	1520	1594	°C			
Final Ratio Data:						
Interference Values (oxide corrected; informational only... not used in this sheet)						
Ce140/Nd144 0.006074167						
Pr141/Nd144 0.007489961						
Sm149/Nd144 0.000629369						
<i>for Ratios &amp; %ISE: use grand mean oxygen corr, interference corr, exp normalized values</i>						
	142/144	143/144	145/144	146/144	148/144	150/144
Ratios 1.1400673	0.513477	0.3501353	0.7219	0.25488071	6.9438591	
%StdErr 0.001495628	0.001545	0.001044	0	0.00293828	0.0035814	
for comparison only 142/144	143/144	145/144	146/144	148/144	150/144	
DePaolo 88, p.14, ln. B': 1.141854	na	0.348416	0.721882	0.241572	na	
<b>FINAL DATA TO REPORT:</b> 146/144 set to 0.7219						
	142/144	143/144	145/144	146/144	148/144	150/144
Ratios 1.141876	0.512084	0.348443	0.721900	0.241565	0.236477	0.140349
± 2 S.E. 0.000034	0.000016	0.000007	0.000000	0.000014	0.000017	0.000010
Epsilon143= -10.80 using (143/144)chur= 0.512638 ± 0.31 (Hamilton et al. 1983)						
<i>linked from Sm sheet</i>						
[Sm147]= 100.904555 nm/g				[Nd144]= 555.46922 nm/g		
± 0.009725				± 0.03985		
[Sm]= 101.167652 ppm				[Nd]= 336.87801 ppm		
± 0.009751				± 0.02417		
TOT ng Sm= 2.438889043				TOT ng Nd= 8.12125293		
Sm147/Nd144= 0.181656 ± 2 S.E. 0.000022 ± 2RSE % 0%						

Full Sample Name: <b>KP1_2.1_9_Nd</b>	Date of TIMS analysis: <b>8/11/2020</b>	Position #: <b>6</b>					
estimated Nd load (ng): <b>25</b>							
<b>Rspike Values Nd {SmNd 0.15 A spike, 6-12-08 calib}</b>							
142/144	143/144	145/144	146/144	148/144	150/144	[Nd150]	
0.830433	0.494001	0.436936	0.885201	0.740574	198.371260	0.125778 nm/g	
Wt Sample (g)= <b>0.00003</b> g							
Wt Spike (g)= <b>0.76352</b> g							
Mass Spectrometer Information:							
Number of cycles measured: <enter!>							
Number of cycles used: <enter!>							
Filament Current range: from <b>3.3</b>	start	<b>3.31</b>	average (from sheet)	Amps			
Beam intensity range: from <b>0.4040554</b>		<b>0.9885467</b>		Volts 144Nd.16O			
Temperature range: from <b>1507</b>		<b>1562</b>		°C			
Final Ratio Data:							
Interference Values (oxide corrected; informational only... not used in this sheet)							
Ce140/Nd144 <b>0.00305761</b>							
Pr141/Nd144 <b>0.0090243</b>							
Sm149/Nd144 <b>6.7948E-05</b>							
<i>for Ratios &amp; %1SE: use grand mean oxygen corr, interference corr, exp normalized values</i>							
	142/144	143/144	145/144	146/144	148/144	150/144	
Ratios	<b>1.1412344</b>	<b>0.512566</b>	<b>0.348996</b>	<b>0.7219</b>	<b>0.24614531</b>	<b>2.5419569</b>	
%StdErr	<b>0.00065962</b>	<b>0.000414</b>	<b>0.0004154</b>	<b>0</b>	<b>0.00093829</b>	<b>0.0010458</b>	
for comparison only	142/144	143/144	145/144	146/144	148/144	150/144	
DePaolo 88, p.14, ln. B':	1.141854	na	0.348416	0.721882	0.241572	na	
FINAL DATA TO REPORT: 146/144 set to 0.7219							
	142/144	143/144	145/144	146/144	148/144	150/144	150t/144s
Ratios	<b>1.141827</b>	<b>0.512093</b>	<b>0.348422</b>	<b>0.721900</b>	<b>0.241589</b>	<b>0.236478</b>	<b>0.424460</b>
± 2 S.E.	<b>0.000015</b>	<b>0.000004</b>	<b>0.000003</b>	<b>0.000000</b>	<b>0.000005</b>	<b>0.000005</b>	<b>0.000009</b>
Epsilon143=	<b>-10.63</b>						using (143/144)chur= <b>0.512638</b>
	<b>± 0.08</b>						(Hamilton et al. 1983)
linked from Sm sheet							
[Sm147]= <b>249.471479</b> nm/g	<b>[Nd144]= 1358.75307</b> nm/g						
± 0.014675	± 0.03229						
[Sm]= <b>250.121946</b> ppm	<b>[Nd]= 824.04932</b> ppm						
± 0.014713	± 0.01958						
TOT ng Sm= <b>7.50365837</b>	TOT ng Nd= <b>24.7214795</b>						
Sm147/Nd144= <b>0.183603</b> ± 2 S.E. <b>0.000012</b> ± 2RSE % <b>0%</b>							

Full Sample Name:	KP1-2.1_10 Nd	Date of TIMS analysis:	7/16/2020	Position #:	4	estimated Nd load (ng):	25														
<b>Rspike Values Nd [SmNd 0.15 A spike, 6-12-08 calib]</b> <table border="1" style="width: 100%; border-collapse: collapse;"> <tr> <td>142/144</td> <td>143/144</td> <td>145/144</td> <td>146/144</td> <td>148/144</td> <td>150/144</td> <td>[Nd150]</td> </tr> <tr> <td>0.830433</td> <td>0.494001</td> <td>0.436936</td> <td>0.885201</td> <td>0.740574</td> <td>198.371260</td> <td>0.125778 nm/g</td> </tr> </table>								142/144	143/144	145/144	146/144	148/144	150/144	[Nd150]	0.830433	0.494001	0.436936	0.885201	0.740574	198.371260	0.125778 nm/g
142/144	143/144	145/144	146/144	148/144	150/144	[Nd150]															
0.830433	0.494001	0.436936	0.885201	0.740574	198.371260	0.125778 nm/g															
Wt Sample (g)=	3.31E-05	g	Wt Spike (g)=	0.87115	g																
Mass Spectrometer Information:																					
Number of cycles measured:	129	Number of cycles used:	105																		
Filament Current range: from	start	average (from sheet)																			
Beam intensity range: from	3.61	3.64		Amps																	
Temperature range: from	1.0246663	0.8811124		°C																	
Final Ratio Data:																					
Interference Values (oxide corrected; informational only... not used in this sheet)																					
Ce140/Nd144	0.001315	Pr141/Nd144	0.003505	Sm149/Nd144	0.000105																
<i>for Ratios &amp; %1SE: use grand mean oxygen corr, interference corr, exp normalized values</i>																					
Ratios	1.141581	0.512411	0.3486756	0.7219	0.24363796	1.2808458															
%StdErr	0.000685	0.000471	0.0004087	0	0.001029924	0.0010651															
for comparison only	142/144	143/144	145/144	146/144	148/144	150/144															
DePaolo 88, p.14, ln. B':	1.141854	na	0.348416	0.721882	0.241572	na															
FINAL DATA TO REPORT: 146/144 set to 0.7219																					
Ratios	1.141846	0.512198	0.348417	0.721900	0.241576	0.236478	0.947190														
± 2 S.E.	0.000016	0.000005	0.000003	0.000000	0.000005	0.000005	0.000020														
Epsilon143=	-8.59			using (143/144)chur=	0.512638																
	±	0.09		(Hamilton et al. 1983)																	
<i>linked from Sm sheet</i>																					
[Sm147]=	##### nm/g		[Nd144]=	3136.60803 nm/g																	
±	0.066782		±	0.10280																	
[Sm]=	##### ppm		[Nd]=	1902.27332 ppm																	
±	0.066956		±	0.06235																	
TOT ng Sm=	20.6869		TOT ng Nd=	62.9430093																	
Sm147/Nd144= 0.198806 ± 2 S.E. 0.000022 ± 2RSE % 0%																					

Full Sample Name: KP 2-1-2	Date of TIMS analysis: 8/7/2010	Position #: 14					
Full Sample Name: eud 122804	estimated Nd load (ng):	Position #: 5					
	Date of TIMS analysis: 4/5/2019						
estimated Nd load (ng): 20	Rspike Values Nd [SmNd 0.15 A spike, 6-12-08 calib]						
142/144 143/144 145/144 146/144 148/144 150/144 [Nd150] 0.830433 0.494001 0.436936 0.885201 0.740574 198.371260 0.125778 nm/g	Rspike Values Nd [SmNd 0.15 A spike, 6-12-08 calib]						
Wt Sample (g)= 2.001±0.1 g	Wt Spike (g)= 0.53225 g						
Wt Sample (g)= 0.000026468 g	Wt Spike (g)= 0.56175 g						
Mass Spectrometer Information:							
Mass Spectrometer Information:	Number of cycles measured: 202						
	Number of cycles used: 171						
	Number of cycles measured: 33						
	Number of cycles used: 29						
	start (from sheet) average (from sheet)						
Filament Current range: from 3.51 to 3.51 Amps							
Beam intensity range: from 0.20 to 0.20 144Nd.16O							
Filament Current range: from <enter!> to <enter!> Amps							
Temperature range: from 0.166055 to 0.6638316 Volts 144Nd.16O							
Final Ratio Data:	Temperature range: from 1560 to 1633 °C						
Final Ratio Data:	Interference Values (oxide corrected; informational only... not used in this sheet)						
Ce140/Nd144 0.000167	Interference Values (oxide corrected; informational only... not used in this sheet)						
Pr141/Nd144 0.003779016							
Sm149/Nd144 0.016097956							
Sm149/Nd144 0.000213278							
for Ratios & %ISE: use grand mean oxygen corr, interference corr, exp normalized values	142/144 143/144 145/144 146/144 148/144 150/144						
for Ratios & %ISE: use grand mean oxygen corr, interference corr, exp normalized values	142/144 143/144 145/144 146/144 148/144 150/144						
for cc	1.14167428	0.512508	0.3485686	0.721900	0.24282397	0.8861335	
%StdErr	0.001151632	0.001328	0.0011156	0	0.00294903	0.0031192	
for comparison only	142/144	143/144	145/144	146/144	148/144	150/144	
DePaolo 88, p.14, ln. B':	1.141854	na	0.348416	0.721882	0.241572	na	
FINAL DATA TO REPORT:						146/144 set to 0.7219	
	142/144	143/144	145/144	146/144	148/144	150/144	150t/144s
Ratios	1.141838	0.512376	0.348408	0.721900	0.241542	0.236478	1.527794
± 2 S.E.	0.000026	0.000014	0.000008	0.000000	0.000014	0.000015	0.000095
Epsilon143=	-5.12	using (143/144)chur=	0.512638				
	± 0.27	(Hamilton et al. 1983)					
linked from Sm sheet							
[Sm147]= 912.018027	nm/g						
± 0.270950							
[Sm]= 914.396004	ppm						
± 0.271657							
TOT ng Sm=	24.20223343						
	Sm147/Nd144= 0.223621						
	± 2 S.E. 0.000068						
	± 2RSE % 0%						
	[Nd144]= 4078.41654 nm/g						
	± 0.30233						
	[Nd]= 2473.45632 ppm						
	± 0.18335						
	TOT ng Nd= 65.4674419						

Full Sample Name: KP\_2\_1\_3 Nd  
 Date of TIMS analysis: 8/7/2019  
 estimated Nd load (ng): 25

Position #: 15

Rspike Values Nd [SmNd 0.15 A spike, 6-12-08 calib]

142/144	143/144	145/144	146/144	148/144	150/144	[Nd150]
0.830433	0.494001	0.436936	0.885201	0.740574	198.371260	0.125778

nm/g

Wt Sample (g)= 2.36E-05 g  
 Wt Spike (g)= 0.59851 g

Mass Spectrometer Information:

Number of cycles measured:	180
Number of cycles used:	153
Filament Current range: from	start 3.61
Beam intensity range: from	average (from sheet) 3.64
Temperature range: from	Amps 0.1830612 0.8649258
	Volts 144Nd.16O
	°C 1480 1562

Final Ratio Data:

Interference Values (oxide corrected; informational only... not used in this sheet)

Ce140/Nd144	0.00019
Pr141/Nd144	0.00252
Sm149/Nd144	2E-05

for Ratios & %1SE: use grand mean oxygen corr, interference corr, exp normalized values

	142/144	143/144	145/144	146/144	148/144	150/144
Ratios	1.141553	0.512222	0.3486218	0.7219	0.24326883	1.0989104
%StdErr	0.0009	0.000467	0.0005293	0	0.00078444	0.0013552
for comparison only	142/144	143/144	145/144	146/144	148/144	150/144
DePaolo 88, p.14, ln. B':	1.141854	na	0.348416	0.721882	0.241572	na

FINAL DATA TO REPORT:

146/144 set to 0.7219

	142/144	143/144	145/144	146/144	148/144	150/144	150t/144s
Ratios	1.141771	0.512045	0.348408	0.721900	0.241566	0.236478	1.148783
± 2 S.E.	0.000021	0.000005	0.000004	0.000000	0.000004	0.000006	0.000031

Epsilon143= -11.56 using (143/144)chur= 0.512638  
 ± 0.09 (Hamilton et al. 1983)

linked from Sm sheet

[Sm147]= ##### nm/g  
 ± 0.076030

[Nd144]= 3671.22275 nm/g

± 0.14887

[Sm]= ##### ppm

[Nd]= 2226.50360 ppm

± 0.076228

± 0.09029

TOT ng Sm= 15.39879

TOT ng Nd= 52.4477414

Sm147/Nd144= 0.177599
± 2 S.E. 0.000022
± 2RSE % 0%

Full Sample Name: KP9\_eud\_1  
 Date of TIMS analysis: #####  
 estimated Nd load (ng): 12  
 Position #: 13

Rspike Values Nd {SmNd 0.15 A spike, 6-12-08 calib}						
142/144	143/144	145/144	146/144	148/144	150/144	[Nd150]
0.830433	0.494001	0.436936	0.885201	0.740574	198.371260	0.125778 nm/g

Wt Sample (g)= 1.14E-05 g  
 Wt Spike (g)= 0.32998 g

Mass Spectrometer Information:

Number of cycles measured:	240
Number of cycles used:	225
start	average (from sheet)
Filament Current range: from 3.3	3.3 Amps
Beam intensity range: from <enter!>	0.0433259 Volts 144Nd.16O
Temperature range: from 1527	1578 °C

Final Ratio Data:

Interference Values (oxide corrected; informational only... not used in this sheet)  
 Ce140/Nd144 0.106166  
 Pr141/Nd144 0.014585  
 Sm149/Nd144 0.000168

for Ratios & %1SE: use grand mean oxygen corr, interference corr, exp normalized values

	142/144	143/144	145/144	146/144	148/144	150/144
Ratios	1.137241	0.515305	0.3524683	0.7219	0.27240644	15.640985
%StdErr	0.003725	0.002854	0.0027816	0	0.00749594	0.009308
for comparison only	142/144	143/144	145/144	146/144	148/144	150/144
DePaolo 88, p.14, ln. B':	1.141854	na	0.348416	0.721882	0.241572	na

#### FINAL DATA TO REPORT: 146/144 set to 0.7219

	142/144	143/144	145/144	146/144	148/144	150/144	150t/144s
Ratios	1.141800	0.512020	0.348474	0.721900	0.241551	0.236365	0.056307
± 2 S.E.	0.000085	0.000029	0.000019	0.000000	0.000036	0.000044	0.000010

$$\text{Epsilon143} = -12.06 \quad \text{using } (143/144)\text{chur} = 0.512638 \\ \pm 0.57 \quad (\text{Hamilton et al. 1983})$$

linked from Sm sheet

$$[\text{Sm147}] = 35.864892 \text{ nm/g} \quad [\text{Nd144}] = 204.70209 \text{ nm/g} \\ \pm 0.010088 \quad \pm 0.03811$$

$$[\text{Sm}] = 35.958406 \text{ ppm} \quad [\text{Nd}] = 124.14663 \text{ ppm} \\ \pm 0.010114 \quad \pm 0.02311$$

$$\text{TOT ng Sm} = 0.410519 \quad \text{TOT ng Nd} = 1.41732002$$

$$\text{Sm147/Nd144} = 0.175205 \\ \pm 2 \text{ S.E.} \quad 0.000059 \\ \pm 2\text{RSE \%} \quad 0\%$$

Full Sample Name: KP9\_eud\_2  
 Date of TIMS analysis: #####  
 Position #: 14  
 estimated Nd load (ng): 15

Rspike Values Nd {SmNd 0.15 A spike, 6-12-08 calib}						
142/144	143/144	145/144	146/144	148/144	150/144	[Nd150]
0.830433	0.494001	0.436936	0.885201	0.740574	198.371260	0.125778 nm/g

Wt Sample (g)= 1.14E-05 g  
 Wt Spike (g)= 0.33061 g

Mass Spectrometer Information:

Number of cycles measured:	35
Number of cycles used:	33
start	average (from sheet)
Filament Current range: from 3.4	3.4 Amps
Beam intensity range: from 0.0784291	0.1568499 Volts 144Nd.16O
Temperature range: from 1547	1592 °C

Final Ratio Data:

Interference Values (oxide corrected; informational only... not used in this sheet)

Ce140/Nd144	0.009369
Pr141/Nd144	0.009176
Sm149/Nd144	6.92E-05

	142/144	143/144	145/144	146/144	148/144	150/144
Ratios	1.139492	0.513985	0.3504785	0.7219	0.25766388	8.3173591
%StdErr	0.007733	0.001619	0.0040231	0	0.0069091	0.0066059
for comparison only	142/144	143/144	145/144	146/144	148/144	150/144
DePaolo 88, p.14, ln. B':	1.141854	na	0.348416	0.721882	0.241572	na

#### FINAL DATA TO REPORT: 146/144 set to 0.7219

	142/144	143/144	145/144	146/144	148/144	150/144	150t/144s
Ratios	1.141698	0.512309	0.348430	0.721900	0.241602	0.236475	0.115053
± 2 S.E.	0.000017	0.000028	0.000000	0.000033	0.000031	0.000015	

$$\text{Epsilon143} = -6.43 \quad \text{using } (143/144)\text{chur} = 0.512638 \\ \pm 0.32 \quad (\text{Hamilton et al. 1983})$$

linked from Sm sheet

$$[\text{Sm147}] = 89.649212 \text{ nm/g} \quad [\text{Nd144}] = 418.15533 \text{ nm/g} \\ \pm 0.014287 \quad \pm 0.05526$$

$$[\text{Sm}] = 89.882962 \text{ ppm} \quad [\text{Nd}] = 253.60062 \text{ ppm} \\ \pm 0.014324 \quad \pm 0.03352$$

$$\text{TOT ng Sm} = 1.028396 \quad \text{TOT ng Nd} = 2.90157146$$

$$\text{Sm147/Nd144} = 0.214392 \\ \pm 2 \text{ S.E.} \quad 0.000044 \\ \pm 2\text{RSE \%} \quad 0\%$$

Full Sample Name: KP9\_eud\_3  
 Date of TIMS analysis: #####  
 estimated Nd load (ng): 15

Position #: 15

Rspike Values Nd {SmNd 0.15 A spike, 6-12-08 calib}						
142/144	143/144	145/144	146/144	148/144	150/144	[Nd150]
0.830433	0.494001	0.436936	0.885201	0.740574	198.371260	0.125778 nm/g

Wt Sample (g)= 1.14E-05 g  
 Wt Spike (g)= 0.3144 g

Mass Spectrometer Information:

Number of cycles measured:	67
Number of cycles used:	44
start	average (from sheet)
Filament Current range: from 3.46	3.48 Amps
Beam intensity range: from 0.1768321	0.3212265 Volts 144Nd.16O
Temperature range: from 1507	1543 °C

Final Ratio Data:

Interference Values (oxide corrected; informational only... not used in this sheet)  
 Ce140/Nd144 0.009426  
 Pr141/Nd144 0.004891  
 Sm149/Nd144 3.79E-05

for Ratios & %1SE: use grand mean oxygen corr, interference corr, exp normalized values

	142/144	143/144	145/144	146/144	148/144	150/144
Ratios	1.138396	0.514816	0.3515368	0.7219	0.26575636	12.356416
%StdErr	0.001217	0.001195	0.00109	0	0.00250124	0.0026179
for comparison only	142/144	143/144	145/144	146/144	148/144	150/144
DePaolo 88, p.14, ln. B':	1.141854	na	0.348416	0.721882	0.241572	na

FINAL DATA TO REPORT: 146/144 set to 0.7219						
	142/144	143/144	145/144	146/144	148/144	150/144
Ratios	1.141860	0.512270	0.348424	0.721900	0.241564	0.236448
± 2 S.E.	0.000028	0.000008	0.000000	0.000012	0.000012	0.000004

$$\text{Epsilon143} = -7.18 \quad \text{using } (143/144)\text{chur} = 0.512638 \\ \pm 0.24 \quad (\text{Hamilton et al. 1983})$$

linked from Sm sheet

$$[\text{Sm147}] = 52.717497 \text{ nm/g} \quad [\text{Nd144}] = 255.25136 \text{ nm/g} \\ \pm 0.010234 \quad \pm 0.01338$$

$$[\text{Sm}] = 52.854951 \text{ ppm} \quad [\text{Nd}] = 154.80348 \text{ ppm} \\ \pm 0.010261 \quad \pm 0.00811$$

$$\text{TOT ng Sm} = 0.604957 \quad \text{TOT ng Nd} = 1.77181877$$

$$\text{Sm147/Nd144} = 0.206532 \\ \pm 2 \text{ S.E.} \quad 0.000042 \\ \pm 2\text{RSE \%} \quad 0\%$$

Full Sample Name: **KP9\_eud\_4**  
Date of TIMS analysis: **#####**  
estimated Nd load (ng): **16**

Rspike Values Nd {SmNd 0.15 A spike, 6-12-08 calib}						
142/144	143/144	145/144	146/144	148/144	150/144	[Nd150]
0.830433	0.494001	0.436936	0.885201	0.740574	198.371260	0.125778 nm/g

Wt Sample (g)= **1.14E-05** g  
Wt Spike (g)= **0.30829** g

Mass Spectrometer Information:

Number of cycles measured:	<enter!>	
Number of cycles used:	<enter!>	
Filament Current range: from	start <enter!>	average (from sheet) <enter!>
Beam intensity range: from	<enter!>	Amps 0.0922148 Volts 144Nd.16O
Temperature range: from	<enter!>	°C <enter!>

Final Ratio Data:

Interference Values (oxide corrected; informational only... not used in this sheet)  
Ce140/Nd144 **0.059779**  
Pr141/Nd144 **0.010306**  
Sm149/Nd144 **0.000142**

for Ratios & %1SE: use grand mean oxygen corr, interference corr, exp normalized values

	142/144	143/144	145/144	146/144	148/144	150/144
Ratios	<b>1.139569</b>	<b>0.514073</b>	<b>0.3506387</b>	<b>0.7219</b>	<b>0.25870708</b>	<b>8.8572121</b>
%StdErr	<b>0.002036</b>	<b>0.001501</b>	<b>0.0020212</b>	<b>0</b>	<b>0.00429281</b>	<b>0.0043564</b>
for comparison only	<b>142/144</b>	<b>143/144</b>	<b>145/144</b>	<b>146/144</b>	<b>148/144</b>	<b>150/144</b>
DePaolo 88, p.14, ln. B':	1.141854	na	0.348416	0.721882	0.241572	na

FINAL DATA TO REPORT: 146/144 set to 0.7219

	142/144	143/144	145/144	146/144	148/144	150/144	150t/144s
Ratios	1.141945	0.512281	0.348451	0.721900	0.241560	0.236473	0.107317
± 2 S.E.	0.000047	0.000015	0.000014	0.000000	0.000021	0.000021	0.000009

Epsilon143= -6.97 using (143/144)chur= 0.512638  
± 0.30 (Hamilton et al. 1983)

linked from Sm sheet

[Sm147]= 75.823423 nm/g [Nd144]= 365.35079 nm/g

± 0.006212 ± 0.03185

[Sm]= 76.021123 ppm

[Nd]= 221.57600 ppm

± 0.006228 ± 0.01932

TOT ng Sm= 0.865881 TOT ng Nd= 2.52375061

Sml47/Nd144= 0.207536
± 2 S.E. 0.000025
± 2RSE % 0%

Full Sample Name: KP9\_eud\_5  
 Date of TIMS analysis: #####  
 estimated Nd load (ng): 15  
 Position #: 17

Rspike Values Nd {SmNd 0.15 A spike, 6-12-08 calib}						
142/144	143/144	145/144	146/144	148/144	150/144	[Nd150]
0.830433	0.494001	0.436936	0.885201	0.740574	198.371260	0.125778 nm/g

Wt Sample (g)= 0.00001 g  
 Wt Spike (g)= 0.27245 g

Mass Spectrometer Information:

Number of cycles measured:	105
Number of cycles used:	98
start	average (from sheet)
Filament Current range: from 3.3	3.36 Amps
Beam intensity range: from 0.1513827	0.3507739 Volts 144Nd.16O
Temperature range: from 1533	1594 °C

Final Ratio Data:

Interference Values (oxide corrected; informational only... not used in this sheet)

Ce140/Nd144	0.012179
Pr141/Nd144	0.004544
Sm149/Nd144	7.13E-05

	142/144	143/144	145/144	146/144	148/144	150/144
Ratios	1.140824	0.51311	0.3494119	0.7219	0.24937102	4.1854618
%StdErr	0.001423	0.001308	0.0007516	0	0.00339189	0.0026247
for comparison only	142/144	143/144	145/144	146/144	148/144	150/144
DePaolo 88, p.14, ln. B':	1.141854	na	0.348416	0.721882	0.241572	na

FINAL DATA TO REPORT: 146/144 set to 0.7219						
	142/144	143/144	145/144	146/144	148/144	150/144
Ratios	1.141858	0.512301	0.348424	0.721900	0.241552	0.236478
± 2 S.E.	0.000033	0.000005	0.000000	0.000016	0.000012	0.000013

Epsilon143= -6.58 using (143/144)chur= 0.512638  
 ± 0.26 (Hamilton et al. 1983)

linked from Sm sheet

[Sm147]= ##### nm/g [Nd144]= 837.14890 nm/g

± 0.010278 ± 0.04429

[Sm]= ##### ppm	[Nd]= 507.70960 ppm
-----------------	---------------------

± 0.010305 ± 0.02686

TOT ng Sm= 1.779653 TOT ng Nd= 5.07709602

Sml47/Nd144= 0.212032
± 2 S.E. 0.000017
± 2RSE % 0%

Full Sample Name: **KP9\_eud\_6**  
 Date of TIMS analysis: **10/18/2020**  
 estimated Nd load (ng): **15**  
 Position #: **18**

Rspike Values Nd {SmNd 0.15 A spike, 6-12-08 calib}						
142/144	143/144	145/144	146/144	148/144	150/144	[Nd150]
0.830433	0.494001	0.436936	0.885201	0.740574	198.371260	0.125778 nm/g

Wt Sample (g)= **0.00001** g  
 Wt Spike (g)= **0.27418** g

Mass Spectrometer Information:

Number of cycles measured:	<b>140</b>
Number of cycles used:	<b>97</b>
Filament Current range: from	<b>start 3.4 average (from sheet) 3.41</b>
Beam intensity range: from	<b>0.2713128 1.0156748</b>
Temperature range: from	<b>1520 1572</b>
	Amps Volts 144Nd.16O °C

Final Ratio Data:

Interference Values (oxide corrected; informational only... not used in this sheet)  
 Ce140/Nd144 **0.003365**  
 Pr141/Nd144 **0.00494**  
 Sm149/Nd144 **2.34E-05**

*for Ratios & %ISE; use grand mean oxygen corr, interference corr, exp normalized values*

	142/144	143/144	145/144	146/144	148/144	150/144
Ratios	<b>1.141616</b>	<b>0.51226456</b>	<b>0.3486314</b>	<b>0.7219</b>	<b>0.24328917</b>	<b>1.1083506</b>
%StdErr	<b>0.000998</b>	<b>0.000535891</b>	<b>0.0005149</b>	<b>0</b>	<b>0.00117509</b>	<b>0.0015977</b>
<i>for comparison only</i>	<b>142/144</b>	<b>143/144</b>	<b>145/144</b>	<b>146/144</b>	<b>148/144</b>	<b>150/144</b>
DePaolo 88, p.14, ln. B':	1.141854	na	0.348416	0.721882	0.241572	na

FINAL DATA TO REPORT: 146/144 set to 0.7219						
	142/144	143/144	145/144	146/144	148/144	150/144
Ratios	<b>1.141837</b>	<b>0.512086</b>	<b>0.348415</b>	<b>0.721900</b>	<b>0.241568</b>	<b>0.236478</b>
± S.E.	<b>0.000023</b>	<b>0.000005</b>	<b>0.000004</b>	<b>0.000000</b>	<b>0.000006</b>	<b>0.000008</b>

$$\text{Epsilon143} = -10.76 \quad \text{using } (143/144)\text{chur} = 0.512638 \\ \pm 0.11 \quad (\text{Hamilton et al. 1983})$$

*linked from Sm sheet*

$$[\text{Sm147}] = \text{##### nm/g} \\ \pm 0.095449$$

$$[\text{Nd144}] = 3918.46217 \text{ nm/g} \\ \pm 0.17131$$

$$[\text{Sm}] = \text{##### ppm} \\ \pm 0.095698$$

$$[\text{Nd}] = 2376.44805 \text{ ppm} \\ \pm 0.10390$$

TOT ng Sm= 7.158552

TOT ng Nd= 23.7644805

$$\text{Sm147/Nd144} = 0.182213 \\ \pm 2 \text{ S.E. } 0.000026 \\ \pm 2\text{RSE \% } 0\%$$

Full Sample Name: KP9\_eud\_7  
 Date of TIMS analysis: #####  
 estimated Nd load (ng): 15

Position #: 19

Rspike Values Nd {SmNd 0.15 A spike, 6-12-08 calib}						
142/144	143/144	145/144	146/144	148/144	150/144	[Nd150]
0.830433	0.494001	0.436936	0.885201	0.740574	198.371260	0.125778 nm/g

Wt Sample (g)= 0.00001 g  
 Wt Spike (g)= 0.27258 g

Mass Spectrometer Information:

Number of cycles measured:	97
Number of cycles used:	62
Filament Current range: from	start 3.3 average (from sheet) 3.34 Amps
Beam intensity range: from	0.089676 0.130408 Volts 144Nd.16O
Temperature range: from	1540 1593 °C

Final Ratio Data:

Interference Values (oxide corrected; informational only... not used in this sheet)

Ce140/Nd144	0.008818
Pr141/Nd144	0.001739
Sm149/Nd144	7.93E-05

for Ratios & %1SE: use grand mean oxygen corr, interference corr, exp normalized values

	142/144	143/144	145/144	146/144	148/144	150/144
Ratios	1.141216	0.512721	0.3490771	0.7219	0.24686585	2.9246793
%StdErr	0.00241	0.001321	0.001895	0	0.00510161	0.0050576
for comparison only	142/144	143/144	145/144	146/144	148/144	150/144
DePaolo 88, p.14, ln. B':	1.141854	na	0.348416	0.721882	0.241572	na

FINAL DATA TO REPORT: 146/144 set to 0.7219

	142/144	143/144	145/144	146/144	148/144	150/144	150t/144s
Ratios	1.141911	0.512170	0.348407	0.721900	0.241550	0.236478	0.362828
± 2 S.E.	0.000055	0.000014	0.000013	0.000000	0.000025	0.000024	0.000037

Epsilon143= -9.13 using (143/144)chur= 0.512638  
 ± 0.26 (Hamilton et al. 1983)

linked from Sm sheet

[Sm147]= ##### nm/g

± 0.021979

[Nd144]= 1243.93984 nm/g

± 0.12640

[Sm]= ##### ppm

± 0.022036

[Nd]= 754.41800 ppm

± 0.07666

TOT ng Sm= 2.426648

TOT ng Nd= 7.54418003

Sm147/Nd144= 0.194570

± 2 S.E. 0.000027

± 2RSE % 0%

Full Sample Name: **KP9\_eud\_8**  
 Date of TIMS analysis: #####  
 estimated Nd load (ng): **15** Position #: **20**

Rspike Values Nd {SmNd 0.15 A spike, 6-12-08 calib}						
142/144	143/144	145/144	146/144	148/144	150/144	[Nd150]
0.830433	0.494001	0.436936	0.885201	0.740574	198.371260	0.125778 nm/g

Wt Sample (g)= **0.00001** g  
 Wt Spike (g)= **0.27285** g

Mass Spectrometer Information:

Number of cycles measured:	<b>110</b>
Number of cycles used:	<b>83</b>
Filament Current range: from	<b>start 3.5</b>
Beam intensity range: from	<b>&lt;enter!&gt; 1.4852408</b>
Temperature range: from	<b>1500 1538</b>
	average (from sheet)
	Amps
	Volts 144Nd.16O
	°C

Final Ratio Data:

Interference Values (oxide corrected; informational only... not used in this sheet)

Ce140/Nd144	<b>0.003088</b>
Pr141/Nd144	<b>0.002319</b>
Sm149/Nd144	<b>3.09E-05</b>

	142/144	143/144	145/144	146/144	148/144	150/144
Ratios	<b>1.141628</b>	<b>0.512279</b>	<b>0.3486205</b>	<b>0.7219</b>	<b>0.24322847</b>	<b>1.0810633</b>
%StdErr	<b>0.00059</b>	<b>0.00039</b>	<b>0.0005244</b>	<b>0</b>	<b>0.00086236</b>	<b>0.0012244</b>
for comparison only	<b>142/144</b>	<b>143/144</b>	<b>145/144</b>	<b>146/144</b>	<b>148/144</b>	<b>150/144</b>
DePaolo 88, p.14, ln. B':	1.141854	na	0.348416	0.721882	0.241572	na

FINAL DATA TO REPORT: 146/144 set to 0.7219						
	142/144	143/144	145/144	146/144	148/144	150/144
Ratios	1.141842	<b>0.512107</b>	0.348411	0.721900	0.241561	0.236478
± 2 S.E.	0.000013	<b>0.000004</b>	0.000000	0.000004	0.000006	0.000029

$$\text{Epsilon143} = -10.36 \quad \text{using } (143/144)_{\text{chur}} = 0.512638 \\ \pm 0.08 \quad (\text{Hamilton et al. 1983})$$

linked from Sm sheet

[Sm147]= ##### nm/g	[Nd144]= 4026.37403 nm/g
± 0.092405	± 0.15843

[Sm]= ##### ppm	[Nd]= 2441.89385 ppm
± 0.092646	± 0.09608

TOT ng Sm= 7.456057 TOT ng Nd= 24.4189385

Sml47/Nd144= 0.184699
± 2 S.E. 0.000024
± 2RSE % 0%

Full Sample Name: <b>CBD_11_10_2_eud1_nd</b>		Position #: <b>13</b>						
Date of TIMS analysis: <b>8/11/2020</b>								
estimated Nd load (ng): <b>20</b>								
<b>Rspike Values Nd {SmNd 0.15 A spike, 6-12-08 calib}</b>								
142/144	143/144	145/144	146/144	148/144	150/144	[Nd150]		
0.830433	0.494001	0.436936	0.885201	0.740574	198.371260	0.125778		
				nm/g				
<b>Wt Sample (g)= 0.00002</b>		<b>Rspike Values Nd {SmNd 0.15 A spike, 6-12-08 calib}</b>						
Wt Sample (g)= <b>0.142/144</b>	<b>0.51034</b>	142/144	143/144	145/144	146/144	148/144	150/144	[Nd150]
Wt Spike (g)= <b>0.830433</b>	<b>0.494001</b>	0.436936	0.885201	0.740574	198.371260	0.125778		nm/g
Mass Spectrometer Information:								
Wt Sample (g)= <b>0.00003</b>	<b>g</b>	Number of cycles measured: <b>18</b>						
Wt Spike (g)= <b>0.76643</b>	<b>g</b>	Number of cycles used: <b>16</b>						
Mass Spectrometer Information:								
Number of cycles measured: Filament Current range: from Number of cycles used: Beam intensity range: from Temperature range: from	start <enter!> <b>0.1563075</b>	average (from sheet) <enter!> <b>0.1717706</b>		Amps				
Final Ratio Data:	start <enter!>	average (from sheet)		Volts 144Nd.16O				
Interference Values (oxide corrected; informational only... not used in this sheet) Ce140/Nd144 <b>0.004279</b>	3.51	3.51		Amps				
Ce140/Nd144 <b>0.004279</b>	0.5769178	0.7968502		Volts 144Nd.16O				
Pr141/Nd144 <b>0.011067</b>	1560	1614		°C				
Final Ratio Data: Sm147/Nd144 <b>0.000124</b>								
Interference Values (oxide corrected; informational only... not used in this sheet) Ce140/Nd144 <b>0.0055</b>								
Pr141/Nd144 <b>0.001757</b>								
<i>for Ratios &amp; %SE: use grand mean oxygen corr, interference corr, exp normalized values</i>								
Sm147/Nd144	142/144	143/144	145/144	146/144	148/144	150/144		
Ratios	<b>1.139686</b>	<b>0.513976</b>	<b>0.3503479</b>	<b>0.7219</b>	<b>0.25659213</b>	<b>7.8170158</b>		
%StdErr	<b>0.005283</b>	<b>0.003715</b>	<b>0.0021773</b>	<b>0</b>	<b>0.00660622</b>	<b>0.0075732</b>		
for comparison only	142/144	143/144	145/144	146/144	148/144	150/144		
DePaolo 88, p.14, ln. B': 1.141854	na	0.348416	0.721882	0.241572	na	yes		
<b>FINAL DATA TO REPORT:</b>				146/144 set to 0.7219				
Ratios	142/144	143/144	145/144	146/144	148/144	150/144		
1.141745	<b>0.512409</b>	0.348430	0.721900	0.241528	0.236476	0.123207		
± 2 S.E.	<b>0.000121</b>	<b>0.000038</b>	0.000015	0.000000	0.000032	0.000036		
Epsilon143=		-4.46	using (143/144)chur=	0.512638				
	±	0.74	(Hamilton et al. 1983)					
<i>linked from Sm sheet</i>								
[Sm147]= 71.658894 nm/g				[Nd144]= 395.43061 nm/g				
± 0.004492				± 0.05991				
[Sm]= 71.845736 ppm				[Nd]= 239.81865 ppm				
± 0.004504				± 0.03633				
TOT ng Sm= 1.436915				TOT ng Nd= 4.796373				
Sm147/Nd144= <b>0.181217</b>								
± 2 S.E. <b>0.000030</b>								
± 2RSE % <b>0%</b>								
<i>± 2RSE /0 - 0/0</i>								

Full Sample Name: CBD\_11\_10\_2\_eud3  
 Date of TIMS analysis: 8/12/2020 Position #: 6  
 estimated Nd load (ng): 25

Rspike Values Nd {SmNd 0.15 A spike, 6-12-08 calib}						
142/144	143/144	145/144	146/144	148/144	150/144	[Nd150]
0.830433	0.494001	0.436936	0.885201	0.740574	198.371260	0.125778 nm/g

Wt Sample (g)= 3.13644E-05 g  
 Wt Spike (g)= 0.80425 g

Mass Spectrometer Information:

Number of cycles measured:	46
Number of cycles used:	46
start	average (from sheet)
Filament Current range: from 3.5	3.59 Amps
Beam intensity range: from 0.0202867	0.034943 Volts 144Nd.160
Temperature range: from 1567	1609 °C

Final Ratio Data:

Interference Values (oxide corrected; informational only... not used in this sheet)

Ce140/Nd144	0.10318067
Pr141/Nd144	0.018161342
Sm149/Nd144	0.00074729

for Ratios & %ISE: use grand mean oxygen corr, interference corr, exp normalized values

	142/144	143/144	145/144	146/144	148/144	150/144
Ratios	1.1275348	0.521031	0.3591312	0.7219	0.31839103	37.665341
%StdErr	0.007017897	0.003715	0.0046781	0	0.01056797	0.0156182
for comparison only	142/144	143/144	145/144	146/144	148/144	150/144
DePaolo 88, p.14, ln. B':	1.141854	na	0.348416	0.721882	0.241572	na

FINAL DATA TO REPORT:

	142/144	143/144	145/144	146/144	148/144	150/144	150t/144s
Ratios	1.141723	0.512574	0.348669	0.721900	0.241488	0.208845	0.018071
± 2 S.E.	0.000160	0.000038	0.000033	0.000000	0.000051	0.000065	0.000006

Epsilon143= -1.25 using (143/144)chur= 0.512638  
 ± 0.74 (Hamilton et al. 1983)

linked from Sm sheet

[Sm147]= 10.279181 nm/g	[Nd144]= 58.28203 nm/g
± 0.014631	± 0.01821

[Sm]= 10.305983 ppm	[Nd]= 35.34658 ppm
± 0.014669	± 0.01104

TOT ng Sm= 0.323240975 TOT ng Nd= 1.10862415

Sm147/Nd144= 0.176370
± 2 S.E. 0.000257
± 2RSE % 0%

Full Sample Name: CBD\_11\_10\_2\_britth\_1  
 Date of TIMS analysis: 8/12/2020 Position #: 8  
 estimated Nd load (ng): 25

Rspike Values Nd {SmNd 0.15 A spike, 6-12-08 calib}						
142/144	143/144	145/144	146/144	148/144	150/144	[Nd150]
0.830433	0.494001	0.436936	0.885201	0.740574	198.371260	0.125778
nm/g						

Wt Sample (g)= 3.11702E-05 g  
 Wt Spike (g)= 0.79861 g

Mass Spectrometer Information:

Number of cycles measured:	65
Number of cycles used:	48
start	average (from sheet)
Filament Current range: from 3.4	3.49 Amps
Beam intensity range: from 0.0652729	0.2143349 Volts 144Nd.16O
Temperature range: from 1513	1589 °C

Final Ratio Data:

Interference Values (oxide corrected; informational only... not used in this sheet)

Ce140/Nd144	0.005934194
Pr141/Nd144	0.010446087
Sm149/Nd144	0.000262861

for Ratios & %ISE: use grand mean oxygen corr, interference corr, exp normalized values

	142/144	143/144	145/144	146/144	148/144	150/144
Ratios	1.139027469	0.514164	0.3510372	0.7219	0.2620155	10.477716
%StdErr	0.001811969	0.001365	0.0017128	0	0.00438184	0.0033402
for comparison only	142/144	143/144	145/144	146/144	148/144	150/144
DePaolo 88, p.14, ln. B':	1.141854	na	0.348416	0.721882	0.241572	na

FINAL DATA TO REPORT:

	142/144	143/144	145/144	146/144	148/144	150/144	150t/144s
Ratios	1.141897	0.512012	0.348423	0.721900	0.241616	0.236466	0.088992
± 2 S.E.	0.000041	0.000014	0.000012	0.000000	0.000021	0.000016	0.000006

Epsilon143= -12.21 using (143/144)chur= 0.512638  
 ± 0.27 (Hamilton et al. 1983)

linked from Sm sheet

[Sm147]= 33.002712 nm/g  
 ± 0.059094

[Sm]= 33.088762 ppm

± 0.059248

TOT ng Sm= 1.031383672

[Nd144]= 286.78188 nm/g  
 ± 0.01917

[Nd]= 173.92594 ppm

± 0.01163

TOT ng Nd= 5.4213082

Sm147/Nd144= 0.115079

± 2 S.E. 0.000206

± 2RSE % 0%

Full Sample Name: <b>CB_02_12</b>	Date of TIMS analysis: <b>7/17/2020</b>	estimated Nd load (ng): <b>25</b>	Position #: <b>7</b>														
<b>Rspike Values Nd {SmNd 0.15 A spike, 6-12-08 calib}</b> <table border="1"> <tr> <th>142/144</th><th>143/144</th><th>145/144</th><th>146/144</th><th>148/144</th><th>150/144</th><th>[Nd150]</th></tr> <tr> <td>0.830433</td><td>0.494001</td><td>0.436936</td><td>0.885201</td><td>0.740574</td><td>198.371260</td><td>0.125778 nm/g</td></tr> </table>				142/144	143/144	145/144	146/144	148/144	150/144	[Nd150]	0.830433	0.494001	0.436936	0.885201	0.740574	198.371260	0.125778 nm/g
142/144	143/144	145/144	146/144	148/144	150/144	[Nd150]											
0.830433	0.494001	0.436936	0.885201	0.740574	198.371260	0.125778 nm/g											
Wt Sample (g)= <b>3.34E-05</b> g	Wt Spike (g)= <b>0.85762</b> g																
Mass Spectrometer Information:																	
Number of cycles measured: <b>68</b> Number of cycles used: <b>49</b>																	
		start	average (from sheet)														
Filament Current range: from	<b>3.36</b>	<b>3.45</b>	Amps														
Beam intensity range: from	<b>0.1682235</b>	<b>2.5435206</b>	Volts 144Nd.16O														
Temperature range: from	<b>1493</b>	<b>1569</b>	°C														
Final Ratio Data:																	
Interference Values (oxide corrected; informational only... not used in this sheet)																	
Ce140/Nd144	<b>0.003252</b>																
Pr141/Nd144	<b>0.002628</b>																
Sm149/Nd144	<b>4.02E-05</b>																
<i>for Ratios &amp; %ISE: use grand mean oxygen corr, interference corr, exp normalized values</i>																	
	142/144	143/144	145/144	146/144	148/144	150/144											
Ratios	<b>1.141668</b>	<b>0.512334</b>	<b>0.3485735</b>	<b>0.7219</b>	<b>0.24199068</b>	<b>0.8886235</b>											
%StdErr	<b>0.000757</b>	<b>0.000796</b>	<b>0.0006589</b>	<b>0</b>	<b>0.01410647</b>	<b>0.0029022</b>											
for comparison only	<b>142/144</b>	<b>143/144</b>	<b>145/144</b>	<b>146/144</b>	<b>148/144</b>	<b>150/144</b>											
DePaolo 88, p.14, ln. B':	1.141854	na	0.348416	0.721882	0.241572	na											
<b>FINAL DATA TO REPORT:</b>																	
146/144 set to 0.7219																	
	142/144	143/144	145/144	146/144	148/144	150/144											
Ratios	<b>1.141832</b>	<b>0.512201</b>	<b>0.348412</b>	<b>0.721900</b>	<b>0.240700</b>	<b>0.236478</b>											
± 2 S.E.	<b>0.000017</b>	<b>0.000008</b>	<b>0.000005</b>	<b>0.000000</b>	<b>0.000068</b>	<b>0.000014</b>											
Epsilon143= -8.53 using (143/144)chur= 0.512638 ± 0.16 (Hamilton et al. 1983)																	
<i>linked from Sm sheet</i>																	
[Sm147]= ##### nm/g	[Nd144]= 4910.36939 nm/g																
± 0.094135	± 0.34583																
[Sm]= ##### ppm	[Nd]= 2978.01465 ppm																
± 0.094381	± 0.20974																
TOT ng Sm= 24.40843	TOT ng Nd= 99.5649763																
Sm147/Nd144= <b>0.148291</b> ± 2 S.E. <b>0.000022</b> ± 2RSE % <b>0%</b>																	

Full Sample Name:	<b>CBD11_10</b>	2 eud 1	
Date of TIMS analysis:	<b>11/23/2020</b>		Position #:
estimated Nd load (ng):			<b>2</b>
<b>Rspike Values Nd {SmNd 0.15 A spike, 6-12-08 calib}</b>			
142/144	143/144	145/144	146/144
0.830433	0.494001	0.436936	0.885201
148/144	150/144	[Nd150]	0.740574
198.371260	0.125778	nm/g	

Wt Sample (g)= **0.00001** g  
 Wt Spike (g)= **0.24632** g

Mass Spectrometer Information:

Number of cycles measured:	<b>193</b>
Number of cycles used:	<b>182</b>
	average
	(from sheet)
Filament Current range: from	<b>3.36</b>
Beam intensity range: from	<b>0.1114387</b>
Temperature range: from	<b>1540</b>
	<b>3.51</b>
	<b>0.0872368</b>
	<b>1590</b>
	Amps
	Volts 144Nd.160
	°C

Final Ratio Data:

Interference Values (oxide corrected; informational only... not used in this sheet)

Ce140/Nd144	<b>0.021873</b>
Pr141/Nd144	<b>0.007666</b>
Sm149/Nd144	<b>8.24E-05</b>

for Ratios & %ISE: use grand mean oxygen corr, interference corr, exp normalized values

	142/144	143/144	145/144	146/144	148/144	150/144	
Ratios	<b>1.141048</b>	<b>0.5128807</b>	<b>0.3490621</b>	0.7219	<b>0.24673442</b>	<b>2.8322928</b>	
%StdErr	<b>0.002804</b>	<b>0.0018657</b>	<b>0.0019759</b>	0	<b>0.00515227</b>	<b>0.0049638</b>	
for comparison only	142/144	143/144	145/144	146/144	148/144	150/144	
DePaolo 88, p.14, ln. B':	1.141854	na	0.348416	0.721882	0.241572	na	

FINAL DATA TO REPORT:

146/144 set to 0.7219

	142/144	143/144	145/144	146/144	148/144	150/144	150t/144s
Ratios	1.141716	0.512351	0.348415	0.721900	0.241603	0.236478	0.376041
± 2 S.E.	0.000064	0.000019	0.000014	0.000000	0.000025	0.000023	0.000037

Epsilon143= -5.60 using (143/144)chur= 0.512638  
 ± 0.37 (Hamilton et al. 1983)

linked from Sm sheet

[Sm147]= ##### nm/g  
 ± 0.020916

[Nd144]= 1165.03804 nm/g  
 ± 0.11625

[Sm]= ##### ppm  
 ± 0.020971

[Nd]= 706.56606 ppm  
 ± 0.07050

TOT ng Sm= 2.02176

TOT ng Nd= 7.06566062

Sm147/Nd144= 0.173085
± 2 S.E. 0.000025
± 2RSE % 0%

Full Sample Name: CBD11\_10 2 eud 2  
 Date of TIMS analysis: 11/24/2020  
 estimated Nd load (ng):

Position #: 4

Rspike Values Nd {SmNd 0.15 A spike, 6-12-08 calib}						
142/144	143/144	145/144	146/144	148/144	150/144	[Nd150]
0.830433	0.494001	0.436936	0.885201	0.740574	198.371260	0.125778
nm/g						

Wt Sample (g)= 0.00001 g  
 Wt Spike (g)= 0.25251 g

Mass Spectrometer Information:

Number of cycles measured:	215
Number of cycles used:	208
start	average (from sheet)
Filament Current range: from	3.16      3.2
Beam intensity range: from	0.1140518      0.1818908
Temperature range: from	1527      1588
	Amps
	Volts 144Nd.160
	° C

Final Ratio Data:

Interference Values (oxide corrected; informational only... not used in this sheet)

Ce140/Nd144 0.01519386  
 Pr141/Nd144 0.00313533  
 Sm149/Nd144 7.3638E-05

for Ratios & %ISE: use grand mean oxygen corr, interference corr, exp normalized values

	142/144	143/144	145/144	146/144	148/144	150/144
Ratios	1.1413738	0.5127715	0.3488462	0.7219	0.24509278	2.0210111
%StdErr	0.00145734	0.0010824	0.0010835	0	0.00194705	0.0026218
for comparison only	142/144	143/144	145/144	146/144	148/144	150/144
DePaolo 88, p.14, ln. B':	1.141854	na	0.348416	0.721882	0.241572	na

FINAL DATA TO REPORT:

146/144 set to 0.7219						
	142/144	143/144	145/144	146/144	148/144	150/144
Ratios	1.141830	0.512409	0.348402	0.721900	0.241567	0.236478
± 2 S.E.	0.000033	0.000011	0.000008	0.000000	0.000009	0.000012
Epsilon143=	-4.48	using (143/144)chur=	0.512638			
	± 0.22	(Hamilton et al. 1983)				

linked from Sm sheet

[Sm147]= 308.026882 nm/g [Nd144]= 1749.45127 nm/g

± 0.026013 ± 0.09521

[Sm]= 308.830025 ppm [Nd]= 1060.99788 ppm

± 0.026080 ± 0.05774

TOT ng Sm= 3.08830025 TOT ng Nd= 10.6099788

Sm147/Nd144= 0.176071  
 ± 2 S.E. 0.000018  
 ± 2RSE % 0%

Full Sample Name: CBD11\_10\_2 eud 3  
 Date of TIMS analysis: 11/24/2020 Position #: 5  
 estimated Nd load (ng):

Rspike Values Nd {SmNd 0.15 A spike, 6-12-08 calib}						
142/144	143/144	145/144	146/144	148/144	150/144	[Nd150]
0.830433	0.494001	0.436936	0.885201	0.740574	198.371260	0.125778
nm/g						

Wt Sample (g)= 0.00001 g  
 Wt Spike (g)= 0.24873 g

#### Mass Spectrometer Information

Number of cycles measured:	177
Number of cycles used:	158
start	average (from sheet)
Filament Current range: from	3.5      3.53
Beam intensity range: from	0.1422713      0.2400054
Temperature range: from	1560      1597
	Amps
	Volts 144Nd16O
	°C

#### Final Ratio Data:

Interference Values (oxide corrected; informational only... not used in this sheet)

Ce140/Nd144	0.012672
Pr141/Nd144	0.002669
Sm149/Nd144	0.000112

for Ratios & %ISE: use grand mean oxygen corr, interference corr, exp normalized values

	142/144	143/144	145/144	146/144	148/144	150/144
Ratios	1.141461	0.5126602	0.3487977	0.7219	0.24470586	1.8365952
%StdErr	0.001189	0.0007747	0.0008225	0	0.00275311	0.0033431
for comparison only	142/144	143/144	145/144	146/144	148/144	150/144
DePaolo 88, p.14, ln. B'	1.141854	na	0.348416	0.721882	0.241572	na

#### FINAL DATA TO REPORT:

146/144 set to 0.7219

	142/144	143/144	145/144	146/144	148/144	150/144	150t/144s
Ratios	1.141870	0.512334	0.348400	0.721900	0.241545	0.236478	0.615287
± 2 S.E.	0.000027	0.000008	0.000006	0.000000	0.000013	0.000016	0.000041

Epsilon143= -5.92 using (143/144)chur= 0.512638  
 ± 0.15 (Hamilton et al. 1983)

linked from Sm sheet

[Sm147]= ##### nm/g                                  [Nd144]= 1924.91079 nm/g

± 0.029448    ± 0.13245

[Sm]= ##### ppm    [Nd]= 1167.40963 ppm

± 0.029524    ± 0.08033

TOT ng Sm= 3.170055

TOT ng Nd= 11.6740963

Sm147/Nd144= 0.164258
± 2 S.E. 0.000019
± 2RSE % 0%

Full Sample Name: CBD11\_10\_2 eud 4  
 Date of TIMS analysis: 11/24/2020 Position #: 6  
 estimated Nd load (ng):

Rspike Values Nd {SmNd 0.15 A spike, 6-12-08 calib}						
142/144	143/144	145/144	146/144	148/144	150/144	[Nd150]
0.830433	0.494001	0.436936	0.885201	0.740574	198.371260	0.125778
nm/g						

Wt Sample (g)= 0.00001 g  
 Wt Spike (g)= 0.24741 g

#### Mass Spectrometer Information:

Number of cycles measured:	119
Number of cycles used:	108
start	average (from sheet)
Filament Current range: from	3.3
Beam intensity range: from	0.0739757
Temperature range: from	1560
	1617
	Amps
	Volts 144Nd16O
	°C

#### Final Ratio Data:

Interference Values (oxide corrected; informational only... not used in this sheet)

Ce140/Nd144	0.046651
Pr141/Nd144	0.006335
Sm149/Nd144	0.000156

for Ratios & %ISE: use grand mean oxygen corr, interference corr, exp normalized values

	142/144	143/144	145/144	146/144	148/144	150/144	
Ratios	1.141471	0.5129231	0.3489985	0.7219	0.2464662	2.7627622	
%StdErr	0.00852	0.0055463	0.0060149	0	0.01185492	0.0135876	
for comparison only	142/144	143/144	145/144	146/144	148/144	150/144	
DePaolo 88, p.14, ln. B'	1.141854	na	0.348416	0.721882	0.241572	na	

#### FINAL DATA TO REPORT:

146/144 set to 0.7219

Ratios	1.142125	0.512408	0.348368	0.721900	0.241470	0.236478	0.386623
± 2 S.E.	0.000195	0.000057	0.000042	0.000000	0.000057	0.000064	0.000105

Epsilon143= -4.48 using (143/144)chur= 0.512638  
 ± 1.11 (Hamilton et al. 1983)

linked from Sm sheet

[Sm147]= ##### nm/g [Nd144]= 1203.12321 nm/g

± 0.029063 ± 0.32718

[Sm]= ##### ppm [Nd]= 729.66375 ppm

± 0.029139 ± 0.19843

TOT ng Sm= 2.181415 TOT ng Nd= 7.29663752

Sm147/Nd144= 0.180841
± 2 S.E. 0.000055
± 2RSE % 0%

Full Sample Name: CBD\_11\_10\_2.edu 5

Date of TIMS analysis: 11/25/2020

Position #: 7

estimated Nd load (ng):

Rspike Values Nd {SmNd 0.15 A spike, 6-12-08 calib}						
142/144	143/144	145/144	146/144	148/144	150/144	[Nd150]
0.830433	0.494001	0.436936	0.885201	0.740574	198.371260	0.125778
nm/g						

Wt Sample (g)= 0.00001 g

Wt Spike (g)= 0.24779 g

Mass Spectrometer Information:

Number of cycles measured: &lt;enter!&gt;

Number of cycles used: &lt;enter!&gt;

	start	average (from sheet)	
Filament Current range: from	3.1	3.16	Amps
Beam intensity range: from	0.18368248	0.2958935	Volts 144Nd.160
Temperature range: from	1547	1583	°C

Final Ratio Data:

Interference Values (oxide corrected; informational only... not used in this sheet)

Ce140/Nd144 0.010206

Pr141/Nd144 0.003847

Sm149/Nd144 5.9E-05

*for Ratios & %ISE: use grand mean oxygen corr, interference corr, exp normalized values*

	142/144	143/144	145/144	146/144	148/144	150/144
Ratios	1.141574	0.51258293	0.34872381	0.7219	0.24408901	1.5185964
%StdErr	0.001308	0.00075285	0.00073924	0	0.00191457	0.0021033
for comparison only	142/144	143/144	145/144	146/144	148/144	150/144
DePaolo 88, p.14, ln. B':	1.141854	na	0.348416	0.721882	0.241572	na

**FINAL DATA TO REPORT:**

146/144 set to 0.7219

Ratios	142/144	143/144	145/144	146/144	148/144	150/144	150t/144s
	1.141901	0.512322	0.348405	0.721900	0.241557	0.236478	0.769984
± 2 S.E.	0.000030	0.000008	0.000005	0.000000	0.000009	0.000010	0.000032

Epsilon143= -6.16 using (143/144)chur= 0.512638  
± 0.15 (Hamilton et al. 1983)*linked from Sm sheet*

[Sm147]= ##### nm/g

[Nd144]= 2399.77529 nm/g

± 0.060312

± 0.11208

[Sm]= ##### ppm

[Nd]= 1455.40293 ppm

± 0.060470

± 0.06797

TOT ng Sm= 3.900037

TOT ng Nd= 14.5540293

Sm147/Nd144= 0.162094

± 2 S.E. 0.000026

± 2RSE % 0%

Full Sample Name: **CBD11\_10** 2 eud 6  
Date of TIMS analysis: **11/25/2020** Position #: **8**  
estimated Nd load (ng):

Rspike Values Nd {SmNd 0.15 A spike, 6-12-08 calib}						
142/144	143/144	145/144	146/144	148/144	150/144	[Nd150]
0.830433	0.494001	0.436936	0.885201	0.740574	198.371260	0.125778
						nm/g

Wt Sample (g)= 0.00001 g  
Wt Spike (g)= 0.247 g

Mass Spectrometer Information:

Number of cycles measured: **233**  
Number of cycles used: **214**

	start	average (from sheet)	
Filament Current range: from	<b>3.45</b>	<b>3.54</b>	Amps
Beam intensity range: from	<b>0.0538764</b>	<b>0.1102072</b>	Volts 144Nd.160
Temperature range: from	<b>1553</b>	<b>1602</b>	°C

### Final Ratio Data:

Interference Values (oxide corrected; informational only... not used in this sheet)  
Ce140/Nd144 **0.015701**  
Pr141/Nd144 **0.003772**  
Sm149/Nd144 **9.52E-05**

for Ratios & %ISE: use grand mean oxygen corr, interference corr, exp normalized values

	142/144	143/144	145/144	146/144	148/144	150/144
Ratios	1.141442	0.5127074	0.3488502	0.7219	0.24495823	1.9700473
%StdErr	0.001972	0.0015569	0.0013124	0	0.00341742	0.0035503
for comparison only	142/144	143/144	145/144	146/144	148/144	150/144
DePaolo 88, p.14, ln. B':	1.141854	na	0.348416	0.721882	0.241572	na

FINAL DATA TO REPORT:			146/144 set to 0.7219				
	142/144	143/144	145/144	146/144	148/144	150/144	150t/144s
Ratios	1.141885	0.512354	0.348419	0.721900	0.241533	0.236478	0.567272
± 2 S.E.	0.000045	0.000016	0.000009	0.000000	0.000017	0.000017	0.000040

Epsilon143=	-5.53	using (143/144)chur=	0.512638
±	0.31	(Hamilton et al. 1983)	

*linked from Sm sheet*

[Sml47]= ##### nm/g  
+ 0.042143

$$[NdI44] = 1762.35509 \text{ nm/g}$$

[S m]= ##### ppm  
+ 0.042253

[Nd]= 1068.82372 ppm

TOT ng Sm= 2.924445

TOT ng Nd= 10.6882372

Sml47/Nd144= 0.165508  
± 2 S.E. 0.000027

128

Full Sample Name: **CBD11\_10** - 2 eud 7  
 Date of TIMS analysis: ##### Position #: **9**  
 estimated Nd load (ng):

Rspike Values Nd [SmNd 0.15 A spike, 6-12-08 calib]						
142/144	143/144	145/144	146/144	148/144	150/144	[Nd150]
0.830433	0.494001	0.436936	0.885201	0.740574	198.371260	0.125778

nm/g

Wt Sample (g)= **0.00001** g  
 Wt Spike (g)= **0.2482** g

Mass Spectrometer Information:

Number of cycles measured:	<b>209</b>
Number of cycles used:	<b>195</b>
start	average
Filament Current range: from	<b>3.45</b> <b>3.53</b>
Beam intensity range: from	<b>0.1203457</b> <b>0.2612121</b>
Temperature range: from	<b>1553</b> <b>1600</b>

Amps  
 Volts 144Nd.16O  
 °C

Final Ratio Data:

Interference Values (oxide corrected; informational only... not used in this sheet)

Ce140/Nd144	<b>0.008095</b>
Pr141/Nd144	<b>0.006467</b>
Sm149/Nd144	<b>5.07E-05</b>

for Ratios & %ISE: use grand mean oxygen corr, interference corr, exp normalized values

	142/144	143/144	145/144	146/144	148/144	150/144
Ratios	<b>1.141484</b>	<b>0.512666</b>	<b>0.3488013</b>	<b>0.7219</b>	<b>0.24470955</b>	<b>1.8290593</b>
%StdErr	<b>0.001354</b>	<b>0.000802</b>	<b>0.0009215</b>	<b>0</b>	<b>0.00191389</b>	<b>0.0022567</b>
for comparison only	<b>142/144</b>	<b>143/144</b>	<b>145/144</b>	<b>146/144</b>	<b>148/144</b>	<b>150/144</b>
DePaolo 88, p.14, ln. B':	1.141854	na	0.348416	0.721882	0.241572	na

FINAL DATA TO REPORT: 146/144 set to 0.7219

	142/144	143/144	145/144	146/144	148/144	150/144	150t/144s
Ratios	<b>1.141891</b>	<b>0.512341</b>	<b>0.348406</b>	<b>0.721900</b>	<b>0.241564</b>	<b>0.236478</b>	<b>0.618238</b>
± 2 S.E.	<b>0.000031</b>	<b>0.000008</b>	<b>0.000006</b>	<b>0.000000</b>	<b>0.000009</b>	<b>0.000011</b>	<b>0.000028</b>

Epsilon143= **-5.78** using (143/144)chur= **0.512638**  
 ± **0.16** (Hamilton et al. 1983)

linked from Sm sheet

[Sm147]= ##### nm/g

± 0.039303

[Nd]= 1930.02270 nm/g

± 0.09264

[Sm]= ##### ppm

± 0.039405

[Nd]= 1170.50988 ppm

± 0.05618

TOT ng Sm= 3.233976

TOT ng Nd= 11.7050988

Sm147/Nd144= **0.167126**

± 2 S.E. 0.000022

± 2RSE % 0%

## Sm Reduction Sheets

This appendix contains the Sm reduction sheets for every sample used in the above study. Sheets appear in the same order as presented in data tables.

Full Sample Name: **KP1\_2.1\_1 Sm**  
 Date of TIMS analysis: **42397**  
 estimated Sm load (ng): **10**

Position #: **2**

Rspike Values Sm {SmNd 0.15 A spike, 6/12/08 calib}

147/152	149/152	[Concentration]
477.2255	1.7429473	0.018992
		nm/g

Normalized to 149/152= 0.51686

Wt. Sample= **2.4107E-05** g  
 Wt. Spike= **0.536385** g

For Sm/Sm, enter Normalized data

	Sml47/Sml52	Sml49/Sml52	Sml54/Sml52	Gd155/Sml52
Ratios	<b>1.2517148</b>	0.51686	<b>0.85178532</b>	<b>0.22364378</b>
%StdErr	<b>0.04823102</b>	0.00000	<b>0.037614439</b>	<b>0.85773097</b>
(ppm)				

Spike subtracted grand mean ratios

	147/152	149/152	152s/147t
Ratios	0.560865	0.516860	1.428564
2 S.E.	0.00054102	0	0.001378022

$$[\text{Sm}147] = 338.55964 \text{ nm/g}$$

$$\pm 0.32736$$

$$[\text{Sm}] = 339.44239 \text{ ppm}$$

$$\pm 0.32821$$

Discrimination= 0.6667 to 0.6667  
 w/Average of 0.6667

Full Sample Name: **KP1\_2.1\_2 Sm**  
 Date of TIMS analysis: **1/29/2020**  
 estimated Sm load (ng): **10**

Position #: **3**

Rspike Values Sm {SmNd 0.15 A spike, 6/12/08 calib}

147/152	149/152	[Concentration]
477.2255	1.7429473	0.018992
		nm/g

Normalized to 149/152= 0.51686

Wt. Sample= **2.4095E-05** g  
 Wt. Spike= **0.53577** g

For Sm/Sm, enter Normalized data

	Sm147/Sm152	Sm149/Sm152	Sm154/Sm152	Gd155/Sm152
Ratios	<b>1.8780165</b>	0.51686	<b>0.85390139</b>	<b>0.00182225</b>
%StdErr	<b>0.00422892</b>	0.00000	<b>0.003604582</b>	<b>0.83434952</b>
(ppm)				

Spike subtracted grand mean ratios

	147/152	149/152	152s/147t
Ratios	0.560865	0.516860	0.744306
2 S.E.	4.7437E-05	0	6.29522E-05

$$[\text{Sm}147] = 176.28365 \text{ nm/g}$$

$$\pm 0.01613$$

<b>[\text{Sm}] = 176.74328 ppm</b>	<b>4.25862941</b>
<b><math>\pm 0.01617</math></b>	

Discrimination= 0.6667 to 0.6667  
 w/Average of 0.6667

Full Sample Name: **KP1\_2.1\_3 Sm**  
 Date of TIMS analysis: **1/29/2020**  
 estimated Sm load (ng): **10**

Position #: **4**

Rspike Values Sm {SmNd 0.15 A spike, 6/12/08 calib}

147/152	149/152	[Concentration]
477.2255	1.7429473	0.018992
		nm/g

Normalized to 149/152= 0.51686

Wt. Sample= **2.4059E-05** g  
 Wt. Spike= **0.535635** g

For Sm/Sm, enter Normalized data

	Sm147/Sm152	Sm149/Sm152	Sm154/Sm152	Gd155/Sm152
Ratios	<b>2.01626801</b>	0.51686	<b>0.854174433</b>	<b>0.01830308</b>
%StdErr	<b>0.00189475</b>	0.00000	<b>0.001425631</b>	<b>1.99169704</b>
(ppm)				

Spike subtracted grand mean ratios

	147/152	149/152	152s/147t
Ratios	0.560865	0.516860	0.672607
2 S.E.	2.1254E-05	0	2.54885E-05

$$[\text{Sm}147] = 159.49973 \text{ nm/g}$$

$$\pm 0.00787$$

$$[\text{Sm}] = 159.91561 \text{ ppm}$$

$$\pm 0.00789$$

Discrimination= 0.6667 to 0.6667  
 w/Average of 0.6667

Full Sample Name: **KP1\_2.1\_4\_Sm**  
 Date of TIMS analysis: **1/29/2020**  
 estimated Sm load (ng): **20**

Position #: **5**

Rspike Values Sm {SmNd 0.15 A spike, 6/12/08 calib}

147/152	149/152	[Concentration]
477.2255	1.7429473	0.018992
nm/g		

Normalized to 149/152= 0.51686

Wt. Sample= **2.403E-05** g  
 Wt. Spike= **0.53473** g

For Sm/Sm, enter Normalized data

	Sml47/Sml52	Sml49/Sml52	Sml54/Sml52	Gd155/Sml52
Ratios	<b>1.8614001</b>	0.51686	<b>0.85406379</b>	<b>0.02669139</b>
%StdErr	<b>0.01046927</b>	0.00000	<b>0.007313807</b>	<b>0.72827473</b>
(ppm)				

Spike subtracted grand mean ratios

	147/152	149/152	152s/147t
Ratios	0.560865	0.516860	0.753950
2 S.E.	0.00011744	0	0.000157866

$$[\text{Sm}147] = 178.70238 \text{ nm/g} \\ \pm 0.03795$$

$[\text{Sm}] = 179.16833 \text{ ppm}$
$\pm 0.03805$

Discrimination= 0.6667 to 0.6667  
 w/Average of 0.6667

Full Sample Name: **KP1\_2.1\_5 Sm**  
 Date of TIMS analysis: **7/21/2020**  
 estimated Sm load (ng): **20**

Position #: **11**

Rspike Values Sm {SmNd 0.15 A spike, 6/12/08 calib}

147/152	149/152	[Concentration]
477.2255	1.7429473	0.018992
		nm/g

Normalized to 149/152= 0.51686

Wt. Sample= **2.9742E-05** g  
 Wt. Spike= **0.75668** g

For Sm/Sm, enter Normalized data

	Sm147/Sm152	Sm149/Sm152	Sm154/Sm152	Gd155/Sm152
Ratios	<b>2.876334</b>	0.51686	<b>0.85523706</b>	<b>0.00694022</b>
%StdErr	<b>0.00438135</b>	0.00000	<b>0.003694891</b>	<b>0.81122819</b>
(ppm)				

Spike subtracted grand mean ratios

	147/152	149/152	152s/147t
Ratios	0.560865	0.516860	0.418871
2 S.E.	4.9147E-05	0	3.67044E-05

$$[\text{Sm}147] = 113.50901 \text{ nm/g} \\ \pm 0.01020$$

$$[\text{Sm}] = 113.80497 \text{ ppm} \\ \pm 0.01023$$

Discrimination= 0.6667 to 0.6667  
 w/Average of 0.6667

Full Sample Name: **KP1\_2.1\_7\_Sm**  
 Date of TIMS analysis: **8/11/2020**  
 estimated Sm load (ng): **20**

Position #: **11**

Rspike Values Sm {SmNd 0.15 A spike, 6/12/08 calib}

147/152	149/152	[Concentration]
477.2255	1.7429473	0.018992
		nm/g

Normalized to 149/152= 0.51686

Wt. Sample= **2.4107E-05** g  
 Wt. Spike= **0.75857** g

For Sm/Sm, enter Normalized data

	Sml47/Sml52	Sml49/Sml52	Sml54/Sml52	Gd155/Sml52
Ratios	<b>3.7517943</b>	0.51686	<b>0.85835619</b>	<b>0.03225917</b>
%StdErr	<b>0.0047649</b>	0.00000	<b>0.003528572</b>	<b>1.2379704</b>
(ppm)				

Spike subtracted grand mean ratios

	147/152	149/152	152s/147t
Ratios	0.560865	0.516860	0.301062
2 S.E.	5.3449E-05	0	2.86907E-05

$$[\text{Sm}147] = 100.90456 \text{ nm/g}$$

$$\pm 0.00973$$

$$[\text{Sm}] = 101.16765 \text{ ppm}$$

$$\pm 0.00975$$

Discrimination= 0.6667 to 0.6667  
 w/Average of 0.6667

Full Sample Name: **P\_1\_2.1\_9\_Sm**  
 Date of TIMS analysis: **8/6/2020**  
 estimated Sm load (ng): **20**

Position #: **12**

Rspike Values Sm {SmNd 0.15 A spike, 6/12/08 calib}

147/152	149/152	[Concentration]
477.2255	1.7429473	0.018992
		nm/g

Normalized to 149/152= 0.51686

Wt. Sample= **0.00003** g  
 Wt. Spike= **0.76352** g

For Sm/Sm, enter Normalized data

	Sm147/Sm152	Sm149/Sm152	Sm154/Sm152	Gd155/Sm152
Ratios	<b>1.629007</b>	0.51686	<b>0.85329728</b>	<b>0.06606277</b>
%StdErr	<b>0.00200376</b>	0.00000	<b>0.00160834</b>	<b>0.9191732</b>
(ppm)				

Spike subtracted grand mean ratios

	147/152	149/152	152s/147t
Ratios	0.560865	0.516860	0.920264
2 S.E.	2.2477E-05	0	3.68799E-05

$$[\text{Sm}147] = 249.47148 \text{ nm/g}$$

$$\pm 0.01467$$

$$[\text{Sm}] = 250.12195 \text{ ppm}$$

$$\pm 0.01471$$

Discrimination= 0.6667 to 0.6667  
 w/Average of 0.6667

Full Sample Name: KP1\_2.1\_10 Sm  
 Date of TIMS analysis: 7/21/2020  
 estimated Sm load (ng): 20  
 Position #: 12

Rspike Values Sm {SmNd 0.15 A spike, 6/12/08 calib}		
147/152	149/152	[Concentration]
477.2255	1.7429473	0.018992 nm/g

Normalized to 149/152= 0.51686

Wt. Sample= 3.3088E-05 g  
 Wt. Spike= 0.87115 g

For Sm/Sm, enter Normalized data			
	Sm147/Sm152	Sm149/Sm152	Sm154/Sm152
Ratios	1.005856	0.51686	0.85127003
%StdErr	0.00140102	0.00000	0.001310737
(ppm)			0.94173502

Spike subtracted grand mean ratios

	147/152	149/152	152s/147t
Ratios	0.560865	0.516860	2.223630
2 S.E.	1.5716E-05	0	6.23071E-05

$$\begin{aligned}
 [\text{Sm}147] &= 623.57690 \text{ nm/g} \\
 &\pm 0.06678
 \end{aligned}$$

$$\begin{aligned}
 [\text{Sm}] &= 625.20281 \text{ ppm} \\
 &\pm 0.06696
 \end{aligned}$$

Discrimination= 0.6667 to 0.6667  
 w/Average of 0.6667

Full Sample Name: **eud\_122804**  
 Date of TIMS analysis: **4/10/2019**  
 estimated Sm load (ng): **20**

Position #: **2**

Rspike Values Sm {SmNd 0.15 A spike, 6/12/08 calib}

147/152	149/152	[Concentration]
477.2255	1.7429473	0.018992
		nm/g

Normalized to 149/152= 0.51686

Wt. Sample= **2.6468E-05** g  
 Wt. Spike= **0.56175** g

For Sm/Sm, enter Normalized data				
	Sm147/Sm152	Sm149/Sm152	Sm154/Sm152	Gd155/Sm152
Ratios	<b>0.80664954</b>	0.51686	<b>0.851564385</b>	<b>0.092915418</b>
%StdErr	<b>0.011536363</b>	0.00000	<b>0.009520048</b>	<b>0.601246711</b>

(ppm)

Spike subtracted grand mean ratios

	147/152	149/152	152s/147t
Ratios	0.560865	0.516860	4.034339
2 S.E.	0.000129407	0	0.000930832

$$[\text{Sm}147] = 912.01803 \text{ nm/g} \\ \pm 0.27095$$

$$[\text{Sm}] = 914.39600 \text{ ppm} \\ \pm 0.27166$$

Discrimination= 0.6667 to 0.6667  
 w/Average of 0.6667

Full Sample Name: **KP 2\_1\_2**  
 Date of TIMS analysis: **8/13/2019**  
 estimated Sm load (ng): **20**

Position #: **18**

Rspike Values Sm {SmNd 0.15 A spike, 6/12/08 calib}

147/152	149/152	[Concentration]
477.2255	1.7429473	0.018992
		nm/g

Normalized to 149/152= 0.51686

Wt. Sample= **2.0551E-05** g  
 Wt. Spike= **0.52225** g

For Sm/Sm, enter Normalized data

	Sm147/Sm152	Sm149/Sm152	Sm154/Sm152	Gd155/Sm152
Ratios	<b>0.94843129</b>	0.51686	<b>0.851657464</b>	<b>0.00385304</b>
%StdErr	<b>0.00233739</b>	0.00000	<b>0.001891702</b>	<b>0.75775676</b>
(ppm)				

Spike subtracted grand mean ratios

	147/152	149/152	152s/147t
Ratios	0.560865	0.516860	2.554649
2 S.E.	2.6219E-05	0	0.000119424

$$[\text{Sm}147] = 691.49666 \text{ nm/g} \\ \pm 0.08820$$

$$[\text{Sm}] = 693.29966 \text{ ppm} \\ \pm 0.08843$$

Discrimination= 0.6667 to 0.6667  
 w/Average of 0.6667

Full Sample Name: **KP\_2\_1\_3 Sm**  
 Date of TIMS analysis: **8/13/2019**  
 estimated Sm load (ng): **20**

Position #: **19**

Rspike Values Sm {SmNd 0.15 A spike, 6/12/08 calib}

147/152	149/152	[Concentration]
477.2255	1.7429473	0.018992
		nm/g

Normalized to 149/152= 0.51686

Wt. Sample= **2.3556E-05** g  
 Wt. Spike= **0.59851** g

For Sm/Sm, enter Normalized data

	Sm147/Sm152	Sm149/Sm152	Sm154/Sm152	Gd155/Sm152
Ratios	<b>0.97172623</b>	0.51686	<b>0.851727063</b>	<b>0.00182225</b>
%StdErr	<b>0.00163136</b>	0.00000	<b>0.001357129</b>	<b>0.83434952</b>
(ppm)				

Spike subtracted grand mean ratios

	147/152	149/152	152s/147t
Ratios	0.560865	0.516860	2.409213
2 S.E.	1.8299E-05	0	7.86057E-05

$$[\text{Sm}147] = 652.00717 \text{ nm/g} \\ \pm 0.07603$$

$$[\text{Sm}] = 653.70720 \text{ ppm} \\ \pm 0.07623$$

Discrimination= 0.6667 to 0.6667  
 w/Average of 0.6667

Full Sample Name:	<b>KP9_eud_1</b>
Date of TIMS analysis:	<b>14-Oct</b>
estimated Sm load (ng):	<b>8</b>
Position #:	<b>3</b>

Rspike Values Sm {SmNd 0.15 A spike, 6/12/08 calib}		
147/152	149/152	[Concentration]
477.2255	1.7429473	0.018992
nm/g		

Normalized to 149/152= 0.51686

Wt. Sample=	<b>1.1417E-05</b>	g	TER on ND sheet
Wt. Spike=	<b>0.32998</b>	g	

---

For Sm/Sm, enter Normalized data				
	Sm147/Sm152	Sm149/Sm152	Sm154/Sm152	Gd155/Sm152
Ratios	<b>8.3852044</b>	0.51686	<b>0.87109809</b>	<b>1.3365445</b>
%StdErr	<b>0.01406031</b>	0.00000	<b>0.011083394</b>	<b>1.4334258</b>
(ppm)				

#### Spike subtracted grand mean ratios

---

	147/152	149/152	152s/147t
Ratios	0.560865	0.516860	0.116495
2 S.E.	0.00015772	0	3.2759E-05

$$\begin{aligned} [\text{Sm147}] &= 35.86489 \text{ nm/g} \\ &\pm 0.01009 \end{aligned}$$

$[\text{Sm}] = 35.95841 \text{ ppm}$
$\pm 0.01011$

Discrimination= 0.6667 to 0.6667  
w/Average of 0.6667

---

Full Sample Name:	<b>KP9_eud_2</b>		
Date of TIMS analysis:	<b>14-Oct</b>	Position #:	<b>4</b>
estimated Sm load (ng):	<b>8</b>		

Rspike Values Sm {SmNd 0.15 A spike, 6/12/08 calib}		
147/152	149/152	[Concentration]
477.2255	1.7429473	0.018992
		nm/g

Normalized to 149/152= 0.51686

Wt. Sample=	<b>1.1442E-05</b>	g	TER on ND sheet
Wt. Spike=	<b>0.33061</b>	g	

---

For Sm/Sm, enter Normalized data				
	Sm147/Sm152	Sm149/Sm152	Sm154/Sm152	Gd155/Sm152
Ratios	<b>3.8552616</b>	0.51686	<b>0.85878747</b>	<b>0.17797404</b>
%StdErr	<b>0.0079374</b>	0.00000	<b>0.007298071</b>	<b>1.5753481</b>
(ppm)				

#### Spike subtracted grand mean ratios

---

	147/152	149/152	152s/147t
Ratios	0.560865	0.516860	0.291276
2 S.E.	8.9036E-05	0	4.62395E-05

$$[\text{Sm}147] = \mathbf{89.64921} \text{ nm/g}$$

$$\pm \mathbf{0.01429}$$

$[\text{Sm}] = \mathbf{89.88296} \text{ ppm}$
$\pm \mathbf{0.01432}$

Discrimination= 0.6667 to 0.6667  
w/Average of 0.6667

---

Full Sample Name:	<b>KP9_eud_3</b>	Position #:	<b>5</b>
Date of TIMS analysis:	<b>14-Oct</b>		
estimated Sm load (ng):	<b>8</b>		

Rspike Values Sm {SmNd 0.15 A spike, 6/12/08 calib}		
147/152	149/152	[Concentration]
477.2255	1.7429473	0.018992
nm/g		

Normalized to 149/152= 0.51686

Wt. Sample=	<b>1.1446E-05</b>	g	TER on ND sheet
Wt. Spike=	<b>0.3144</b>	g	

---

For Sm/Sm, enter Normalized data				
	Sm147/Sm152	Sm149/Sm152	Sm154/Sm152	Gd155/Sm152
Ratios	<b>5.7740006</b>	0.51686	<b>0.86333353</b>	<b>0.22508447</b>
%StdErr	<b>0.00969664</b>	0.00000	<b>0.006190726</b>	<b>1.7587097</b>
(ppm)				

#### Spike subtracted grand mean ratios

---

	147/152	149/152	152s/147t
Ratios	0.560865	0.516860	0.180178
2 S.E.	0.00010877	0	3.49424E-05

$$\begin{aligned} [\text{Sm}147] &= 52.71750 \text{ nm/g} \\ &\pm 0.01023 \end{aligned}$$

$[\text{Sm}] = 52.85495 \text{ ppm}$
$\pm 0.01026$

Discrimination= 0.6667 to 0.6667  
w/Average of 0.6667

---

Full Sample Name:	<b>KP9_eud_4</b>	
Date of TIMS analysis:	<b>10/15/2020</b>	Position #:
estimated Sm load (ng):	<b>8</b>	<b>6</b>

Rspike Values Sm {SmNd 0.15 A spike, 6/12/08 calib}		
147/152	149/152	[Concentration]
477.2255	1.7429473	0.018992
		nm/g

Normalized to 149/152= 0.51686

Wt. Sample=	<b>0.00001139</b>	g	TER on ND sheet
Wt. Spike=	<b>0.30829</b>	g	

---

For Sm/Sm, enter Normalized data				
	Sm147/Sm152	Sm149/Sm152	Sm154/Sm152	Gd155/Sm152
Ratios	<b>4.1957704</b>	0.51686	<b>0.85962025</b>	<b>0.14390081</b>
%StdErr	<b>0.00404699</b>	0.00000	<b>0.00348308</b>	<b>2.2787963</b>
(ppm)				

#### Spike subtracted grand mean ratios

---

	147/152	149/152	152s/147t
Ratios	0.560865	0.516860	0.263002
2 S.E.	4.5396E-05	0	2.12873E-05

$$\begin{aligned} [\text{Sm}147] &= 75.82342 \text{ nm/g} \\ &\pm 0.00621 \end{aligned}$$

$[\text{Sm}] = 76.02112 \text{ ppm}$
$\pm 0.00623$

Discrimination= 0.6667 to 0.6667  
w/Average of 0.6667

---

Full Sample Name: **KP9\_eud\_5**  
 Date of TIMS analysis: **10/15/2020**  
 estimated Sm load (ng): **<enter!>**  
 Position #: **7**

Rspike Values Sm {SmNd 0.15 A spike, 6/12/08 calib}		
147/152	149/152	[Concentration]
477.2255	1.7429473	0.018992
		nm/g

Normalized to 149/152= 0.51686

**Wt. Sample=** **0.00001** g      TER on ND sheet  
**Wt. Spike=** **0.27245** g

---

For Sm/Sm, enter Normalized data				
	Sm147/Sm152	Sm149/Sm152	Sm154/Sm152	Gd155/Sm152
Ratios	<b>2.1588476</b>	0.51686	<b>0.85463052</b>	<b>0.07517494</b>
%StdErr	<b>0.00251219</b>	0.00000	<b>0.001796412</b>	<b>2.8135351</b>
(ppm)				

#### Spike subtracted grand mean ratios

---

	147/152	149/152	152s/147t
Ratios	0.560865	0.516860	0.611658
2 S.E.	2.818E-05	0	3.0732E-05

$$\begin{aligned}
 [\text{Sm}147] &= 177.50248 \text{ nm/g} \\
 &\pm 0.01028
 \end{aligned}$$

$[\text{Sm}] = 177.96530 \text{ ppm}$ $\pm 0.01030$
--

Discrimination= 0.6667 to 0.6667  
 w/Average of 0.6667

---

Full Sample Name:	KP9_eud_6
Date of TIMS analysis:	10/15/2020
estimated Sm load (ng):	<enter!>
Position #:	8

Rspike Values Sm {SmNd 0.15 A spike, 6/12/08 calib}		
147/152	149/152	[Concentration]
477.2255	1.7429473	0.018992
		nm/g

Normalized to 149/152= 0.51686

Wt. Sample=	0.00001	g	TER on ND sheet
Wt. Spike=	0.27418	g	

---

For Sm/Sm, enter Normalized data				
	Sm147/Sm152	Sm149/Sm152	Sm154/Sm152	Gd155/Sm152
Ratios	0.96576551	0.51686	0.85162048	0.02770532
%StdErr	0.0035237	0.00000	0.002884068	0.519644
(ppm)				

#### Spike subtracted grand mean ratios

	147/152	149/152	152s/147t
Ratios	0.560865	0.516860	0.85162048
2 S.E.	4.9987E-05	0	0.00018E205

$$\begin{aligned} [\text{Sm147}] &= 743.00000 \text{ nm/g} \\ &\pm 0.09398 \end{aligned}$$

[Sm]= 715.85523 ppm
± 0.09570

Discrimination= 0.6667 to 0.6667  
w/Average of 0.6667

---

Full Sample Name:	KP9_eud-7
Date of TIMS analysis:	10/15/2020
estimated Sm load (ng):	<enter!>
Position #:	9

Rspike Values Sm {SmNd 0.15 A spike, 6/12/08 calib}		
147/152	149/152	[Concentration]
477.2255	1.7429473	0.018992
		nm/g

Normalized to 149/152= 0.51686

Wt. Sample=	0.00001	g	TER on ND sheet
Wt. Spike=	0.27258	g	

---

For Sm/Sm, enter Normalized data				
	Sm147/Sm152	Sm149/Sm152	Sm154/Sm152	Gd155/Sm152
Ratios	1.7386366	0.51686	0.85417701	0.05633245
%StdErr	0.00409911	0.00000	0.008712509	0.45920331
(ppm)				

#### Spike subtracted grand mean ratios

---

	147/152	149/152	152s/147t
Ratios	0.560865	0.516860	0.833629
2 S.E.	4.5981E-05	0	6.83427E-05

$$\begin{aligned} [\text{Sm}147] &= 242.03371 \text{ nm/g} \\ &\pm 0.02198 \end{aligned}$$

[Sm]= 242.66478 ppm
± 0.02204

Discrimination= 0.6667 to 0.6667  
w/Average of 0.6667

---

Full Sample Name:	KP9_eud_8
Date of TIMS analysis:	10/16/2020
estimated Sm load (ng):	<enter!>
Position #:	10

Rspike Values Sm {SmNd 0.15 A spike, 6/12/08 calib}		
147/152	149/152	[Concentration]
477.2255	1.7429473	0.018992
		nm/g

Normalized to 149/152= 0.51686

Wt. Sample=	0.00001	g	TER on ND sheet
Wt. Spike=	0.27285	g	

For Sm/Sm, enter Normalized data				
	Sm147/Sm152	Sm149/Sm152	Sm154/Sm152	Gd155/Sm152
Ratios	0.94779723	0.51686	0.85164181	0.02572892
%StdErr	0.0018085	0.00000	0.001822589	1.7592161
(ppm)				

#### Spike subtracted grand mean ratios

	147/152	149/152	152s/147t
Ratios	0.560865	0.516860	2.558853
2 S.E.	2.0287E-05	0	9.25538E-05

$$\begin{aligned} [\text{Sm}147] &= 743.66669 \text{ nm/g} \\ &\pm 0.09241 \end{aligned}$$

[Sm]= 745.60571 ppm
± 0.09265

Discrimination= 0.6667 to 0.6667  
w/Average of 0.6667

Full Sample Name: **11\_10\_2\_eud1\_Sm**  
 Date of TIMS analysis: **8/7/2020**  
 estimated Sm load (ng): **10**  
 Position #: **13**

Rspike Values Sm {SmNd 0.15 A spike, 6/12/08 calib}		
147/152	149/152	[Concentration]
477.2255	1.7429473	0.018992 nm/g

Normalized to 149/152= 0.51686

**Wt. Sample=** **0.00002** g  
**Wt. Spike=** **0.51034** g

For Sm/Sm, enter Normalized data			
	Sml47/Sml52	Sml49/Sml52	Sml54/Sml52
Ratios	<b>4.1871475</b>	0.51686	<b>0.8594772</b>
%StdErr	<b>0.00306958</b>	0.00000	<b>0.002684929</b>
(ppm)			<b>0.34264929</b>

#### Spike subtracted grand mean ratios

	147/152	149/152	152s/147t
Ratios	0.560865	0.516860	0.263652
2 S.E.	3.4432E-05	0	1.61861E-05

$$\begin{aligned}
 [\text{Sm}147] &= 71.65889 \text{ nm/g} \\
 &\pm 0.00449
 \end{aligned}$$

$[\text{Sm}] = 71.84574 \text{ ppm}$ $\pm 0.00450$
---

Discrimination= 0.6667 to 0.6667  
 w/Average of 0.6667

Full Sample Name: **CBD\_11\_10\_2\_EUD2\_Sm**  
 Date of TIMS analysis: **8/7/2020**  
 estimated Sm load (ng): **20**

Position #: **14**

Rspike Values Sm {SmNd 0.15 A spike, 6/12/08 calib}

147/152	149/152	[Concentration]
477.2255	1.7429473	0.018992
		nm/g

Normalized to 149/152= 0.51686

Wt. Sample= **0.00003** g  
 Wt. Spike= **0.76643** g

For Sm/Sm, enter Normalized data

	Sm147/Sm152	Sm149/Sm152	Sm154/Sm152	Gd155/Sm152
Ratios	<b>5.201059</b>	0.51686	<b>0.86186997</b>	<b>0.04638127</b>
%StdErr	<b>0.00238809</b>	0.00000	<b>0.001847613</b>	<b>1.4602183</b>
(ppm)				

Spike subtracted grand mean ratios

	147/152	149/152	152s/147t
Ratios	0.560865	0.516860	0.203733
2 S.E.	2.6788E-05	0	9.73068E-06

$$[\text{Sm}147] = 55.43988 \text{ nm/g}$$

$$\pm 0.00270$$

$$[\text{Sm}] = 55.58443 \text{ ppm}$$

$$\pm 0.00271$$

Discrimination= 0.6667 to 0.6667  
 w/Average of 0.6667

Full Sample Name: D\_11\_10\_2\_eud\_3  
 Date of TIMS analysis: 7/22/2020  
 estimated Sm load (ng): 20

Position #: 14

Rspike Values Sm {SmNd 0.15 A spike, 6/12/08 calib}

147/152	149/152	[Concentration]
477.2255	1.7429473	0.018992
		nm/g

Normalized to 149/152= 0.51686

Wt. Sample= 3.1364E-05 g  
 Wt. Spike= 0.80425 g

For Sm/Sm, enter Normalized data

	Sml47/Sml52	Sml49/Sml52	Sml54/Sml52	Gd155/Sml52
Ratios	21.0878379	0.51686	0.907180689	0.93036874
%StdErr	0.07116749	0.00000	0.063514396	3.86454263

(ppm)

Spike subtracted grand mean ratios

	147/152	149/152	152s/147t
Ratios	0.560865	0.516860	0.037635
2 S.E.	0.00079831	0	5.35682E-05

$$[\text{Sm}147] = 10.27918 \text{ nm/g}$$

$$\pm 0.01463$$

$$[\text{Sm}] = 10.30598 \text{ ppm}$$

$$\pm 0.01467$$

Discrimination= 0.6667 to 0.6667  
 w/Average of 0.6667

Full Sample Name: **\_11\_10\_2\_brith\_1**  
 Date of TIMS analysis: **7/22/2020**  
 estimated Sm load (ng): **20**

Position #: **13**

Rspike Values Sm {SmNd 0.15 A spike, 6/12/08 calib}

147/152	149/152	[Concentration]
477.2255	1.7429473	0.018992
		nm/g

Normalized to 149/152= 0.51686

Wt. Sample= **3.117E-05** g  
 Wt. Spike= **0.79861** g

For Sm/Sm, enter Normalized data

	Sml47/Sml52	Sml49/Sml52	Sml54/Sml52	Gd155/Sml52
Ratios	<b>8.12134361</b>	0.51686	<b>0.871484499</b>	<b>0.08912726</b>
%StdErr	<b>0.08952899</b>	0.00000	<b>0.130529134</b>	<b>0.03679161</b>
(ppm)				

Spike subtracted grand mean ratios

	147/152	149/152	152s/147t
Ratios	0.560865	0.516860	0.120933
2 S.E.	0.00100427	0	0.000216541

$$[\text{Sm}147] = 33.00271 \text{ nm/g}$$

$$\pm 0.05909$$

$$[\text{Sm}] = 33.08876 \text{ ppm}$$

$$\pm 0.05925$$

Discrimination= 0.6667 to 0.6667  
 w/Average of 0.6667

Full Sample Name: CB\_02\_12\_Sm  
Date of TIMS analysis: 7/30/2020  
estimated Sm load (ng): 10

Position #: 15

Rspike Values Sm {SmNd 0.15 A spike, 6/12/08 calib}

147/152	149/152	[Concentration]
477.2255	1.7429473	0.018992
nm/g		

Normalized to 149/152= 0.51686

Wt. Sample= 3.3433E-05 g  
Wt. Spike= 0.85762 g

For Sm/Sm, enter Normalized data

	Sm147/Sm152	Sm149/Sm152	Sm154/Sm152	Gd155/Sm152
Ratios	0.93243935	0.51686	0.85162639	0.00622707
%StdErr	0.00186341	0.00000	0.001667226	1.9080804
(ppm)				

Spike subtracted grand mean ratios

	147/152	149/152	152s/147t
Ratios	0.560865	0.516860	2.665047
2 S.E.	2.0902E-05	0	9.93216E-05

$$[\text{Sm}147] = 728.16385 \text{ nm/g}$$
$$\pm 0.09414$$

$$[\text{Sm}] = 730.06245 \text{ ppm}$$
$$\pm 0.09438$$

Discrimination= 0.6667 to 0.6667  
w/Average of 0.6667

Full Sample Name: **CBD11\_10\_2** eud 1  
 Date of TIMS analysis: **11/27/2020**  
 estimated Sm load (ng): **<enter!>**

Position #: **13**

Rspike Values Sm {SmNd 0.15 A spike, 6/12/08 calib}

147/152	149/152	[Concentration]
477.2255	1.7429473	0.018992
		nm/g

Normalized to 149/152= 0.51686

Wt. Sample= **0.00001** g  
 Wt. Spike= **0.24632** g

TER on ND sheet

For Sm/Sm, enter Normalized data

	Sm147/Sm152	Sm149/Sm152	Sm154/Sm152	Gd155/Sm152
Ratios	<b>1.8369742</b>	0.51686	<b>0.85375342</b>	<b>0.0679827</b>
%StdErr	<b>0.00486307</b>	0.00000	<b>0.003777442</b>	<b>3.5661836</b>
(ppm)				

Spike subtracted grand mean ratios

	147/152	149/152	152s/147t
Ratios	0.560865	0.516860	0.768581
2 S.E.	5.455E-05	0	7.47533E-05

$$[\text{Sm}147] = 201.65021 \text{ nm/g} \\ \pm 0.02092$$

$$[\text{Sm}] = 202.17599 \text{ ppm} \\ \pm 0.02097$$

Discrimination= 0.6667 to 0.6667  
 w/Average of 0.6667

Full Sample Name: **D11\_10\_2 eud 2**  
 Date of TIMS analysis: **11/2/2020**  
 estimated Sm load (ng): **<enter!>**

Position #: **14**

Rspike Values Sm {SmNd 0.15 A spike, 6/12/08 calib}

147/152	149/152	[Concentration]
477.2255	1.7429473	0.018992
		nm/g

Normalized to 149/152= 0.51686

Wt. Sample= **0.00001** g  
 Wt. Spike= **0.25251** g

TER on ND sheet

For Sm/Sm, enter Normalized data			
Sm147/Sm152	Sm149/Sm152	Sm154/Sm152	Gd155/Sm152
<b>1.4210696</b>	0.51686	<b>0.85295387</b>	<b>0.06696124</b>
<b>0.00326832</b>	0.00000	<b>0.002857222</b>	<b>1.5849907</b>
(ppm)			

Spike subtracted grand mean ratios

	147/152	149/152	152s/147t
Ratios	0.560865	0.516860	1.145252
2 S.E.	3.6662E-05	0	7.48609E-05

$$\begin{aligned} [\text{Sm147}] &= 308.02688 \text{ nm/g} \\ &\pm 0.02601 \end{aligned}$$

$$\begin{aligned} [\text{Sm}] &= 308.83002 \text{ ppm} \\ &\pm 0.02608 \end{aligned}$$

Discrimination= 0.6667 to 0.6667  
 w/Average of 0.6667

Full Sample Name: **D11\_10\_2 eud 3**  
 Date of TIMS analysis: **11/27/2020**  
 estimated Sm load (ng): **<enter!>**

Position #: **15**

Rspike Values Sm {SmNd 0.15 A spike, 6/12/08 calib}

147/152	149/152	[Concentration]
477.2255	1.7429473	0.018992
		nm/g

Normalized to 149/152= 0.51686

Wt. Sample= **0.00001** g  
 Wt. Spike= **0.24873** g

TER on ND sheet

For Sm/Sm, enter Normalized data

	Sm147/Sm152	Sm149/Sm152	Sm154/Sm152	Gd155/Sm152
Ratios	<b>1.3866424</b>	0.51686	<b>0.85276922</b>	<b>0.03820581</b>
%StdErr	<b>0.00373227</b>	0.00000	<b>0.003235288</b>	<b>1.2189067</b>
(ppm)				

Spike subtracted grand mean ratios

	147/152	149/152	152s/147t
Ratios	0.560865	0.516860	1.193434
2 S.E.	4.1866E-05	0	8.90845E-05

$$[\text{Sm}147] = 316.18105 \text{ nm/g} \\ \pm 0.02945$$

$$[\text{Sm}] = 317.00545 \text{ ppm} \\ \pm 0.02952$$

Discrimination= 0.6667 to 0.6667  
 w/Average of 0.6667

Full Sample Name: **D11\_10\_2 eud 4**  
 Date of TIMS analysis: **11/27/2020**  
 estimated Sm load (ng): **<enter!>**

Position #: **16**

Rspike Values Sm {SmNd 0.15 A spike, 6/12/08 calib}

147/152	149/152	[Concentration]
477.2255	1.7429473	0.018992
		nm/g

Normalized to 149/152= 0.51686

Wt. Sample= **0.00001** g  
 Wt. Spike= **0.24741** g

TER on ND sheet

For Sm/Sm, enter Normalized data

	Sm147/Sm152	Sm149/Sm152	Sm154/Sm152	Gd155/Sm152
Ratios	<b>1.74991595</b>	0.51686	<b>0.853904353</b>	<enter!>
%StdErr	<b>0.00639265</b>	0.00000	<b>0.007054912</b>	<enter!>
(ppm)				

Spike subtracted grand mean ratios

	147/152	149/152	152s/147t
Ratios	0.560865	0.516860	0.825622
2 S.E.	7.1708E-05	0	0.000105558

$$[\text{Sm}147] = 217.57423 \text{ nm/g} \\ \pm 0.02906$$

$$[\text{Sm}] = 218.14153 \text{ ppm} \\ \pm 0.02914$$

Discrimination= 0.6667 to 0.6667  
 w/Average of 0.6667

Full Sample Name: **D\_11\_10\_2.edu 5**  
 Date of TIMS analysis: **11/28/2020**  
 Position #: **17**  
 estimated Sm load (ng): **<enter!>**

Rspike Values Sm {SmNd 0.15 A spike, 6/12/08 calib}

147/152	149/152	[Concentration]
477.2255	1.7429473	0.018992
		nm/g

Normalized to 149/152= 0.51686

**Wt. Sample=** **0.00001** g  
**Wt. Spike=** **0.24779** g

TER on ND sheet

For Sm/Sm, enter Normalized data

	Sm147/Sm152	Sm149/Sm152	Sm154/Sm152	Gd155/Sm152
Ratios	<b>1.2306502</b>	0.51686	<b>0.85231509</b>	<b>0.04667569</b>
%StdErr	<b>0.00695061</b>	0.00000	<b>0.004668435</b>	<b>1.5743044</b>
(ppm)				

Spike subtracted grand mean ratios

	147/152	149/152	152s/147t
Ratios	0.560865	0.516860	1.473822
2 S.E.	7.7967E-05	0	0.000204879

$$\begin{aligned}
 [\text{Sm}147] &= 388.98941 \text{ nm/g} \\
 &\pm 0.06031
 \end{aligned}$$

$$\begin{aligned}
 [\text{Sm}] &= 390.00366 \text{ ppm} \\
 &\pm 0.06047
 \end{aligned}$$

Discrimination= 0.6667 to 0.6667  
 w/Average of 0.6667

Full Sample Name: **D11\_10\_2 eud 6**  
Date of TIMS analysis: **11/28/2020**  
estimated Sm load (ng): **<enter!>**

Position #: **18**

Rspike Values Sm {SmNd 0.15 A spike, 6/12/08 calib}

147/152	149/152	[Concentration]
477.2255	1.7429473	0.018992
		nm/g

Normalized to 149/152= 0.51686

Wt. Sample= **0.00001** g  
Wt. Spike= **0.247** g

TER on ND sheet

For Sm/Sm, enter Normalized data

	Sm147/Sm152	Sm149/Sm152	Sm154/Sm152	Gd155/Sm152
Ratios	<b>1.4491788</b>	0.51686	<b>0.85291252</b>	<b>0.05393064</b>
%StdErr	<b>0.00674427</b>	0.00000	<b>0.004772217</b>	<b>1.4305155</b>
(ppm)				

Spike subtracted grand mean ratios

	147/152	149/152	152s/147t
Ratios	0.560865	0.516860	1.108681
2 S.E.	7.5652E-05	0	0.000149545

$$[\text{Sm}147] = 291.68398 \text{ nm/g}$$
$$\pm 0.04214$$

$$[\text{Sm}] = 292.44451 \text{ ppm}$$
$$\pm 0.04225$$

Discrimination= 0.6667 to 0.6667  
w/Average of 0.6667

Full Sample Name: D11\_10\_2 eud 7  
Date of TIMS analysis: 11/28/2020  
estimated Sm load (ng): <enter!>

Position #: 19

Rspike Values Sm {SmNd 0.15 A spike, 6/12/08 calib}

147/152	149/152	[Concentration]
477.2255	1.7429473	0.018992
		nm/g

Normalized to 149/152= 0.51686

Wt. Sample= 0.00001 g  
Wt. Spike= 0.2482 g

TER on ND sheet

For Sm/Sm, enter Normalized data

	Sm147/Sm152	Sm149/Sm152	Sm154/Sm152	Gd155/Sm152
Ratios	1.3687491	0.51686	0.85297575	0.06731696
%StdErr	0.0053865	0.00000	0.004624163	1.3222343
(ppm)				

Spike subtracted grand mean ratios

	147/152	149/152	152s/147t
Ratios	0.560865	0.516860	1.220099
2 S.E.	6.0422E-05	0	0.000131441

$$[\text{Sm}147] = 322.55659 \text{ nm/g}$$
$$\pm 0.03930$$

$$[\text{Sm}] = 323.39761 \text{ ppm}$$
$$\pm 0.03941$$

Discrimination= 0.6667 to 0.6667  
w/Average of 0.6667

Full Sample Name: **D11\_10\_2 eud 8**  
Date of TIMS analysis: **11/29/2020**  
estimated Sm load (ng): **<enter!>**

Position #: **20**

Rspike Values Sm {SmNd 0.15 A spike, 6/12/08 calib}

147/152	149/152	[Concentration]
477.2255	1.7429473	0.018992
		nm/g

Normalized to 149/152= 0.51686

Wt. Sample= **0.00001** g  
Wt. Spike= **0.24829** g

TER on ND sheet

For Sm/Sm, enter Normalized data

	Sm147/Sm152	Sm149/Sm152	Sm154/Sm152	Gd155/Sm152
Ratios	<b>1.4821257</b>	0.51686	<b>0.85308126</b>	<b>0.04919407</b>
%StdErr	<b>0.01887947</b>	0.00000	<b>0.01366086</b>	<b>1.1187333</b>
(ppm)				

Spike subtracted grand mean ratios

	147/152	149/152	152s/147t
Ratios	0.560865	0.516860	1.068657
2 S.E.	0.00021178	0	0.000403514

$$[\text{Sm}147] = 282.62239 \text{ nm/g}$$
$$\pm 0.10764$$

$$[\text{Sm}] = 283.35929 \text{ ppm}$$
$$\pm 0.10792$$

Discrimination= 0.6667 to 0.6667  
w/Average of 0.6667

## 7.0 APPENDIX 3: DATA TABLES

Table 7. LA-ICP-MS elemental concentration data.

<b>Sample</b>	<b><math>^{147}\text{Sm}/^{144}\text{Nd}</math></b>	<b>Na</b>	<b>Cl</b>	<b>Ca</b>	<b>Mn</b>	<b>Fe</b>	<b>Zr</b>	<b>Be</b>	<b>Mg</b>
		<i>Wt %</i>	<i>ppm</i>	<i>ppm</i>					
Eud_LV01_1	0.12379	12.17	0.88	8.31	1.65	3.07	9.52	2.06	366
Eud_LV01_2	0.12454	12.13	0.90	8.07	1.59	3.06	9.35	1.24	374
Eud_LV01_3	0.12499	12.90	1.01	8.74	1.65	3.17	10.00	1.26	397
Eud_LV01_4	0.12462	12.72	1.02	8.54	1.62	3.10	9.81	1.07	398
Eud_LV01_5	0.12373	12.02	1.04	7.91	1.71	3.22	8.97	2.8	297
Eud_LV01_6	0.1246	12.52	1.13	8.18	1.59	2.92	9.21	1.22	350
Eud_LV01_7	0.12255	13.42	1.30	9.21	1.82	3.36	9.92	1.21	486
Eud_LV01_8	0.12129	13.27	1.27	9.21	1.86	3.27	9.40	0.52	523
Eud_LV01_9	0.12462	12.65	1.13	8.49	1.64	3.57	9.76	1.47	380
Eud_LV01_10	0.12386	12.62	1.16	8.36	1.73	3.63	9.80	1.3	313

<b>Sample</b>	<b><math>^{147}\text{Sm}/^{144}\text{Nd}</math></b>	<b>Na</b>	<b>Cl</b>	<b>Ca</b>	<b>Mn</b>	<b>Fe</b>	<b>Zr</b>	<b>Be</b>	<b>Mg</b>
Eud_LV01_11	0.12481	11.60	1.04	8.72	1.69	3.47	9.78	1.52	370
Eud_LV01_12	0.12536	12.12	0.97	8.49	1.61	3.49	10.01	1.21	416
Eud_LV01_13	0.12145	13.17	0.93	9.02	1.84	3.25	9.85	0.62	545
Eud_LV01_14	0.12271	13.03	0.92	9.00	1.84	3.23	9.70		548
Eud_LV01_15	0.12502	12.96	0.88	8.73	1.67	3.24	10.24		435
Eud_LV01_16	0.12509	12.52	0.86	8.76	1.70	3.04	10.00	0.06	452
Eud_LV01_17	0.12413	11.31	1.20	9.06	1.70	3.32	9.86	1.34	348
Eud_LV01_18	0.12495	12.89	1.17	9.01	1.63	3.42	9.87		442
Eud_NK_1	0.18978	10.23	0.22	5.73	1.82	2.25	10.25	1.66	151.7
Eud_NK_2	0.1892	10.04	0.22	6.20	1.87	2.31	10.22	3.9	147.7
Eud_NK_3	0.18921	10.68	0.30	6.02	1.91	2.42	10.60	1.82	148.9
Eud_NK_4	0.18969	10.40	0.28	5.97	1.93	2.34	10.66	3	156.3
Eud_NK_5	0.1892	10.51	0.30	5.45	1.80	2.25	9.64	1.84	139
Eud_NK_6	0.1896	10.41	0.29	5.55	1.79	2.24	9.63	2.32	134.7
Eud_NK_7	0.18979	10.51	0.31	6.08	1.86	2.49	9.91	2.94	149.4
Eud_NK_8	0.18906	10.68	0.31	5.87	1.86	2.49	9.99	2.86	150.2
Eud_NK_9	0.18885	10.34	0.30	5.76	1.85	2.66	10.00	2.15	145.5
Eud_NK_10	0.18911	10.57	0.25	5.73	1.85	2.62	10.03	1.28	150.2
Eud_NK_11	0.18884	10.53	0.23	5.80	1.83	2.62	10.18	1.84	147
Eud_NK_12	0.1885	10.73	0.25	5.85	1.84	2.60	10.13		145.3
Eud_NK_13	0.18872	10.47	0.20	5.63	1.81	2.47	10.12	1.14	151.1
Eud_NK_14	0.18938	10.56	0.23	5.67	1.89	2.53	10.43	2.35	138.7
Eud_NK_15	0.18892	10.54	0.21	5.87	1.91	2.36	10.40	1.83	157.5
Eud_NK_16	0.18913	10.39	0.21	5.77	1.88	2.32	10.20	2.3	140.2
Eud_NK_17	0.1888	10.70	0.33	6.17	1.83	2.52	10.42	1.93	153
Eud_NK_18	0.1888	10.30	0.36	5.87	1.82	2.51	10.33	1.61	145.6

<b>Sample</b>	<b><math>^{147}\text{Sm}/^{144}\text{Nd}</math></b>	<b>Na</b>	<b>Cl</b>	<b>Ca</b>	<b>Mn</b>	<b>Fe</b>	<b>Zr</b>	<b>Be</b>	<b>Mg</b>
CBD11_02_1	0.1879	10.43	0.86	8.23	0.36	4.90	9.89	1.07	
CBD11_02_2	0.1872	11.02	0.82	8.16	0.38	4.83	9.84	2.38	12.7
CBD11_02_3	0.1896	11.08	0.92	7.94	0.35	4.78	9.49	0.88	10.2
CBD11_02_4	0.1874	11.72	0.94	7.85	0.35	4.89	9.55	1.11	
CBD11_02_5	0.1835	11.71	0.88	8.12	0.38	4.87	9.61	1.34	10.2
CBD11_02_6	0.185	11.57	0.90	7.92	0.36	4.87	9.41	1.14	9.5
CBD11_02_7	0.1919	11.53	0.95	7.81	0.34	4.67	9.25		
CBD11_02_8	0.1846	11.58	0.94	7.92	0.36	4.70	9.46	0.95	11.5
CBD11_02_9	0.1841	11.51	0.87	7.89	0.38	4.90	9.36	1.2	
CBD11_02_10	0.1887	11.23	0.92	7.58	0.34	4.64	9.09	0.82	11
CBD11_02_11	0.1844	10.25	0.89	7.57	0.34	4.63	8.90	1.02	
CBD11_02_12	0.1892	10.45	1.01	7.60	0.32	4.82	8.99		
CBD11_02_13	0.19099	10.72	0.97	7.20	0.32	4.54	8.59	1.12	7.9
CBD11_02_16	0.18565	11.38	1.01	7.89	0.36	4.78	9.12	0.74	8
CBD11_02_17	0.1878	11.35	0.97	7.62	0.37	4.85	8.95	1.13	12
CBD11_02_18	0.1858	11.71	1.05	8.39	0.37	4.96	9.79	1.43	11.5
CBD11_02_19	0.1797	11.44	0.97	7.54	0.36	4.78	9.01		7.9
CBD11_02_20	0.1751	11.33	0.99	7.60	0.36	4.82	9.04	1.44	7.3
CBD11_02_21	0.1829	11.19	0.95	8.09	0.38	5.35	9.62	1.04	
CBD11_02_22	0.1905	11.26	0.97	7.88	0.36	5.30	9.66	0.65	7.3
CBD11_02_23	0.1923	11.44	1.11	7.57	0.34	5.19	9.29	0.96	8.4
CBD11_02_24	0.1857	11.78	1.05	7.70	0.34	5.31	9.31	1.18	
CBD11_02_25	0.1837	11.11	0.95	7.41	0.34	5.25	9.09	1.13	11.9
CBD11_02_26	0.188	10.85	1.08	7.55	0.32	5.13	8.99		14.6
CBD11_02_27	0.1882	11.68	0.91	7.52	0.34	5.38	9.26	1.5	6.5

<b>Sample</b>	<b><math>^{147}\text{Sm}/^{144}\text{Nd}</math></b>	<b>Na</b>	<b>Cl</b>	<b>Ca</b>	<b>Mn</b>	<b>Fe</b>	<b>Zr</b>	<b>Be</b>	<b>Mg</b>
CBD11_02_28	0.1874	11.11	0.88	7.47	0.34	5.69	8.96	1.69	7.9
CBD11_02_29	0.1851	11.51	0.93	7.61	0.34	5.24	9.07	0.76	11.3
CBD11_02_30	0.1881	11.20	0.88	7.38	0.32	5.19	8.90	1.15	
KP8_1_3_1	0.2358	9.56	0.86	11.62	1.23	1.36	9.82	3.8	728
KP8_1_3_2	0.2338	9.34	0.80	11.06	1.21	1.32	9.44	4.5	733
KP8_1_3_3	0.2391	9.43	0.74	11.18	1.14	1.33	9.51	6.1	697
KP8_1_3_4	0.2388	9.29	0.73	11.87	1.15	1.31	9.62	5.7	715
KP8_1_3_5	0.2463	9.79	0.68	11.16	1.13	1.33	9.79	4.7	710
KP8_1_3_6	0.2446	9.25	0.66	11.08	1.11	1.29	9.17	4.7	689
KP8_1_3_7	0.2357	9.01	0.57	10.22	1.10	1.25	8.88	4.3	674
KP8_1_3_8	0.2353	9.74	0.71	11.00	1.18	1.34	9.30	5.1	733
KP8_1_3_11	0.2119	9.10	0.74	11.38	1.31	1.38	9.75	6.2	748
KP8_1_3_18	0.2224	9.65	0.66	10.17	1.22	1.31	8.96	4.6	759
KP8_1_3_19	0.2127	9.67	0.61	10.06	1.30	1.31	8.67	4.7	759
KP8_1_3_20	0.2091	9.20	0.56	10.05	1.29	1.30	8.57	4.2	770
KP9_2_2_1	0.1951	9.55	0.55	10.71	1.39	1.90	10.11	3.9	388
KP9_2_2_2	0.1965	9.34	0.55	10.62	1.39	1.86	9.88	3.6	473
KP9_2_2_3	0.1982	9.27	0.56	10.22	1.37	1.85	9.86	3.18	514
KP9_2_2_4	0.1966	9.75	0.58	10.48	1.39	1.90	9.83	3.2	580
KP9_2_2_5	0.1986	9.45	0.53	10.48	1.36	1.81	9.86	2.03	544
KP9_2_2_6	0.2005	9.72	0.52	10.46	1.31	1.77	9.85	1.95	551
KP9_2_2_7	0.2011	9.46	0.49	10.33	1.27	1.73	9.65	2.52	539
KP9_2_2_8	0.2013	9.50	0.52	10.59	1.29	1.74	9.82	1.53	543
KP9_2_2_9	0.2024	9.71	0.50	10.46	1.27	1.66	9.84	2.36	546
KP9_2_2_10	0.2037	9.62	0.51	10.32	1.28	1.65	9.74	2.7	547

<b>Sample</b>	<b><math>^{147}\text{Sm}/^{144}\text{Nd}</math></b>	<b>Na</b>	<b>Cl</b>	<b>Ca</b>	<b>Mn</b>	<b>Fe</b>	<b>Zr</b>	<b>Be</b>	<b>Mg</b>
KP9_2_2_11	0.1944	9.19	0.53	11.28	1.47	1.70	10.45	3.3	529
KP9_2_2_12	0.196	8.89	0.62	11.13	1.34	1.55	9.77	3.9	535
KP9_2_2_13	0.1947	9.55	0.68	10.13	1.42	1.55	9.79	2.7	608
KP9_2_2_14	0.1984	9.44	0.66	10.64	1.43	1.60	9.73	2.9	612
KP9_2_2_15	0.2039	9.82	0.70	10.17	1.32	1.55	9.32	3.1	598
KP9_2_2_16	0.204	9.99	0.72	10.07	1.36	1.57	9.44	2.29	598
KP9_2_2_17	0.2084	9.87	0.69	10.10	1.35	1.53	9.54	2.33	590
KP9_2_2_18	0.2078	9.48	0.74	10.25	1.37	1.57	9.55	2.64	575
KP9_2_2_19	0.2065	9.65	0.70	10.29	1.41	1.58	9.55	2.6	593
KP9_2_2_20	0.2032	9.68	0.70	10.24	1.47	1.56	9.56	2.61	634
KP9_2_2_21	0.211	9.47	0.69	10.20	1.33	1.56	9.61	3.1	636
KP9_2_2_22	0.2113	10.01	0.70	10.30	1.34	1.56	9.44	2.18	578
KP9_2_2_23	0.2112	9.62	0.69	10.41	1.36	1.56	9.57	2.74	605
KP9_2_2_24	0.213	9.73	0.73	10.03	1.33	1.55	9.46	2.84	589
KP9_2_2_25	0.2111	9.02	0.66	10.90	1.29	1.71	9.21	5.4	685
KP9_2_2_26	0.2139	10.16	0.72	10.48	1.35	1.60	9.53	3	607
KP9_2_2_27	0.2163	9.94	0.74	10.23	1.31	1.58	9.41	2.6	604
KP9_2_2_28	0.2182	10.12	0.75	10.52	1.35	1.57	9.59	1.83	594
KP9_2_2_29	0.2182	9.73	0.70	10.01	1.28	1.53	9.41	2.91	596
KP9_2_2_30	0.2229	9.62	0.70	10.15	1.25	1.56	9.49	2.41	590
KP9_2_2_31	0.221	9.85	0.73	10.34	1.23	1.52	9.36	2.29	571
KP9_2_2_32	0.2164	9.39	0.72	9.93	1.25	1.54	9.24	2.66	576
KP9_2_2_33	0.2157	9.78	0.74	10.22	1.33	1.56	9.56	1.32	595
KP9_2_2_34	0.214	9.89	0.70	10.29	1.31	1.55	9.27	3.5	584
KP9_2_2_35	0.2247	9.54	0.76	9.81	1.18	1.47	8.96	2.78	534
KP9_2_2_36	0.2219	9.45	0.69	9.96	1.15	1.46	9.07	2.32	528
KP9_2_2_37	0.2228	9.38	0.70	10.04	1.21	1.50	9.29	1.57	551

<b>Sample</b>	<b><math>^{147}\text{Sm}/^{144}\text{Nd}</math></b>	<b>Na</b>	<b>Cl</b>	<b>Ca</b>	<b>Mn</b>	<b>Fe</b>	<b>Zr</b>	<b>Be</b>	<b>Mg</b>
KP9_2_2_38	0.1982	9.51	0.69	10.09	1.47	1.49	9.27	3.3	606
KP9_2_2_39	0.2139	9.58	0.71	9.96	1.26	1.46	9.23	3.7	556
KP9_2_2_40	0.2006	9.33	0.63	10.02	1.37	1.42	9.03	1.69	584
KP9_2_2_41	0.1924	9.27	0.64	9.68	1.41	1.41	9.12	1.9	586
KP9_2_2_42	0.1943	9.17	0.57	9.85	1.31	1.46	9.10	2.3	469
Eud_LV01_1	0.1212	12.87	1.01	9.71	1.88	2.90	10.64	3.9	500
Eud_LV01_2	0.12103	12.61	1.03	9.65	1.85	2.92	10.74	1.33	523
Eud_LV01_3	0.12452	12.28	0.91	8.44	1.62	3.16	9.84	0.75	402
Eud_LV01_4	0.12478	12.22	0.92	8.36	1.61	3.00	9.46	0.77	386
Eud_LV01_5	0.12217	13.23	1.06	9.42	1.85	3.43	10.02	2.43	452
Eud_LV01_6	0.12129	13.10	1.08	9.32	1.96	3.33	9.86	1.31	506
Eud_LV01_7	0.12132	13.24	1.12	9.35	1.93	3.34	10.01	4.1	498
Eud_LV01_8	0.12421	13.05	1.11	8.80	1.69	3.52	10.06	2.47	422
Eud_LV01_9	0.12447	12.90	1.18	8.88	1.70	3.48	10.28	0.64	444
Eud_LV01_10	0.12428	13.22	1.25	8.83	1.72	3.54	9.97		428
Eud_LV01_11	0.12471	12.55	1.32	9.01	1.68	3.36	10.09	0.97	454
Eud_LV01_12	0.12394	12.71	1.22	8.97	1.69	3.41	9.97	3.5	433
Eud_LV01_13	0.12172	13.15	1.40	9.21	1.89	3.03	10.01	2.5	491
Eud_LV01_14	0.12129	12.85	1.36	9.32	1.93	3.02	9.97	3.42	475
Eud_LV01_15	0.12063	13.31	1.54	9.50	1.92	3.04	10.07	0.99	540
Eud_LV01_16	0.12149	13.37	1.57	9.66	1.93	2.97	9.85	2.34	519
Eud_LV01_17	0.12081	13.27	1.60	9.75	1.93	2.97	10.22		534
Eud_LV01_18	0.12068	13.09	1.73	9.63	1.90	3.08	10.04	1.98	521
Eud_NK_1	0.19107	10.52	0.27	6.02	1.97	2.45	10.36	2.51	143.3
Eud_NK_2	0.18994	10.91	0.28	5.93	1.93	2.50	10.30	1.02	147.9
Eud_NK_3	0.1894	11.07	0.26	5.96	1.98	2.45	10.32	1.9	137.1

<b>Sample</b>	<b><math>^{147}\text{Sm}/^{144}\text{Nd}</math></b>	<b>Na</b>	<b>Cl</b>	<b>Ca</b>	<b>Mn</b>	<b>Fe</b>	<b>Zr</b>	<b>Be</b>	<b>Mg</b>
Eud_NK_4	0.191	10.71	0.28	6.24	1.94	2.50	10.50	1.77	152.7
Eud_NK_5	0.1914	11.13	0.30	6.21	1.97	2.59	10.82	1.42	146.5
Eud_NK_6	0.1902	11.04	0.28	6.21	1.97	2.52	10.77	1.48	149.5
Eud_NK_7	0.18936	10.61	0.29	6.06	1.92	2.47	10.64	1.65	152
Eud_NK_8	0.18895	11.02	0.32	6.01	1.92	2.43	10.64	1.88	148.2
Eud_NK_9	0.18969	10.42	0.32	5.92	1.89	2.33	10.39	1.47	143.3
Eud_NK_10	0.18915	10.52	0.35	6.02	1.91	2.42	10.65	1.23	147.9
Eud_NK_11	0.19019	10.81	0.36	6.04	1.90	2.41	10.68	2.32	151.5
Eud_NK_12	0.1895	10.77	0.35	6.00	1.91	2.39	10.66		154
Eud_NK_13	0.1904	11.43	0.43	6.27	2.06	2.49	11.17	1.86	154.9
Eud_NK_14	0.1896	10.98	0.37	6.13	1.94	2.41	10.73	1.8	156.1
Eud_NK_15	0.1892	10.86	0.44	6.12	1.92	2.43	10.79	0.89	151.4
Eud_NK_16	0.18881	10.95	0.39	6.22	1.90	2.36	10.83	1.91	156.5
<hr/>									
KP1_2_1	0.20313	9.66	0.90	10.70	1.08	2.19	10.43	3.04	404
KP1_2_2	0.19086	9.81	0.82	10.54	1.18	1.93	9.79	4.5	463
KP1_2_3	0.1902	9.82	0.75	10.14	1.25	1.89	9.74	3.5	509
KP1_2_4	0.198	9.91	0.78	10.16	1.13	1.74	9.38	3.6	464
KP1_2_5	0.19013	10.14	0.73	10.22	1.23	1.80	9.47	5.5	506
KP1_2_6	0.1916	10.02	0.75	10.01	1.19	1.80	9.37	4.8	492
KP1_2_7	0.19355	9.96	0.77	10.13	1.24	1.90	9.59	5.3	500
KP1_2_8	0.20088	10.07	0.74	10.50	1.11	1.82	9.49	4.4	457
KP1_2_9	0.1901	9.87	0.79	9.96	1.21	1.82	9.29	4.6	466
KP1_2_10	0.1931	10.03	0.77	10.24	1.16	1.80	9.50	4.5	445
KP1_2_11	0.1908	9.78	0.80	8.98	1.05	1.96	9.01		389
KP1_2_12	0.1886	10.30	0.81	9.59	1.17	1.91	9.31	1.56	471
KP1_2_13	0.1861	9.81	0.71	9.28	1.20	1.84	8.98	3.09	496
KP1_2_14	0.1878	9.70	0.73	9.13	1.15	1.77	8.79	5.1	479

<b>Sample</b>	<b><math>^{147}\text{Sm}/^{144}\text{Nd}</math></b>	<b>Na</b>	<b>Cl</b>	<b>Ca</b>	<b>Mn</b>	<b>Fe</b>	<b>Zr</b>	<b>Be</b>	<b>Mg</b>
KP1_2_15	0.1914	9.52	0.74	9.40	1.14	1.73	8.93	2.44	478
KP1_2_16	0.1922	9.68	0.78	9.47	1.12	1.77	9.15	3.2	490
KP1_2_17	0.1877	9.34	0.73	8.80	1.11	1.74	8.69	3.2	479
KP1_2_18	0.1917	9.37	0.75	8.24	0.86	1.64	8.65	3.1	378
KP1_2_19	0.1922	10.22	0.88	8.86	0.99	2.16	9.18	2.9	387
KP1_2_20	0.1954	10.12	0.85	9.00	0.97	2.02	9.12	2.22	370
KP1_2_21	0.2	9.58	0.86	8.92	0.94	1.88	8.76	1.73	354
KP1_2_22	0.2001	9.92	1.02	10.33	1.12	2.17	10.09	1.5	410
KP1_2_23	0.1893	10.20	0.89	10.61	1.24	1.90	10.11	2.53	513
KP1_2_24	0.1886	9.98	0.86	10.16	1.18	1.86	9.73	1.97	496
KP1_2_25	0.1931	9.87	0.93	9.95	1.11	1.84	9.70	2.68	485
KP1_2_26	0.1921	10.10	0.90	9.84	1.19	1.84	9.42	2.55	513
KP1_2_27	0.1907	10.12	0.90	10.10	1.21	1.81	9.40	2.18	511
KP1_2_28	0.1896	10.14	0.90	9.93	1.14	1.80	9.50	2.77	483
KP1_2_29	0.1877	10.26	0.92	9.94	1.13	1.89	9.48	2.16	464
KP1_2_30	0.1874	9.87	0.90	9.48	1.02	1.91	9.16	2.9	397
CBD11_10_1	0.188	10.39	0.93	8.64	0.54	5.16	10.42		10.4
CBD11_10_2	0.1749	10.55	1.10	7.74	0.47	4.87	9.74	1.19	
CBD11_10_3	0.1867	10.50	0.85	8.00	0.50	4.87	9.69	1.01	9.6
CBD11_10_4	0.1715	10.77	0.94	7.73	0.42	4.61	9.35	0.87	
CBD11_10_5	0.182	10.09	0.80	7.75	0.46	4.74	9.53	1.19	11.6
CBD11_10_6	0.1768	10.79	0.88	7.76	0.45	4.79	9.30		7.8
CBD11_10_7	0.1728	11.77	0.95	8.14	0.45	4.93	10.01	1.12	8.4
CBD11_10_8	0.1839	11.15	0.83	7.95	0.46	4.87	9.51		8.5
CBD11_10_9	0.159	10.78	1.00	7.50	0.43	4.62	9.20	1.45	
CBD11_10_10	0.195	10.98	0.76	7.61	0.43	4.64	9.21	0.99	

<b>Sample</b>	<b><math>^{147}\text{Sm}/^{144}\text{Nd}</math></b>	<b>Na</b>	<b>Cl</b>	<b>Ca</b>	<b>Mn</b>	<b>Fe</b>	<b>Zr</b>	<b>Be</b>	<b>Mg</b>
CBD11_10_11	0.2067	10.68	0.92	8.22	0.46	5.24	9.73	1.4	23
CBD11_10_12	0.1978	11.09	1.08	8.08	0.43	4.83	9.90	1.62	
CBD11_10_13	0.1996	10.34	1.00	7.83	0.43	4.66	9.55	1.09	11.9
CBD11_10_14	0.1886	10.85	0.96	7.85	0.44	4.74	9.50		8.5
CBD11_10_15	0.1967	10.90	0.97	7.94	0.43	4.76	9.44	1.4	9.7

p

<b>Sample</b>	<b>Al</b>	<b>K</b>	<b>Ti</b>	<b>Ga</b>	<b>Rb</b>	<b>Sr</b>	<b>Y</b>	<b>Nb</b>	<b>Mo</b>	<b>Sn</b>
	<i>ppm</i>									
Eud_LV01_1	748	3348	3240	71.7	6.82	9520	2416	3893	7.03	54.3
Eud_LV01_2	752	3306	3230	68.5	7.3	9120	2348	3682	6.1	49.8
Eud_LV01_3	832	3469	3350	67.9	7.07	9550	2520	3875	6.9	49.3
Eud_LV01_4	810	3438	3270	70.3	6.72	9450	2491	3872	7.47	53
Eud_LV01_5	1410	2210	2740	64.8	6.99	8800	2452	4530	6.5	58.4
Eud_LV01_6	740	3315	3000	64	6.55	8820	2333	3603	6.11	39.7
Eud_LV01_7	741	3860	3294	82.9	8.28	12230	2754	5550	10.9	56.9
Eud_LV01_8	754	3929	3350	84.5	9.25	13130	2765	6310	12	58.4
Eud_LV01_9	805	3499	3120	65	7.09	9450	2458	3947	6.51	49.3
Eud_LV01_10	831	3380	3220	66.2	7.25	9470	2507	3922	8.2	43.2
Eud_LV01_11	806	3550	3190	67.7	7.23	9760	2564	3869	7.5	50.5
Eud_LV01_12	846	3520	3280	65.6	7	9690	2556	3890	7.8	50.6
Eud_LV01_13	711	3690	3450	84.2	7.88	12750	2763	6350	11.8	53.9
Eud_LV01_14	716	3688	3590	81.3	8.72	12470	2827	6050	12.4	52.6
Eud_LV01_15	864	3614	3280	67.7	6.84	9890	2650	3910	6.94	53.3
Eud_LV01_16	858	3550	3300	67.4	6.48	9900	2626	3850	6.65	52.4
Eud_LV01_17	850	3588	3110	70.3	7.36	9860	2566	3930	7	47.2
Eud_LV01_18	839	3620	3110	66.5	7.19	9740	2591	3888	6.48	52.6
<hr/>										
Eud_NK_1	1938	4090	557	80.3	40.4	719	16840	3964	1.77	133.4
Eud_NK_2	2015	5080	552	81.1	38.4	761	17070	4100	2.16	139.3
Eud_NK_3	1976	4500	575	82.3	42	744	17210	4107	2.2	140.7
Eud_NK_4	2016	4690	582	77.9	39.6	747	17120	4080	2.04	145.3
Eud_NK_5	1832	4080	508	75	40.8	698	16000	3769	1.59	129.4
Eud_NK_6	1810	4130	533	72.7	41	694	15980	3800	1.16	125.6
Eud_NK_7	2035	4940	534	75.4	41.4	743	16980	4025	1.7	135.5
Eud_NK_8	2038	4720	495	76.8	41.1	735	17080	3980	1.32	129.2

<b>Sample</b>	<b>Al</b>	<b>K</b>	<b>Ti</b>	<b>Ga</b>	<b>Rb</b>	<b>Sr</b>	<b>Y</b>	<b>Nb</b>	<b>Mo</b>	<b>Sn</b>
Eud_NK_9	1942	4580	507	77.9	40.9	739	16690	4067	1.95	129.5
Eud_NK_10	1864	4280	526	75.4	41.1	715	16560	4020	1.55	129
Eud_NK_11	1898	4150	537	76.9	41.9	722	16660	4052	1.76	133.3
Eud_NK_12	1897	4350	522	77.8	42.3	731	16590	4032	1.78	130.8
Eud_NK_13	1878	4280	540	76.8	39.6	710	16470	3936	1.64	130.4
Eud_NK_14	1915	4240	523	79.1	43.2	724	16660	4061	1.8	132.3
Eud_NK_15	1961	4450	532	79.1	42.4	736	17250	4120	1.73	135.6
Eud_NK_16	1882	4370	495	76.9	43.3	713	16580	3891	2.13	131.2
Eud_NK_17	1935	5240	516	80.6	43.2	738	17110	4090	1.7	136.7
Eud_NK_18	1873	5280	502	80.3	41.8	725	16770	4070	1.49	134.6
CBD11_02_1	819	3770	867	115.4	11.74	295.6	5740	770	4.32	204.5
CBD11_02_2	3240	1860	763	114.1	10.97	320.7	5730	1229	4.39	245.9
CBD11_02_3	851	3890	593	117.4	11.37	294.5	5840	969	3.87	291
CBD11_02_4	843	3840	661	115.3	11.42	289.4	5560	785	3.42	175.1
CBD11_02_5	807	4510	622	112.6	14.3	355	5830	1595	2.58	179.7
CBD11_02_6	824	4060	702	112.1	12.13	318	5570	1107	4.6	148.7
CBD11_02_7	838	3930	554	114.2	9.95	281.2	5620	773	3.92	291.3
CBD11_02_8	811	4220	666	112.9	10.77	318.7	5570	1135	4.15	156.2
CBD11_02_9	803	4100	667	110.6	11.51	332	5640	1381	1.96	155.3
CBD11_02_10	799	3530	636	111.4	10.95	286.8	5510	924	4.19	223.9
CBD11_02_11	702	3010	642	116.5	12.47	381	5240	1683	0.94	137.3
CBD11_02_12	835	3695	363	119.2	13.04	357.8	5730	1497	5.81	70.4
CBD11_02_13	860	3423	276	121.4	11.72	359.3	5860	1427	5.09	82.8
CBD11_02_16	808	2300	443	126.3	12.55	404.5	5820	2054	6.53	95.4
CBD11_02_17	819	2630	357	115.6	9.37	385	5740	1933	6.2	74.8

<b>Sample</b>	<b>Al</b>	<b>K</b>	<b>Ti</b>	<b>Ga</b>	<b>Rb</b>	<b>Sr</b>	<b>Y</b>	<b>Nb</b>	<b>Mo</b>	<b>Sn</b>
CBD11_02_18	1001	1896	293	138	7.27	414	6500	2080	6.8	59.7
CBD11_02_19	900	3900	279	120.4	11.67	375	6010	1883	6.94	57.7
CBD11_02_20	882	3177	300	117.7	11.51	371	5970	1825	6.34	52.3
CBD11_02_21	781	4350	510	117.7	15.57	385	5970	1958	0.86	111.3
CBD11_02_22	823	4170	425	117.7	14.71	371	6110	1677	5.32	70
CBD11_02_23	988	3760	236	133.3	13.68	360.2	6340	1520	5.04	111.6
CBD11_02_24	992	3830	257	128.6	13.4	335.1	6360	1182	5.76	92.1
CBD11_02_25	845	1609	430	111.5	11.75	325	5910	1183	5.18	76.7
CBD11_02_26	2810	1690	294	120.4	8.57	329	6140	1160	5.19	98.4
CBD11_02_27	809	4110	470	111.6	14.12	344.5	5940	1366	4.98	79.6
CBD11_02_28	956	2090	613	109.4	8.39	330.2	5770	1332	4.68	74.4
CBD11_02_29	843	4160	446	115.3	14.44	359.7	5820	1542	5.04	92.7
CBD11_02_30	872	3873	329	120.9	13.99	356	5900	1496	4.29	52.9
KP8_1_3_1	1615	3024	663	124.6	63.7	1032	20970	3730	11.1	133.8
KP8_1_3_2	1600	5050	679	115	69.8	1018	21140	3902	13.7	141.5
KP8_1_3_3	1551	4580	751	117	67.4	968	19800	3049	4.59	144.4
KP8_1_3_4	1539	4730	779	116.5	71.6	1012	20150	3171	6.2	165.5
KP8_1_3_5	1502	5100	823	120	70.7	957	19710	2751	5.34	181.8
KP8_1_3_6	1408	5050	771	111.8	68.4	931	19270	2816	6.36	179.9
KP8_1_3_7	1339	4870	699	103.9	66.2	926	18240	3095	4.13	174.3
KP8_1_3_8	1423	5280	726	112.3	70.4	956	19340	3438	6.4	170.6
KP8_1_3_11	1657	3730	665	120.5	73.2	1102	23290	4480	13	164.8
KP8_1_3_18	1437	4870	579	112.7	63.6	1001	19000	4350	10.4	145.9
KP8_1_3_19	1272	5090	519	107.4	62.1	1016	17330	5270	8.6	136.5
KP8_1_3_20	1175	4800	561	104.8	63.9	1017	16980	5490	7.2	133.8

<b>Sample</b>	<b>Al</b>	<b>K</b>	<b>Ti</b>	<b>Ga</b>	<b>Rb</b>	<b>Sr</b>	<b>Y</b>	<b>Nb</b>	<b>Mo</b>	<b>Sn</b>
KP9_2_2_1	373	3208	1012	114.6	60.2	886	22560	4480	7.7	264.2
KP9_2_2_2	379	6170	1062	109.6	60.2	871	21760	4370	8.6	233
KP9_2_2_3	392	6560	1044	107.1	56.9	854	21590	4240	8.9	265
KP9_2_2_4	451	4380	1020	106.4	57.9	863	21390	4260	12	182.7
KP9_2_2_5	517	6310	948	104	58	845	21600	3829	11.4	178.6
KP9_2_2_6	597	4130	912	105.3	55.8	834	21620	3628	10.8	178.7
KP9_2_2_7	662	5940	955	103	55.2	813	21750	3413	9.58	173.9
KP9_2_2_8	728	5390	981	102.3	57.5	813	21970	3335	7.7	161.1
KP9_2_2_9	756	5280	1026	105.9	55.1	817	22610	3310	6.02	185.3
KP9_2_2_10	801	5080	1065	104.8	53.8	812	22270	3296	5.76	185.5
<hr/>										
KP9_2_2_11	718	6200	1037	119.9	53.2	971	23000	5140	5.1	271.4
KP9_2_2_12	840	6390	1499	113	56.7	899	23550	3645	2.08	282.9
KP9_2_2_13	753	5600	1477	112.5	46.4	922	23720	4440	1.56	250.4
KP9_2_2_14	684	5620	1614	110.5	46.6	928	24430	4330	1.98	253
KP9_2_2_15	649	5500	1646	108.9	44.8	869	24110	3863	2.3	242.4
KP9_2_2_16	565	5630	1806	112.5	45.2	893	25050	4079	1.76	259.7
KP9_2_2_17	498	5650	1905	110.4	44.6	870	24920	3850	2.28	252.3
KP9_2_2_18	446	5780	2019	111.9	44.7	907	25390	4300	2.54	248
KP9_2_2_19	392	5650	2044	114.4	47.2	921	25250	4559	1.98	253.4
KP9_2_2_20	413	5850	2068	110.2	47.7	941	25110	5150	2.31	270
KP9_2_2_21	452	5580	2289	111.7	48	889	26020	3705	2.18	266.1
KP9_2_2_22	399	2901	2279	110.1	42.9	882	25340	3781	2	251.8
KP9_2_2_23	407	5830	2166	111.6	49.3	895	25530	3958	1.92	242.1
KP9_2_2_24	397	5770	2175	109.2	47.9	866	25060	3813	1.81	240
KP9_2_2_25	533	2370	2280	109.3	20.8	948	24900	3820	2.05	245
KP9_2_2_26	405	3145	2204	111.4	49	909	26340	3751	2.07	261.3

<b>Sample</b>	<b>Al</b>	<b>K</b>	<b>Ti</b>	<b>Ga</b>	<b>Rb</b>	<b>Sr</b>	<b>Y</b>	<b>Nb</b>	<b>Mo</b>	<b>Sn</b>
KP9_2_2_27	414	5720	2206	110.7	49.1	865	25460	3594	1.49	268.6
KP9_2_2_28	413	4300	2199	109.9	49.5	879	26180	3534	1.39	272
KP9_2_2_29	416	5020	2150	113.8	48.2	858	25440	3321	1.21	259.8
KP9_2_2_30	460	5890	2309	112.7	48.2	847	25750	2830	1.59	270.3
KP9_2_2_31	461	5820	2190	113.1	45.1	825	25380	2913	1.77	264.8
KP9_2_2_32	441	5740	2167	108.6	47	835	24710	3300	2.01	269.8
KP9_2_2_33	484	5840	2350	113.1	48	868	25870	3546	2.04	283.5
KP9_2_2_34	490	5930	2370	113.3	47	881	25500	3584	2.6	291
KP9_2_2_35	537	5720	2417	107.8	46.2	789	24340	2509	1.67	272.5
KP9_2_2_36	557	5550	2360	112.5	45.8	803	25100	2450	1.7	275.5
KP9_2_2_37	629	5620	2450	103	46.1	794	24860	2553	2.08	266.2
KP9_2_2_38	590	5670	2010	108.9	47.5	934	23890	5760	2.65	257.6
KP9_2_2_39	754	5650	1915	108.2	46.3	841	23720	3465	2.62	213.2
KP9_2_2_40	762	5610	1600	106.1	46.5	895	23170	4580	2.53	185.5
KP9_2_2_41	657	5850	1099	104.7	48.2	906	22200	5360	4.1	160.9
KP9_2_2_42	487	5160	753	105	53.2	868	21880	5000	9.6	175.8
<hr/>										
Eud_LV01_1	814	3930	3710	92.3	8.99	13640	2939	6690	13	57.5
Eud_LV01_2	800	3963	3780	88.3	8.9	13480	2881	6450	11.1	57.7
Eud_LV01_3	808	3233	3170	62.6	6.68	9400	2454	3838	6.7	42
Eud_LV01_4	807	3241	3120	64.1	6.65	9470	2443	3819	5.93	43.4
Eud_LV01_5	735	3646	3440	78.7	8.31	12060	2811	5700	11.1	57.7
Eud_LV01_6	737	3740	3560	84.5	9.15	13160	2909	6370	12.8	55.9
Eud_LV01_7	748	3760	3340	81.4	8.3	12810	2866	6210	12.1	60.2
Eud_LV01_8	774	3417	3120	66	7.13	9910	2565	4207	7.17	45.1
Eud_LV01_9	800	3484	3220	64.9	7.25	9800	2576	3983	8.4	46.4
Eud_LV01_10	804	3484	3200	65.7	7.08	9920	2544	4061	7.3	49.6
Eud_LV01_11	792	3551	3160	67.4	7.13	10220	2576	4283	7.9	50

<b>Sample</b>	<b>Al</b>	<b>K</b>	<b>Ti</b>	<b>Ga</b>	<b>Rb</b>	<b>Sr</b>	<b>Y</b>	<b>Nb</b>	<b>Mo</b>	<b>Sn</b>
Eud_LV01_12	878	3580	3160	66.3	7.45	9930	2602	4370	8.7	48.3
Eud_LV01_13	726	3881	3370	86.8	8.8	13020	2866	6430	12.9	56.8
Eud_LV01_14	745	3830	3400	86.3	8.93	13040	2855	6440	11.9	52.7
Eud_LV01_15	765	3910	3540	85.4	8.44	13680	2899	6530	11.6	56.7
Eud_LV01_16	744	3864	3490	88.7	8.28	13180	2931	6420	10.9	56.5
Eud_LV01_17	767	4050	3630	90.2	8.58	13550	2955	6570	13.5	54
Eud_LV01_18	746	4070	3550	87.7	8.43	13620	2922	6580	12.7	58.8
<hr/>										
Eud_NK_1	1939	6990	536	77	42.1	765	18010	4370	1.72	130.1
Eud_NK_2	1950	6070	511	78	44.5	749	17840	4300	1.78	134.6
Eud_NK_3	1951	5940	546	79.3	45.2	751	17940	4290	2.01	134.5
Eud_NK_4	1944	4960	516	80.3	43.3	763	18180	4360	1.74	140.3
Eud_NK_5	2004	5480	558	81.7	44.2	774	18760	4460	1.91	137.8
Eud_NK_6	1989	5630	530	80.4	44.8	786	18630	4450	1.84	135.4
Eud_NK_7	1933	7490	515	80.6	43.8	759	17930	4360	1.95	136.3
Eud_NK_8	1948	5250	563	79.1	43.2	754	18040	4400	1.84	137.8
Eud_NK_9	1913	7350	503	79.1	42.6	751	17990	4350	1.69	128.3
Eud_NK_10	1997	9150	564	81.6	43.5	765	17950	4380	1.96	127.5
Eud_NK_11	1963	6280	537	79.6	42.4	752	17980	4372	1.89	133.5
Eud_NK_12	1968	6410	528	79.5	44	768	18240	4370	1.91	131.7
Eud_NK_13	2156	4910	575	81.7	45.1	799	19130	4580	2.23	140.9
Eud_NK_14	2024	5290	541	77.6	43.8	779	18310	4470	1.52	131.2
Eud_NK_15	2059	5770	527	79.9	43.5	774	18170	4360	1.72	129.1
Eud_NK_16	2035	5200	559	79.4	43.4	784	18530	4390	2.18	140
<hr/>										
KP1_2_1	306	6240	1113	247.5	48.1	1374	21300	3184	12.6	182.5
KP1_2_2	455	5970	1561	227.8	49.5	1500	20090	4500	7.36	72.6
KP1_2_3	494	5740	1745	225.8	48.3	1559	20080	4870	5	60.4

<b>Sample</b>	<b>Al</b>	<b>K</b>	<b>Ti</b>	<b>Ga</b>	<b>Rb</b>	<b>Sr</b>	<b>Y</b>	<b>Nb</b>	<b>Mo</b>	<b>Sn</b>
KP1_2_4	545	5620	1988	224.2	45.7	1461	19720	3586	2.91	51.8
KP1_2_5	519	5730	1926	222.9	47.5	1603	19490	4645	3.01	53.3
KP1_2_6	528	5620	1926	215.2	47	1520	19230	4315	3.05	59.5
KP1_2_7	504	5570	1917	214.9	46.6	1540	19490	4530	4.18	63.6
KP1_2_8	573	5620	2059	224.6	44.8	1408	19740	3562	5.25	74.4
KP1_2_9	513	5420	1763	215.1	45.9	1519	19220	4495	3.05	60.2
KP1_2_10	558	4950	1910	217.2	45.1	1470	19650	4110	3.14	73
KP1_2_11	267	5450	791	215.9	41.8	1325	18380	3640	10.1	54.1
KP1_2_12	406	5730	1530	204.4	43.3	1402	18910	4300	5.48	51.4
KP1_2_13	476	5500	1644	197.7	44.2	1474	18420	4920	4.1	72
KP1_2_14	461	5360	1660	199.8	41.5	1414	18160	4500	3.99	76.9
KP1_2_15	478	5280	1770	196.3	41.6	1422	18170	4430	3.97	66.9
KP1_2_16	441	5340	1887	201.3	43.2	1417	18300	4170	4.67	58.2
KP1_2_17	348	5230	1679	192.5	40.4	1365	17270	4050	4.4	37
KP1_2_18	344	4900	1048	186.2	41.4	1103	17580	2000	9.3	17.3
KP1_2_19	302	3731	708	211	44.6	1271	18390	3216	8.6	35.3
KP1_2_20	302	4350	875	219.6	43.7	1286	18830	3368	8.7	150.3
KP1_2_21	282	5190	812	204.8	42.9	1203	18060	2738	8.7	90.7
KP1_2_22	284	5520	1000	230.9	46	1368	20430	3760	13.2	170.8
KP1_2_23	459	6020	1785	221.3	47.4	1558	19830	5010	5.45	75.8
KP1_2_24	417	5820	1475	217.4	46	1481	19290	4708	7.08	80.6
KP1_2_25	450	5780	1790	208.1	43.8	1450	19150	3960	4.78	53.2
KP1_2_26	494	5830	1746	213.4	44.5	1502	18800	4710	3.78	65.3
KP1_2_27	474	5740	1704	211.1	44.2	1520	19200	4730	4.84	62.7
KP1_2_28	470	5830	1538	215	43.3	1446	19270	4470	6.3	90.7
KP1_2_29	408	5830	1289	219.3	45.5	1413	19210	4320	9.8	100.5
KP1_2_30	345	5800	843	219.1	42.7	1303	18940	3628	10.9	148.1

<b>Sample</b>	<b>Al</b>	<b>K</b>	<b>Ti</b>	<b>Ga</b>	<b>Rb</b>	<b>Sr</b>	<b>Y</b>	<b>Nb</b>	<b>Mo</b>	<b>Sn</b>
CBD11_10_1	895	2703	746	121.9	13.09	460	6860	2701	0.82	152.2
CBD11_10_2	2050	5970	311	107.3	19.5	366.2	6190	2059	7.5	48.3
CBD11_10_3	725	5340	678	109.8	18.3	432	6280	2744	0.89	129.5
CBD11_10_4	829	5550	279	99.1	18.1	285.7	6000	1145	8.6	77.9
CBD11_10_5	766	2760	613	93.4	19.9	360.7	6040	2057	2.27	91.3
CBD11_10_6	759	5160	477	95.6	19	326.4	5440	1650	6.6	58.4
CBD11_10_7	832	5610	439	101.5	20.02	312	5430	1287	6.5	76.6
CBD11_10_8	787	6340	559	98.3	19.7	348.2	6160	1921	6.43	69.3
CBD11_10_9	824	5390	299	97.5	17.29	290.5	5150	1271	4.66	54.8
CBD11_10_10	775	5420	577	90.3	20.9	301.9	5620	1289	5.01	101.6
CBD11_10_11	3200	4170	1100	109.3	14.8	389	6140	1930	0.66	151.7
CBD11_10_12	829	4630	324	105.5	14.6	318	6610	1155	7.7	98.4
CBD11_10_13	6110	2448	325	99.3	11.58	318	6610	1474	7.5	47.6
CBD11_10_14	815	5280	400	96.7	18.7	357	6570	1841	6.7	37.4
CBD11_10_15	820	4820	398	94.5	17.03	336	6580	1643	7.4	43.6
CBD11_10_21	671	5300	543	578	17.9	1080	8400	4110	11.3	53.7
CBD11_10_22	687	5210	539	461	18.3	753	7850	2526	9	68.3
CBD11_10_23	686	5390	455	504	17.1	814	7860	2640	8.6	42.1
CBD11_10_25	640	4460	188	518	16	906	7660	3480	9.9	41.8
CBD11_10_26	682	3400	480	512	15.7	864	7440	2990	8.1	36
CBD11_10_29	600	4760	461	391	15.8	651	6680	2130	5.7	72.8
CBD11_10_31	620	5560	140	356	17.7	668	6470	2500	2.5	96

<b>Sample</b>	<b>Sb</b>	<b>Ba</b>	<b>La</b>	<b>Ce</b>	<b>Pr</b>	<b>Nd</b>	<b>Sm</b>	<b>Eu</b>	<b>Gd</b>	<b>Tb</b>
	<i>ppm</i>									
Eud_LV01_1		531	3139	6080	615	2323	458.2	137.6	424	71.5
Eud_LV01_2	0.79	516	3023	5920	592	2266	448.8	133.2	418	71.1
Eud_LV01_3		525	3185	6230	622	2361	473	143.1	439	74.8
Eud_LV01_4	0.86	532	3156	6150	620	2346	468	141.1	429	75.2
Eud_LV01_5	2.44	469	3273	5950	602	2286	456	127.8	408	69.5
Eud_LV01_6		498	2938	5610	574	2181	441	133.9	407	67.5
Eud_LV01_7	0.49	642	3760	7000	691	2584	509.6	154.9	457	81.3
Eud_LV01_8		650	3978	7230	702	2645	516	155.6	463	81.1
Eud_LV01_9	1.59	505	3127	6060	605	2325	465.4	140.2	418	74.4
Eud_LV01_10	3.3	506	3262	6240	624	2386	475	145	426	75.3
Eud_LV01_11		516	3202	6150	614	2348	473	143.5	430	74.3
Eud_LV01_12	0.57	516	3169	6050	618	2339	472.5	143.3	429	75.6
Eud_LV01_13	0.63	663	4040	7290	715	2657	517	155.7	471	82
Eud_LV01_14		630	3940	7120	714	2642	519	153.4	473	80
Eud_LV01_15	0.7	520	3225	6190	630	2426	487	150.9	445	77
Eud_LV01_16		512	3195	6070	620	2399	482	146.4	428	77.9
Eud_LV01_17	0.99	525	3296	6250	623	2371	471	145	427	73.8
Eud_LV01_18	0.71	511	3216	6090	627	2363	474	139.9	410	74
Eud_NK_1	0.71	590	3778	7670	893	3886	1180	157.1	1557	338.1
Eud_NK_2	0.98	600	3867	7840	909	3971	1197	158.1	1580	337.2
Eud_NK_3	0.63	611	3958	7990	926	4034	1228	165.3	1576	351.1
Eud_NK_4	0.64	602	3900	7910	928	4020	1226	159.3	1590	340.1
Eud_NK_5		550	3555	7230	830	3696	1130	150	1461	311.1
Eud_NK_6	0.72	556	3570	7090	831	3654	1124	147.9	1437	312.5
Eud_NK_7		579	3727	7570	876	3877	1183	153.2	1519	336.3
Eud_NK_8		598	3700	7530	869	3855	1179	156.9	1500	334.6

<b>Sample</b>	<b>Sb</b>	<b>Ba</b>	<b>La</b>	<b>Ce</b>	<b>Pr</b>	<b>Nd</b>	<b>Sm</b>	<b>Eu</b>	<b>Gd</b>	<b>Tb</b>
Eud_NK_9		576	3710	7510	859	3818	1159	153.2	1509	325.8
Eud_NK_10	0.9	595	3750	7520	869	3834	1161	154.7	1515	328
Eud_NK_11	0.46	583	3728	7550	869	3830	1163	154.3	1510	322.9
Eud_NK_12	0.57	588	3763	7580	874	3846	1165	153.2	1501	330.9
Eud_NK_13		586	3662	7430	852	3774	1141	152.4	1497	323.3
Eud_NK_14	0.66	586	3746	7560	866	3838	1165	152	1516	323.9
Eud_NK_15	0.76	613	3840	7560	889	3941	1196	161.7	1553	335.4
Eud_NK_16		591	3642	7380	865	3810	1157	151.4	1485	320.3
Eud_NK_17	0.56	599	3870	7700	888	3918	1184	156.2	1530	332.2
Eud_NK_18	0.48	582	3755	7530	879	3875	1171	153.9	1531	332.5
 CBD11_02_1		877	1193	3014	362	1730	521	74.9	664	136.2
CBD11_02_2		862	1388	3210	385.9	1807	542	79.4	705	139.7
CBD11_02_3		873	1283	3070	375.9	1737	528	73.6	700	142.4
CBD11_02_4		908	1177	2930	362	1699	514	70.2	672	137.5
CBD11_02_5		861	1689	3550	405	1810	538	77.2	688	140.1
CBD11_02_6		849	1425	3225	378	1741	517	71.8	666	140.2
CBD11_02_7		883	1152	2934	365.8	1717	532	73.9	706	141.5
CBD11_02_8		892	1398	3160	374	1719	507	72.6	646	132.3
CBD11_02_9		875	1536	3310	385	1720	515	72.9	668	135.7
CBD11_02_10		872	1240	2973	359	1664	505	70.8	674	134.3
 CBD11_02_11		911	1581	3155	346.9	1553	462	66.1	587	123.4
CBD11_02_12		917	1514	3222	367	1706	522	70.9	649	137.8
CBD11_02_13		941	1448	3235	365.6	1730	536	71.4	686	141
 CBD11_02_16		966	1811	3647	404	1857	556	78	702	144.1
CBD11_02_17		923	1757	3650	410	1933	587	77.7	710	141.9

<b>Sample</b>	<b>Sb</b>	<b>Ba</b>	<b>La</b>	<b>Ce</b>	<b>Pr</b>	<b>Nd</b>	<b>Sm</b>	<b>Eu</b>	<b>Gd</b>	<b>Tb</b>
CBD11_02_18		1043	1946	3980	460	2217	665	90.6	794	157.3
CBD11_02_19		928	1713	3746	431	2011	582	81.6	723	147.3
CBD11_02_20		913	1699	3797	445	2098	596	82.6	722	145.3
CBD11_02_21		907	1796	3670	406	1847	543	78.1	678	144.7
CBD11_02_22		927	1651	3660	408	1928	589	80.8	735	155.3
CBD11_02_23		1005	1561	3790	457	2230	691	91.6	835	166.5
CBD11_02_24		1002	1432	3692	466	2302	684	90.1	815	160.4
CBD11_02_25		859	1473	3570	429	2126	632	83.6	756	147.8
CBD11_02_26		936	1433	3504	434	2194	664	87.5	803	156.7
CBD11_02_27		862	1513	3373	394	1812	548	79.2	700	142.7
CBD11_02_28	1.64	843	1407	3252	383.5	1800	540	76	666	140.3
CBD11_02_29		915	1579	3649	432	2126	632	81.5	749	148.5
CBD11_02_30		932	1495	3343	386	1842	556	79.3	712	146.2
KP8_1_3_1	0.48	964	2313	3308	319.3	1331	503	89	938	274.1
KP8_1_3_2		914	2380	3436	317	1328	500	84.1	909	269
KP8_1_3_3		905	1929	2933	296.2	1238	475	83.5	870	254.5
KP8_1_3_4		947	2001	3060	302	1294	496	85.8	883	257.8
KP8_1_3_5	0.89	899	1746	2710	281.4	1243	494	82.7	905	259.5
KP8_1_3_6	0.79	871	1744	2699	279	1214	476	82.7	859	248.6
KP8_1_3_7	0.95	831	1839	2756	286.5	1197	452	75.9	835	238.3
KP8_1_3_8	0.98	884	1997	2981	299.1	1252	475	79.1	866	249
KP8_1_3_11	0.67	898	3610	6460	469	1828	621	102.4	1088	313.6
KP8_1_3_18	0.77	877	2432	3330	315	1243	443	75.1	824	238.7
KP8_1_3_19		829	2530	3420	325	1240	426	72.3	774	223
KP8_1_3_20		788	2612	3540	326	1251	419	67.3	755	215.3

<b>Sample</b>	<b>Sb</b>	<b>Ba</b>	<b>La</b>	<b>Ce</b>	<b>Pr</b>	<b>Nd</b>	<b>Sm</b>	<b>Eu</b>	<b>Gd</b>	<b>Tb</b>
KP9_2_2_1	0.63	872	4250	6750	674	2749	863	129.8	1329	348
KP9_2_2_2		850	4075	6460	648	2657	838	122.6	1277	330.2
KP9_2_2_3		840	3870	6130	622	2539	812	120.9	1234	320
KP9_2_2_4		812	3850	6120	609	2520	794	121	1229	312.5
KP9_2_2_5		824	3611	5820	588	2457	787	118	1209	316.7
KP9_2_2_6		822	3508	5680	584	2420	782	121.4	1195	316.4
KP9_2_2_7		809	3365	5480	573	2393	772	117.6	1172	311.4
KP9_2_2_8		800	3326	5450	573	2393	777	118.4	1200	317.3
KP9_2_2_9		809	3357	5550	577	2418	786	119.8	1205	324.9
KP9_2_2_10		816	3332	5410	576	2393	783	120.4	1211	324.1
KP9_2_2_11	0.56	937	4290	6670	669	2723	850	129.4	1250	331.1
KP9_2_2_12		851	3603	5800	599	2489	783	122.1	1174	321.4
KP9_2_2_13		854	3612	5780	588	2406	756	118	1158	326.5
KP9_2_2_14		847	3477	5620	578	2346	751	119.3	1182	330
KP9_2_2_15		847	3092	5130	536	2207	721	115.4	1164	328
KP9_2_2_16		867	3119	5235	535	2232	731	116.1	1201	347.6
KP9_2_2_17		855	2972	5000	519	2161	723	112.8	1194	343.2
KP9_2_2_18		882	3090	5170	524	2191	731	111.4	1221	354.2
KP9_2_2_19		860	3110	5150	536	2205	731	113.7	1228	365
KP9_2_2_20		848	3317	5420	553	2241	731	112.1	1272	367.7
KP9_2_2_21	0.78	873	2965	4990	526	2178	741	117.5	1285	373
KP9_2_2_22		857	2980	4910	511	2164	734	111	1297	377
KP9_2_2_23		855	2986	5050	520	2157	734	116.8	1279	378.7
KP9_2_2_24		847	2928	4890	505	2129	731	112.8	1293	375
KP9_2_2_25		847	3021	5000	529	2239	762	115.7	1322	376
KP9_2_2_26	0.56	878	3060	5020	531	2248	771	117.1	1355	392

<b>Sample</b>	<b>Sb</b>	<b>Ba</b>	<b>La</b>	<b>Ce</b>	<b>Pr</b>	<b>Nd</b>	<b>Sm</b>	<b>Eu</b>	<b>Gd</b>	<b>Tb</b>
KP9_2_2_27		873	2866	4870	504	2137	742	113.7	1343	384.9
KP9_2_2_28	0.56	850	2901	4910	506.6	2153	756	116.1	1342	389
KP9_2_2_29	0.65	852	2768	4710	497	2122	743	111.2	1320	384
KP9_2_2_30	0.64	886	2548	4490	489	2099	750	113.3	1331	388
KP9_2_2_31		841	2547	4480	475	2058	731	110.7	1311	375.8
KP9_2_2_32		847	2705	4620	490	2078	723	111.2	1283	366
KP9_2_2_33	0.7	875	2851	4880	516	2196	760	113.6	1336	384
KP9_2_2_34		864	2770	4910	516	2164	745	115.8	1311	376.9
KP9_2_2_35		833	2286	4230	453	2012	725	109.1	1273	366
KP9_2_2_36		826	2296	4280	465	2004	720	112.8	1261	365
KP9_2_2_37	0.87	777	2374	4320	467	2026	727	112.9	1275	369
KP9_2_2_38		854	3410	5570	553	2246	717	113.7	1190	346.4
KP9_2_2_39		828	2699	4680	495	2077	719	113.4	1181	343.9
KP9_2_2_40		819	3245	5360	541	2210	714	111.8	1131	329.1
KP9_2_2_41		788	3610	5740	569	2269	701	106.1	1111	307
KP9_2_2_42		797	3459	5640	561	2294	716	111.7	1104	311.7
Eud_LV01_1	0.72	710	4313	7960	756	2880	548	169.6	507	86.9
Eud_LV01_2		692	4186	7810	746	2855	540	168.4	517	87
Eud_LV01_3	0.9	504	3088	6040	614	2344	466.7	143.4	432	73.3
Eud_LV01_4	0.34	505	3035	5960	614	2317	463	136.7	418	73.2
Eud_LV01_5	2.6	583	3823	7150	722	2668	524.9	154.5	458	82
Eud_LV01_6		651	4000	7470	741	2733	536	160.9	480	84.3
Eud_LV01_7	0.73	651	4010	7400	726	2723	530	158.3	486	86.1
Eud_LV01_8	0.57	504	3238	6210	633	2406	481	144.5	430	74.3
Eud_LV01_9	0.35	506	3204	6340	627	2436	483	145	447	76.8
Eud_LV01_10		508	3245	6160	626	2417	478.5	145.5	429	75.3
Eud_LV01_11		522	3325	6350	654	2461	490	145.6	447	76.1

<b>Sample</b>	<b>Sb</b>	<b>Ba</b>	<b>La</b>	<b>Ce</b>	<b>Pr</b>	<b>Nd</b>	<b>Sm</b>	<b>Eu</b>	<b>Gd</b>	<b>Tb</b>
Eud_LV01_12	2.28	520	3328	6290	649	2463	488	144	442	76.8
Eud_LV01_13	0.45	694	4029	7330	724	2726	532	159.2	479	85.1
Eud_LV01_14	0.49	699	4090	7360	723	2710	527	158	479	83.2
Eud_LV01_15		689	4200	7570	753	2783	543	163.5	492	85.1
Eud_LV01_16	0.43	697	4112	7550	749	2775	547	161.2	494	86.2
Eud_LV01_17	0.38	704	4300	7900	756	2833	552	164.2	511	88.5
Eud_LV01_18	0.5	696	4230	7640	746	2773	542	162.3	509	84.2
Eud_NK_1	0.58	589	3843	7830	929	4067	1258	167.2	1619	359
Eud_NK_2	0.73	593	3893	7810	919	4048	1244	160.6	1630	348.9
Eud_NK_3	0.77	598	3850	7930	934	4098	1251	162.3	1635	356.8
Eud_NK_4	0.77	617	3950	8070	941	4157	1268	162.6	1653	359
Eud_NK_5	0.65	608	4060	8200	938	4239	1295	168.4	1685	371
Eud_NK_6		621	4050	8190	947	4230	1284	166.2	1675	360
Eud_NK_7	0.41	614	3960	7980	923	4153	1253	163.7	1667	357.3
Eud_NK_8	0.8	599	4012	8100	919	4153	1250	166.6	1632	361.2
Eud_NK_9		582	3960	7950	925	4109	1245	162.2	1610	356.5
Eud_NK_10	0.69	605	3990	8240	939	4200	1268	165.7	1679	363
Eud_NK_11	0.71	596	4015	8050	929	4121	1255	165.5	1621	355.5
Eud_NK_12	0.4	591	3980	8120	938	4150	1260	168.3	1635	356
Eud_NK_13	0.51	637	4240	8560	1001	4310	1325	174.2	1724	373
Eud_NK_14	0.51	620	4040	8250	945	4193	1285	171.5	1689	361.8
Eud_NK_15	0.38	617	4110	8270	950	4180	1277	165.5	1696	359
Eud_NK_16	0.44	622	4140	8320	953	4182	1273	169.5	1671	362
KP1_2_1	0.92	1963	3528	5560	571	2299	763	116.7	1142	308.4
KP1_2_2	1.14	1833	4230	6260	603	2317	720	115.5	1065	287.6
KP1_2_3	1.13	1776	4380	6350	612	2300	713	109.8	1056	286.4

<b>Sample</b>	<b>Sb</b>	<b>Ba</b>	<b>La</b>	<b>Ce</b>	<b>Pr</b>	<b>Nd</b>	<b>Sm</b>	<b>Eu</b>	<b>Gd</b>	<b>Tb</b>
KP1_2_4	1.2	1773	3657	5560	561	2191	707	111.6	1053	284.2
KP1_2_5	0.79	1752	4238	6200	601	2283	704	109.6	1024	278.7
KP1_2_6	1.36	1696	3956	5730	558	2206	685	107.4	1020	270.7
KP1_2_7	1.34	1718	4004	5880	574	2233	700	110.7	1023	275.7
KP1_2_8	1.03	1748	3447	5240	539	2164	707	113.9	1032	284
KP1_2_9	1.18	1692	4120	6030	579	2230	686	105	1020	277.5
KP1_2_10	1.07	1698	3930	5860	569	2209	689	114.4	1033	276.7
KP1_2_11		1694	3630	5500	544	2153	659	104.1	973	264.5
KP1_2_12	1	1636	4020	5900	560	2219	674	106.5	987	267.2
KP1_2_13	1.03	1572	4370	6230	585	2211	660	103.2	996	266.2
KP1_2_14	1.16	1532	4010	5880	559	2152	651	103.3	983	266.7
KP1_2_15	0.75	1545	3980	5860	546	2128	657	99	984	265.6
KP1_2_16	0.95	1596	3950	5720	540	2115	658	102.9	964	265.3
KP1_2_17		1506	3810	5680	535	2059	618	100.8	922	250.1
KP1_2_18		1490	2898	4720	483	1991	611	96.6	919	251.2
KP1_2_19		1682	3420	5340	528	2151	665	102.5	974	265.7
KP1_2_20	0.65	1717	3429	5340	528	2169	679	105	1011	271.1
KP1_2_21		1646	2920	4720	477	1975	631	99.4	955	259.2
KP1_2_22	0.66	1826	3460	5400	541	2213	705	109.2	1093	291
KP1_2_23	1.4	1748	4460	6520	595	2360	710	112.4	1077	291
KP1_2_24	1.09	1677	4340	6390	585	2287	692	109.1	1016	282.5
KP1_2_25	1.1	1679	3891	5740	543	2174	668	106	1032	272.8
KP1_2_26	0.92	1666	4110	6020	566	2217	682	107.4	1012	275.1
KP1_2_27	0.95	1656	4146	6070	563	2226	682	109.4	1041	274
KP1_2_28	0.69	1701	4120	6100	566	2260	686	107.9	1034	273.1
KP1_2_29	0.87	1733	4160	6180	577	2285	682	109.2	1033	279.7
KP1_2_30	0.73	1713	3860	5800	564	2291	683	109.6	1015	268.7

<b>Sample</b>	<b>Sb</b>	<b>Ba</b>	<b>La</b>	<b>Ce</b>	<b>Pr</b>	<b>Nd</b>	<b>Sm</b>	<b>Eu</b>	<b>Gd</b>	<b>Tb</b>
CBD11_10_1	0.26	928	2048	3844	411.3	1809	542	83.2	718	155.5
CBD11_10_2		836	1833	4160	493	2352	657	92.3	794	149.6
CBD11_10_3		869	1982	3577	372	1628	485	74.7	635	142.1
CBD11_10_4		770	1439	3800	479	2291	627	90.8	767	151.9
CBD11_10_5		722	1787	3728	419	1903	555	81.5	696	142.1
CBD11_10_6		740	1585	3621	422.8	1989	563	82	656	131.7
CBD11_10_7		816	1395	3590	450	2188	604	90.6	696	131
CBD11_10_8		757	1609	3595	425.8	1966	577	85.8	707	141.1
CBD11_10_9		757	1552	3942	495	2263	573	90.1	650	126.3
CBD11_10_10		723	1271	2694	324.9	1525	473.5	70.3	629	131
CBD11_10_11	0.33	836	1525	2860	305	1325	443	63.8	645	138.2
CBD11_10_12		815	1240	3229	422	2166	685	95	830	168.7
CBD11_10_13		785	1354	3170	390	1925	611	86.4	790	158.1
CBD11_10_14		741	1695	3769	449	2153	652	92.9	820	160
CBD11_10_15		745	1529	3430	406	1953	617	84.6	807	163
CBD11_10_21	0.37	4700	5070	9540	1010	4240	991	125.8	1097	210
CBD11_10_22		3640	3650	7590	828	3450	817	110.6	920	184.8
CBD11_10_23		3950	3890	7680	799	3300	777	103.6	896	184.9
CBD11_10_25		4100	4360	8260	864	3490	797	106.4	923	170.4
CBD11_10_26		4030	4030	7470	798	3210	735	98	810	169
CBD11_10_29		3070	3180	6680	731	3010	697	89	760	150
CBD11_10_31		2790	3310	6360	660	2740	643	81.6	719	142

<b>Sample</b>	<b>Dy</b>	<b>Ho</b>	<b>Er</b>	<b>Tm</b>	<b>Yb</b>	<b>Lu</b>	<b>Hf</b>	<b>Ta</b>	<b>W</b>	<b>Pb</b>
	<i>ppm</i>									
Eud_LV01_1	451	94.6	258.9	37.4	251.2	31.9	2011	450	132.1	12.08
Eud_LV01_2	445	93.8	254.2	37.2	246.2	31.6	1953	408.2	119.7	11.9
Eud_LV01_3	478	98.8	273.9	38.6	268.5	33.9	2052	424	126.5	13.84
Eud_LV01_4	468	97.8	272.8	38.6	264.8	32.4	2031	427.3	124.7	14.2
Eud_LV01_5	435	94.1	251.4	36.9	238.1	31.3	1833	409	167.9	29
Eud_LV01_6	431	89.7	250.2	36.7	236	32.3	1881	405	115	12
Eud_LV01_7	494	104.8	294.8	42.5	265.7	36.5	1930	528	195	21.1
Eud_LV01_8	496	106.4	295.8	42.9	267.8	36.2	1886	574	228.7	25
Eud_LV01_9	460	93.9	259.9	36.3	248.4	32.5	1938	425	120.3	13.3
Eud_LV01_10	464	96.3	268.1	38.8	250.2	33.7	1988	424	124.2	14.3
Eud_LV01_11	470	98.2	271.8	39.9	258.1	34.9	1975	422	128.5	27.5
Eud_LV01_12	475	99	273.7	40.5	260.1	34.2	2013	413	123.2	27.1
Eud_LV01_13	512	105.6	291.7	42.8	277.4	36.3	1936	580	230	24
Eud_LV01_14	506	107.8	298.8	42.4	282.4	37.7	1905	534	212.4	23.5
Eud_LV01_15	491	99.7	281.4	42	257.9	35.4	2024	417	124	14.2
Eud_LV01_16	482	98.4	275.5	40.3	265	35.2	1986	415	121.6	12.4
Eud_LV01_17	466	95.8	275.9	39.9	261.5	34.1	2026	420	130.2	31.6
Eud_LV01_18	477	98.2	278.4	39.8	259	34.1	2030	419	122.5	15.4
<hr/>										
Eud_NK_1	2484	589	1765	269.9	1919	252.4	2214	201	24.4	249
Eud_NK_2	2531	595	1777	276.7	1960	255.7	2247	201	24.4	284
Eud_NK_3	2555	608	1798	281.9	1994	262.7	2327	207	25.8	192
Eud_NK_4	2546	597	1801	286.6	1975	261.3	2275	205.5	26.5	192
Eud_NK_5	2290	553	1697	265.3	1773	239.1	2059	190.7	21.3	169.5
Eud_NK_6	2263	549	1665	257.9	1764	239.7	2048	187.5	22.4	189.4
Eud_NK_7	2432	565	1771	273.5	1812	247.5	2147	197.8	23.5	213
Eud_NK_8	2390	570	1780	273.8	1803	249	2123	195.4	22.5	134.1

<b>Sample</b>	<b>Dy</b>	<b>Ho</b>	<b>Er</b>	<b>Tm</b>	<b>Yb</b>	<b>Lu</b>	<b>Hf</b>	<b>Ta</b>	<b>W</b>	<b>Pb</b>
Eud_NK_9	2353	565	1730	268.5	1822	245.7	2150	193.2	22.7	199.5
Eud_NK_10	2415	572	1708	266.6	1814	245.6	2120	194.5	23.6	189.5
Eud_NK_11	2416	563	1696	266.6	1831	245.8	2161	190.9	21.7	187.6
Eud_NK_12	2412	561	1747	271.6	1843	246.8	2172	196.9	25.1	193.4
Eud_NK_13	2396	552	1699	261.2	1793	239	2150	189.7	21.8	188.9
Eud_NK_14	2454	567	1725	269.5	1856	242.4	2165	194.3	24.6	195.3
Eud_NK_15	2473	565	1757	273.3	1866	250.5	2184	198.4	23.8	501
Eud_NK_16	2404	555	1691	268.2	1797	238.2	2129	191.5	23.4	184.4
Eud_NK_17	2434	576	1787	276.9	1893	254.5	2265	202.9	25.1	203.3
Eud_NK_18	2448	561	1752	277.1	1863	251.7	2228	201.6	23.9	199.3
CBD11_02_1	977	230.6	662	96.4	614	76.5	1851	109.5	22.7	2.66
CBD11_02_2	982	230.9	656	95.3	601	76.2	1921	155.1	36.4	3.32
CBD11_02_3	996	230.4	640	88.7	570	69	1745	106.9	23.4	3.39
CBD11_02_4	966	223.2	627	89.4	572	69.8	1808	86.4	20.9	2.93
CBD11_02_5	993	230.4	667	96.8	611	76.1	1921	160.5	54.2	4.77
CBD11_02_6	978	221.7	628	87.6	557	68.8	1830	110.4	31.7	2.89
CBD11_02_7	1001	221.2	607	85.4	535	64	1805	90	21.2	2.89
CBD11_02_8	943	218.6	640	93.1	590	72.4	1830	136.4	33.2	3.47
CBD11_02_9	954	226.4	636	93.7	598	72	1849	133.6	44.1	3.96
CBD11_02_10	955	213.2	603	87.9	537	67.3	1667	102.8	22.5	3.74
CBD11_02_11	859	202.2	613	88.7	540	70	1809	143.5	65.5	4.57
CBD11_02_12	951	220.5	649	93.7	552	72.7	1807	142.3	60.3	3.09
CBD11_02_13	969	230.5	674	96.1	563	74.9	1804	158.7	65.1	4.02
CBD11_02_16	991	225.4	658	93.9	569	72.9	2092	236.3	98.1	6.57
CBD11_02_17	963	224	646	93.9	551	72	2011	206.9	92.2	2.38

<b>Sample</b>	<b>Dy</b>	<b>Ho</b>	<b>Er</b>	<b>Tm</b>	<b>Yb</b>	<b>Lu</b>	<b>Hf</b>	<b>Ta</b>	<b>W</b>	<b>Pb</b>
CBD11_02_18	1101	251	741	105.3	621	81.9	2195	227	90.9	4.87
CBD11_02_19	1006	231.7	699	97.3	585	77.5	1951	194.5	88.1	6.35
CBD11_02_20	985	228.2	688	97.6	577	75.2	1959	195.4	86.8	6.37
CBD11_02_21	990	231.4	682	97.8	594	77.7	1837	177.7	67.6	7.09
CBD11_02_22	1042	240.6	680	96.3	574	73.1	1978	169	64.6	6.65
CBD11_02_23	1102	250.6	707	99.1	601	75.6	1908	154.3	60.5	7.6
CBD11_02_24	1084	248.7	693	99.4	608	76.9	1922	105.8	42.3	4.18
CBD11_02_25	1029	229.8	665	94	568	73.5	1892	112.3	42.5	5.39
CBD11_02_26	1064	242.5	684	97.8	591	72.2	1854	108	41.8	4.56
CBD11_02_27	1010	234.8	665	96.9	589	73	1840	129.5	53.1	4.8
CBD11_02_28	974	225.7	652	94.6	557	70.8	1784	111	49.9	3.73
CBD11_02_29	1010	231	662	95.1	562	70.8	1912	155.2	66	3.4
CBD11_02_30	998	232.8	666	95.5	568	72.6	1908	154.8	58	4.16
KP8_1_3_1	2531	736	2667	471	3239	395	1856	554	597	92.3
KP8_1_3_2	2540	729	2670	471	3220	395	1829	531	734	77
KP8_1_3_3	2375	675	2498	444	3062	378	1757	306.1	1056	95.5
KP8_1_3_4	2404	693	2532	450	3060	390	1762	500	921	99.3
KP8_1_3_5	2353	688	2484	450	3090	389	1805	310	1126	85.7
KP8_1_3_6	2283	656	2438	432	2987	369	1726	275.5	1068	89.8
KP8_1_3_7	2191	616	2258	408	2791	352	1624	506	1036	82.4
KP8_1_3_8	2313	664	2453	433	3034	374	1782	450	811	89.6
KP8_1_3_11	2903	819	2910	507	3430	423	1788	681	839	224
KP8_1_3_18	2258	655	2428	410	2880	347	1772	813	327	81.2
KP8_1_3_19	2103	595	2220	381	2680	328	1707	795	244	84.7
KP8_1_3_20	2011	572	2126	368	2633	319	1676	797	240	86.9

<b>Sample</b>	<b>Dy</b>	<b>Ho</b>	<b>Er</b>	<b>Tm</b>	<b>Yb</b>	<b>Lu</b>	<b>Hf</b>	<b>Ta</b>	<b>W</b>	<b>Pb</b>
KP9_2_2_1	3032	823	2919	492	3401	419	1966	874	296	68.2
KP9_2_2_2	2910	799	2851	489	3400	421	1970	860	323	67.5
KP9_2_2_3	2848	776	2807	491	3370	426	1960	845	279	65
KP9_2_2_4	2817	784	2801	489	3388	430	1976	858	287.1	66.5
KP9_2_2_5	2846	790	2853	512	3448	437	1995	843	285.7	63.5
KP9_2_2_6	2869	789	2891	508	3519	443	1956	855	310	70.7
KP9_2_2_7	2841	784	2880	510	3552	442	1918	830	323	64.9
KP9_2_2_8	2898	804	2936	521	3552	442	1957	851	345	66.8
KP9_2_2_9	2932	820	2959	525	3658	451	1971	841	299.1	68.8
KP9_2_2_10	2901	810	2944	522	3565	442	1950	821	280.2	71.3
KP9_2_2_11	2974	825	3092	552	3780	478	2027	927	300	71.6
KP9_2_2_12	2945	836	3030	545	3706	476	2060	950	445	101.8
KP9_2_2_13	3033	847	3124	553	3680	464	2045	1087	550	62.6
KP9_2_2_14	3077	875	3194	555	3670	452	2096	1101	635	79.1
KP9_2_2_15	3030	871	3138	541	3502	438	1937	796	277.1	69.2
KP9_2_2_16	3154	901	3198	546	3474	435.3	1993	807	211.6	60.7
KP9_2_2_17	3201	916	3187	526	3413	421	1893	718	146.9	31.7
KP9_2_2_18	3290	915	3161	530	3340	412	1913	739	161.1	16.5
KP9_2_2_19	3264	926	3158	522	3255	404	1924	790	184.2	23.7
KP9_2_2_20	3355	928	3152	508	3253	397	1861	748	126.5	29.1
KP9_2_2_21	3418	933	3230	513	3259	398	1768	566	71.9	532
KP9_2_2_22	3437	927	3147	508	3215	388	1762	540	69.2	19.7
KP9_2_2_23	3422	931	3133	498	3179	387.8	1775	591	79.8	21.1
KP9_2_2_24	3378	916	3124	490	3135	376.6	1751	556	80.8	26.9
KP9_2_2_25	3330	911	3017	488	3052	366.5	1710	555	82.3	1390
KP9_2_2_26	3508	947	3204	511	3192	388	1817	592	82.5	157

<b>Sample</b>	<b>Dy</b>	<b>Ho</b>	<b>Er</b>	<b>Tm</b>	<b>Yb</b>	<b>Lu</b>	<b>Hf</b>	<b>Ta</b>	<b>W</b>	<b>Pb</b>
KP9_2_2_27	3461	928	3135	500	3105	375.6	1783	605	85	34.8
KP9_2_2_28	3479	946	3196	513	3183	383	1793	581	78	37.3
KP9_2_2_29	3480	933	3128	504	3155	389	1759	556	60.2	32.2
KP9_2_2_30	3460	943	3209	507	3179	394	1769	475	38.8	33.9
KP9_2_2_31	3407	910	3100	506	3157	383.2	1718	447	37.4	36.4
KP9_2_2_32	3302	892	3071	482	3117	378	1678	535	51.5	31.7
KP9_2_2_33	3459	934	3182	518	3269	396	1786	554	52.3	700
KP9_2_2_34	3404	922	3156	513	3253	397	1778	483	56.2	39.8
KP9_2_2_35	3277	900	3122	494	3178	380	1712	383	31.3	33.5
KP9_2_2_36	3306	891	3097	503	3170	390	1733	378.1	35.9	175
KP9_2_2_37	3274	900	3150	513	3292	393	1755	384	36.9	18.1
KP9_2_2_38	3098	863	2999	498	3206	394.1	1765	797	138.8	50.3
KP9_2_2_39	3114	848	3061	512	3375	416	1714	585	112.4	58.4
KP9_2_2_40	2985	811	3016	504	3380	423	1906	959	329	70.1
KP9_2_2_41	2818	783	2851	487	3310	417	2012	1088	776	74.1
KP9_2_2_42	2762	779	2840	487	3365	424	1782	848	273.3	74.7
<hr/>										
Eud_LV01_1	553	116.1	317.1	47.3	302	40	2121	601	251.8	26.3
Eud_LV01_2	559	116.9	319.9	47.2	303	40.2	2082	582	236.2	27.4
Eud_LV01_3	473	97.1	269.1	38.5	256.6	33.8	2032	418	121.3	18.9
Eud_LV01_4	461	94.6	264.7	37.3	247.9	33.7	2028	429	123.4	16.2
Eud_LV01_5	511	106	300	42.3	278	36.8	1994	520	194	22.5
Eud_LV01_6	523	108.7	309	43.9	287	38.6	2030	588	231	23.4
Eud_LV01_7	518	108.1	308.7	44.4	286.3	37.8	2022	572	219.4	22.7
Eud_LV01_8	468	98.4	274.2	39.3	256	34.2	2050	424	123.9	17.2
Eud_LV01_9	465	99.9	276.1	39.7	258.9	34.8	2070	434.6	126.7	17.7
Eud_LV01_10	471	97.7	273.7	39.2	259.8	34.2	2058	446	129.7	19.3
Eud_LV01_11	464	98.6	278.6	39.4	260.5	35.6	2069	431	136.1	17.7

<b>Sample</b>	<b>Dy</b>	<b>Ho</b>	<b>Er</b>	<b>Tm</b>	<b>Yb</b>	<b>Lu</b>	<b>Hf</b>	<b>Ta</b>	<b>W</b>	<b>Pb</b>
Eud_LV01_12	473	100.3	274.8	39.5	260.2	35.8	2054	428	132.6	18.7
Eud_LV01_13	525	109.9	308.1	44.8	276.4	39.4	1966	569	220	23.2
Eud_LV01_14	516	109.1	298.4	43.4	283	38.3	1962	584	225.4	21.4
Eud_LV01_15	521	109.9	307	44.3	283.2	39.6	2017	594	233.8	22.2
Eud_LV01_16	542	111.6	309.8	44	293.6	39.1	2002	582	227.4	21.9
Eud_LV01_17	550	113.8	313	45.2	302	40.6	2031	610	241.5	21.8
Eud_LV01_18	533	110.4	303	45.4	291	38.1	2000	590	229.3	23.3
Eud_NK_1	2606	606	1930	297.8	1966	272.5	2281	236.2	23.9	213.4
Eud_NK_2	2606	601	1898	289.7	1950	269.3	2273	234.9	23	217.2
Eud_NK_3	2574	608	1888	289.7	1960	268.4	2274	236.6	26.2	221.7
Eud_NK_4	2639	611	1923	295.2	2011	274.2	2306	231.7	26.1	211.6
Eud_NK_5	2680	637	1955	308.7	2017	277.9	2359	236.1	23.6	216.9
Eud_NK_6	2651	621	1970	302	2041	278.9	2323	228	25.9	218.8
Eud_NK_7	2586	613	1894	298.2	2002	272.6	2291	232.9	25.5	213.3
Eud_NK_8	2604	616	1921	298.7	2004	273.3	2314	233.6	25.5	4400
Eud_NK_9	2584	608	1881	289.6	1962	266	2287	230	25.4	216.9
Eud_NK_10	2639	632	1936	294.7	2016	273.9	2314	237.5	24.9	210.1
Eud_NK_11	2560	615	1877	290.1	1958	274.5	2281	231.7	23.7	219.3
Eud_NK_12	2611	616	1903	295.8	2009	273.3	2320	239.7	25.6	214.2
Eud_NK_13	2725	643	1977	304.6	2030	283.5	2390	251.2	24.5	212.9
Eud_NK_14	2687	620	1914	299.9	1984	272.6	2314	244.1	24.7	219.1
Eud_NK_15	2633	636	1932	296.5	2007	274.4	2275	236.1	24.4	211.8
Eud_NK_16	2666	626	1901	300	2005	273.2	2308	241.9	26	200.6
KP1_2_1	2671	743	2722	476	3275	411	1833	390	369	103.3
KP1_2_2	2480	696	2558	446	3069	388.2	1753	494	187.8	106.4
KP1_2_3	2434	691	2506	445	3052	387	1839	704	230.7	103

<b>Sample</b>	<b>Dy</b>	<b>Ho</b>	<b>Er</b>	<b>Tm</b>	<b>Yb</b>	<b>Lu</b>	<b>Hf</b>	<b>Ta</b>	<b>W</b>	<b>Pb</b>
KP1_2_4	2404	685	2532	443	2998	380.9	1811	535	440	104
KP1_2_5	2405	677	2481	439	3011	381.3	1908	753	332.4	117
KP1_2_6	2345	659	2455	428	2915	370.6	1855	725	378	99.2
KP1_2_7	2414	671	2507	440	3004	378	1803	387	1145	100.5
KP1_2_8	2403	680	2543	449	3110	387.1	1706	306	664	94.2
KP1_2_9	2355	669	2467	432	2961	371.8	1846	751	846	127.1
KP1_2_10	2382	668	2500	434	2977	374	1812	581	377	107
KP1_2_11	2285	637	2342	405	2770	349	1553	448	670	86
KP1_2_12	2323	659	2434	426	2882	366	1655	483	181.2	85.4
KP1_2_13	2290	649	2397	419	2837	363	1753	707	192.2	94
KP1_2_14	2248	641	2355	415	2812	366.2	1734	613	206.7	97
KP1_2_15	2264	642	2347	409.5	2862	362	1741	632	203	96.5
KP1_2_16	2257	643	2381	419	2916	368	1631	555	227.8	94.5
KP1_2_17	2147	607	2215	395	2748	349	1587	525	225	90.4
KP1_2_18	2138	616	2265	387	2703	336	1385	216.7	321	78
KP1_2_19	2267	633	2352	407	2787	359	1563	356.6	265	81.4
KP1_2_20	2304	654	2416	414	2855	356	1468	351	260	93.1
KP1_2_21	2205	622	2275	408	2792	346	1504	328	281	88.3
KP1_2_22	2539	713	2567	458	3120	397	1744	421	557	94.8
KP1_2_23	2505	697	2612	460	3158	392	1931	689	225.4	108
KP1_2_24	2409	678	2517	439	3007	381.2	1873	668	220.6	102.3
KP1_2_25	2393	675	2464	437	2982	378.7	1727	391	450	100.5
KP1_2_26	2414	672	2465	434	3029	376	1833	627	228.5	104.5
KP1_2_27	2359	668	2474	435	2992	375	1849	672	231.7	102.7
KP1_2_28	2398	675	2473	434	2947	377	1712	582	393	101.8
KP1_2_29	2426	675	2478	439	2946	377.4	1682	622	236.1	99.6
KP1_2_30	2389	664	2430	427	2925	368	1660	536	284.6	88.7

<b>Sample</b>	<b>Dy</b>	<b>Ho</b>	<b>Er</b>	<b>Tm</b>	<b>Yb</b>	<b>Lu</b>	<b>Hf</b>	<b>Ta</b>	<b>W</b>	<b>Pb</b>
CBD11_10_1	1123	269.4	826	122.3	762	99.7	2033	214.9	61.3	6.94
CBD11_10_2	1073	238.7	702	98.3	598	76.4	2238	219.6	85	6.42
CBD11_10_3	1011	239.2	730	109.2	663	89.5	1853	210.9	64.6	7.36
CBD11_10_4	1051	237.1	681	94.3	581	74.7	1815	111.4	37	4.4
CBD11_10_5	992	231.8	682	99	621	79	2080	187	66.2	5.42
CBD11_10_6	889	204.8	587	84.8	521	66.6	2024	183.5	70.5	5.43
CBD11_10_7	889	208.9	610	87.2	544	72.1	2181	140.6	62.1	4.54
CBD11_10_8	1003	231.6	680	99.4	610	81.4	2057	237.5	102.9	5.6
CBD11_10_9	878	203.1	585	83.5	502	65.8	1898	110.8	29	5
CBD11_10_10	920	213.7	656	94.7	573	75	1786	142.6	42.3	4.9
CBD11_10_11	992	234	705	101.9	632	85.9	1980	155.3	38.1	6.81
CBD11_10_12	1113	251.3	725	99.5	580	73.2	1989	89.4	34	5.84
CBD11_10_13	1075	252.3	707	100.4	602	77.1	2106	114.1	49.9	3.25
CBD11_10_14	1118	251.3	718	97.3	593	74.2	2104	193.7	68.1	8.4
CBD11_10_15	1100	262.4	725	100.3	601	72.3	1979	170.9	58.4	6
CBD11_10_21	1434	327	939	141.6	851	114.6	2790	430	213	11.1
CBD11_10_22	1265	305	889	131.1	813	106.6	2240	275	135	6.01
CBD11_10_23	1272	301	869	127.3	810	104.2	2330	293	139.2	6.2
CBD11_10_25	1228	287	856	122.2	759	101.4	2400	368	202	9.3
CBD11_10_26	1189	284	866	126.5	808	101.5	2340	340	178	4.99
CBD11_10_29	1015	239	711	104.3	649	86	1960	229	115	5.7
CBD11_10_31	1009	238	707	100	625	82.5	1800	262	132	7.9

<b>Sample</b>	<b>Th</b>	<b>U</b>
	<i>ppm</i>	<i>ppm</i>
Eud_LV01_1	21.1	48.5
Eud_LV01_2	22.9	50.2
Eud_LV01_3	23.4	51.2
Eud_LV01_4	22.4	49.6
Eud_LV01_5	219	85.5
Eud_LV01_6	20.9	47.1
Eud_LV01_7	24.6	48
Eud_LV01_8	25.9	46.1
Eud_LV01_9	29.3	49.1
Eud_LV01_10	29.4	49.5
Eud_LV01_11	25.8	49.6
Eud_LV01_12	23.64	51.3
Eud_LV01_13	26.5	46.8
Eud_LV01_14	27.6	50.6
Eud_LV01_15	23.8	51.5
Eud_LV01_16	23.8	50.4
Eud_LV01_17	24.5	50
Eud_LV01_18	24.8	51.2
Eud_NK_1	15.89	32.5
Eud_NK_2	15.38	33.7
Eud_NK_3	16.6	33.7
Eud_NK_4	16.15	33.5
Eud_NK_5	14.6	30.6
Eud_NK_6	14.39	30.9
Eud_NK_7	16	30.4

<b>Sample</b>	<b>Th</b>	<b>U</b>
Eud_NK_8	15.95	31.5
Eud_NK_9	15.14	31.3
Eud_NK_10	14.71	30.3
Eud_NK_11	14.6	31.8
Eud_NK_12	15.9	32.8
Eud_NK_13	15.5	31.2
Eud_NK_14	15.1	32.7
Eud_NK_15	15.1	32.4
Eud_NK_16	16.3	31.2
Eud_NK_17	16	33.4
Eud_NK_18	16.08	33
CBD11_02_1	8.61	56.8
CBD11_02_2	17.2	37.4
CBD11_02_3	13.15	72.6
CBD11_02_4	8.81	56.9
CBD11_02_5	8.16	32.2
CBD11_02_6	7.68	33.7
CBD11_02_7	12.35	65.8
CBD11_02_8	7.87	43.5
CBD11_02_9	6.93	29.2
CBD11_02_10	10.55	63.6
CBD11_02_11	5.98	27.9
CBD11_02_12	6.18	23.5
CBD11_02_13	6.3	24.5
CBD11_02_16	6.55	21.9

<b>Sample</b>	<b>Th</b>	<b>U</b>
CBD11_02_17	6.48	16.2
CBD11_02_18	9.2	17.7
CBD11_02_19	6.18	16.76
CBD11_02_20	5.96	13.26
 CBD11_02_21	6.67	20.4
CBD11_02_22	5.54	21.8
CBD11_02_23	9.05	28.6
CBD11_02_24	8.3	25.8
CBD11_02_25	6.2	17.73
CBD11_02_26	7.73	26.9
CBD11_02_27	5.42	18.2
CBD11_02_28	5.17	15.32
CBD11_02_29	7.27	23.1
CBD11_02_30	5.51	16.7
 KP8_1_3_1	9.68	14.96
KP8_1_3_2	10.77	12.72
KP8_1_3_3	10.74	21.1
KP8_1_3_4	13.9	27.9
KP8_1_3_5	13.69	33.2
KP8_1_3_6	13.66	35.3
KP8_1_3_7	14.3	32.9
KP8_1_3_8	15.2	32.7
KP8_1_3_11	15.7	20.8
 KP8_1_3_18	8.8	13.3
KP8_1_3_19	11.35	16.9

<b>Sample</b>	<b>Th</b>	<b>U</b>
KP8_1_3_20	12.21	18.5
KP9_2_2_1	13.72	38.2
KP9_2_2_2	17.6	50.1
KP9_2_2_3	20.4	51
KP9_2_2_4	21.1	41.8
KP9_2_2_5	22	43
KP9_2_2_6	22.3	43.4
KP9_2_2_7	23	45.1
KP9_2_2_8	24	45.3
KP9_2_2_9	23.1	48
KP9_2_2_10	24.2	46.7
KP9_2_2_11	28.3	58.8
KP9_2_2_12	28.6	59.9
KP9_2_2_13	32.7	56.2
KP9_2_2_14	33.8	51.5
KP9_2_2_15	32	45.8
KP9_2_2_16	32.4	42.1
KP9_2_2_17	29.7	40.4
KP9_2_2_18	30.7	36.6
KP9_2_2_19	29.3	37.5
KP9_2_2_20	29.6	40.3
KP9_2_2_21	26.6	46.6
KP9_2_2_22	23.8	38.5
KP9_2_2_23	24	36.2
KP9_2_2_24	21.8	36.9
KP9_2_2_25	31.6	53.1

<b>Sample</b>	<b>Th</b>	<b>U</b>
KP9_2_2_26	22.2	39.6
KP9_2_2_27	21.2	38.7
KP9_2_2_28	21.6	40.3
KP9_2_2_29	20.5	38.5
KP9_2_2_30	20.3	42.3
KP9_2_2_31	21.8	41.6
KP9_2_2_32	22	39.5
KP9_2_2_33	23.9	44.7
KP9_2_2_34	25.9	45.7
KP9_2_2_35	23.8	45.1
KP9_2_2_36	26.5	45.9
KP9_2_2_37	27.3	49.3
KP9_2_2_38	32.2	49.7
KP9_2_2_39	27.9	48
KP9_2_2_40	30	46.7
KP9_2_2_41	29.8	43.7
KP9_2_2_42	26.8	45.3
Eud_LV01_1	30	51.1
Eud_LV01_2	29.4	51.8
Eud_LV01_3	24	51.7
Eud_LV01_4	21.6	50.6
Eud_LV01_5	41.2	45.6
Eud_LV01_6	27.8	50.1
Eud_LV01_7	27.3	49.8
Eud_LV01_8	22.9	50.5
Eud_LV01_9	23.2	51.5
Eud_LV01_10	22.6	50

<b>Sample</b>	<b>Th</b>	<b>U</b>
Eud_LV01_11	22.8	51.2
Eud_LV01_12	42.9	52
Eud_LV01_13	27.4	49.3
Eud_LV01_14	26.1	48.1
Eud_LV01_15	27.8	48
Eud_LV01_16	28.4	49.4
Eud_LV01_17	29.1	50.1
Eud_LV01_18	27.2	50.7
Eud_NK_1	15.92	31.6
Eud_NK_2	15.8	29.3
Eud_NK_3	16.7	30.1
Eud_NK_4	15.6	31.9
Eud_NK_5	16.68	32.7
Eud_NK_6	16.62	31
Eud_NK_7	15.6	29.7
Eud_NK_8	16.4	30.2
Eud_NK_9	16.1	31.2
Eud_NK_10	16.08	33
Eud_NK_11	16.72	32.1
Eud_NK_12	16.6	30.2
Eud_NK_13	16.5	33.5
Eud_NK_14	16.4	32
Eud_NK_15	16.56	30.9
Eud_NK_16	17.11	31.7
KP1_2_1	6.48	64.4
KP1_2_2	12.19	49.3

<b>Sample</b>	<b>Th</b>	<b>U</b>
KP1_2_3	16.6	47.4
KP1_2_4	17.7	47.5
KP1_2_5	19.8	46.3
KP1_2_6	21.3	50.1
KP1_2_7	20.8	51
KP1_2_8	21.1	57.4
KP1_2_9	19.7	50.4
KP1_2_10	18.8	51
KP1_2_11	5.58	31.4
KP1_2_12	10.03	39.6
KP1_2_13	14.14	51.2
KP1_2_14	14.62	51.9
KP1_2_15	15.9	49.8
KP1_2_16	14.2	49.9
KP1_2_17	11.3	38.6
KP1_2_18	4.64	16.1
KP1_2_19	5.07	20.9
KP1_2_20	5.75	54.3
KP1_2_21	4.85	41.9
KP1_2_22	7	66
KP1_2_23	17.9	55.6
KP1_2_24	15.99	54.4
KP1_2_25	12.97	45
KP1_2_26	16.84	50.3
KP1_2_27	16.9	51.4
KP1_2_28	13.74	57.2
KP1_2_29	10.17	53.7

<b>Sample</b>	<b>Th</b>	<b>U</b>
KP1_2_30	7.2	60.1
CBD11_10_1	6.81	37.9
CBD11_10_2	4.37	19.6
CBD11_10_3	5.58	30.4
CBD11_10_4	4.65	31.5
CBD11_10_5	6.4	26.8
CBD11_10_6	3.27	22.2
CBD11_10_7	3.99	29.3
CBD11_10_8	3.9	25.3
CBD11_10_9	4.27	18
CBD11_10_10	4.96	21.8
CBD11_10_11	5.61	45.4
CBD11_10_12	4.91	34.6
CBD11_10_13	3.27	23
CBD11_10_14	3.4	16.4
CBD11_10_15	3.47	19.09
CBD11_10_21	30.1	27.9
CBD11_10_22	23.5	26.5
CBD11_10_23	29.4	20.4
CBD11_10_25	30.4	22.3
CBD11_10_26	30.3	20.7
CBD11_10_29	23	27.6
CBD11_10_31	24.3	33.3

Table 2: Analytical Uncertainty

Sample	$^{147}\text{Sm}/^{144}\text{Nd}$	Na <i>ppm</i>	Cl <i>ppm</i>	Ca <i>ppm</i>	Mn <i>ppm</i>	Fe <i>ppm</i>	Zr <i>ppm</i>	Be <i>ppm</i>
Eud_LV01_1	0.12379	3000	490	3500	490	800	2400	0.81
Eud_LV01_2	0.12454	3200	460	4300	390	820	2000	0.56
Eud_LV01_3	0.12499	3200	510	3300	440	810	2800	0.53
Eud_LV01_4	0.12462	3000	490	4000	410	770	2700	0.53
Eud_LV01_5	0.12373	3200	540	3900	480	2300	2600	1
Eud_LV01_6	0.1246	4100	550	3800	390	900	2600	0.57
Eud_LV01_7	0.12255	3300	590	3200	390	770	2300	0.55
Eud_LV01_8	0.12129	2800	540	3300	510	850	2400	0.42
Eud_LV01_9	0.12462	3000	550	3300	430	850	2300	0.62
Eud_LV01_10	0.12386	3000	590	4100	540	1100	2400	0.62
Eud_LV01_11	0.12481	3500	530	4400	480	940	2800	0.69
Eud_LV01_12	0.12536	4000	550	3800	400	1000	3000	0.59
Eud_LV01_13	0.12145	2900	550	4500	530	820	2700	0.47
Eud_LV01_14	0.12271	3300	460	4800	510	940	3100	
Eud_LV01_15	0.12502	3500	430	3700	390	920	3100	
Eud_LV01_16	0.12509	3500	480	3700	480	870	3100	0.12
Eud_LV01_17	0.12413	3600	730	4000	440	940	2900	0.6
Eud_LV01_18	0.12495	3300	630	3600	450	880	2700	
Eud_NK_1	0.18978	2600	360	2800	410	700	2400	0.69
Eud_NK_2	0.1892	2900	290	2600	520	670	3000	1.1
Eud_NK_3	0.18921	2400	480	2100	470	660	2700	0.74
Eud_NK_4	0.18969	3000	370	3100	560	920	3300	1
Eud_NK_5	0.1892	2500	310	3000	470	600	2800	0.68
Eud_NK_6	0.1896	2800	430	2800	500	790	3100	0.96

<b>Sample</b>	<b><math>^{147}\text{Sm}/^{144}\text{Nd}</math></b>	<b>Na</b>	<b>Cl</b>	<b>Ca</b>	<b>Mn</b>	<b>Fe</b>	<b>Zr</b>	<b>Be</b>
Eud_NK_7	0.18979	2800	460	3100	450	720	2500	0.92
Eud_NK_8	0.18906	2600	530	2800	520	620	2800	0.84
Eud_NK_9	0.18885	2500	460	2900	490	750	2400	0.91
Eud_NK_10	0.18911	2600	430	2500	560	730	3000	0.58
Eud_NK_11	0.18884	3000	330	2700	480	960	3500	0.74
Eud_NK_12	0.1885	2500	410	2700	470	710	3000	
Eud_NK_13	0.18872	2400	310	3000	500	790	3300	0.56
Eud_NK_14	0.18938	3300	250	2700	550	760	3100	0.92
Eud_NK_15	0.18892	3500	290	3200	530	790	3100	0.68
Eud_NK_16	0.18913	2400	300	2900	470	510	2800	1
Eud_NK_17	0.1888	2800	450	2700	450	820	3100	0.85
Eud_NK_18	0.1888	3000	480	3700	520	810	3600	0.85
CBD11_02_1	0.1879	2900	550	3300	110	1500	3100	0.51
CBD11_02_2	0.1872	3400	500	3600	120	1600	2900	0.93
CBD11_02_3	0.1896	3300	660	3400	100	1300	2800	0.46
CBD11_02_4	0.1874	3800	770	3700	100	1500	2900	0.58
CBD11_02_5	0.1835	3600	670	3600	120	1800	3000	0.73
CBD11_02_6	0.185	3500	600	3800	110	2000	2900	0.62
CBD11_02_7	0.1919	3500	670	3400	110	1400	2400	
CBD11_02_8	0.1846	4400	650	3600	100	1600	3000	0.54
CBD11_02_9	0.1841	3800	640	4200	110	1300	2800	0.65
CBD11_02_10	0.1887	3200	560	3600	100	1400	2700	0.56
CBD11_02_11	0.1844	2900	460	3100	81	1300	2100	0.51
CBD11_02_12	0.1892	2500	640	3900	80	1400	2500	
CBD11_02_13	0.19099	3000	640	2800	85	850	2200	0.57

<b>Sample</b>	<b><math>^{147}\text{Sm}/^{144}\text{Nd}</math></b>	<b>Na</b>	<b>Cl</b>	<b>Ca</b>	<b>Mn</b>	<b>Fe</b>	<b>Zr</b>	<b>Be</b>
CBD11_02_16	0.18565	3100	500	2800	84	1100	2400	0.41
CBD11_02_17	0.1878	2900	590	3000	100	1300	2400	0.52
CBD11_02_18	0.1858	5000	590	5800	170	2100	3300	0.96
CBD11_02_19	0.1797	3000	590	3300	110	1200	2400	
CBD11_02_20	0.1751	3600	580	3500	110	1400	2800	0.63
CBD11_02_21	0.1829	2700	500	4000	100	1300	3100	0.54
CBD11_02_22	0.1905	3100	530	3200	96	1400	2800	0.36
CBD11_02_23	0.1923	2700	640	3800	100	1600	2800	0.53
CBD11_02_24	0.1857	3200	610	3200	93	1400	2500	0.53
CBD11_02_25	0.1837	3600	570	3200	120	1900	3000	0.57
CBD11_02_26	0.188	3200	580	3800	83	1400	2700	
CBD11_02_27	0.1882	2900	540	3000	75	1300	2700	0.75
CBD11_02_28	0.1874	3100	640	4000	88	1600	2500	0.72
CBD11_02_29	0.1851	2900	540	3200	83	1400	2300	0.47
CBD11_02_30	0.1881	3200	530	3100	78	1500	2500	0.58
KP1_2_1	0.2358	3300	490	4600	370	500	2700	1.1
KP1_2_2	0.2338	2100	480	4300	250	470	2900	1.3
KP1_2_3	0.2391	2600	530	5200	330	420	3300	1.6
KP1_2_4	0.2388	4100	720	5200	390	520	3500	1.6
KP1_2_5	0.2463	3200	570	4700	400	460	3200	1.2
KP1_2_6	0.2446	2700	650	5000	330	440	2500	1.1
KP1_2_7	0.2357	2900	590	4900	340	500	2900	1.2
KP1_2_8	0.2353	2800	450	4200	350	500	2400	1.2
KP1_2_11	0.2119	2800	470	5300	520	490	3600	1.4
KP1_2_18	0.2224	3100	510	5400	440	520	3200	1.4

<b>Sample</b>	<b><math>^{147}\text{Sm}/^{144}\text{Nd}</math></b>	<b>Na</b>	<b>Cl</b>	<b>Ca</b>	<b>Mn</b>	<b>Fe</b>	<b>Zr</b>	<b>Be</b>
KP1_2_19	0.2127	3400	530	6400	520	600	2900	1.7
KP1_2_20	0.2091	3200	430	5500	410	510	3200	1.4
KP9_2_2_1	0.1951	2700	360	4200	340	530	2600	1.1
KP9_2_2_2	0.1965	2500	340	4300	350	510	2800	1
KP9_2_2_3	0.1982	2300	290	3900	380	610	3400	0.93
KP9_2_2_4	0.1966	2800	370	4000	420	540	3000	1.1
KP9_2_2_5	0.1986	3000	410	4100	350	550	3300	0.72
KP9_2_2_6	0.2005	2800	320	3800	440	620	3100	0.71
KP9_2_2_7	0.2011	2900	310	3700	290	500	2600	0.88
KP9_2_2_8	0.2013	2300	380	3300	330	540	2900	0.65
KP9_2_2_9	0.2024	2400	400	4500	350	510	2800	0.84
KP9_2_2_10	0.2037	2400	320	3500	280	460	2900	0.72
KP9_2_2_11	0.1944	2500	430	4000	380	590	3000	1.1
KP9_2_2_12	0.196	2600	420	4000	340	490	2300	1.2
KP9_2_2_13	0.1947	2500	430	4100	370	400	2500	1
KP9_2_2_14	0.1984	2400	440	3900	430	500	3300	1
KP9_2_2_15	0.2039	2600	400	4700	320	440	2600	1.1
KP9_2_2_16	0.204	2600	430	3000	300	460	2400	0.97
KP9_2_2_17	0.2084	2300	430	3700	360	490	3100	0.96
KP9_2_2_18	0.2078	2500	420	3800	380	530	3100	0.95
KP9_2_2_19	0.2065	2500	390	5200	400	470	2800	1
KP9_2_2_20	0.2032	2700	460	3500	420	460	2600	0.97
KP9_2_2_21	0.211	2500	400	3700	360	500	3300	1
KP9_2_2_22	0.2113	2800	440	4300	320	490	2400	0.77
KP9_2_2_23	0.2112	2600	400	3500	320	450	2500	0.84
KP9_2_2_24	0.213	3000	480	3200	350	530	2600	0.97

<b>Sample</b>	<b><math>^{147}\text{Sm}/^{144}\text{Nd}</math></b>	<b>Na</b>	<b>Cl</b>	<b>Ca</b>	<b>Mn</b>	<b>Fe</b>	<b>Zr</b>	<b>Be</b>
KP9_2_2_25	0.2111	2300	350	5100	340	880	3000	1.3
KP9_2_2_26	0.2139	2800	340	3600	380	510	3200	1.1
KP9_2_2_27	0.2163	2000	410	3100	360	470	2500	0.86
KP9_2_2_28	0.2182	2400	440	4300	260	400	2400	0.63
KP9_2_2_29	0.2182	2100	390	3400	310	520	2700	0.84
KP9_2_2_30	0.2229	3000	450	3800	330	480	2600	0.84
KP9_2_2_31	0.221	2600	530	3900	320	470	2200	0.98
KP9_2_2_32	0.2164	2100	560	4300	310	410	2100	0.84
KP9_2_2_33	0.2157	3100	480	4300	340	550	2700	0.66
KP9_2_2_34	0.214	2300	480	4000	330	500	2400	1.1
KP9_2_2_35	0.2247	2600	550	3500	320	500	2500	0.96
KP9_2_2_36	0.2219	2500	680	3800	260	500	2900	0.9
KP9_2_2_37	0.2228	2600	660	4400	350	390	2700	0.77
KP9_2_2_38	0.1982	2600	470	4300	410	400	2600	1.2
KP9_2_2_39	0.2139	2600	580	4000	360	550	2900	1.3
KP9_2_2_40	0.2006	2800	470	5200	420	540	2900	0.85
KP9_2_2_41	0.1924	2900	460	4900	440	500	2600	1
KP9_2_2_42	0.1943	2400	520	5000	310	510	2500	1.1
Eud_LV01_1	0.1212	2900	390	3300	500	790	2200	1
Eud_LV01_2	0.12103	3100	520	3500	460	800	3300	0.67
Eud_LV01_3	0.12452	3300	390	3300	370	790	2300	0.51
Eud_LV01_4	0.12478	3100	450	3800	430	850	2700	0.42
Eud_LV01_5	0.12217	3700	490	3800	480	990	2900	0.89
Eud_LV01_6	0.12129	3500	570	4300	530	1000	2500	0.62
Eud_LV01_7	0.12132	3600	550	4400	510	950	3200	1
Eud_LV01_8	0.12421	3600	600	4100	380	880	2600	0.85
Eud_LV01_9	0.12447	3200	700	4100	420	1000	2900	0.42

<b>Sample</b>	<b><math>^{147}\text{Sm}/^{144}\text{Nd}</math></b>	<b>Na</b>	<b>Cl</b>	<b>Ca</b>	<b>Mn</b>	<b>Fe</b>	<b>Zr</b>	<b>Be</b>
Eud_LV01_10	0.12428	3200	660	3100	540	1000	2300	
Eud_LV01_11	0.12471	3200	570	3300	410	990	2500	0.55
Eud_LV01_12	0.12394	4000	730	5000	440	970	2600	1.1
Eud_LV01_13	0.12172	3300	720	4400	460	1000	2900	1
Eud_LV01_14	0.12129	3400	780	4400	520	910	3100	0.96
Eud_LV01_15	0.12063	4100	710	4800	600	980	3100	0.55
Eud_LV01_16	0.12149	3300	760	4200	480	940	2600	0.88
Eud_LV01_17	0.12081	4400	980	5100	540	1000	2900	
Eud_LV01_18	0.12068	3400	720	4200	520	900	2900	0.78
Eud_NK_1	0.19107	2600	400	2500	510	650	2200	0.99
Eud_NK_2	0.18994	3100	380	2700	490	790	3000	0.58
Eud_NK_3	0.1894	2800	340	2800	570	710	2900	0.83
Eud_NK_4	0.191	3400	390	3100	580	800	2800	0.68
Eud_NK_5	0.1914	2800	400	2300	600	710	3600	0.59
Eud_NK_6	0.1902	3400	440	3700	580	880	3000	0.65
Eud_NK_7	0.18936	2600	430	3300	540	810	3100	0.66
Eud_NK_8	0.18895	3300	350	2800	400	690	3100	0.82
Eud_NK_9	0.18969	3100	400	3400	570	680	3100	0.75
Eud_NK_10	0.18915	3300	470	3500	580	740	3400	0.61
Eud_NK_11	0.19019	2800	350	2900	450	730	3000	0.92
Eud_NK_12	0.1895	2700	490	3400	560	850	3000	
Eud_NK_13	0.1904	3200	620	3000	640	780	3500	0.76
Eud_NK_14	0.1896	3300	440	3100	520	750	3200	0.81
Eud_NK_15	0.1892	3300	500	3300	560	1000	3400	0.5
Eud_NK_16	0.18881	3200	520	3500	570	750	2700	0.74
KP1_2_1	0.20313	2600	450	3500	230	570	2700	0.93

<b>Sample</b>	<b><math>^{147}\text{Sm}/^{144}\text{Nd}</math></b>	<b>Na</b>	<b>Cl</b>	<b>Ca</b>	<b>Mn</b>	<b>Fe</b>	<b>Zr</b>	<b>Be</b>
KP1_2_2	0.19086	2300	400	3900	280	610	2300	1.3
KP1_2_3	0.1902	2300	410	3500	370	630	3000	1.2
KP1_2_4	0.198	2200	440	3700	260	510	2500	1.1
KP1_2_5	0.19013	2300	480	3400	260	440	2600	1.3
KP1_2_6	0.1916	2700	420	3600	250	540	2300	1.1
KP1_2_7	0.19355	2400	360	4500	350	620	2800	1.3
KP1_2_8	0.20088	2200	400	3800	240	420	2200	1.3
KP1_2_9	0.1901	2200	430	4000	300	480	2400	1.2
KP1_2_10	0.1931	2500	550	3800	310	530	2700	1.1
KP1_2_11	0.1908	2800	540	4700	300	760	3000	
KP1_2_12	0.1886	3300	460	3400	330	640	3100	0.89
KP1_2_13	0.1861	2800	480	3900	320	540	2400	0.95
KP1_2_14	0.1878	2700	560	3500	370	610	3300	1.5
KP1_2_15	0.1914	2600	740	4500	330	560	2700	0.96
KP1_2_16	0.1922	2400	500	4400	310	600	3300	1
KP1_2_17	0.1877	2600	640	5100	350	700	2800	1.2
KP1_2_18	0.1917	1900	580	5100	250	650	2700	1.3
KP1_2_19	0.1922	2800	730	3800	330	720	3400	1.3
KP1_2_20	0.1954	2700	600	4200	240	750	2800	0.98
KP1_2_21	0.2	3000	720	4400	360	750	3600	0.83
KP1_2_22	0.2001	3400	620	5200	420	970	3500	0.74
KP1_2_23	0.1893	3100	530	4200	330	570	3500	0.87
KP1_2_24	0.1886	2600	610	4500	290	510	2800	0.74
KP1_2_25	0.1931	2700	530	4100	270	590	2500	0.91
KP1_2_26	0.1921	3500	540	4500	350	720	3100	0.88
KP1_2_27	0.1907	2300	570	4000	370	520	2800	0.91
KP1_2_28	0.1896	2500	640	4100	290	590	3300	0.97

<b>Sample</b>	<b><math>^{147}\text{Sm}/^{144}\text{Nd}</math></b>	<b>Na</b>	<b>Cl</b>	<b>Ca</b>	<b>Mn</b>	<b>Fe</b>	<b>Zr</b>	<b>Be</b>
KP1_2_29	0.1877	3000	550	4300	330	620	2600	0.85
KP1_2_30	0.1874	2700	520	4200	240	590	2600	1
CBD11_10_1	0.188	2400	600	3700	130	1400	2500	
CBD11_10_2	0.1749	2500	560	3500	140	1400	2600	0.66
CBD11_10_3	0.1867	2600	570	3900	140	1300	3100	0.5
CBD11_10_4	0.1715	2500	710	3600	95	1500	2700	0.6
CBD11_10_5	0.182	2600	470	3300	130	1300	2600	0.65
CBD11_10_6	0.1768	3000	630	3200	130	1200	2500	
CBD11_10_7	0.1728	2700	550	3500	130	1300	3000	0.65
CBD11_10_8	0.1839	3100	430	3700	120	1600	2400	
CBD11_10_9	0.159	3000	750	3400	120	1300	2500	0.76
CBD11_10_10	0.195	3200	630	3900	110	1400	2600	0.56
CBD11_10_11	0.2067	3400	730	5100	220	1300	5400	0.7
CBD11_10_12	0.1978	2500	660	3100	120	1300	3000	0.81
CBD11_10_13	0.1996	2800	730	2900	130	1300	2500	0.54
CBD11_10_14	0.1886	2800	700	2600	130	1600	3100	
CBD11_10_15	0.1967	2900	670	3700	120	1600	2900	0.73
CBD11_10_21	0.1455	5900	1300	8400	370	2000	4900	1.3
CBD11_10_22	0.1465	4900	840	4200	210	1600	3200	
CBD11_10_23	0.146	5600	780	5700	260	1600	4300	0.54
CBD11_10_25	0.1415	5100	910	6400	290	2900	4300	0.9
CBD11_10_26	0.1421	4900	1300	8000	360	2800	7200	0.49
CBD11_10_29	0.1432	7700	1300	8000	320	2800	6200	1.4
CBD11_10_31	0.145	6600	2000	9200	330	3200	5500	0.79

<b>Sample</b>	<b>Mg</b> <i>ppm</i>	<b>Al</b> <i>ppm</i>	<b>K</b> <i>ppm</i>	<b>Ti</b> <i>ppm</i>	<b>Ga</b> <i>ppm</i>	<b>Rb</b> <i>ppm</i>	<b>Sr</b> <i>ppm</i>	<b>Y</b> <i>ppm</i>
Eud_LV01_1	15	28	91	120	2.6	0.48	200	59
Eud_LV01_2	15	26	90	98	2.6	0.56	200	48
Eud_LV01_3	16	30	93	94	2.1	0.58	230	60
Eud_LV01_4	16	27	90	95	2.5	0.56	240	60
Eud_LV01_5	22	340	150	110	2.2	0.53	250	69
Eud_LV01_6	15	25	89	140	2.2	0.49	240	66
Eud_LV01_7	17	23	100	120	2.8	0.62	350	52
Eud_LV01_8	22	28	98	120	2.9	0.7	310	69
Eud_LV01_9	13	22	81	87	2.6	0.52	230	49
Eud_LV01_10	16	23	110	110	2.4	0.58	230	60
Eud_LV01_11	15	27	87	110	2.3	0.61	220	64
Eud_LV01_12	17	29	74	120	2.2	0.55	220	52
Eud_LV01_13	20	22	100	140	2.7	0.45	300	61
Eud_LV01_14	18	24	88	120	3.3	0.69	340	73
Eud_LV01_15	17	26	91	140	2.3	0.62	260	71
Eud_LV01_16	18	33	120	130	3.1	0.47	300	75
Eud_LV01_17	14	32	87	130	3.1	0.47	230	72
Eud_LV01_18	17	30	110	130	2.6	0.64	230	61
Eud_NK_1	8.4	51	110	38	2.6	1.5	15	370
Eud_NK_2	8.2	58	190	41	3.2	1.5	22	460
Eud_NK_3	8.6	46	150	35	2.5	1.5	17	340
Eud_NK_4	9.7	79	180	41	3	1.6	22	440
Eud_NK_5	8.3	47	110	42	2.3	1.8	18	380
Eud_NK_6	8.9	64	120	36	2.5	1.5	22	510

<b>Sample</b>	<b>Mg</b>	<b>Al</b>	<b>K</b>	<b>Ti</b>	<b>Ga</b>	<b>Rb</b>	<b>Sr</b>	<b>Y</b>
Eud_NK_7	9.7	73	170	42	2.6	1.7	21	410
Eud_NK_8	9.5	70	140	39	2.5	1.7	21	400
Eud_NK_9	9	60	120	42	2.6	1.7	18	410
Eud_NK_10	8.7	63	130	34	2.9	1.8	16	420
Eud_NK_11	10	56	110	42	2.7	1.5	19	410
Eud_NK_12	8.9	47	99	46	2.4	1.8	15	320
Eud_NK_13	9.6	56	120	37	2.7	1.7	19	370
Eud_NK_14	9.5	58	100	44	3.2	1.8	20	430
Eud_NK_15	9.5	57	130	39	3.2	1.4	22	460
Eud_NK_16	7.8	50	110	43	2.2	1.4	17	360
Eud_NK_17	10	61	130	46	3.2	1.8	17	450
Eud_NK_18	9.9	63	160	43	3.2	1.5	22	530
CBD11_02_1		31	120	48	4.5	0.75	9.1	150
CBD11_02_2	4.5	190	110	49	3.7	0.82	9	150
CBD11_02_3	3.5	28	110	36	4	0.64	7.7	160
CBD11_02_4		35	110	45	4.3	0.79	8.5	130
CBD11_02_5	4	35	160	56	4	1	13	180
CBD11_02_6	3.6	38	140	51	4.1	0.92	11	160
CBD11_02_7		37	150	43	3.2	0.83	8.2	160
CBD11_02_8	4.3	34	140	52	3.4	0.74	8.8	150
CBD11_02_9		31	120	45	4.3	0.95	12	160
CBD11_02_10	3.9	34	140	48	3.6	0.75	8.7	130
CBD11_02_11		23	240	43	3.5	0.78	9.8	110
CBD11_02_12		29	98	32	3.4	0.73	9.9	160
CBD11_02_13	3.5	30	90	31	3.8	0.76	9.6	120

<b>Sample</b>	<b>Mg</b>	<b>Al</b>	<b>K</b>	<b>Ti</b>	<b>Ga</b>	<b>Rb</b>	<b>Sr</b>	<b>Y</b>
CBD11_02_16	3.2	31	150	39	3.6	0.83	9.4	120
CBD11_02_17	3.4	28	120	39	3.5	0.57	10	140
CBD11_02_18	4.5	55	83	42	6.3	0.75	13	220
CBD11_02_19	3	33	100	38	4.4	0.63	10	160
CBD11_02_20	2.7	30	82	35	3.8	0.75	10	150
CBD11_02_21		26	110	38	3.8	0.87	11	160
CBD11_02_22	3.3	23	120	31	3.3	0.74	10	180
CBD11_02_23	3.2	38	100	32	5	0.67	9.9	170
CBD11_02_24		28	110	30	3.4	0.7	7.8	150
CBD11_02_25	3.4	28	50	40	3.9	0.78	11	150
CBD11_02_26	3.2	200	63	27	4.3	0.68	10	180
CBD11_02_27	3	30	120	31	3.3	0.8	9.2	150
CBD11_02_28	2.4	48	140	52	3.4	0.67	9.5	140
CBD11_02_29	3.3	29	110	38	3.7	0.85	8.7	140
CBD11_02_30		36	98	29	3.8	0.77	8.9	140
KP1_2_1	27	53	81	47	3.4	2.2	28	490
KP1_2_2	29	51	150	42	3.7	2.4	28	510
KP1_2_3	33	53	140	48	4.2	2.6	29	500
KP1_2_4	35	69	190	71	4.5	3.2	43	650
KP1_2_5	30	57	140	45	4.9	2.4	28	590
KP1_2_6	29	45	150	55	4.1	2.1	27	570
KP1_2_7	28	50	150	57	3.6	2.6	26	530
KP1_2_8	31	49	150	44	3.9	2.4	25	480
KP1_2_11	29	75	110	59	6.3	3.1	35	740
KP1_2_18	42	57	160	45	5	2.5	38	680

<b>Sample</b>	<b>Mg</b>	<b>Al</b>	<b>K</b>	<b>Ti</b>	<b>Ga</b>	<b>Rb</b>	<b>Sr</b>	<b>Y</b>
KP1_2_19	36	66	190	49	5	2.6	40	700
KP1_2_20	30	47	150	37	4.6	2.4	32	590
KP9_2_2_1	15	15	79	58	3.4	1.9	23	560
KP9_2_2_2	16	19	160	60	3.3	2.2	21	570
KP9_2_2_3	20	16	180	65	3.7	2	25	650
KP9_2_2_4	20	19	140	50	3.5	1.9	28	600
KP9_2_2_5	20	22	200	52	3.4	2.3	23	610
KP9_2_2_6	18	24	130	53	3.9	2.2	23	580
KP9_2_2_7	21	23	150	45	3.8	1.9	21	510
KP9_2_2_8	19	24	140	66	2.6	1.9	21	490
KP9_2_2_9	19	26	150	57	3.1	1.7	21	560
KP9_2_2_10	21	25	110	61	2.8	1.9	21	480
KP9_2_2_11	21	27	160	53	4.9	2.1	24	570
KP9_2_2_12	22	29	170	60	3.6	2.1	22	540
KP9_2_2_13	24	26	170	62	4.1	1.6	24	540
KP9_2_2_14	24	28	140	71	3.2	2.1	24	670
KP9_2_2_15	24	22	140	81	4	1.4	23	630
KP9_2_2_16	17	20	140	71	3.3	1.9	17	440
KP9_2_2_17	24	19	140	85	3.4	1.8	23	620
KP9_2_2_18	23	20	190	94	4	1.5	24	670
KP9_2_2_19	23	18	130	76	3.4	1.9	24	590
KP9_2_2_20	24	20	160	89	4.1	1.6	24	640
KP9_2_2_21	30	22	150	84	3.9	1.6	24	690
KP9_2_2_22	18	17	75	82	3.4	2	21	570
KP9_2_2_23	23	18	150	91	3.3	1.5	21	660
KP9_2_2_24	20	15	160	87	3.9	1.6	20	560

<b>Sample</b>	<b>Mg</b>	<b>Al</b>	<b>K</b>	<b>Ti</b>	<b>Ga</b>	<b>Rb</b>	<b>Sr</b>	<b>Y</b>
KP9_2_2_25	42	30	66	84	2.9	1.9	35	640
KP9_2_2_26	23	13	85	95	4.2	1.9	22	690
KP9_2_2_27	22	15	140	88	3.9	2.1	20	540
KP9_2_2_28	22	17	130	89	2.8	1.6	21	600
KP9_2_2_29	19	18	120	79	3.2	1.6	22	630
KP9_2_2_30	25	17	170	100	3.7	1.9	22	600
KP9_2_2_31	22	18	160	91	3.5	1.9	19	650
KP9_2_2_32	20	18	130	91	3.6	1.9	18	560
KP9_2_2_33	24	21	170	110	4.1	2	22	660
KP9_2_2_34	21	21	150	110	3.7	1.6	21	560
KP9_2_2_35	19	23	150	110	3.9	1.8	22	600
KP9_2_2_36	21	24	150	110	3.7	2.1	24	740
KP9_2_2_37	28	26	170	110	3.6	1.6	21	690
KP9_2_2_38	22	23	120	87	3.3	2	22	530
KP9_2_2_39	22	35	150	87	3.4	1.8	25	650
KP9_2_2_40	20	32	170	84	4.3	2.3	25	590
KP9_2_2_41	25	28	170	65	3.9	2.2	25	650
KP9_2_2_42	20	24	160	53	3.8	2.1	21	500
Eud_LV01_1	16	26	110	130	2.5	0.56	280	65
Eud_LV01_2	21	24	85	120	2.8	0.76	280	67
Eud_LV01_3	16	26	89	110	2.4	0.4	210	54
Eud_LV01_4	16	28	95	130	2.1	0.55	220	64
Eud_LV01_5	18	26	95	120	2.3	0.71	300	61
Eud_LV01_6	16	29	96	170	2.6	0.66	330	79
Eud_LV01_7	19	26	110	96	2.9	0.66	270	64
Eud_LV01_8	15	22	88	110	2.1	0.5	230	56
Eud_LV01_9	16	25	95	97	2.4	0.48	250	64

<b>Sample</b>	<b>Mg</b>	<b>Al</b>	<b>K</b>	<b>Ti</b>	<b>Ga</b>	<b>Rb</b>	<b>Sr</b>	<b>Y</b>
Eud_LV01_10	16	24	75	130	2.2	0.57	220	55
Eud_LV01_11	15	30	87	110	2.1	0.63	250	65
Eud_LV01_12	19	56	100	120	2.5	0.62	290	64
Eud_LV01_13	21	26	93	120	2.8	0.66	310	70
Eud_LV01_14	21	27	100	140	3.1	0.72	310	71
Eud_LV01_15	22	30	110	140	3.6	0.59	400	82
Eud_LV01_16	20	28	89	140	3.1	0.62	270	69
Eud_LV01_17	17	23	100	150	3.2	0.59	380	78
Eud_LV01_18	19	28	120	130	3.4	0.69	380	72
 Eud_NK_1	8.5	50	200	41	2.9	1.7	19	430
Eud_NK_2	8.7	62	170	50	2.6	1.7	20	460
Eud_NK_3	8.2	56	160	42	2.7	1.7	21	500
Eud_NK_4	7.9	56	150	43	2.4	1.4	18	440
Eud_NK_5	9	50	120	46	2.9	1.7	19	470
Eud_NK_6	9.4	61	170	43	2.9	1.4	25	510
Eud_NK_7	6.7	65	220	43	3.1	1.8	18	470
Eud_NK_8	9.2	58	120	54	2.4	1.6	17	390
Eud_NK_9	9.4	53	200	42	3.2	1.6	21	490
Eud_NK_10	9	74	350	46	3.1	2.1	25	510
Eud_NK_11	9.2	55	170	40	2.2	1.8	18	450
Eud_NK_12	11	58	210	43	2.7	2.1	24	480
Eud_NK_13	9.8	84	160	43	2.7	1.8	22	560
Eud_NK_14	9.9	72	140	43	2.4	1.6	22	490
Eud_NK_15	8.9	75	220	40	3.4	1.9	24	470
Eud_NK_16	8.6	61	160	40	2.7	1.7	22	500
 KP1_2_1	19	15	190	52	6.4	1.8	30	420

<b>Sample</b>	<b>Mg</b>	<b>Al</b>	<b>K</b>	<b>Ti</b>	<b>Ga</b>	<b>Rb</b>	<b>Sr</b>	<b>Y</b>
KP1_2_2	14	20	130	72	5.4	1.4	40	430
KP1_2_3	20	24	150	72	7.3	1.7	42	640
KP1_2_4	17	18	140	86	6.7	1.8	35	460
KP1_2_5	18	18	100	80	5.6	1.7	36	400
KP1_2_6	18	19	130	78	5.8	1.6	35	410
KP1_2_7	20	22	150	86	5.5	1.5	41	510
KP1_2_8	14	19	140	92	6	1.5	30	470
KP1_2_9	18	19	130	78	5.9	1.5	37	450
KP1_2_10	18	22	120	92	6.1	1.7	35	470
KP1_2_11	18	18	190	58	6.9	2	38	560
KP1_2_12	19	16	160	78	5.7	1.5	37	520
KP1_2_13	17	19	150	92	6	1.7	39	470
KP1_2_14	21	26	160	73	7.6	1.9	33	500
KP1_2_15	23	23	160	93	6.7	1.8	37	550
KP1_2_16	19	23	150	87	6	1.8	39	530
KP1_2_17	25	22	190	110	5.9	2.1	42	530
KP1_2_18	19	21	150	84	6.4	2	33	560
KP1_2_19	21	21	99	55	6.8	2	42	600
KP1_2_20	17	17	130	58	6.5	1.9	34	510
KP1_2_21	16	23	250	55	6.8	2.1	35	490
KP1_2_22	19	18	170	69	8.1	2.2	47	730
KP1_2_23	20	21	160	69	6.2	1.8	39	550
KP1_2_24	17	20	160	70	6.8	1.8	39	530
KP1_2_25	19	21	160	79	5.9	1.6	37	450
KP1_2_26	21	22	150	94	6.3	1.6	41	500
KP1_2_27	17	17	170	90	5.8	1.6	37	490
KP1_2_28	18	20	160	73	5.6	1.8	37	530

<b>Sample</b>	<b>Mg</b>	<b>Al</b>	<b>K</b>	<b>Ti</b>	<b>Ga</b>	<b>Rb</b>	<b>Sr</b>	<b>Y</b>
KP1_2_29	19	17	170	62	6.3	1.8	35	550
KP1_2_30	14	13	150	55	6.7	1.7	36	540
CBD11_10_1	4	45	84	58	3.8	0.89	12	160
CBD11_10_2		290	150	38	3.5	1.1	9.2	180
CBD11_10_3	4.4	28	150	52	3	1.1	10	160
CBD11_10_4		29	190	32	3	1.1	8.1	170
CBD11_10_5	2.8	26	110	41	3	1.2	9	120
CBD11_10_6	3.4	24	110	32	2.8	1.1	8.8	120
CBD11_10_7	3.7	30	150	36	3.5	0.96	12	140
CBD11_10_8	3.3	30	200	43	3.4	1	8.8	150
CBD11_10_9		30	160	42	3.1	0.99	8.2	130
CBD11_10_10		27	130	39	3	1.1	7.5	120
CBD11_10_11	15	1700	260	100	3.7	1.1	23	370
CBD11_10_12		29	140	41	3.4	0.86	8.4	180
CBD11_10_13	3.4	350	81	37	3.3	0.86	10	160
CBD11_10_14	4.2	31	170	42	3.2	1	10	190
CBD11_10_15	3.4	35	150	32	3.5	0.77	10	180
CBD11_10_21		34	350	76	24	1.7	55	340
CBD11_10_22	4.5	34	200	63	22	1	28	280
CBD11_10_23	6.5	41	260	51	20	1.5	37	250
CBD11_10_25	7	34	170	77	15	1.2	27	190
CBD11_10_26	4.4	47	170	73	23	1.5	47	340
CBD11_10_29	8.7	61	230	98	25	2.2	46	510
CBD11_10_31	11	110	330	92	28	1.8	46	440

<b>Sample</b>	<b>Nb</b> <i>ppm</i>	<b>Mo</b> <i>ppm</i>	<b>Sn</b> <i>ppm</i>	<b>Sb</b> <i>ppm</i>	<b>Ba</b> <i>ppm</i>	<b>La</b> <i>ppm</i>	<b>Ce</b> <i>ppm</i>	<b>Pr</b> <i>ppm</i>
Eud_LV01_1	91	0.89	2.7		15	75	140	17
Eud_LV01_2	71	1	2.1	0.41	18	62	110	11
Eud_LV01_3	85	1.1	2.5		17	76	150	16
Eud_LV01_4	90	0.99	2.7	0.3	16	83	170	17
Eud_LV01_5	140	1.1	4.1	0.53	16	92	170	19
Eud_LV01_6	91	0.91	2		17	86	130	17
Eud_LV01_7	230	1.2	2.8	0.26	24	110	160	16
Eud_LV01_8	140	1.5	3		20	98	160	14
Eud_LV01_9	86	0.82	2.5	0.44	17	72	140	15
Eud_LV01_10	95	1.2	2	0.5	18	89	160	15
Eud_LV01_11	85	1.3	2.8		18	77	140	14
Eud_LV01_12	84	1.1	2.2	0.33	15	61	130	13
Eud_LV01_13	170	1.3	2.6	0.29	24	120	220	17
Eud_LV01_14	150	1.3	2.8		24	110	200	19
Eud_LV01_15	110	0.92	2.5	0.26	15	89	170	16
Eud_LV01_16	100	0.97	2.4		18	98	190	16
Eud_LV01_17	110	1	2.5	0.32	18	84	180	17
Eud_LV01_18	91	0.98	2.7	0.28	18	85	150	16
<hr/>								
Eud_NK_1	86	0.35	5.2	0.37	18	88	140	21
Eud_NK_2	100	0.59	4	0.38	20	98	210	24
Eud_NK_3	83	0.59	5	0.38	21	87	190	22
Eud_NK_4	110	0.46	5.7	0.35	20	110	220	28
Eud_NK_5	97	0.38	4.4		20	90	160	19
Eud_NK_6	110	0.38	5	0.35	23	110	200	23

<b>Sample</b>	<b>Nb</b>	<b>Mo</b>	<b>Sn</b>	<b>Sb</b>	<b>Ba</b>	<b>La</b>	<b>Ce</b>	<b>Pr</b>
Eud_NK_7	88	0.46	4.3		20	90	160	19
Eud_NK_8	100	0.41	4.6		21	95	180	22
Eud_NK_9	93	0.47	4.9		17	92	200	22
Eud_NK_10	110	0.47	5	0.4	21	100	190	23
Eud_NK_11	91	0.43	5.6	0.28	20	93	200	22
Eud_NK_12	86	0.48	4.7	0.32	21	82	170	19
Eud_NK_13	91	0.51	4.8		17	92	180	18
Eud_NK_14	95	0.46	5.1	0.35	20	84	200	20
Eud_NK_15	110	0.43	5.7	0.31	21	110	210	26
Eud_NK_16	82	0.58	5		19	90	160	17
Eud_NK_17	100	0.52	5.1	0.27	19	100	200	24
Eud_NK_18	110	0.5	5.1	0.24	22	99	220	26
CBD11_02_1	21	0.84	7.8		26	36	96	11
CBD11_02_2	32	0.92	9.2		29	33	100	9.5
CBD11_02_3	24	0.81	12		27	31	81	8.6
CBD11_02_4	22	0.64	6.9		29	34	83	11
CBD11_02_5	80	0.66	7.3		34	61	130	15
CBD11_02_6	28	1.3	7.2		26	40	91	11
CBD11_02_7	21	0.86	9.6		24	35	85	8.6
CBD11_02_8	32	0.81	6.2		31	47	100	12
CBD11_02_9	95	0.63	6.5		28	73	120	13
CBD11_02_10	20	0.8	8.1		28	30	74	10
CBD11_02_11	40	0.33	4.7		22	39	78	8.5
CBD11_02_12	36	0.79	3.1		33	41	89	11
CBD11_02_13	30	0.93	4		29	36	75	9.1

<b>Sample</b>	<b>Nb</b>	<b>Mo</b>	<b>Sn</b>	<b>Sb</b>	<b>Ba</b>	<b>La</b>	<b>Ce</b>	<b>Pr</b>
CBD11_02_16	45	0.86	5.3		28	45	84	10
CBD11_02_17	40	1	4.9		32	42	95	10
CBD11_02_18	74	1.5	4.3		43	84	170	17
CBD11_02_19	45	0.82	2.7		31	49	89	11
CBD11_02_20	49	0.91	2.8		25	48	92	12
CBD11_02_21	49	0.32	5.5		28	52	100	11
CBD11_02_22	40	0.88	2.6		29	42	98	11
CBD11_02_23	52	0.72	4.8		36	43	110	13
CBD11_02_24	29	0.87	3.8		26	30	77	11
CBD11_02_25	28	0.89	3.6		24	42	100	11
CBD11_02_26	31	0.88	5.5		35	34	99	14
CBD11_02_27	33	0.78	3.3		30	34	71	10
CBD11_02_28	28	0.74	3.4	0.62	27	35	80	8.4
CBD11_02_29	38	0.78	4.4		23	39	91	12
CBD11_02_30	40	0.68	2.6		30	37	86	10
KP1_2_1	100	1.3	4.5	0.26	36	64	81	7.9
KP1_2_2	94	1.5	5.3		27	66	76	7.7
KP1_2_3	81	0.86	5.2		29	64	83	7.9
KP1_2_4	94	1	7.5		33	76	110	11
KP1_2_5	77	0.96	6.1	0.39	33	57	100	9.2
KP1_2_6	75	0.94	5.9	0.41	26	50	77	7.8
KP1_2_7	80	0.81	5.7	0.44	28	52	82	8.4
KP1_2_8	86	1.3	5.5	0.42	30	57	85	9.2
KP1_2_11	140	1.7	6.8	0.35	32	110	370	19
KP1_2_18	150	1.5	5.6	0.34	36	93	120	12

<b>Sample</b>	<b>Nb</b>	<b>Mo</b>	<b>Sn</b>	<b>Sb</b>	<b>Ba</b>	<b>La</b>	<b>Ce</b>	<b>Pr</b>
KP1_2_19	210	1.3	6.9		32	110	150	15
KP1_2_20	170	1.2	5.4		27	97	130	12
KP9_2_2_1	110	1	9.6		27	110	170	19
KP9_2_2_2	110	1.1	18		27	96	170	15
KP9_2_2_3	120	1	13		30	110	170	19
KP9_2_2_4	120	1.1	4.9		29	110	170	15
KP9_2_2_5	92	1.2	6		26	97	150	17
KP9_2_2_6	82	1.3	5.7	0.33	27	88	160	16
KP9_2_2_7	79	0.97	5.3		22	82	120	13
KP9_2_2_8	89	1	4.4		22	80	130	15
KP9_2_2_9	70	0.98	6.4		26	84	140	15
KP9_2_2_10	75	0.88	6		23	75	130	12
KP9_2_2_11	120	1	8.5		28	110	170	19
KP9_2_2_12	81	0.57	8.2	0.31	27	73	150	14
KP9_2_2_13	100	0.47	7.1		27	94	140	15
KP9_2_2_14	100	0.55	8.3	0.25	28	92	140	17
KP9_2_2_15	83	0.62	6.3		22	80	130	13
KP9_2_2_16	88	0.42	6.9		23	53	92	13
KP9_2_2_17	90	0.56	8.2		22	76	120	14
KP9_2_2_18	120	0.66	7.3		26	84	140	14
KP9_2_2_19	99	0.57	7.2	0.26	24	80	130	14
KP9_2_2_20	110	0.61	7.8		30	81	140	14
KP9_2_2_21	91	0.51	7.9	0.31	28	79	130	16
KP9_2_2_22	78	0.55	7.2		25	67	120	11
KP9_2_2_23	91	0.56	6.2		24	76	120	11
KP9_2_2_24	95	0.44	5.8	0.25	25	82	140	12

<b>Sample</b>	<b>Nb</b>	<b>Mo</b>	<b>Sn</b>	<b>Sb</b>	<b>Ba</b>	<b>La</b>	<b>Ce</b>	<b>Pr</b>
KP9_2_2_25	110	0.47	8.7	0.27	30	98	130	20
KP9_2_2_26	98	0.53	7.3	0.27	24	72	150	16
KP9_2_2_27	78	0.44	7.9		24	72	110	12
KP9_2_2_28	69	0.39	7.8	0.27	21	73	110	9.5
KP9_2_2_29	74	0.38	7.1	0.28	23	68	110	14
KP9_2_2_30	72	0.57	9.4	0.31	31	83	110	12
KP9_2_2_31	68	0.48	8.2		22	72	100	11
KP9_2_2_32	68	0.62	7.5		24	78	84	11
KP9_2_2_33	98	0.61	8.4	0.35	27	84	120	14
KP9_2_2_34	71	0.64	8		22	67	100	12
KP9_2_2_35	71	0.53	9.5		28	65	110	13
KP9_2_2_36	56	0.51	8.6		28	67	120	12
KP9_2_2_37	67	0.66	7.7	0.33	30	68	110	14
KP9_2_2_38	120	0.6	8.4		25	96	120	13
KP9_2_2_39	80	0.77	6.7		29	80	120	16
KP9_2_2_40	120	0.65	7.9		33	99	150	16
KP9_2_2_41	150	1.1	4.5		31	130	170	19
KP9_2_2_42	120	1.3	6.4		24	93	120	14
Eud_LV01_1	150	1.4	3.1	0.27	18	90	160	17
Eud_LV01_2	140	1.3	2.6		21	92	170	16
Eud_LV01_3	79	1	2.4	0.28	16	81	140	16
Eud_LV01_4	92	0.87	2.4	0.21	16	77	160	16
Eud_LV01_5	190	1.3	2.7	0.49	16	91	160	16
Eud_LV01_6	150	1.4	2.8		21	110	210	22
Eud_LV01_7	180	1.3	2.8	0.3	21	110	160	18
Eud_LV01_8	96	0.96	2.5	0.26	18	80	140	14
Eud_LV01_9	83	1.2	2.3	0.22	18	90	150	15

<b>Sample</b>	<b>Nb</b>	<b>Mo</b>	<b>Sn</b>	<b>Sb</b>	<b>Ba</b>	<b>La</b>	<b>Ce</b>	<b>Pr</b>
Eud_LV01_10	83	1	2.2		18	66	140	16
Eud_LV01_11	91	1	2		17	82	160	13
Eud_LV01_12	130	1.1	2.7	0.4	19	84	160	17
Eud_LV01_13	160	1.5	2.8	0.21	24	99	210	17
Eud_LV01_14	160	1.5	2.3	0.21	23	100	190	19
Eud_LV01_15	180	1.3	2.8		22	120	220	21
Eud_LV01_16	160	1.1	2.6	0.22	22	88	170	20
Eud_LV01_17	170	1.6	2.9	0.18	21	110	230	21
Eud_LV01_18	160	1.6	2.8	0.21	23	110	210	18
Eud_NK_1	92	0.45	4.8	0.26	19	81	180	20
Eud_NK_2	100	0.41	4.8	0.3	19	89	170	20
Eud_NK_3	100	0.54	4.9	0.34	19	100	230	23
Eud_NK_4	110	0.48	5	0.28	22	110	240	25
Eud_NK_5	110	0.62	5.6	0.29	16	120	220	21
Eud_NK_6	120	0.48	5.2		21	110	230	28
Eud_NK_7	110	0.47	5.6	0.2	22	110	190	22
Eud_NK_8	99	0.43	4.8	0.33	17	77	170	20
Eud_NK_9	120	0.49	5		19	100	190	25
Eud_NK_10	120	0.44	4.2	0.25	23	120	260	27
Eud_NK_11	97	0.59	4.9	0.23	20	93	180	23
Eud_NK_12	120	0.54	4.5	0.23	18	110	220	26
Eud_NK_13	110	0.55	6	0.22	20	120	240	28
Eud_NK_14	120	0.44	5.3	0.22	23	120	230	26
Eud_NK_15	140	0.51	4.7	0.19	23	130	240	31
Eud_NK_16	110	0.56	4	0.21	20	120	170	24
KP1_2_1	59	1.2	7.7	0.28	50	79	130	13

<b>Sample</b>	<b>Nb</b>	<b>Mo</b>	<b>Sn</b>	<b>Sb</b>	<b>Ba</b>	<b>La</b>	<b>Ce</b>	<b>Pr</b>
KP1_2_2	100	0.87	3.6	0.28	44	100	160	14
KP1_2_3	120	0.92	2.6	0.34	56	110	170	18
KP1_2_4	88	0.61	2.3	0.35	48	84	130	13
KP1_2_5	91	0.83	2.5	0.28	42	87	110	13
KP1_2_6	95	0.71	2.9	0.31	45	97	120	12
KP1_2_7	110	0.74	2.9	0.33	51	95	140	18
KP1_2_8	75	0.91	3.1	0.31	40	71	120	12
KP1_2_9	95	0.64	2.4	0.31	45	100	160	15
KP1_2_10	110	0.67	3	0.29	44	100	130	15
KP1_2_11	110	1.4	3.2		56	110	140	15
KP1_2_12	110	0.97	2.8	0.29	48	100	150	14
KP1_2_13	120	0.69	2.9	0.31	48	130	150	15
KP1_2_14	130	0.9	3.9	0.44	46	110	130	16
KP1_2_15	100	0.93	3.5	0.34	37	110	170	15
KP1_2_16	120	0.86	3.2	0.35	53	120	160	14
KP1_2_17	120	1.1	2.5		50	120	180	15
KP1_2_18	59	1.6	1.9		50	81	110	13
KP1_2_19	98	1	2.3		57	130	150	17
KP1_2_20	86	1.3	7.1	0.34	52	89	160	14
KP1_2_21	88	1.3	4.8		58	100	160	16
KP1_2_22	110	1.5	7.9	0.28	65	120	180	20
KP1_2_23	130	0.82	3.3	0.37	53	130	180	14
KP1_2_24	95	0.97	2.7	0.31	51	120	170	13
KP1_2_25	100	0.88	2.8	0.38	41	96	130	13
KP1_2_26	130	0.8	3.5	0.32	50	120	170	18
KP1_2_27	110	0.83	3.3	0.28	44	92	140	15
KP1_2_28	120	1.1	3.8	0.31	51	110	140	15

<b>Sample</b>	<b>Nb</b>	<b>Mo</b>	<b>Sn</b>	<b>Sb</b>	<b>Ba</b>	<b>La</b>	<b>Ce</b>	<b>Pr</b>
KP1_2_29	100	1.1	4.7	0.33	48	100	160	16
KP1_2_30	91	1.4	5.7	0.27	52	100	150	14
CBD11_10_1	58	0.31	5.6		32	48	90	7.9
CBD11_10_2	54	1.2	2.9		27	44	100	13
CBD11_10_3	70	0.37	4		26	49	86	12
CBD11_10_4	29	2.1	3.3		24	38	100	12
CBD11_10_5	54	0.49	4.5	0.2	21	40	79	11
CBD11_10_6	45	1	2.5		20	36	75	8.8
CBD11_10_7	71	1.1	3.3		25	61	110	13
CBD11_10_8	60	0.92	3.1		24	45	95	9.2
CBD11_10_9	31	0.85	2.3		26	38	90	13
CBD11_10_10	30	0.96	3		21	26	66	8.4
CBD11_10_11	110	0.3	6.5		47	82	160	17
CBD11_10_12	24	1.3	4.6		26	31	77	11
CBD11_10_13	45	1.1	2.2		25	43	100	11
CBD11_10_14	50	1.2	2.6		24	46	96	12
CBD11_10_15	51	1.1	2.3		24	44	110	10
CBD11_10_21	180	2.5	2.6		280	240	410	36
CBD11_10_22	64	3.1	6.9	0.3	150	140	290	32
CBD11_10_23	92	1.6	3.1		140	170	310	27
CBD11_10_25	120	1.8	3	0.33	190	160	310	31
CBD11_10_26	130	1.7	4.6		180	230	330	44
CBD11_10_29	170	1.8	4.3		230	230	510	56
CBD11_10_31	170	1.2	14		200	260	520	50

<b>Sample</b>	<b>Nd</b> <i>ppm</i>	<b>Sm</b> <i>ppm</i>	<b>Eu</b> <i>ppm</i>	<b>Gd</b> <i>ppm</i>	<b>Tb</b> <i>ppm</i>	<b>Dy</b> <i>ppm</i>	<b>Ho</b> <i>ppm</i>	<b>Er</b> <i>ppm</i>
Eud_LV01_1	49	9.7	3.9	12	2.4	17	3	9
Eud_LV01_2	40	9.1	3.8	12	2.2	12	2.2	7.8
Eud_LV01_3	52	10	3.8	13	2.5	13	2.9	6.6
Eud_LV01_4	51	10	4.8	14	2	12	3.2	8.3
Eud_LV01_5	61	13	5.4	16	2.7	14	2.9	8.8
Eud_LV01_6	54	11	5.2	13	2.4	12	2.8	7.6
Eud_LV01_7	46	8.6	4.4	15	2.6	13	2.7	7.6
Eud_LV01_8	53	11	3.8	14	2.3	15	3.5	8.3
Eud_LV01_9	48	9.6	4.2	11	2.4	12	3.1	7.1
Eud_LV01_10	55	11	4.5	15	2.3	16	2.6	8.2
Eud_LV01_11	52	10	4.2	13	2.6	14	3.4	8.3
Eud_LV01_12	44	9	4.1	14	2.3	15	3	7.7
Eud_LV01_13	57	11	4.3	15	2.6	15	3.5	8.8
Eud_LV01_14	61	12	4	13	2.2	15	3.3	9.5
Eud_LV01_15	54	11	4.7	17	2.2	13	3.4	8.5
Eud_LV01_16	59	12	5.3	15	2.9	20	3	9.4
Eud_LV01_17	55	11	4.4	14	2.4	14	2.9	8.3
Eud_LV01_18	51	10	5.6	11	2.7	13	2.9	8.9
Eud_NK_1	78	24	4.3	39	8.1	58	15	44
Eud_NK_2	93	31	5.5	43	9.9	67	17	51
Eud_NK_3	83	23	4.1	43	9.3	57	15	39
Eud_NK_4	110	33	5.3	41	8.7	70	17	54
Eud_NK_5	69	22	4.2	35	7.2	52	14	43
Eud_NK_6	99	30	5.7	49	9.1	75	17	43

<b>Sample</b>	<b>Nd</b>	<b>Sm</b>	<b>Eu</b>	<b>Gd</b>	<b>Tb</b>	<b>Dy</b>	<b>Ho</b>	<b>Er</b>
Eud_NK_7	82	24	4.4	38	8.3	57	13	48
Eud_NK_8	88	26	5.8	42	8.8	72	14	44
Eud_NK_9	83	25	4.8	40	7.7	64	14	43
Eud_NK_10	87	27	5.1	41	10	66	16	43
Eud_NK_11	83	26	4.9	45	8.5	56	17	53
Eud_NK_12	66	22	4.3	35	7.8	57	13	39
Eud_NK_13	80	25	4.8	40	8.5	60	15	50
Eud_NK_14	79	25	5.3	40	8.1	59	13	43
Eud_NK_15	98	31	5.2	50	8.8	69	15	51
Eud_NK_16	70	22	5.5	35	8.4	59	15	40
Eud_NK_17	86	27	5	42	8.4	65	14	42
Eud_NK_18	96	30	5.2	44	9.2	64	16	54
CBD11_02_1	41	12	3.3	22	4.4	26	7.1	19
CBD11_02_2	45	15	3.2	22	5.1	31	7.5	20
CBD11_02_3	39	13	2.4	22	4.6	32	5.6	20
CBD11_02_4	46	14	2.6	29	5.3	33	8	25
CBD11_02_5	52	15	3	26	4.2	37	9	22
CBD11_02_6	47	15	3.2	24	5.4	35	7.9	22
CBD11_02_7	39	14	2.8	21	4.7	31	8.3	20
CBD11_02_8	46	13	2.9	24	4.6	32	7.7	22
CBD11_02_9	41	12	3.4	22	4.5	30	6.4	17
CBD11_02_10	35	12	3.3	26	4.5	26	7.3	16
CBD11_02_11	31	10	2.4	16	2.9	20	5.2	18
CBD11_02_12	40	13	2.8	21	4.2	28	6.3	17
CBD11_02_13	38	11	2.9	21	4.9	28	6	21

<b>Sample</b>	<b>Nd</b>	<b>Sm</b>	<b>Eu</b>	<b>Gd</b>	<b>Tb</b>	<b>Dy</b>	<b>Ho</b>	<b>Er</b>
CBD11_02_16	39	13	2.7	17	4.3	27	6.6	16
CBD11_02_17	43	12	2.7	22	3.7	25	5.7	18
CBD11_02_18	69	21	5.1	34	6.4	44	8.7	35
CBD11_02_19	50	16	3.1	26	4.6	29	7.7	21
CBD11_02_20	50	14	3.3	22	3.3	29	8	19
CBD11_02_21	46	14	2.6	22	4.8	32	7.1	22
CBD11_02_22	43	14	2.8	24	4.6	26	7.6	18
CBD11_02_23	65	19	3.4	26	6.1	33	7.3	22
CBD11_02_24	43	13	3.5	27	4.8	30	6.2	16
CBD11_02_25	55	14	3.1	18	5.3	34	6.7	17
CBD11_02_26	61	18	3.4	29	4.9	34	7.7	22
CBD11_02_27	35	10	2.9	19	4.6	28	5.5	16
CBD11_02_28	42	13	2.8	17	4.4	29	7.2	20
CBD11_02_29	48	13	2.8	24	4.9	28	5.9	18
CBD11_02_30	43	12	2.8	21	4.1	31	6.1	19
KP1_2_1	31	12	3.4	26	8	79	18	73
KP1_2_2	33	12	3.3	26	8.4	73	20	66
KP1_2_3	33	14	3.3	30	9.2	71	21	66
KP1_2_4	38	15	3.9	34	8.5	85	25	87
KP1_2_5	33	13	3.6	29	7.1	69	19	81
KP1_2_6	30	13	3.4	27	8.5	67	20	81
KP1_2_7	34	13	3.2	28	7.4	68	20	75
KP1_2_8	29	11	3.3	28	7.8	61	18	65
KP1_2_11	67	20	4.5	32	9.9	98	28	100
KP1_2_18	42	15	3.2	34	8.4	97	25	84

<b>Sample</b>	<b>Nd</b>	<b>Sm</b>	<b>Eu</b>	<b>Gd</b>	<b>Tb</b>	<b>Dy</b>	<b>Ho</b>	<b>Er</b>
KP1_2_19	46	16	3.5	32	10	85	24	91
KP1_2_20	34	11	3.3	27	7.7	59	20	76
KP9_2_2_1	68	20	4.5	35	10	83	21	81
KP9_2_2_2	55	17	4	35	8.6	77	21	72
KP9_2_2_3	70	22	3.4	41	10	81	24	86
KP9_2_2_4	61	20	3.9	37	9.5	92	22	96
KP9_2_2_5	64	19	3.6	36	9.9	86	24	80
KP9_2_2_6	62	19	3.8	34	7.9	92	21	85
KP9_2_2_7	49	16	3.5	33	8.9	68	20	67
KP9_2_2_8	55	18	4.2	36	8.4	80	25	85
KP9_2_2_9	50	18	3.8	34	8.4	71	22	76
KP9_2_2_10	47	16	4.1	31	9	67	17	72
KP9_2_2_11	64	20	4	44	9.7	84	22	73
KP9_2_2_12	47	15	3.3	25	7.3	69	20	75
KP9_2_2_13	57	18	4.5	27	9.8	82	23	85
KP9_2_2_14	62	19	5.1	36	10	92	29	86
KP9_2_2_15	52	19	4.8	41	10	84	23	90
KP9_2_2_16	38	14	3.5	31	9.1	70	22	73
KP9_2_2_17	44	15	3.3	33	7.6	84	24	80
KP9_2_2_18	52	19	4.1	37	9.5	100	25	86
KP9_2_2_19	47	16	3.7	32	10	74	24	84
KP9_2_2_20	47	15	4.4	32	8	89	28	88
KP9_2_2_21	54	18	3.9	37	11	99	23	100
KP9_2_2_22	44	16	3.3	36	9.8	92	24	83
KP9_2_2_23	43	15	4.6	30	9.3	87	24	74
KP9_2_2_24	51	17	4.2	37	11	92	24	83

<b>Sample</b>	<b>Nd</b>	<b>Sm</b>	<b>Eu</b>	<b>Gd</b>	<b>Tb</b>	<b>Dy</b>	<b>Ho</b>	<b>Er</b>
KP9_2_2_25	77	23	4.6	50	10	100	29	89
KP9_2_2_26	59	20	3.6	39	11	95	21	89
KP9_2_2_27	37	14	3.7	33	8.3	88	20	71
KP9_2_2_28	42	15	3.6	30	8.7	88	24	78
KP9_2_2_29	47	18	4.1	42	11	100	25	85
KP9_2_2_30	50	18	3.8	41	10	89	27	89
KP9_2_2_31	44	15	4.3	40	9.4	81	24	70
KP9_2_2_32	38	15	3.7	34	11	84	24	72
KP9_2_2_33	47	16	4.2	33	11	94	22	75
KP9_2_2_34	43	15	3.9	43	8.9	84	23	73
KP9_2_2_35	47	18	4.8	38	9.7	97	25	87
KP9_2_2_36	47	17	5.3	43	11	94	25	87
KP9_2_2_37	50	19	4.3	46	11	92	25	91
KP9_2_2_38	47	14	3.6	38	9.9	70	20	81
KP9_2_2_39	48	17	4.3	40	9.9	85	23	77
KP9_2_2_40	57	18	4.1	35	9.8	81	22	92
KP9_2_2_41	54	19	4.7	36	11	79	25	73
KP9_2_2_42	48	17	3.8	38	8.7	82	19	78
Eud_LV01_1	58	11	4.9	15	2.4	16	3	8.4
Eud_LV01_2	61	13	4.2	14	2.7	14	3.2	8.9
Eud_LV01_3	44	9.1	4.3	11	2.1	14	3.1	8.1
Eud_LV01_4	51	10	4.8	13	2.4	13	2.8	8
Eud_LV01_5	47	9.5	5.3	13	2.7	15	3.2	8.7
Eud_LV01_6	67	13	5.9	16	2.6	18	3.3	11
Eud_LV01_7	51	12	5.1	15	2.4	14	3.2	8.8
Eud_LV01_8	49	11	4.8	14	2.2	13	3.3	8.6
Eud_LV01_9	51	10	4.7	16	2.6	13	3.2	7

<b>Sample</b>	<b>Nd</b>	<b>Sm</b>	<b>Eu</b>	<b>Gd</b>	<b>Tb</b>	<b>Dy</b>	<b>Ho</b>	<b>Er</b>
Eud_LV01_10	47	9.3	4.2	14	2.3	14	2.8	8.4
Eud_LV01_11	48	9.3	4.1	13	2.1	13	3	9
Eud_LV01_12	51	11	5	15	2.1	12	2.9	8.3
Eud_LV01_13	58	12	5.1	16	2.7	16	3	8.8
Eud_LV01_14	60	11	5.9	17	2.6	15	3.7	9
Eud_LV01_15	69	14	5.7	17	2.7	14	3.6	10
Eud_LV01_16	55	13	4.6	17	2.3	15	2.9	9.5
Eud_LV01_17	68	14	5.7	18	3	20	3.2	12
Eud_LV01_18	68	14	5.4	20	3	16	4.2	11
<hr/>								
Eud_NK_1	84	25	4.9	46	8.3	63	16	48
Eud_NK_2	90	24	5	41	9.7	68	14	50
Eud_NK_3	97	32	6.3	53	9.6	76	15	49
Eud_NK_4	98	30	5.1	45	10	73	17	63
Eud_NK_5	92	30	6.7	44	11	67	18	49
Eud_NK_6	110	33	5.6	46	11	66	18	54
Eud_NK_7	96	30	4.7	53	9.4	71	16	56
Eud_NK_8	71	23	4.7	43	8.5	64	15	46
Eud_NK_9	91	29	4.8	45	9.5	68	17	48
Eud_NK_10	110	34	5.5	51	11	75	17	63
Eud_NK_11	77	24	4.6	44	9	55	14	48
Eud_NK_12	100	31	5.1	54	11	76	17	51
Eud_NK_13	110	37	5.7	50	10	81	19	65
Eud_NK_14	98	31	5.9	49	9.9	73	16	49
Eud_NK_15	110	37	6.2	50	12	86	21	65
Eud_NK_16	88	28	5.8	39	10	69	18	50
<hr/>								
KP1_2_1	45	14	3.9	30	7.2	64	16	56

<b>Sample</b>	<b>Nd</b>	<b>Sm</b>	<b>Eu</b>	<b>Gd</b>	<b>Tb</b>	<b>Dy</b>	<b>Ho</b>	<b>Er</b>
KP1_2_2	53	15	4.6	30	7.4	62	16	58
KP1_2_3	63	19	4.2	32	8.8	70	19	73
KP1_2_4	45	15	3.9	29	7.5	54	17	58
KP1_2_5	40	13	3.1	26	6.9	55	17	54
KP1_2_6	45	15	3.3	29	7.3	59	15	55
KP1_2_7	50	17	4	29	7.9	69	19	72
KP1_2_8	40	15	3.6	26	6.9	56	14	60
KP1_2_9	46	14	4	29	7.7	62	17	65
KP1_2_10	50	17	3.8	28	7.6	66	16	66
KP1_2_11	59	19	4.1	41	8.4	76	24	76
KP1_2_12	52	15	3.9	24	6.7	61	18	72
KP1_2_13	47	15	3.8	29	7.4	60	16	68
KP1_2_14	50	16	4.4	35	6.7	62	18	66
KP1_2_15	50	15	4.1	27	8.1	56	18	59
KP1_2_16	55	18	3.9	36	8.9	64	20	66
KP1_2_17	52	16	4.2	35	7.5	71	18	74
KP1_2_18	52	17	4.1	35	8	69	20	84
KP1_2_19	58	17	3.9	35	8.6	67	22	69
KP1_2_20	48	16	3.3	31	8.1	62	19	67
KP1_2_21	55	19	3.6	33	9.5	75	20	71
KP1_2_22	70	23	3.9	42	12	89	24	91
KP1_2_23	61	19	4.6	36	11	86	18	75
KP1_2_24	56	17	3.7	26	8.6	68	17	66
KP1_2_25	50	16	3.7	27	6.7	60	18	71
KP1_2_26	61	18	3.9	35	9.1	72	18	77
KP1_2_27	48	15	4.1	30	7	58	18	63
KP1_2_28	56	16	3.9	33	7.8	66	18	62

<b>Sample</b>	<b>Nd</b>	<b>Sm</b>	<b>Eu</b>	<b>Gd</b>	<b>Tb</b>	<b>Dy</b>	<b>Ho</b>	<b>Er</b>
KP1_2_29	55	18	3.9	29	7.9	65	18	69
KP1_2_30	53	15	3.6	26	7.6	73	17	71
CBD11_10_1	33	10	3	19	4.2	30	6.2	20
CBD11_10_2	51	15	3.5	23	4.5	32	6.7	19
CBD11_10_3	32	11	3.5	17	3.8	24	6.9	19
CBD11_10_4	53	15	3.5	26	4.3	31	7.3	19
CBD11_10_5	39	11	2.6	21	4.2	28	6.1	18
CBD11_10_6	37	11	3.6	21	3.4	20	4.9	13
CBD11_10_7	52	15	3.3	20	3.9	27	5.7	17
CBD11_10_8	44	13	2.9	21	4.1	32	7	17
CBD11_10_9	50	14	3	22	3.5	25	7.5	15
CBD11_10_10	27	9	2.7	20	3.8	23	6.3	19
CBD11_10_11	75	24	4.2	41	9	62	15	40
CBD11_10_12	43	14	3.2	27	4.6	27	7.6	18
CBD11_10_13	48	16	3.3	25	5.6	30	7.8	19
CBD11_10_14	50	15	3	28	4.7	35	7	19
CBD11_10_15	50	15	3.6	26	4.7	34	9	21
CBD11_10_21	160	40	7	60	11	69	15	44
CBD11_10_22	130	35	6.8	42	8.7	61	18	48
CBD11_10_23	110	31	4.7	39	8.6	70	12	40
CBD11_10_25	130	37	8.3	48	9	71	16	45
CBD11_10_26	150	35	6.1	46	8.8	56	17	58
CBD11_10_29	220	54	10	64	11	93	21	55
CBD11_10_31	190	52	9.7	77	14	91	22	63

<b>Sample</b>	<b>Tm</b> <i>ppm</i>	<b>Yb</b> <i>ppm</i>	<b>Lu</b> <i>ppm</i>	<b>Hf</b> <i>ppm</i>	<b>Ta</b> <i>ppm</i>	<b>W</b> <i>ppm</i>	<b>Pb</b> <i>ppm</i>	<b>Th</b> <i>ppm</i>
Eud_LV01_1	1.4	8	1.3	50	12	6.2	0.99	1.1
Eud_LV01_2	1.5	7.5	1.3	45	8.7	4.7	1.3	1.3
Eud_LV01_3	1.5	8.7	1.4	49	11	5	0.95	1.2
Eud_LV01_4	1.3	8.5	1.2	53	9.2	6	1	1.3
Eud_LV01_5	1.6	8.8	1.4	51	11	8.1	13	13
Eud_LV01_6	1.5	10	1.3	51	10	4.8	1.1	1.1
Eud_LV01_7	1.5	8.4	1.7	40	17	12	1.3	1.3
Eud_LV01_8	1.4	8.7	1.6	40	12	7.1	1.5	1.3
Eud_LV01_9	1.4	7.2	1.1	48	12	5.3	1.1	1.6
Eud_LV01_10	1.7	7.2	1.5	53	11	5.3	2.7	2.3
Eud_LV01_11	1.3	8.5	1.5	52	11	4.2	2	1.2
Eud_LV01_12	1.5	7.9	1.4	51	8.8	4.7	4.4	0.8
Eud_LV01_13	1.4	9.4	1.4	52	20	8.9	2.1	1.2
Eud_LV01_14	1.5	8.9	1.6	52	16	8.8	1.9	1.4
Eud_LV01_15	1.7	9.4	1.3	58	12	5.1	1.4	1.3
Eud_LV01_16	1.5	11	1.5	58	12	5.4	1.3	1.2
Eud_LV01_17	1.4	8.5	1.5	56	11	4.4	4.3	1.4
Eud_LV01_18	1.6	8.7	1.6	49	11	4.9	1.2	1.2
Eud_NK_1	5.6	48	6.3	58	5	1.7	67	0.85
Eud_NK_2	8	53	8.1	58	5.2	2.2	48	0.98
Eud_NK_3	6.1	48	6.7	57	6	1.9	15	1
Eud_NK_4	9.1	55	7.8	80	6.4	2.3	22	0.92
Eud_NK_5	7.2	45	5.8	45	4.8	1.8	8	1
Eud_NK_6	8.5	55	6.5	61	5.4	1.7	6.6	0.96

<b>Sample</b>	<b>Tm</b>	<b>Yb</b>	<b>Lu</b>	<b>Hf</b>	<b>Ta</b>	<b>W</b>	<b>Pb</b>	<b>Th</b>
Eud_NK_7	6.5	44	7.1	54	5.1	2.1	32	1
Eud_NK_8	6	51	6.6	58	5.5	2.1	9	0.87
Eud_NK_9	6.7	44	6.3	56	4.6	1.7	6.3	0.88
Eud_NK_10	8.1	52	6.2	61	5.4	2.1	6.1	0.99
Eud_NK_11	7.1	48	6.4	53	6.1	2	6	1.1
Eud_NK_12	6.8	40	6.4	58	4.6	1.4	5.9	1.1
Eud_NK_13	7.1	50	6.2	52	4.9	2.1	6.4	1.2
Eud_NK_14	7.2	48	6.4	51	4.7	2.3	7.1	1
Eud_NK_15	8.7	56	8	68	6.4	1.8	84	1.1
Eud_NK_16	7.3	43	5.9	52	4.9	1.8	5.6	1.1
Eud_NK_17	7.5	54	6.3	55	6.2	1.7	6.9	1
Eud_NK_18	8.7	61	7.7	63	6	2.3	6.6	0.94
CBD11_02_1	3.3	21	2.4	54	3.9	1.7	0.55	0.66
CBD11_02_2	3.3	22	2.9	48	4.8	2.9	0.64	1.3
CBD11_02_3	3	19	2.1	47	3.3	2	0.56	0.93
CBD11_02_4	3.2	19	2.9	50	3	1.9	0.54	0.88
CBD11_02_5	3.4	23	2.7	57	5.1	3.8	0.8	0.78
CBD11_02_6	3.3	20	3	58	3.7	2.4	0.62	0.73
CBD11_02_7	3.1	18	2.3	49	3.1	2.2	0.63	0.78
CBD11_02_8	3.4	19	2.6	62	4.9	2.5	0.67	0.79
CBD11_02_9	3.6	16	2.2	56	6.3	4.4	0.75	0.71
CBD11_02_10	3	20	2.4	44	3.2	1.9	0.71	0.66
CBD11_02_11	2.8	16	2.4	49	4.1	2.9	0.69	0.49
CBD11_02_12	3	17	2.9	47	4.2	3.2	0.54	0.49
CBD11_02_13	2.7	18	2.4	47	4.6	3.3	0.57	0.53

<b>Sample</b>	<b>Tm</b>	<b>Yb</b>	<b>Lu</b>	<b>Hf</b>	<b>Ta</b>	<b>W</b>	<b>Pb</b>	<b>Th</b>
CBD11_02_16	2.9	20	2.2	50	7.1	3.9	0.8	0.56
CBD11_02_17	2.7	15	2.3	46	5.5	3.7	0.48	0.62
CBD11_02_18	4.9	29	2.9	86	8.7	5.3	0.75	1
CBD11_02_19	3.1	19	2.8	50	5.6	4.1	0.77	0.49
CBD11_02_20	2.7	18	2.3	59	6.4	3.2	0.64	0.49
CBD11_02_21	4.1	20	2.9	55	4.9	3.2	0.83	0.59
CBD11_02_22	2.8	19	2.4	51	3.8	3.1	0.74	0.48
CBD11_02_23	3.6	23	2.9	55	5.5	3.3	1.1	0.75
CBD11_02_24	2.8	17	2.2	46	2.9	3	0.67	0.63
CBD11_02_25	2.8	20	3.2	48	3.4	2.4	0.68	0.43
CBD11_02_26	3.6	23	2.4	59	3.9	2.8	0.61	0.61
CBD11_02_27	3.2	15	2.4	40	3.6	2.5	0.71	0.54
CBD11_02_28	3.5	17	2.1	54	2.8	3	0.71	0.44
CBD11_02_29	3.1	16	2.4	51	4.1	3.3	0.65	0.63
CBD11_02_30	2.7	16	2.3	54	5.4	3.5	0.59	0.49
KP1_2_1	12	82	11	55	17	17	5	0.86
KP1_2_2	13	99	12	56	12	17	3.9	0.81
KP1_2_3	13	90	11	51	9.7	33	5.4	0.83
KP1_2_4	16	100	13	72	18	27	6.2	1
KP1_2_5	14	94	12	53	12	33	4.4	0.94
KP1_2_6	13	82	12	46	7.3	30	4.8	0.76
KP1_2_7	15	94	11	49	15	27	3.9	1.1
KP1_2_8	13	99	10	52	12	27	4.4	1
KP1_2_11	18	130	16	65	23	30	14	1.1
KP1_2_18	15	110	15	61	25	12	3.9	0.66

<b>Sample</b>	<b>Tm</b>	<b>Yb</b>	<b>Lu</b>	<b>Hf</b>	<b>Ta</b>	<b>W</b>	<b>Pb</b>	<b>Th</b>
KP1_2_19	16	100	15	72	29	11	5.1	0.85
KP1_2_20	12	85	12	57	24	11	4.2	0.87
KP9_2_2_1	14	93	12	62	24	11	3.1	0.84
KP9_2_2_2	13	93	11	50	21	11	3	0.98
KP9_2_2_3	15	110	13	61	25	11	3.4	1.3
KP9_2_2_4	12	88	12	58	24	9.1	3.5	1.3
KP9_2_2_5	15	98	13	56	24	9.4	3.1	1.2
KP9_2_2_6	13	91	12	54	24	11	3.6	1.4
KP9_2_2_7	12	82	12	49	19	10	3.5	1.1
KP9_2_2_8	15	93	12	51	20	11	2.7	1.2
KP9_2_2_9	13	96	12	47	21	8.1	3.1	1
KP9_2_2_10	14	88	11	54	21	8.7	3.2	1
KP9_2_2_11	15	100	14	62	25	11	3.8	1.5
KP9_2_2_12	13	88	11	43	22	13	4.4	1.2
KP9_2_2_13	14	100	12	59	28	15	3.3	2
KP9_2_2_14	14	110	13	64	30	20	3.9	1.4
KP9_2_2_15	16	98	12	48	20	8.1	3.4	1.5
KP9_2_2_16	14	70	9.3	49	19	8.1	2.9	1.7
KP9_2_2_17	13	87	12	46	19	5.5	1.8	1.5
KP9_2_2_18	15	100	12	48	22	7.6	1.3	1.4
KP9_2_2_19	14	87	12	52	22	6.3	1.7	1.3
KP9_2_2_20	11	86	10	46	17	5.4	1.8	1.3
KP9_2_2_21	15	87	14	56	18	3.9	72	1.5
KP9_2_2_22	12	74	11	47	14	3.2	1.6	1.4
KP9_2_2_23	11	82	8.9	42	13	4.1	1.5	1.1
KP9_2_2_24	12	90	9.7	44	14	3.9	2.2	1.3

<b>Sample</b>	<b>Tm</b>	<b>Yb</b>	<b>Lu</b>	<b>Hf</b>	<b>Ta</b>	<b>W</b>	<b>Pb</b>	<b>Th</b>
KP9_2_2_25	13	84	9.9	52	15	4.2	160	2.3
KP9_2_2_26	13	79	10	50	16	4.6	33	1.4
KP9_2_2_27	11	81	9.4	40	15	4.1	1.8	1.2
KP9_2_2_28	13	74	10	41	13	4	2.5	1.2
KP9_2_2_29	14	90	12	45	15	3.7	1.8	1.1
KP9_2_2_30	13	83	12	48	11	2.3	1.7	1.3
KP9_2_2_31	13	88	8.6	50	13	2.7	1.9	1.5
KP9_2_2_32	13	76	11	39	14	3.1	2.1	1.1
KP9_2_2_33	14	78	10	48	13	3.2	130	1.5
KP9_2_2_34	13	83	10	46	12	3.2	2.7	1.3
KP9_2_2_35	15	91	11	47	12	2.2	3	1.3
KP9_2_2_36	14	86	10	51	9.2	2.8	20	1.7
KP9_2_2_37	13	94	12	51	10	2.6	1.7	1.5
KP9_2_2_38	12	68	9.7	42	19	5.9	3	1.7
KP9_2_2_39	15	94	11	43	15	6.5	3.5	1.6
KP9_2_2_40	16	100	13	58	29	13	4	1.9
KP9_2_2_41	14	110	13	58	29	24	3.9	1.8
KP9_2_2_42	14	87	11	46	20	9.9	4.3	1.5
Eud_LV01_1	1.8	11	1.3	59	15	8.9	1.8	1.2
Eud_LV01_2	1.5	10	1.7	54	11	6.7	1.7	1.4
Eud_LV01_3	1.6	8.1	1.1	48	9.8	4.4	1.7	1.3
Eud_LV01_4	1.4	8.8	1.1	52	11	5.5	1.5	1.1
Eud_LV01_5	1.4	9	1.3	51	14	11	1.5	2
Eud_LV01_6	1.6	11	1.5	56	14	7.2	1.8	1.2
Eud_LV01_7	1.5	9.9	1.3	49	16	9.5	1.7	1.4
Eud_LV01_8	1.6	9.2	1.6	52	10	5.2	1.2	1.2
Eud_LV01_9	1.6	8.3	1.2	51	9.9	5.2	1.4	1.2

<b>Sample</b>	<b>Tm</b>	<b>Yb</b>	<b>Lu</b>	<b>Hf</b>	<b>Ta</b>	<b>W</b>	<b>Pb</b>	<b>Th</b>
Eud_LV01_10	1.5	7.7	1.3	47	10	5.2	1.5	1.2
Eud_LV01_11	1.4	7.9	1.5	49	11	3.8	1.5	1.1
Eud_LV01_12	1.3	8.6	1.3	57	12	6.4	3	7.2
Eud_LV01_13	1.6	9.3	1.6	53	14	6.8	1.7	1.4
Eud_LV01_14	1.5	9	1.4	52	14	8.4	1.6	1.4
Eud_LV01_15	1.7	9.6	1.6	57	18	9.4	1.6	1.4
Eud_LV01_16	1.5	9.1	1.6	53	16	5.5	1.7	1.2
Eud_LV01_17	2.1	11	1.8	56	17	9	1.9	1.4
Eud_LV01_18	1.9	11	1.7	54	15	7.6	1.8	1.3
<hr/>								
Eud_NK_1	7.2	54	7	60	5.8	2	6.1	0.93
Eud_NK_2	7.8	52	8.1	60	6	2	6.6	1.1
Eud_NK_3	7.5	51	7.2	61	6.5	2.3	8.3	1.1
Eud_NK_4	8.7	60	7.4	71	6.2	2.1	7.2	1
Eud_NK_5	7.9	58	7.4	60	7.5	1.9	7.6	0.86
Eud_NK_6	9.2	62	8.8	70	6.4	2.1	7.3	0.95
Eud_NK_7	9.1	56	8.1	58	6.4	2.1	7.6	1
Eud_NK_8	8	46	6.9	60	5.6	1.9	4300	1.1
Eud_NK_9	8.3	52	7.1	59	6.3	1.9	7.6	1
Eud_NK_10	9.8	63	8.7	67	7.1	1.9	7.5	0.8
Eud_NK_11	7.1	44	7.3	53	5.7	2.1	5.7	0.87
Eud_NK_12	8.7	61	8.5	64	6.7	1.9	6.6	1.1
Eud_NK_13	8.7	64	8.4	75	7.2	2	8	1.1
Eud_NK_14	7.7	53	8.2	72	8	2.2	7.8	1
Eud_NK_15	9.8	65	9.1	72	8	2	8.5	0.93
Eud_NK_16	8.2	51	7.5	59	6.8	1.7	6.9	0.98
<hr/>								
KP1_2_1	12	68	10	48	10	13	4.9	0.62

<b>Sample</b>	<b>Tm</b>	<b>Yb</b>	<b>Lu</b>	<b>Hf</b>	<b>Ta</b>	<b>W</b>	<b>Pb</b>	<b>Th</b>
KP1_2_2	13	79	9.7	41	11	7.6	4.1	0.88
KP1_2_3	12	96	13	53	21	9.3	4.7	1.1
KP1_2_4	10	73	8.9	48	12	12	4.8	1.1
KP1_2_5	11	69	9.3	47	16	9.2	11	1.2
KP1_2_6	11	71	9.9	43	18	11	4.2	1.3
KP1_2_7	11	80	10	44	11	29	4.6	1
KP1_2_8	11	77	9.1	43	6.5	21	4.9	1.3
KP1_2_9	11	78	9.8	48	20	46	8.2	1.1
KP1_2_10	13	76	11	43	16	10	4.8	1.1
KP1_2_11	13	110	11	49	16	21	4.4	0.58
KP1_2_12	13	68	10	46	12	6.4	4.1	0.79
KP1_2_13	11	82	10	43	17	8	4.2	0.84
KP1_2_14	12	80	9	55	17	8.2	4.7	0.94
KP1_2_15	9.7	75	13	45	17	6.8	5	1.1
KP1_2_16	13	85	12	48	16	7.8	3.7	0.84
KP1_2_17	13	90	12	42	16	11	3.8	1.1
KP1_2_18	13	86	12	42	9.5	16	4.1	0.54
KP1_2_19	12	82	11	46	9.2	10	4.4	0.54
KP1_2_20	11	84	10	48	10	9.9	4.3	0.53
KP1_2_21	15	86	12	62	13	12	4.4	0.57
KP1_2_22	17	110	14	63	21	27	5.1	0.73
KP1_2_23	15	90	11	55	21	8.7	4.3	1.2
KP1_2_24	12	83	8.8	51	17	6.3	4.4	0.96
KP1_2_25	11	77	9.1	47	13	24	3.8	0.81
KP1_2_26	12	94	10	52	17	8.6	4.4	0.98
KP1_2_27	11	92	10	52	18	8.1	4.3	1.1
KP1_2_28	13	86	12	47	18	13	3.8	0.86

<b>Sample</b>	<b>Tm</b>	<b>Yb</b>	<b>Lu</b>	<b>Hf</b>	<b>Ta</b>	<b>W</b>	<b>Pb</b>	<b>Th</b>
KP1_2_29	12	81	9.6	40	17	7.1	4.3	0.72
KP1_2_30	11	76	12	41	17	9.3	3.9	0.59
CBD11_10_1	3.1	21	2.9	50	5.5	3.5	0.82	0.66
CBD11_10_2	3.5	18	2.5	56	6.8	4.4	0.83	0.43
CBD11_10_3	3.3	18	2.8	58	5.8	4	0.92	0.51
CBD11_10_4	3.5	20	2.7	56	3.7	2.6	0.66	0.52
CBD11_10_5	2.7	19	2.7	49	6	3.8	0.96	0.8
CBD11_10_6	2.1	14	2.1	49	4.5	3.7	0.71	0.45
CBD11_10_7	2.4	16	2.5	61	9.8	5.2	0.65	0.46
CBD11_10_8	3.3	17	2.8	55	6.1	3.8	0.94	0.5
CBD11_10_9	3	16	2.1	49	2.5	2	0.81	0.51
CBD11_10_10	3.2	15	2.8	50	4	2.9	0.74	0.59
CBD11_10_11	6.4	40	4.9	110	9.5	3.5	0.93	0.66
CBD11_10_12	3.4	18	2.4	49	2.6	2.4	0.76	0.48
CBD11_10_13	3.6	18	3	56	3.5	3	0.92	0.42
CBD11_10_14	3.1	20	2.7	58	5.6	4.5	1	0.43
CBD11_10_15	2.9	21	2.6	59	4.8	3.7	0.78	0.43
CBD11_10_21	6.1	33	8.7	130	23	14	2.2	2.7
CBD11_10_22	5.5	34	5.7	110	15	7	0.97	1.7
CBD11_10_23	5.8	47	6	110	14	9.4	1.1	2
CBD11_10_25	6.9	47	7	140	22	14	1.7	2.4
CBD11_10_26	6.9	51	7.3	120	19	14	0.84	2.6
CBD11_10_29	8.8	69	11	200	26	11	1.3	2.9
CBD11_10_31	10	60	8.2	170	26	14	2	3.4

**Sample**                   **U**

*ppm*

Sample	U
Eud_LV01_1	2.1
Eud_LV01_2	2
Eud_LV01_3	2.1
Eud_LV01_4	1.6
Eud_LV01_5	4.5
Eud_LV01_6	1.8
Eud_LV01_7	1.7
Eud_LV01_8	1.6
Eud_LV01_9	1.6
Eud_LV01_10	1.9
Eud_LV01_11	1.8
Eud_LV01_12	1.6
Eud_LV01_13	1.8
Eud_LV01_14	1.5
Eud_LV01_15	2.2
Eud_LV01_16	2.1
Eud_LV01_17	1.9
Eud_LV01_18	2.1
Eud_NK_1	1.7
Eud_NK_2	1.4
Eud_NK_3	1.6
Eud_NK_4	1.4
Eud_NK_5	1.4

<b>Sample</b>	<b>U</b>
Eud_NK_6	1.7
Eud_NK_7	1.2
Eud_NK_8	1.5
Eud_NK_9	1.5
Eud_NK_10	1.6
Eud_NK_11	1.4
Eud_NK_12	1.4
Eud_NK_13	1.5
Eud_NK_14	1.7
Eud_NK_15	1.6
Eud_NK_16	1.3
Eud_NK_17	1.5
Eud_NK_18	1.7
 CBD11_02_1	3.5
CBD11_02_2	1.7
CBD11_02_3	2.8
CBD11_02_4	2.8
CBD11_02_5	1.7
CBD11_02_6	1.9
CBD11_02_7	2.5
CBD11_02_8	2.8
CBD11_02_9	1.2
CBD11_02_10	2.9
 CBD11_02_11	1.3
CBD11_02_12	1.4
CBD11_02_13	1.3

**Sample                  U**

CBD11_02_16	1.8
CBD11_02_17	1.1
CBD11_02_18	1.3
CBD11_02_19	0.95
CBD11_02_20	0.74
CBD11_02_21	1.2
CBD11_02_22	1
CBD11_02_23	1.3
CBD11_02_24	1.4
CBD11_02_25	0.89
CBD11_02_26	1.6
CBD11_02_27	1.1
CBD11_02_28	0.98
CBD11_02_29	1.4
CBD11_02_30	1.1
KP1_2_1	0.97
KP1_2_2	0.91
KP1_2_3	1.2
KP1_2_4	1.5
KP1_2_5	1.6
KP1_2_6	1.7
KP1_2_7	1.5
KP1_2_8	1.5
KP1_2_11	1.6

<b>Sample</b>	<b>U</b>
KP1_2_18	1
KP1_2_19	1.3
KP1_2_20	1.3
KP9_2_2_1	1.9
KP9_2_2_2	3.4
KP9_2_2_3	2.8
KP9_2_2_4	1.5
KP9_2_2_5	1.9
KP9_2_2_6	1.8
KP9_2_2_7	1.5
KP9_2_2_8	1.9
KP9_2_2_9	1.6
KP9_2_2_10	1.7
KP9_2_2_11	2.5
KP9_2_2_12	2.1
KP9_2_2_13	2
KP9_2_2_14	2.2
KP9_2_2_15	1.9
KP9_2_2_16	1.7
KP9_2_2_17	1.7
KP9_2_2_18	1.7
KP9_2_2_19	1.9
KP9_2_2_20	1.5
KP9_2_2_21	2.9
KP9_2_2_22	1.5
KP9_2_2_23	1.6

<b>Sample</b>	<b>U</b>
KP9_2_2_24	1.7
KP9_2_2_25	3
KP9_2_2_26	1.6
KP9_2_2_27	1.4
KP9_2_2_28	1.9
KP9_2_2_29	1.7
KP9_2_2_30	1.5
KP9_2_2_31	1.6
KP9_2_2_32	1.6
KP9_2_2_33	2.1
KP9_2_2_34	1.9
KP9_2_2_35	2.2
KP9_2_2_36	1.6
KP9_2_2_37	2.4
KP9_2_2_38	2.1
KP9_2_2_39	2.3
KP9_2_2_40	2.3
KP9_2_2_41	1.9
KP9_2_2_42	2
Eud_LV01_1	1.8
Eud_LV01_2	1.8
Eud_LV01_3	1.9
Eud_LV01_4	1.5
Eud_LV01_5	1.5
Eud_LV01_6	2
Eud_LV01_7	2
Eud_LV01_8	1.9

<b>Sample</b>	<b>U</b>
Eud_LV01_9	1.8
Eud_LV01_10	1.8
Eud_LV01_11	1.8
Eud_LV01_12	1.9
Eud_LV01_13	2
Eud_LV01_14	2
Eud_LV01_15	1.9
Eud_LV01_16	1.8
Eud_LV01_17	2.3
Eud_LV01_18	2
Eud_NK_1	1.4
Eud_NK_2	1.6
Eud_NK_3	1.1
Eud_NK_4	1.4
Eud_NK_5	1.5
Eud_NK_6	1.1
Eud_NK_7	1.5
Eud_NK_8	1.8
Eud_NK_9	1.6
Eud_NK_10	1.4
Eud_NK_11	1.3
Eud_NK_12	1.6
Eud_NK_13	1.7
Eud_NK_14	1.8
Eud_NK_15	1.7
Eud_NK_16	1.5

<b>Sample</b>	<b>U</b>
KP1_2_1	2.4
KP1_2_2	2.3
KP1_2_3	2.1
KP1_2_4	2.1
KP1_2_5	1.6
KP1_2_6	1.7
KP1_2_7	2
KP1_2_8	1.9
KP1_2_9	1.9
KP1_2_10	1.9
KP1_2_11	1.5
KP1_2_12	1.6
KP1_2_13	1.9
KP1_2_14	2.5
KP1_2_15	2.3
KP1_2_16	2.1
KP1_2_17	2.3
KP1_2_18	1.1
KP1_2_19	1.7
KP1_2_20	2.9
KP1_2_21	2.3
KP1_2_22	2.6
KP1_2_23	2.2
KP1_2_24	2
KP1_2_25	2
KP1_2_26	2.3
KP1_2_27	2.1

<b>Sample</b>	<b>U</b>
KP1_2_28	2.1
KP1_2_29	1.9
KP1_2_30	1.8
 CBD11_10_1	2.1
CBD11_10_2	1.2
CBD11_10_3	1.9
CBD11_10_4	1.3
CBD11_10_5	1.4
CBD11_10_6	1.3
CBD11_10_7	1.2
CBD11_10_8	1.3
CBD11_10_9	1
CBD11_10_10	1.1
 CBD11_10_11	3.8
CBD11_10_12	1.7
CBD11_10_13	1.3
CBD11_10_14	0.83
CBD11_10_15	0.93
 CBD11_10_21	2.2
CBD11_10_22	1.9
CBD11_10_23	1.6
CBD11_10_25	2
CBD11_10_26	2.4
CBD11_10_29	3.5
CBD11_10_31	5.3



## 8.0 APPENDIX 4: SAMPLE INVENTORY

Table 8. Inventory of all samples acquired in the course of this study.

Sample ID	Locality	Coordinates	Sample Type
<b>KP 1</b>	Kipawa	46.80783, -78.50404	Hand sample, polished chip
<b>KP 2</b>	Kipawa	46.80783, -78.50405	Hand sample
<b>KP 3</b>	Kipawa	46.80783, -78.50406	Hand sample
<b>KP 4</b>	Kipawa	46.80783, -78.50407	Hand sample
<b>KP 5</b>	Kipawa	46.80783, -78.50408	Hand sample
<b>KP 6</b>	Kipawa	46.80783, -78.50409	Hand sample
<b>KP 7</b>	Kipawa	46.80783, -78.50410	Hand sample
<b>KP 8</b>	Kipawa	46.80783, -78.50411	Hand sample, polished chip
<b>KP 9</b>	Kipawa	46.80783, -78.50412	Hand sample, polished chip, thin section
<b>KP 10</b>	Kipawa	46.80783, -78.50413	Hand sample
<b>KP 11</b>	Kipawa	46.80783, -78.50414	Hand sample
<b>KP 12</b>	Kipawa	46.80783, -78.50415	Hand sample, thin section
<b>KP 13</b>	Kipawa	46.80783, -78.50416	Hand sample, thin section
<b>KP 14</b>	Kipawa	46.80783, -78.50417	Hand sample
<b>KP 15</b>	Kipawa	46.80783, -78.50418	Hand sample
<b>KP 16</b>	Kipawa	46.80783, -78.50419	Hand sample
<b>KM 134</b>	Kipawa	46.807, -78.504	Drill core, polished chip, thin section
<b>CB 02-2</b>	Red Wine- Cabernet		Drill core, polished chip, thin section
<b>PR 03</b>	Red Wine- Pinot Rose		Drill core, polished chip, thin section
<b>CBD 11-10-1</b>	Red Wine- Cabernet		Drill core, polished chip
<b>CBD 11-10-2</b>	Red Wine- Cabernet		Drill core, polished chip

## 9.0 APPENDIX 5: SUPPLIMENTAL IMAGES

### Figure from Appendix 5

Figure 44. Sample KP 3 .....	255
Figure 45. Sample KP 4 .....	256
Figure 46. Sample KP 5 .....	257
Figure 47. Sample KP 6 .....	258
Figure 48. Sample KP 7 .....	259
Figure 49. Sample KP 8 .....	260
Figure 50. Sample KP 9 .....	261
Figure 51. Sample KP 10 .....	262
Figure 52. Sample KP 11 .....	263
Figure 53. Sample KP 12 .....	264
Figure 54. Sample KP 13 .....	265
Figure 55. Sample KP 13.1 .....	266
Figure 56. Sample KP 14 .....	267
Figure 57. Sample KP 15 .....	268
Figure 58. Sample KP 16 .....	269
Figure 59. BSE image and overlaid EDS identifications of eudialyte in sample KP 9 .....	270
Figure 60. BSE image and overlaid EDS identifications of eudialyte in sample KP 9 .....	271
Figure 61. BSE image of sample KP 8 .....	272
Figure 62. BSE image and overlaid EDS identifications of eudialyte in sample KP 8 .....	273
Figure 63. Galena (white) in sample KP 8 .....	274
Figure 64. True color image of KM 134 .....	275
Figure 65. BSE image and overlaid EDS identifications of eudialyte in sample KM 134 .....	276
Figure 66. BSE image and overlaid EDS identifications of eudialyte in sample KM 134 .....	277
Figure 67. BSE image and overlaid EDS identifications of eudialyte in sample KM 134 .....	278
Figure 68. BSE image and overlaid EDS identifications of eudialyte in sample KM 134 .....	279
Figure 69. BSE image and overlaid EDS identifications of eudialyte in sample KM 134 .....	280
Figure 70 BSE image and overlaid EDS identifications of eudialyte in sample KM 134 .....	281
Figure 71. BSE image and overlaid EDS identifications of eudialyte in sample CBD 11-10-2 .....	282
Figure 72. BSE image and overlaid EDS identifications of eudialyte in sample CBD 11-10-2 .....	283
Figure 73. BSE image and overlaid EDS identifications of eudialyte in sample CBD 11-10-2 .....	283
Figure 74. BSE image and overlaid EDS identifications of eudialyte in sample CBD 11-10-2 .....	283
Figure 75. BSE image and overlaid EDS identifications of eudialyte in sample PR 03-11 .....	283
Figure 76. BSE image and overlaid EDS identifications of eudialyte in sample PR 03-11 .....	283
Figure 77. BSE image and overlaid EDS identifications of eudialyte in sample PR 03-11 .....	283

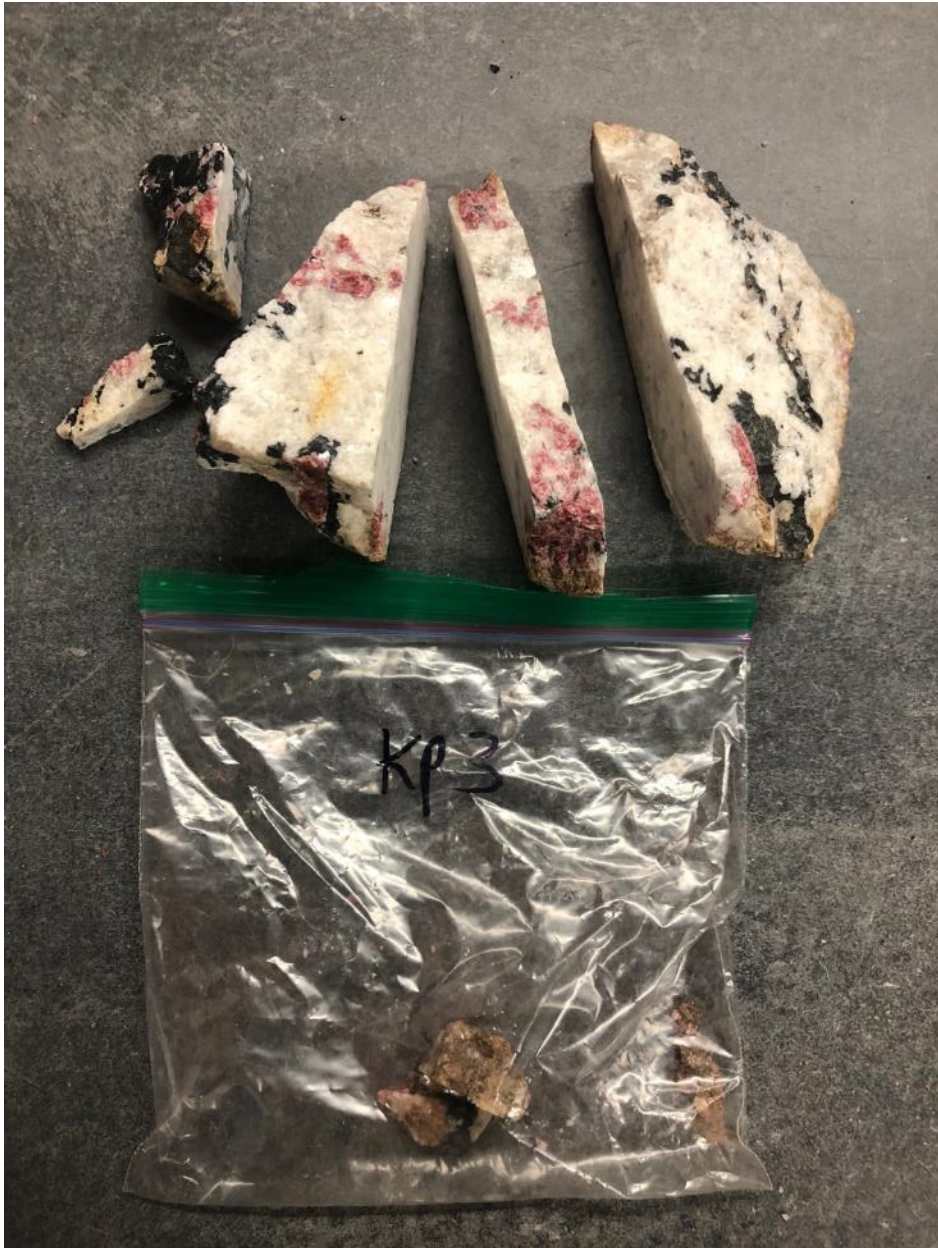


Figure 44. Sample KP 3



Figure 45. Sample KP 4



Figure 46. Sample KP 5

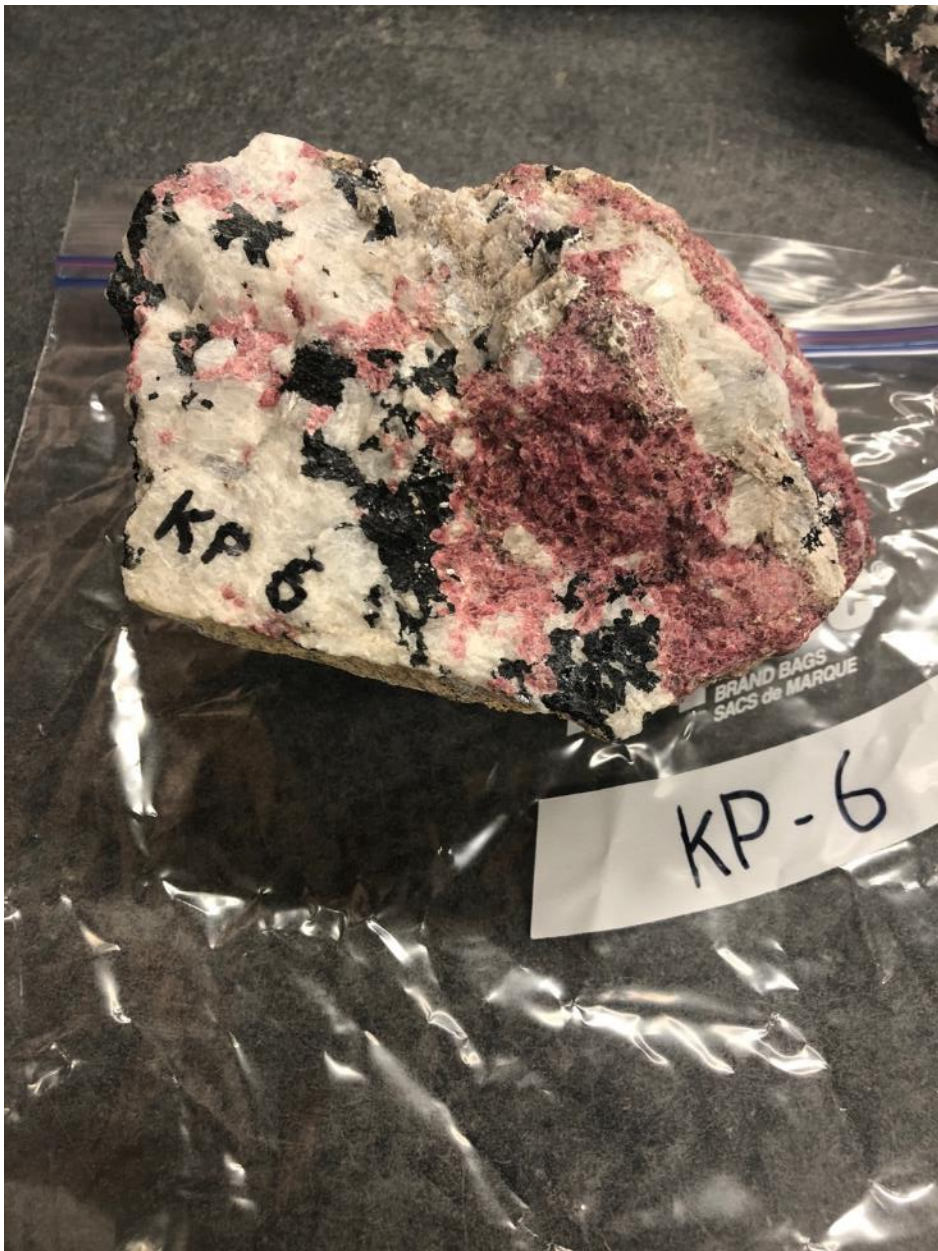


Figure 47. Sample KP 6

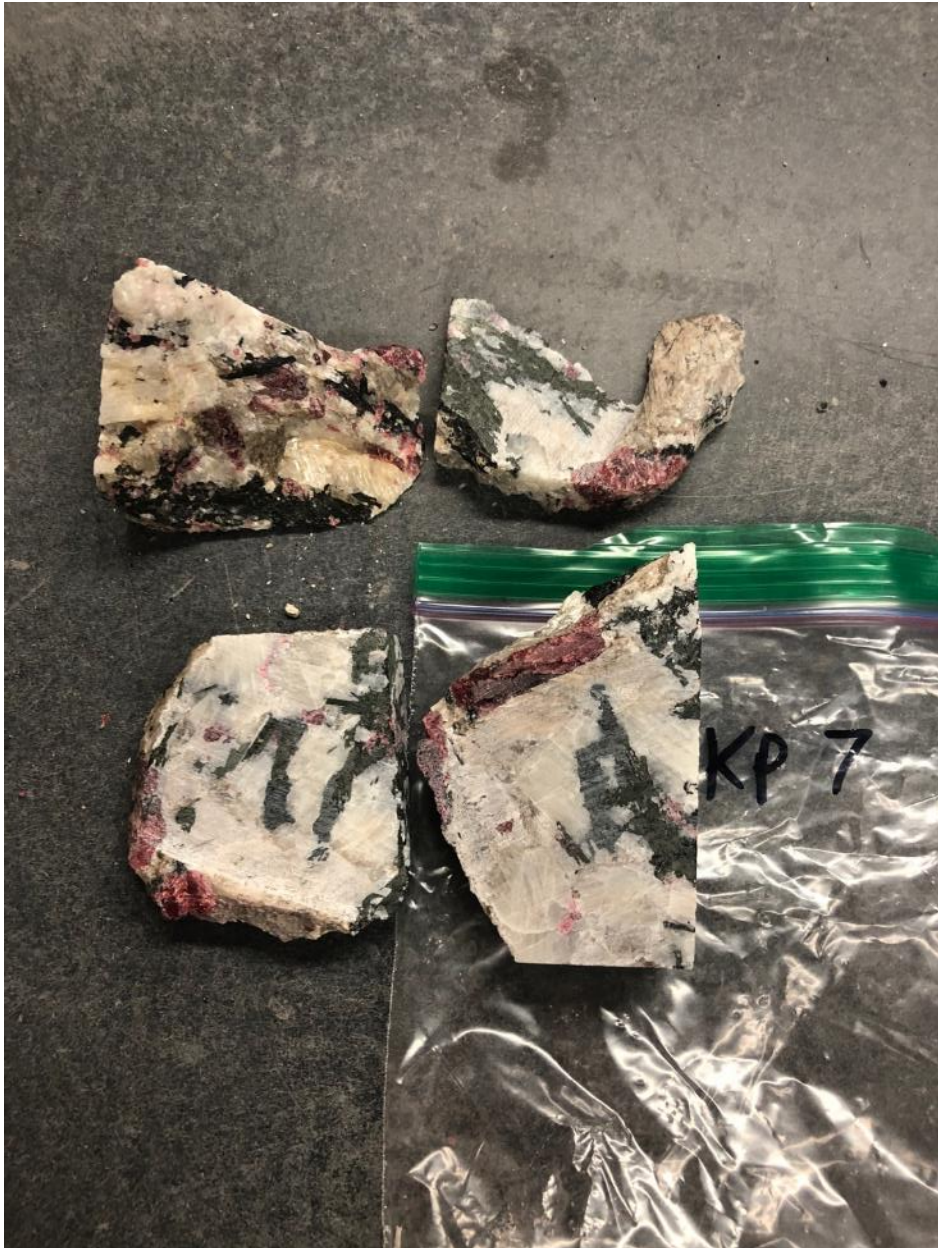


Figure 48. Sample KP 7



Figure 49. Sample KP 8



Figure 50. Sample KP 9



Figure 51. Sample KP 10



Figure 52. Sample KP 11

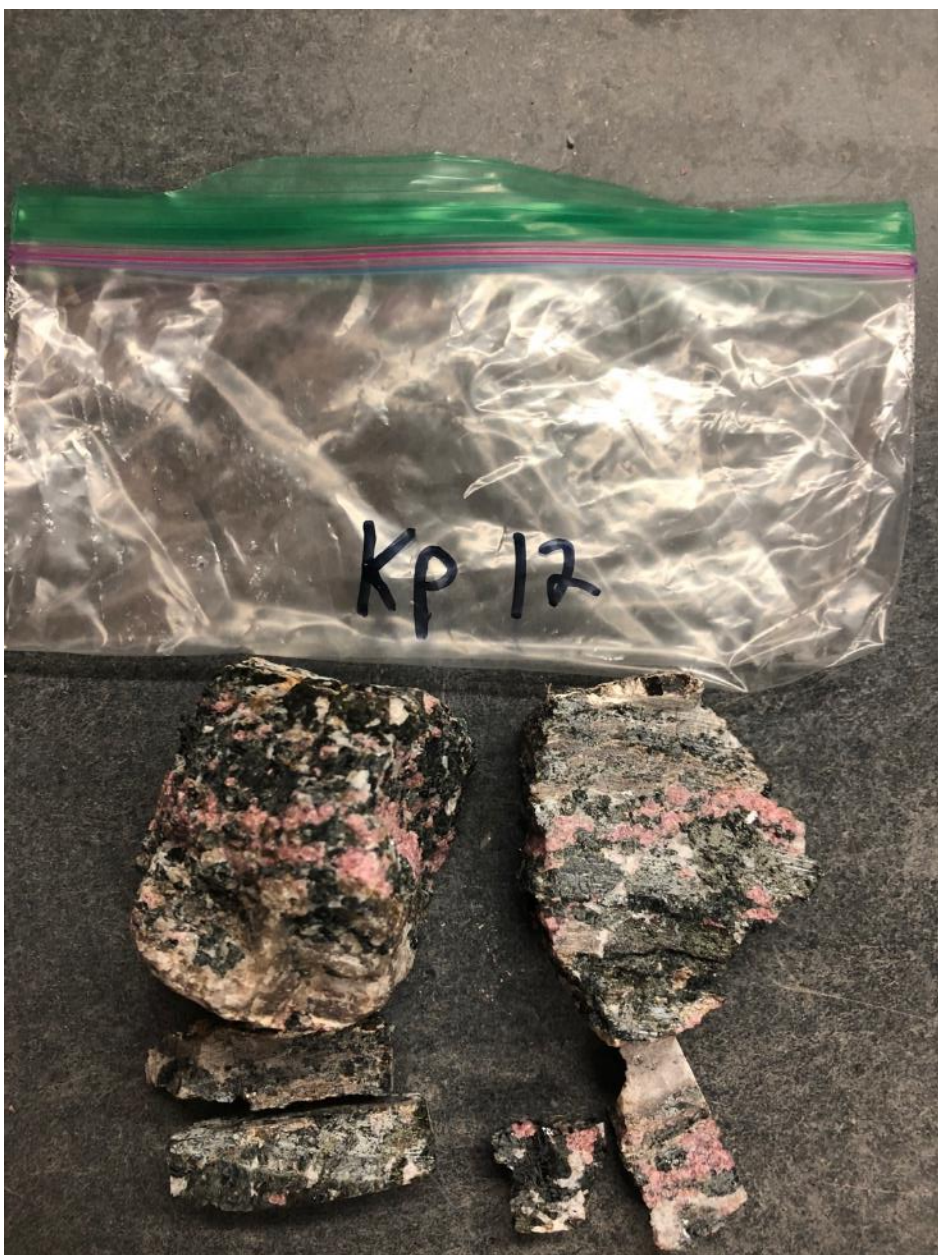


Figure 53. Sample KP 12



Figure 54. Sample KP 13

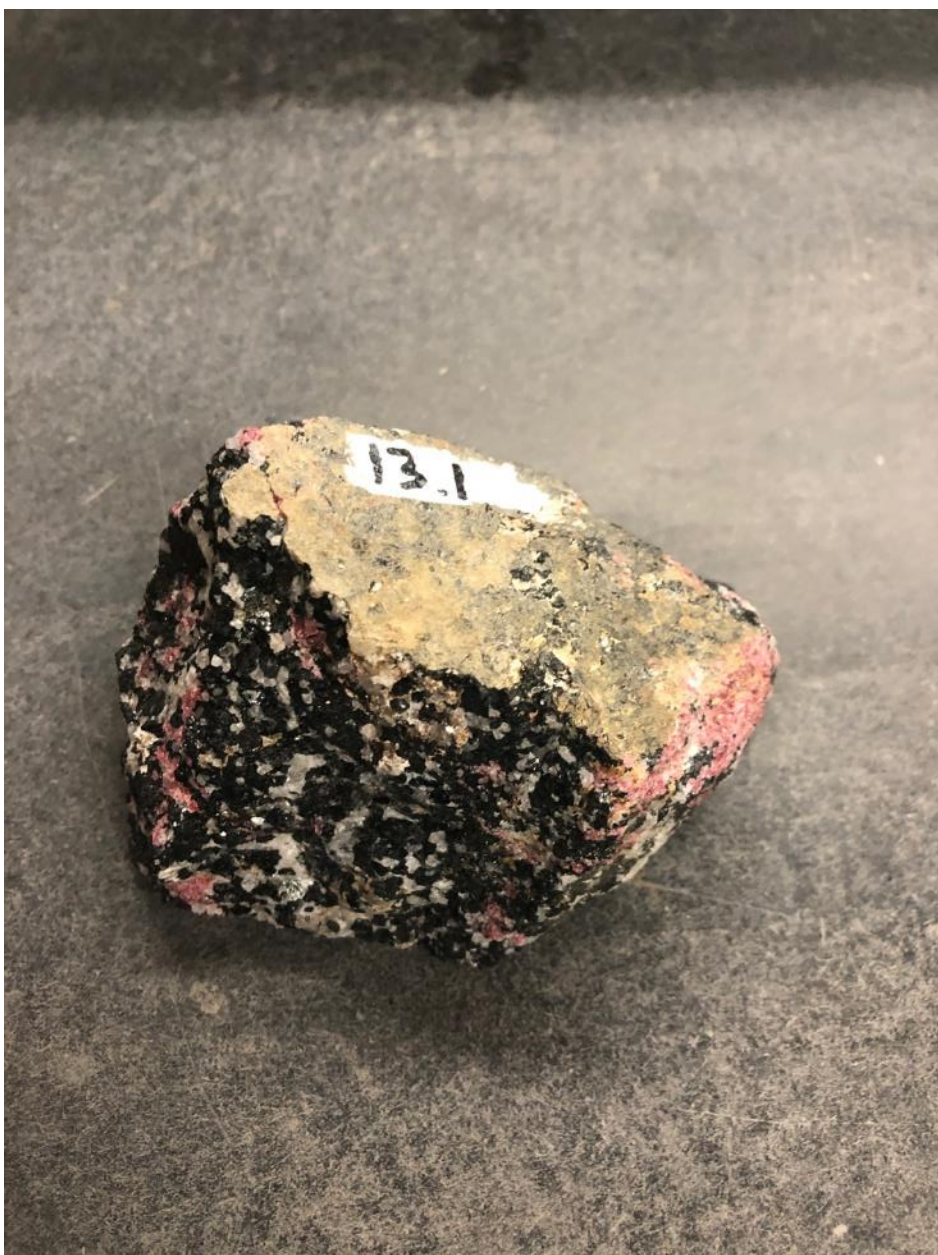


Figure 55. Sample KP 13.1

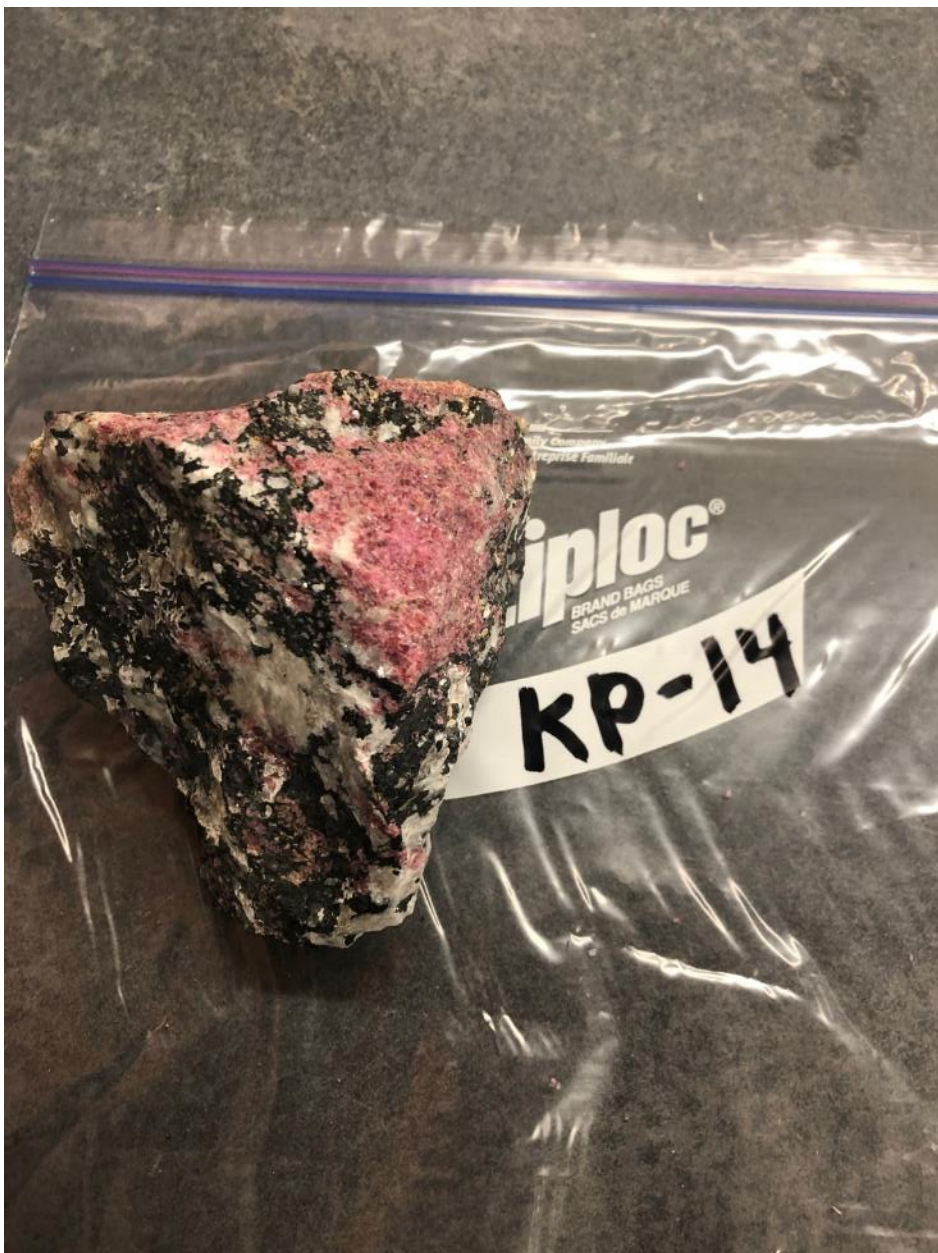


Figure 56. Sample KP 14

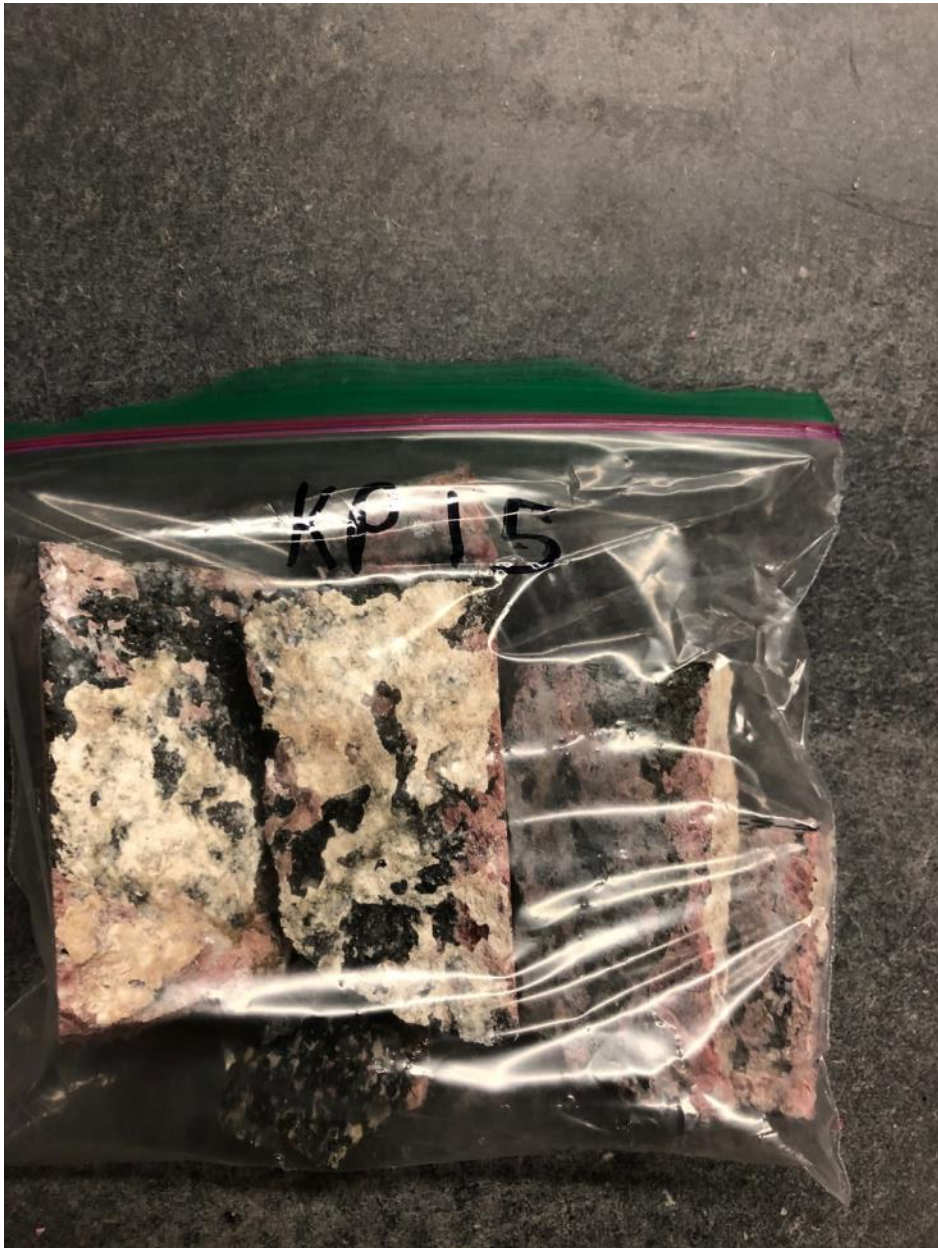


Figure 57. Sample KP 15



Figure 58. Sample KP 16.

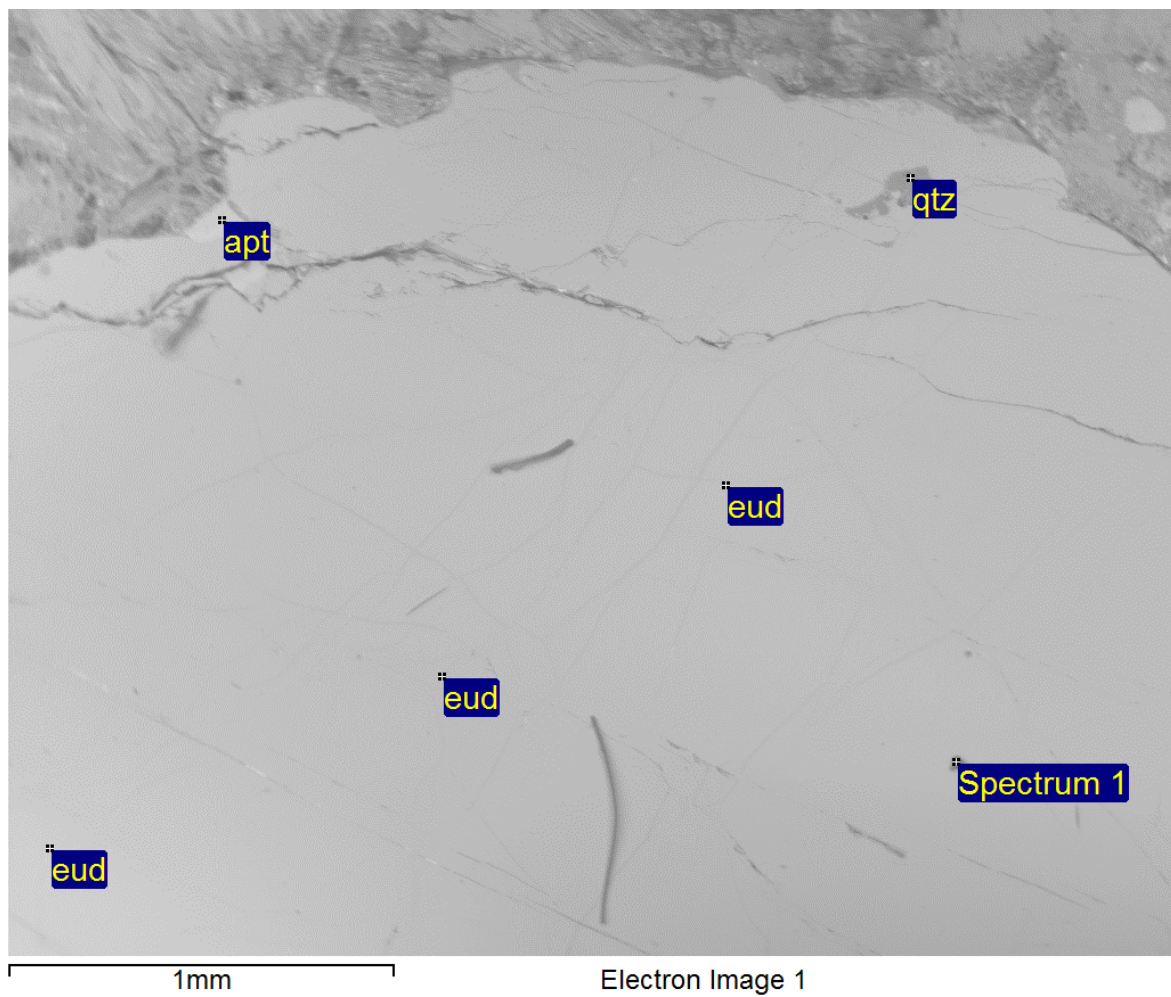


Figure 59. BSE image and overlaid EDS identifications of eudialyte in sample KP 9

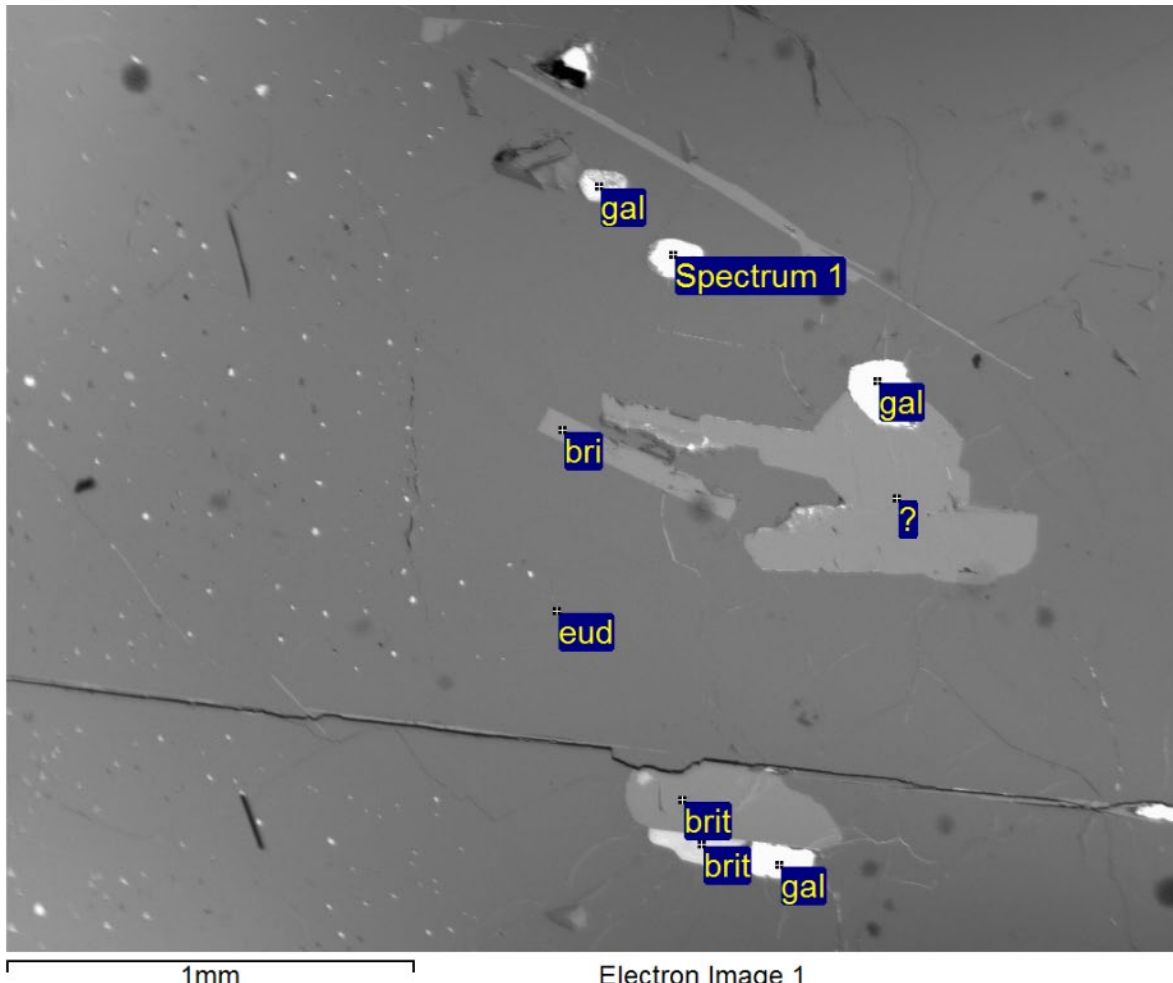


Figure 60. BSE image and overlaid EDS identifications of eudialyte in sample KP 9

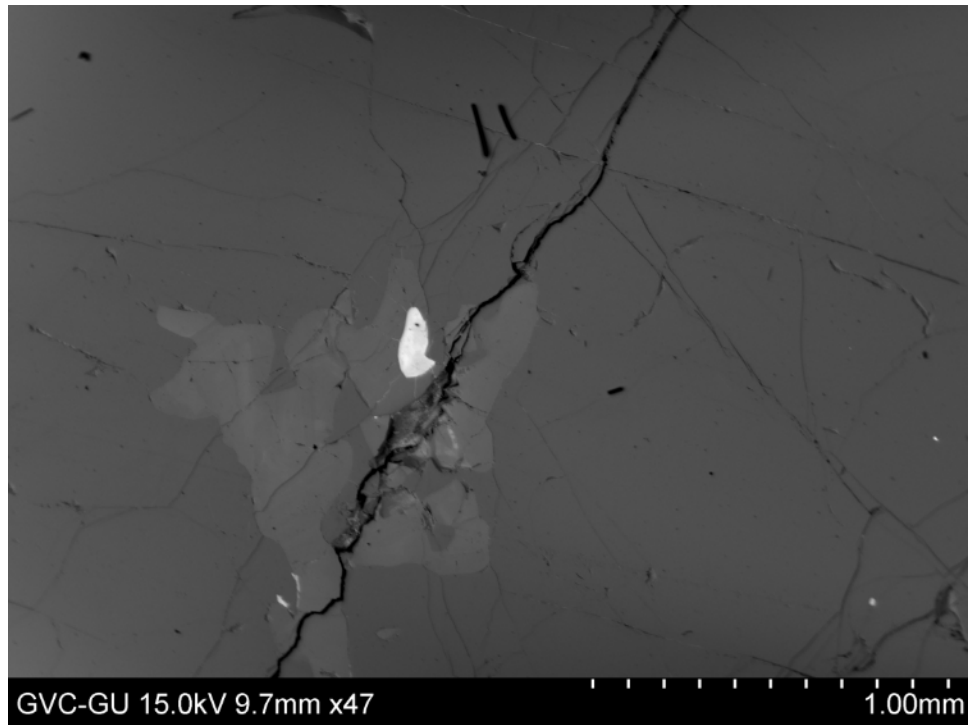


Figure 61. BSE image of sample KP 8

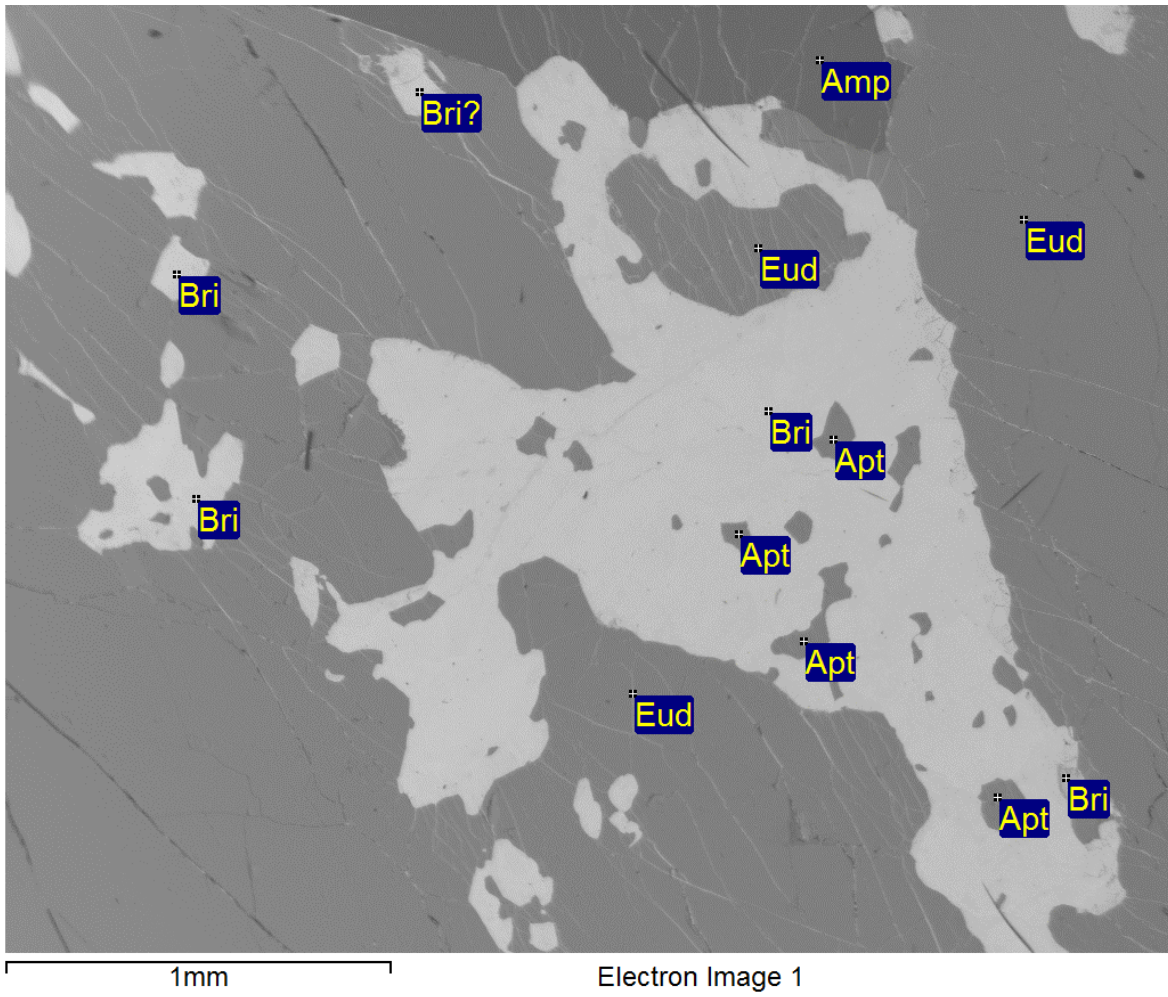


Figure 62. BSE image and overlaid EDS identifications of eudialyte in sample KP 8

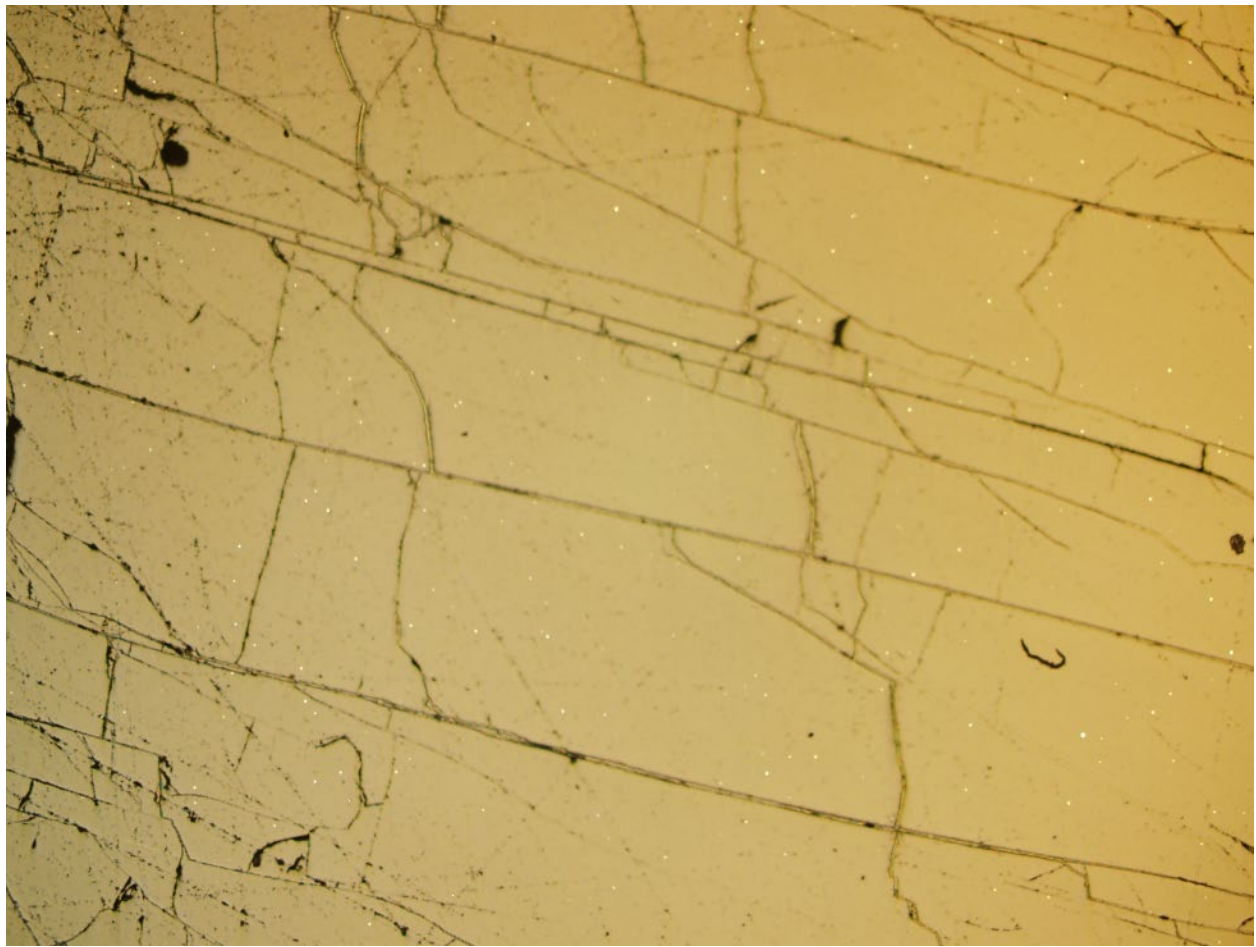


Figure 63. Galena (white) in sample KP 8



Figure 64. True color image of KM 134

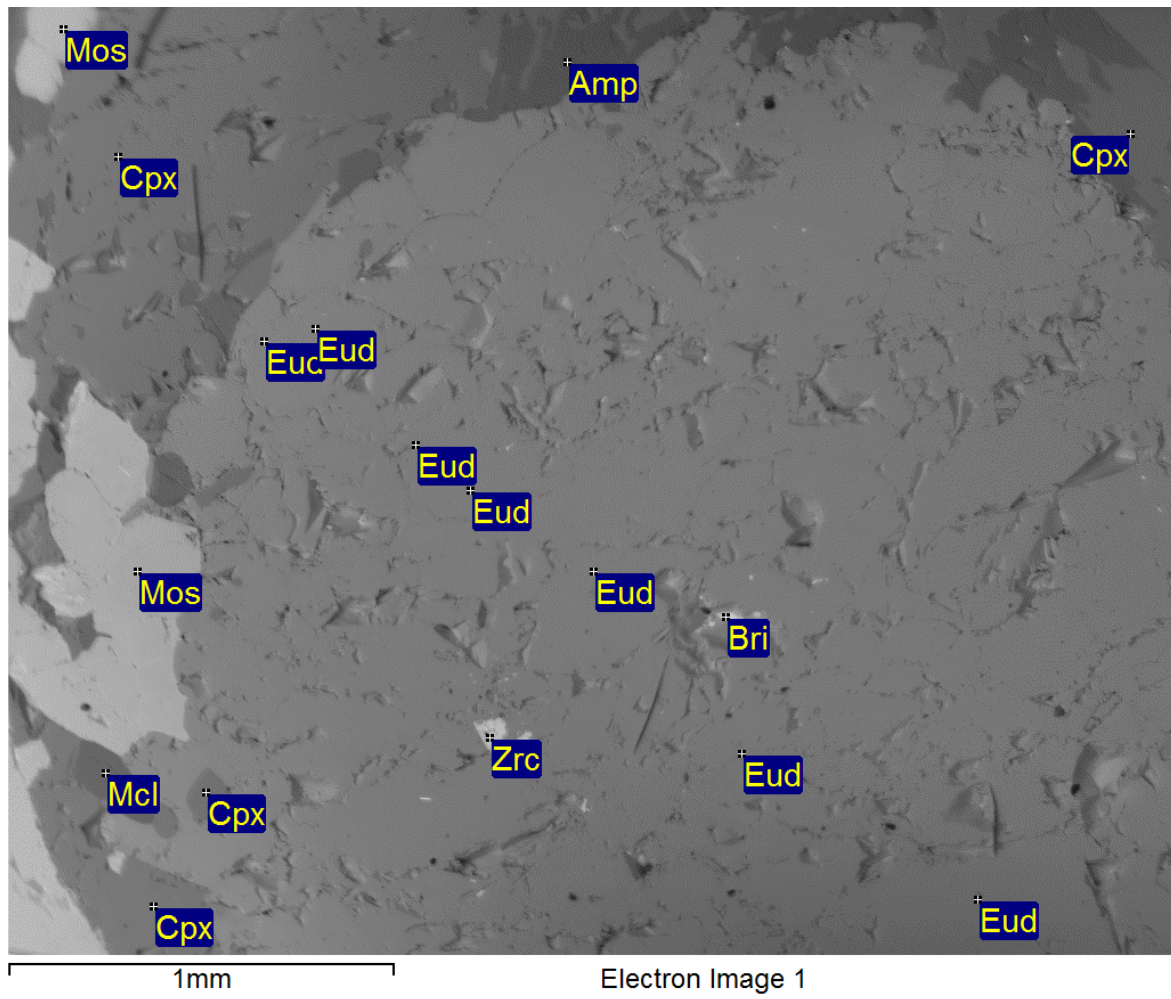


Figure 65. BSE image and overlaid EDS identifications of eudialyte in sample KM 134

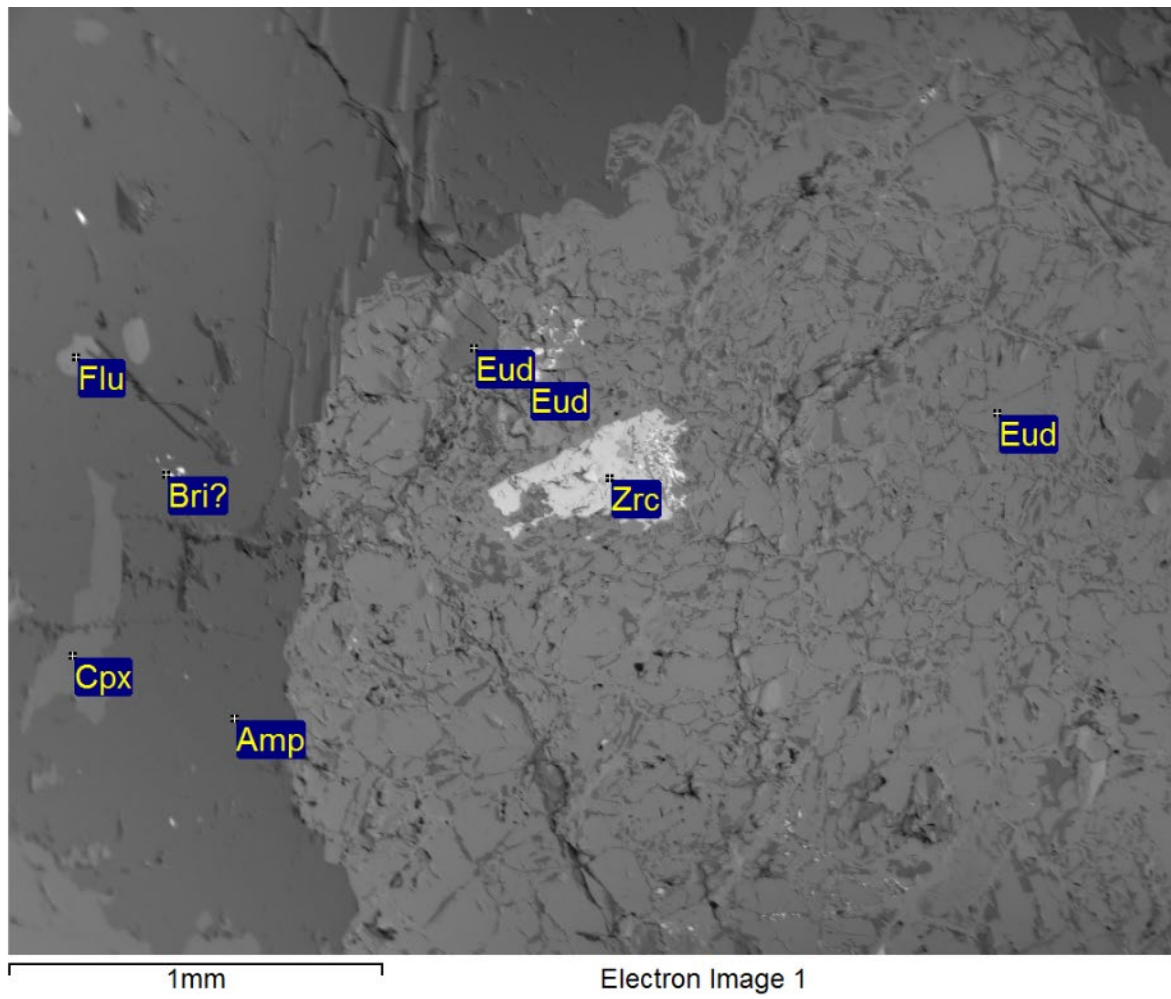


Figure 66. BSE image and overlaid EDS identifications of eudialyte in sample KM 134

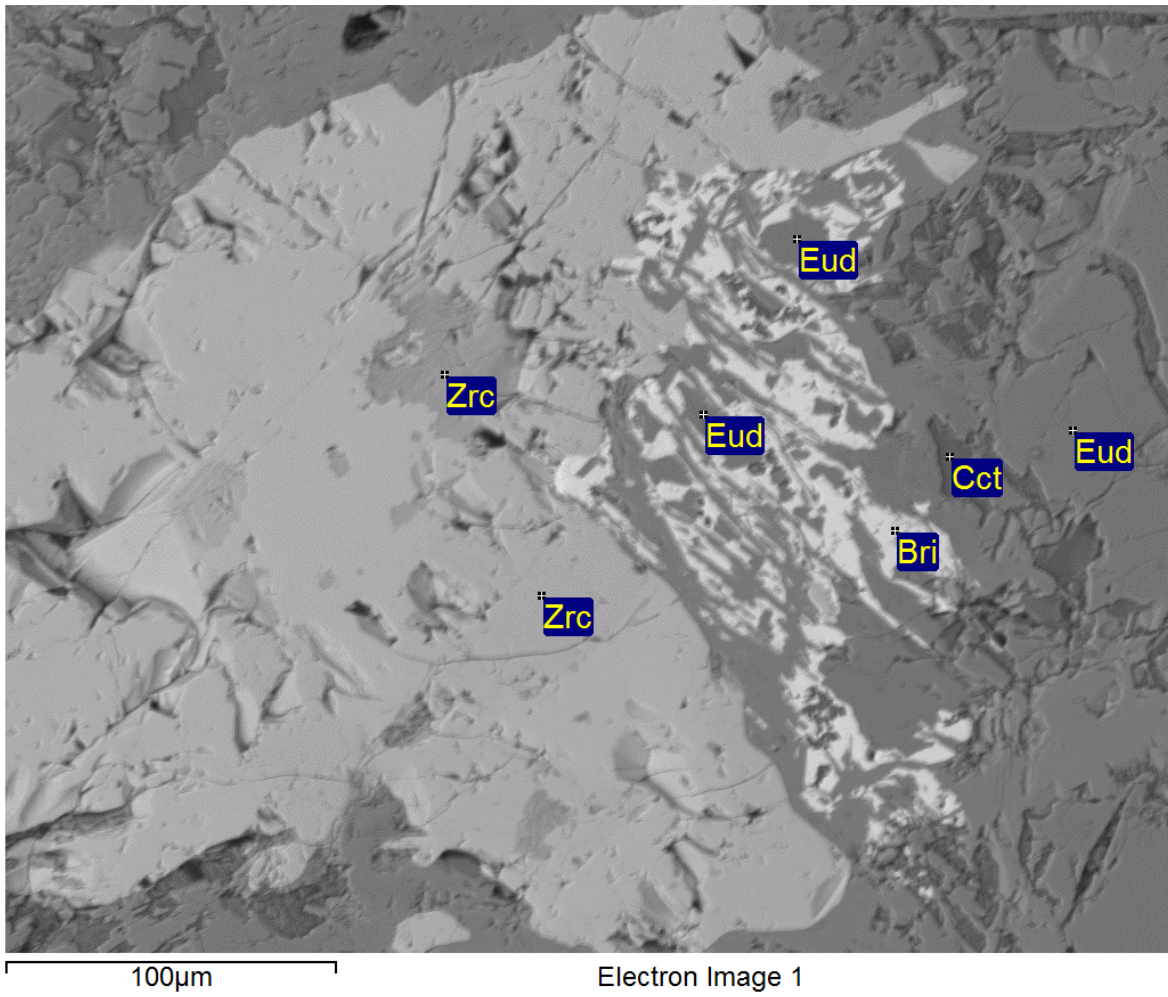


Figure 67. BSE image and overlaid EDS identifications of eudialyte in sample KM 134

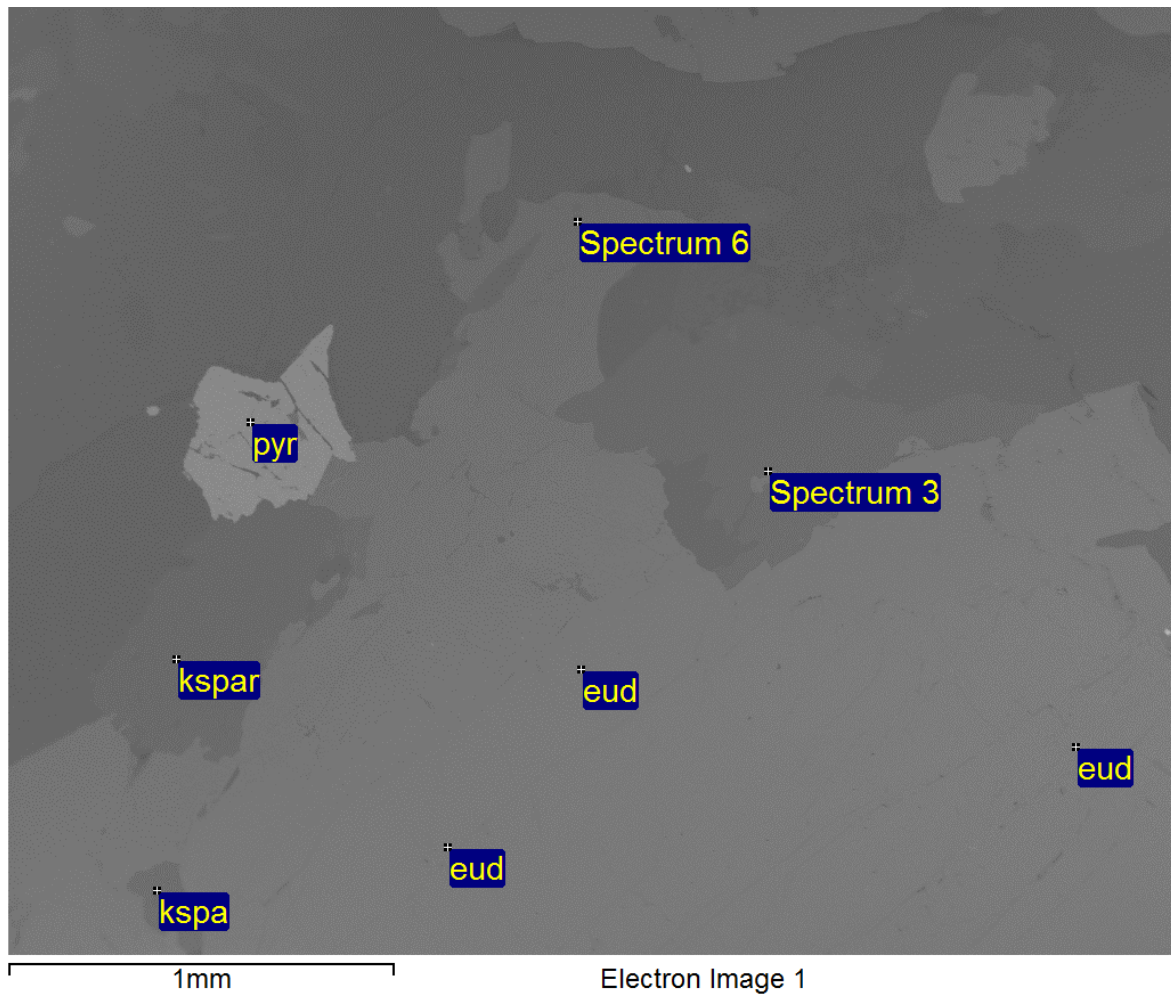


Figure 68. BSE image and overlaid EDS identifications of eudialyte in sample KM 134

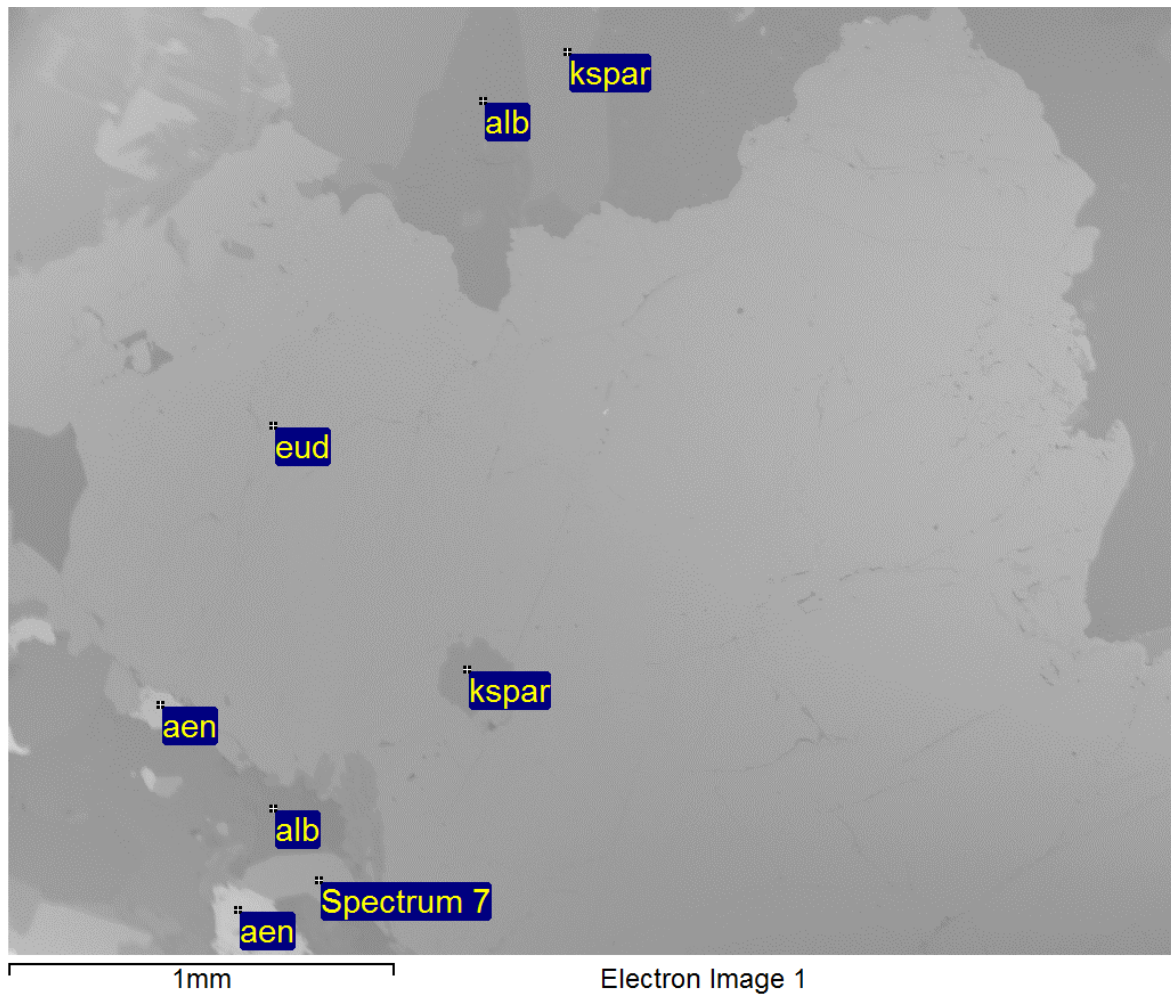


Figure 69. BSE image and overlaid EDS identifications of eudialyte in sample KM 134

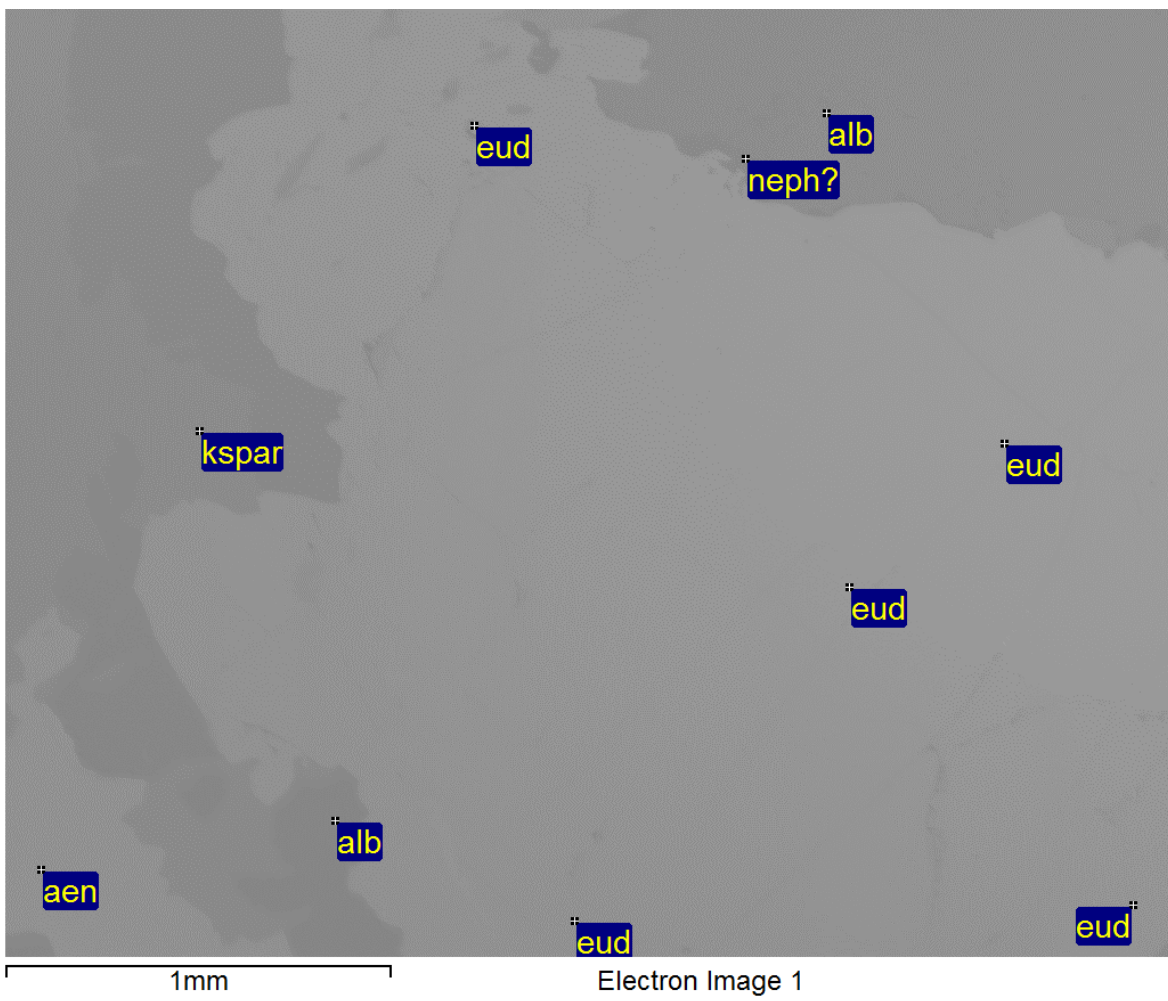


Figure 70 BSE image and overlaid EDS identifications of eudialyte in sample KM 134

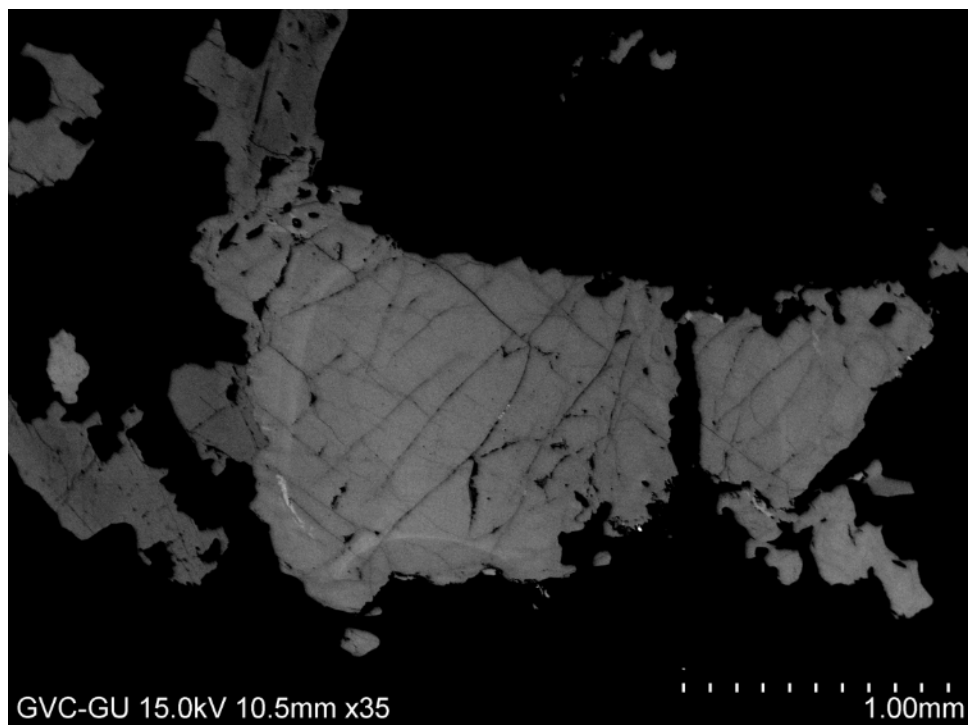


Figure 71. BSE image and overlaid EDS identifications of eudialyte in sample CBD 11-10-2

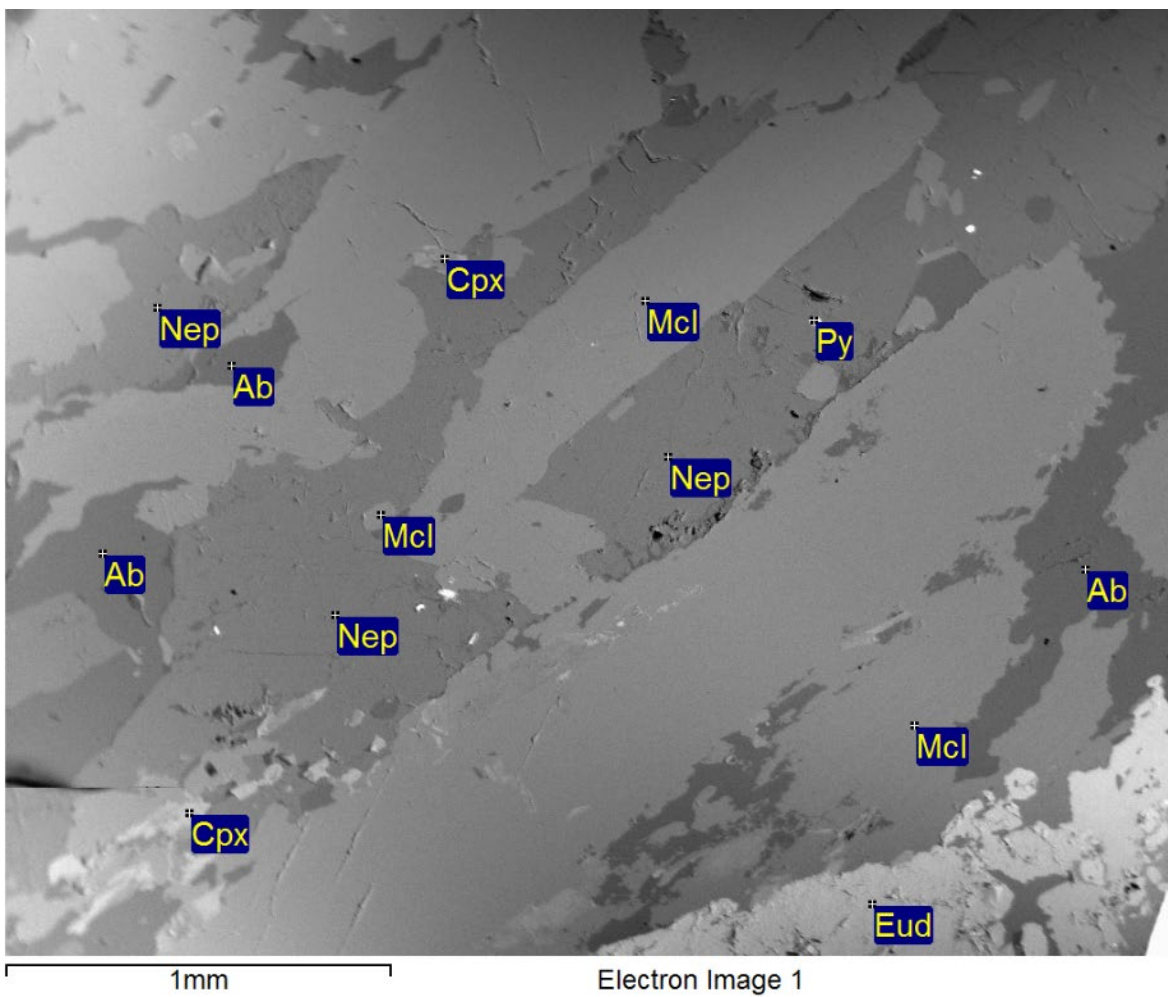


Figure 72. BSE image and overlaid EDS identifications of eudialyte in sample CBD 11-10-2

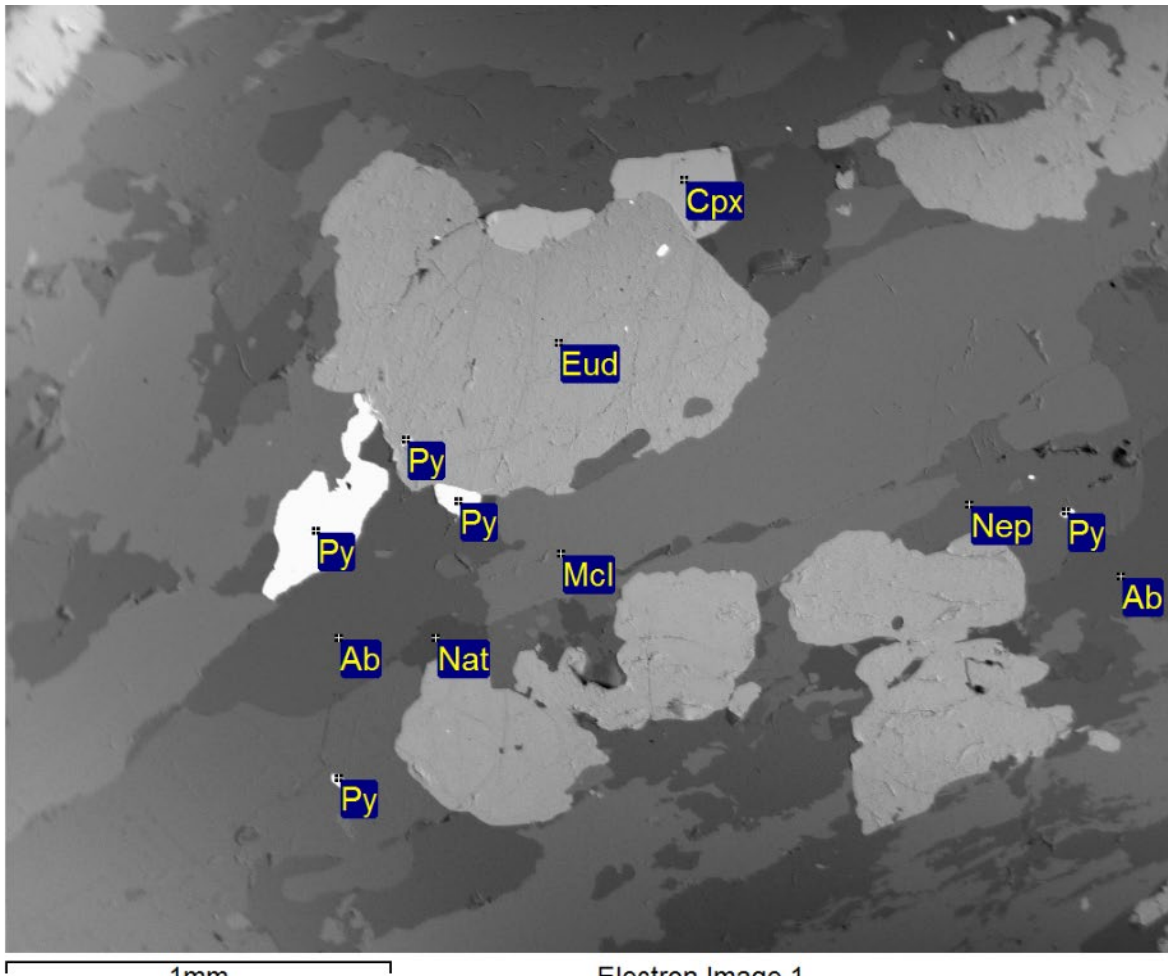


Figure 73. BSE image and overlaid EDS identifications of eudialyte in sample CBD 11-10-2

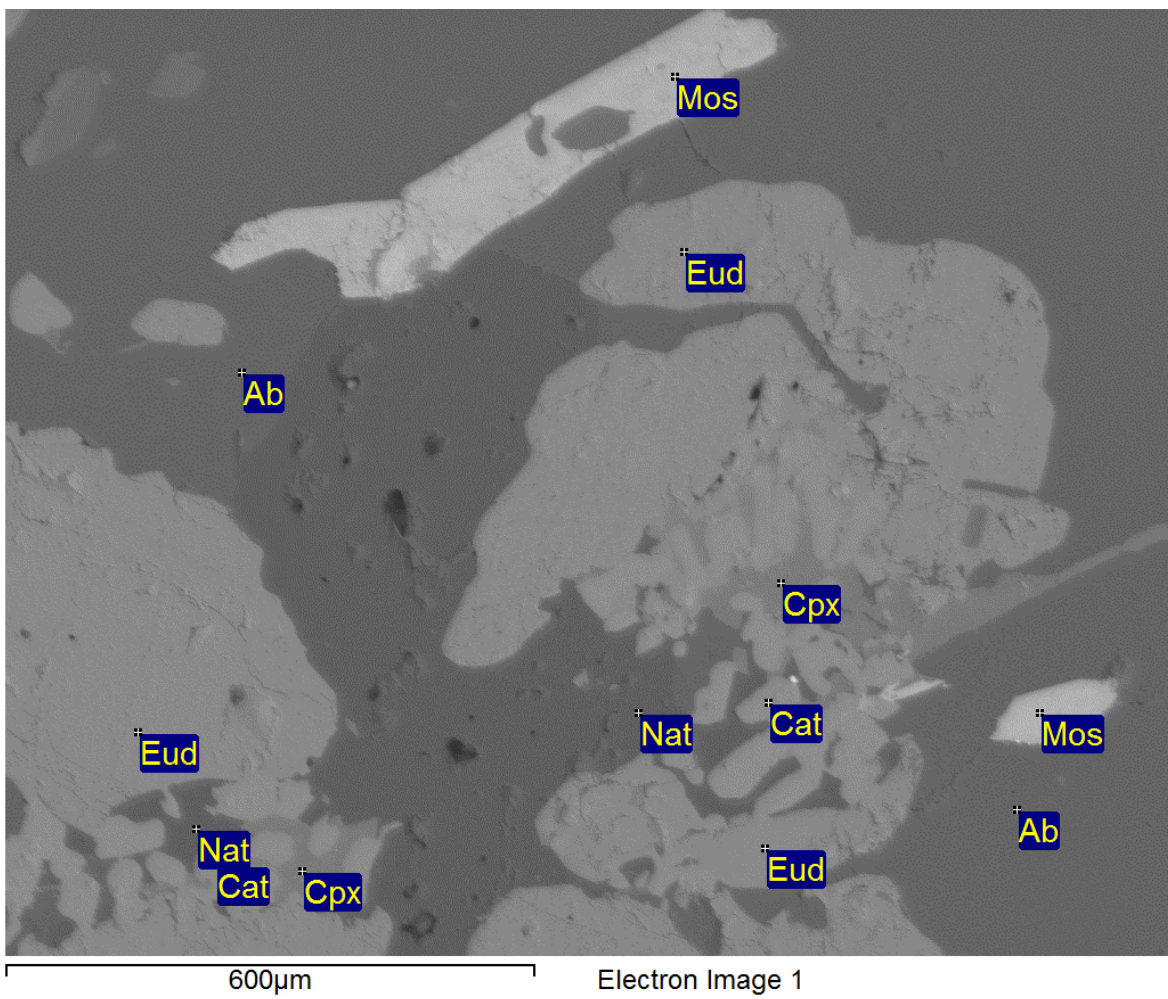


Figure 74. BSE image and overlaid EDS identifications of eudialyte in sample CBD 11-10-2

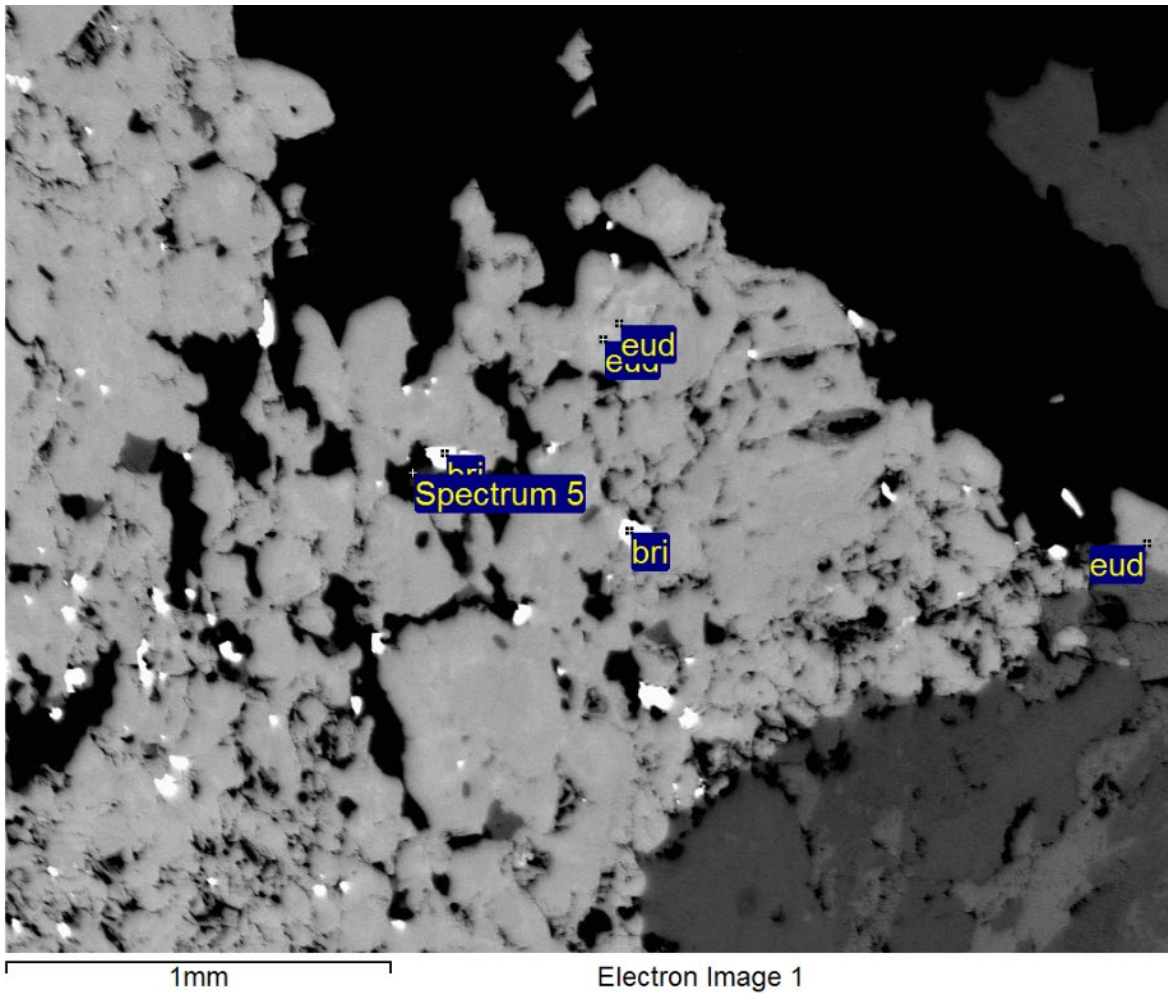


Figure 75. BSE image and overlaid EDS identifications of eudialyte in sample PR 03-11

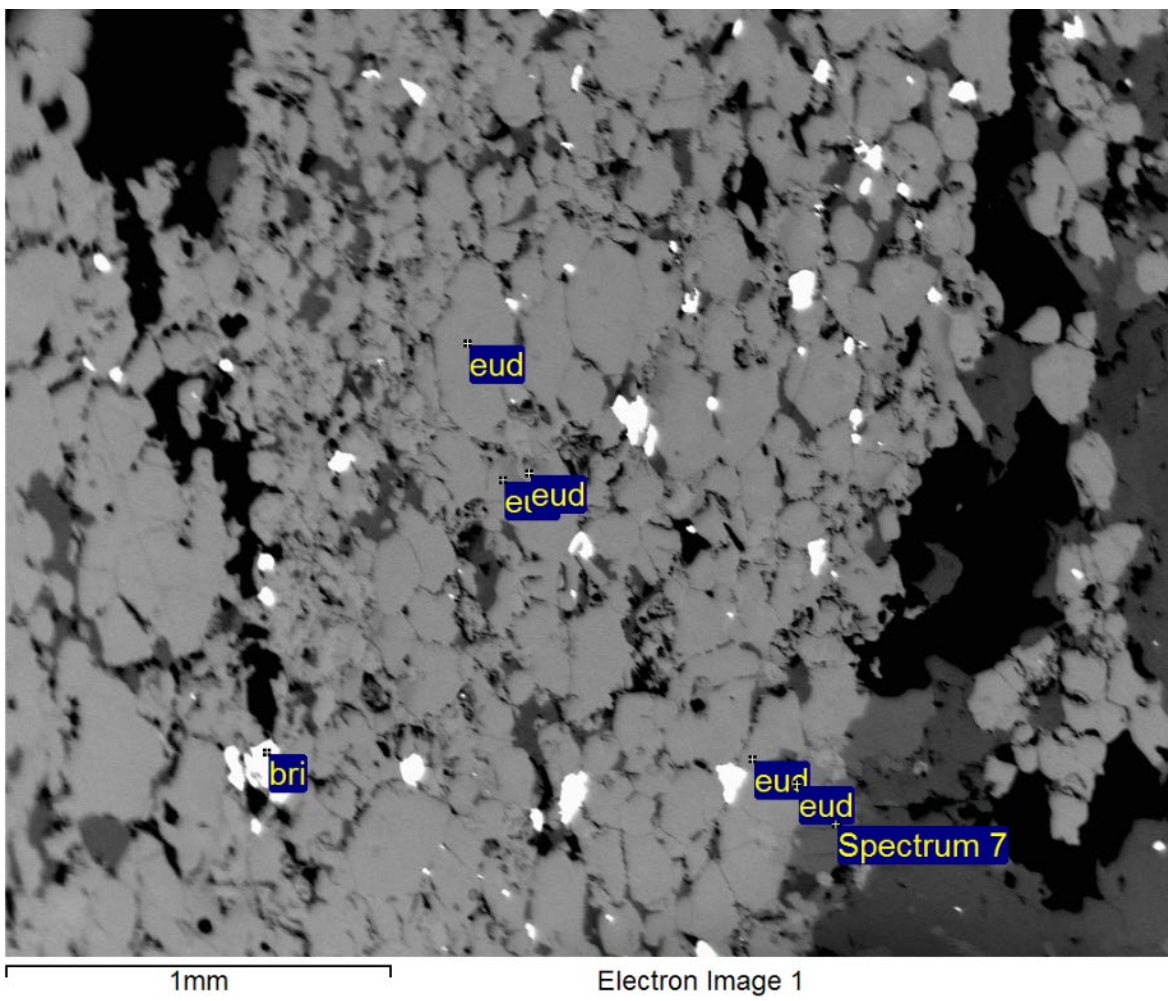


Figure 76. BSE image and overlaid EDS identifications of eudialyte in sample PR 03-11

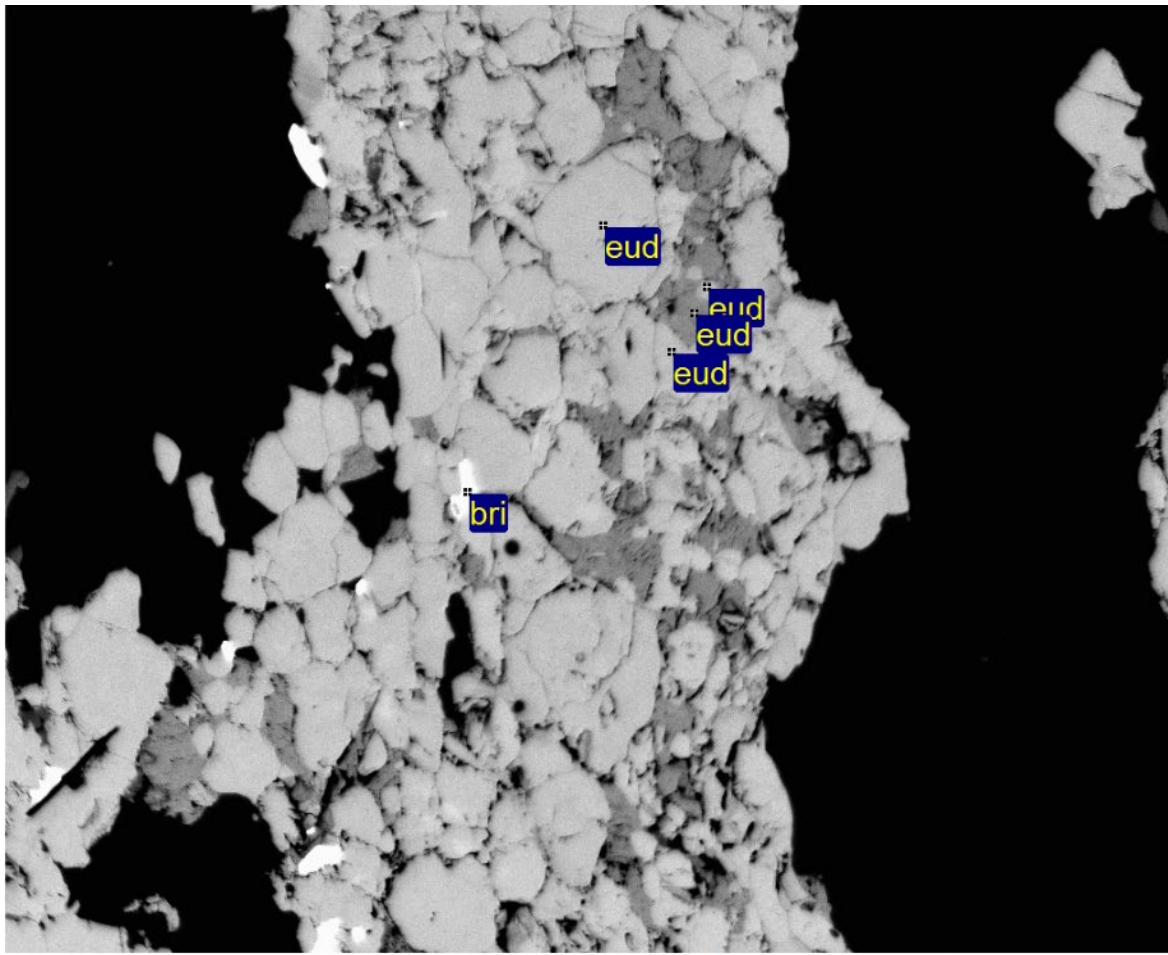


Figure 77. BSE image and overlaid EDS identifications of eudialyte in sample PR 03-11

